
# RHEOLOGICAL MODELLING OF SELF-COMPACTING CONCRETE

**AYE MONN MONN SHEINN**

*M.Eng.(Structural.), Asian Institute of Technology*

**A THESIS SUBMITTED FOR**

**THE DEGREE OF DOCTOR OF PHILOSOPHY**

**DEPARTMENT OF CIVIL ENGINEERING**

**NATIONAL UNIVERSITY OF SINGAPORE**

**2007**

## ACKNOWLEDGEMENTS

The author wishes to express deep appreciation and sincere gratitude to her supervisors, Professor S.T. Quek and Dr. C.T Tam for their invaluable guidance, encouragement, helpful criticism and suggestions throughout this research. Without their constructive ideas, devotion and encouragement, this study would not have been in this form. Special thanks and appreciation also goes to her former supervisor Associate Professor W.S. Ho for his valuable advice and discussion on this research. The author would like to express her heartfelt gratitude to Associate Professor M.H. Zhang and K.C. Ong for their valuable suggestions and also for serving as members of the Thesis Committee.

Thanks also go to all the dedicated technical staffs of The Concrete and Structural Engineering Laboratory, Department of Civil Engineering, for their kind help throughout the experimental work. Special thanks are also due to Mr B.C. Sit, Assistance Lab Manager, for his patient, tolerance and untiring cooperation. The author would like to express her real appreciation to her friends and classmates for their help and encouragement throughout the research study.

The author is grateful to The National University of Singapore for awarding NUS Research Scholarship, which enabled the author to pursue her study. Sincere thanks are due to RDC Concrete, Eng Seng Construction Pte. Ltd, JPL Industries Pte. Ltd, Ssangyong Cement Pte. Ltd and WR Grace (Singapore) Pte Ltd for providing assistance and necessary materials for experimental study.

## ACKNOWLEDGEMENTS

The author reiterates her gratitude to her parents, sisters and brothers, for their understanding, warm support and constant encouragement. Last, but not the least, special recognition must go to her husband, Wen Bin, who has given her tremendous support and inspiration over the years. To whom this work is dedicated.

## TABLE OF CONTENTS

The development of self-compacting concrete (SCC) has offered the best solutions to several of the most obvious needs in the development of concrete construction. However, SCC is a complex mixture containing different constituents; with interactions between these various materials which can cause wide variations in workability and even give negative results from the expected properties. Determining workability and other desired properties of SCC by testing concrete at site is not always an option due to high cost. The estimation of workability of SCC in terms of rheological parameters will promote both systemization and automation of concrete construction work.

The main objective of this research is to develop a model to predict the workability of SCC by predicting the rheological properties (especially yield stress and plastic viscosity) of self-compacting concrete from the properties of its mix constituents. From the estimation of workability of SCC in terms of rheological parameters, the mix design method of SCC for tropical areas will be proposed and the suitability of proposed mix design will be verified by conducting the trial mixes under laboratory conditions and batching plant conditions.

The study is focused firstly on the developing the rheological model on paste fraction of SCC. Secondly, the rheology study extends from paste to mortar and then to concrete. The key factors affecting the rheology from paste to concrete are determined experimentally. In order to study the basic parameters and influencing key factors, such as particle concentration, size distribution, particle geometrical shape and degree of particle flocculation, a series of parametric studies and rheological tests have been proposed. The inter-dependency between mix constituents and rheological parameters is presented as analytical models with the unknown factors in the

relationship determined from the experimental data. The levels and accuracy of analytical models will then be confirmed with the combination of different mix constituents and varying mix proportions.

It was found that the properties of Self-compacting concrete in the fresh and hardened stages are mainly affected by physical and chemical properties of its mix constituents. In paste fraction of SCC, the major controlling factors of paste rheology are both chemical (reactivity) and physical (shape and surface texture) effects of powder used. However, it was found that in rheology of mortar fractions, the physical effects (physical shape and size) contributed from fine aggregate influenced the rheological behavior more than the reactivity of the powder. Similar phenomenon was found also in concrete rheology, as the size range of particle became wider compared to the paste fraction. The flow diameter or flowability of SCC has a close relation with yield stress while the resistance to segregation of SCC is determined by plastic viscosity. According to the verification results, it seems that the proposed rheological model is suitable to predict the yield stress and plastic viscosity of SCC with satisfactory accuracy ($R^2$ = 0.84 and 0.82 respectively).

With the understanding of the factors on rheology of SCC, it is possible to predict the workability of SCC from its paste fraction by combining the additional physical effect contributed from aggregate. A series of concrete mixes which are designed according to the proposed mix design method fulfill the desired fresh properties of SCC as well as desired strength development in the hardened stage. Thus, the proposed model has a potential to optimize the mix proportions of SCC during the actual production process.

## LIST OF NOTATIONS

| | |
|---|---|
| SCC | Self-Compacting Concrete |
| $f_c$ | strength of the hardened concrete |
| *K1, K2* | empirical constant |
| *w/c* | water to cement ratio |
| *SP* | superplasticizer |
| $\tau$ | shear stress (Pa) |
| $\tau_0$ | yield stress (Pa) |
| $\gamma^\circ$ | shear rate or strain rate ($s^{-1}$) = $d\gamma/dt$ |
| $\eta$ | viscosity (Pa.s) |
| $F$ | shear force (N) |
| $A$ | area of plane parallel to force ($m^2$) |
| $\eta_c$ | viscosity of fluid phase |
| $k$ | shape factor of suspended particles |
| $\phi$ | solid volume concentration of suspension system |
| $T_p$ | thickness of paste on the surface of aggregate |
| $P_e$ | volume of excess paste |
| $S_{all}$ | total surface area of aggregate |
| $V_p$ | total volume of paste |
| $P_c$ | volume of paste to fill the voids between the compacted aggregates |
| $\boldsymbol{V_{SP}}$ | volume of suspended particles ($m^3$) |
| $\boldsymbol{V_{SM}}$ | volume of suspending medium ($m^3$) |
| $\boldsymbol{V_v}$ | volume of voids ($m^3$) |
| $\boldsymbol{T_W}$ | thickness of water film around the powder particles (um) |
| $\boldsymbol{V_W}$ | volume of water ($m^3$) |

## LIST OF NOTATIONS

| | |
|---|---|
| $\boldsymbol{V_V}$ | volume of voids in the compacted powder ($m^3$) |
| $\boldsymbol{S_{SP}}$ | total surface area of cement and filler ($m^2$) |
| $\boldsymbol{V_{SP}}$ | total volume of cement and filler ($m^3$) |
| $\tau_p$ | yield stress of paste |
| $\eta_p$ | plastic viscosity of paste |
| $\eta_0$ | plastic viscosity of suspending medium |
| $1/\psi_{Li}$ | angularity factor of individual suspended particle i, |
| $d_{0i}^{v}$ | diameter of the sphere of the same volume as irregular particle |
| $. d_{0i}^{s}$ | diameter of the sphere of the same surface area as irregular particle |
| $1/\psi_{LR}$ | average angularity factor of suspended particle group in the system |
| $S_{SPi}$ | specific surface area ($m^2/m^3$) of individual suspended particle i |
| $V_{SPi}$ | volume ($m^3$) of individual suspended particle i |
| $d_{max}$ | maximum size of different type of powder in the particle group |
| $d_{min}$ | minimum size of different type of powder in the particle group |
| $\delta_i$ | reactivity factor of individual suspended particle i. |
| $\delta_R$ | average reactivity factor of suspended particle group |
| $\alpha_i$ | repulsion factor of individual suspended particle i. |
| $\alpha_{rep}$ | average repulsion factor of suspended particle group |
| $D_{sp}$ | dosage of superplasticizer in the system in percentage of solid volume |
| $\tau_m$ | yield stress of mortar |
| $\eta_m$ | plastic viscosity of mortar |
| $G_s$ | solid volume percentage of sand (%) |
| $V_s$ | volume ratio of sand with respect to total volume of mortar |

## LIST OF NOTATIONS

| | |
|---|---|
| $\sigma_s$ | specific surface area of sand |
| $\in$ | void content (%) |
| $SM$ | surface modulus |
| $p_i$ | weight fraction of individual group |
| $\tau_c$ | yield stress of concrete |
| $\eta_c$ | plastic viscosity of concrete |
| $T_m$ | thickness of excess mortar |
| $G_g$ | solid volume percentage of coarse aggregate (%) |
| $V_g$ | volume ratio of aggregate with respect to total volume of concrete |
| $\sigma_g$ | specific surface area of aggregate. |
| OPC | Ordinary Portland cement |
| LS | Limestone powder |
| GR | Granite crusher dust (Granite powder) |
| GGBS | Ground granulated blast furnace slag |
| CY | Cyclone Slag |
| DC | Dust Collector Slag |
| $T_{50}$ | Time recorded for the concrete diameter to reach 500 mm in Slump Test |
| $T_{final}$ | Time recorded for the flow completely stopped in Slump Test |
| $D_{final}$ | The average flow diameter of final flow, D1 & D2 |
| $Rc$ | Relative funnel speed |
| $T_{200}$ | Time for the flow reached to 200 mm in L Box Test |
| $T_{500}$ | Time for the flow reached to 500 mm in L Box Test |
| $H_{br}$ | Blocking ratio, H2/H1 |
| $V_{pw}$ | Paste volume in the mix |
| $Vg_{min}$ | Void content of compacted coarse aggregate |

## LIST OF NOTATIONS

| | |
|---|---|
| $Vs_{min}$ | Void content of compacted sand |
| $Nga$ | Coarse to total aggregate ratios |
| $Nga_{min}$ | Coarse-total aggregate ratio which gives the minimum void content in aggregate binary mixture |
| $V_{min}$ | Minimum void content in aggregate binary mixture |
| $D_{ss}$ | Average distance between the aggregate particles |
| $D_{av}$ | Average diameter of aggregate |
| $M_i$ | Percentage of retaining on the corresponding sieve of aggregate group i |
| $Nb$ | Blocking aggregate ratio |
| $Dc$ | Reinforcement clear spacing |
| $Vai$ | Volume of aggregate group i |
| $Vbi$ | Blocking volume of aggregate i |
| $Vgm$ | Volume of coarse aggregate group m |
| $Vbgm$ | Blocking volume of coarse aggregate group |
| $Vsn$ | Volume of fine aggregate group n |
| $Vbsn$ | Blocking volume of fine aggregate group m |

## LIST OF FIGURES

## LIST OF TABLES

## LIST OF TABLES



.

# CHAPTER 1

# INTRODUCTION

## 1.1 Background

As construction technology advances, concrete structures become more massive and taller than before, requiring high performance in strength and durability of concrete. Increasing structural performance has led to increase in reinforcement volumes and need for closely spaced smaller diameter bars [*RILEM Report 23, 2000*]. Thus, sometimes, there are not enough spaces to use poker vibrators for consolidation process. The operation of the consolidation process with the aid of vibrators will also be restricted when formwork configuration has long inclined components such as inclined columns. Confined and enclosed spaces, very high casting height, long cantilever access area, etc., would also limit the accessibility of workers and the usage of poker vibrators. Moreover, the noise generated from the use of these vibrators would sometimes restrict the working hours for both cast-in-situ and precast concreting processes.

In addition, consolidation process with the use of vibrators requires extra workers at each discharge point to ensure proper compaction, particularly in space congested with reinforcing bars. For example, to cast the raft foundation of a large commercial building, it is required to handle the placement of some 2500 $m^3$ of fresh concrete. Often the crew is mainly made up of semi-skilled and unskilled workers, which results in not only low productivity but also poor works which may lead to "honeycombs" affecting future durability. [*RILEM Report 23, 2000*]. Therefore in recent year, the gradual reduction in the number of skill workers has led to a similar reduction in the quality of concrete structures [*Okamur, et.al, 1999*].

Self-compacting concrete, (herein after refers as SCC), a new composite material, which has the ability to flow under its own weight over a long distance without segregation and to achieve consolidation without the use of vibrators, seems to be one of the solutions to solve all those construction related problems. The use of SCC could potentially reduce the required labors for the above-mentioned operation by more than 50% (Fig. 1.1) *[RILEM, 1999]*.

**Traditional Vibrated Concrete**

**Self-Compacting Concrete**

Fig. 1.1 Comparison of construction site using Traditional Vibrated Concrete and Self-Compacting Concrete *(source photo: Axim Italcementi Group)*

Complete elimination of compaction work gives not only the environmental friendly quiet revolution but also higher productivity with a reduction in manpower and increase in the construction speed. This may then shorten the construction period and save the overall construction cost [*RILEM, 1999, Ho. et. al 2001a,b*]**.**

.

## 1.2 Benefits of Using SCC

As discussed by Ho [*Ho, et. al, 2001c,d,e*], the benefits of using SCC in general construction can be addressed with two important issues, which concern the economic development of the Nation. The first issue deals with the *buildability* in construction and the other relates to ecological *sustainability* through utilization of wastes.

Improved 'buildability' has been the main driver in SCC applications, which could result in a reduced number of workers on site as well as improved productivity and better quality concrete, particularly in areas with congested reinforcement. For example, in the construction of a large LNG tank for the OSAKA Gas Company, and by using some 12,000 $m^3$ of SCC, the number of concrete workers was reduced from 150 to 50. The construction period of the structure shortened from 22 to 18 months *[Nishizaki et. al, 1999]*. Moreover in numerous projects, direct savings in overall cost of between 5 to 15% have been recorded [*Petersson , 2000a*].

*Buildability* will also be improved through the use of SCC by providing safer working environment throughout the concreting process. There are no cables, transformers and vibration equipments hindering the work during the concreting process. In addition, the use of SCC giving to a silent work place with reduced physical work. For normal concrete, the noise generated from vibrators sometimes would restrict the working hours in the production of both cast-in-situ concrete and precast elements. The 10% reduction in noise level [*Skarendahl, 2000b*] is of particular significance to enclosed spaces in precast factories. Noise due to vibration can exceed 100dB [*Petersson, 2000a*].

*Sustainability* will be enhanced by a holistic approach which takes into account in the design phase, issues such as waste utilization, waste emission and energy consumption, ease of construction, durability and maintenance. The Return on Investment (ROI) is expected to be high considering the size of the industry, annually producing about 12 million cubic meter of concrete. As an example, for a construction cost of $500 per cubic meter finished structural concrete and a targeted market penetration of SCC of 10% p.a. and an 'average' cost saving of 10%, the amount of saving for the industry is some $60 million p.a for the estimated annual volume of 12 million cubic meters.[*Tan et. al, 2001*]. This represents a very attractive ROI of 240 per year or 2400 over 10 years. The ROI would be even higher if indirect benefits such as health and safety, productivity, and social issues from foreign workers are taken into account. These savings would have flow-on effects to the other sectors of the economy [*Ho et al, 2001d,e, 2002a,b*]

For pre-cast manufacturers, the use of SCC offers additional benefits. Instead of elements being cast horizontally in an open form, they can now be produced vertically or in an inclined position with double-sided formwork. Thus, this SCC technology can be of advantage in better use of space in factories, possibilities of automation, better off-form architectural finish on both surfaces, and lower energy and maintenance costs [*Tam et. al, 2002]*

## 1.3 Statement of the Problems

The first prototype of self-compacting concrete (SCC) was introduced in 1988 in Japan [Ozawa *et al* ,1989]. and later exploited in Sweden and other countries around Europe. However, even after 13 years of successful applications and despite its many advantages [*Okamura and Ouchi, 1999, Skarendahl , 2000a*], the adoption and

application of SCC technology in general construction has been slow. According to Okamura during his keynote lecture in Stockholm [*Okamura and Ouchi, 1999*], only about 0.5% of ready-mixed concrete in Japan utilized SCC. The usage is even lower in other countries [*Skarendahl,, 2000a, Petersson, 2000a]*. Such a low usage was mainly due to its substantially high initial supply cost, and partly due to the tight quality control and the semi-empirical prescriptive mix design methods in SCC production. In Sweden, the production of SCC is well established and the cost factor is about 1.2 to 1.4 while in Germany, it is around 1.5 [*Skarendahl., 2001*]. In Singapore, the application of SCC is at its infancy and currently this cost factor is about 1.8 for precast concrete production [*Tan et.al, 2001*] and between 2.0 and 2.5 for ready-mixed concrete [*Doraipandian, 2001*].

To increase the usage of SCC in general construction, it is required to find a way to reduce the high cost of SCC either by replacing the expensive traditionally used fillers, limestone powder, with low cost local materials, or by introducing suitable construction technique such as the application of a sandwich concept in layered construction for raft foundations. [*Ho et al, 2001a,b,c,d*].

Besides the supply cost, a proper mix design is particularly important when such technology is applied and traditional vibrated concrete is replaced with SCC in a tropical environment like Singapore. It is clear that the high temperature and humidity in the tropics tend to alter the rheology of cement paste, thus affecting the cracking potential, morphology and long term performance of the resultant concrete. To ensure the workability requirements in the fresh stage and the strength development in the hardened stage of SCC, the local tropic environment shall be considered in the mix design methods.

There have been several mix-design methods for SCC reported by different researchers based on their locally available materials and environmental conditions as well as local practice. In 1993, Okamura, who is the pioneer of SCC technology, proposed a mix design method [*Okamura and Ouchi,, 1999*]. However, the drawback of his method is that it is applicable to mixes containing a limited range of Japanese materials which are not available in other areas. The Laboratory Central Des Ponts et Chausses (LCPC), the Swedish Cement and Concrete Research Institute (CBI), research group in mainland China and Taiwan all have proposed different mix design methods for SCC. The LCPC's approach is developed on the basis of BTRHEOM Rheometer and RENE LCPC software [*Ferraris and Larrard, 1998*]. It is difficult for others to adopt their method without the equipment and their software. CBI's approach makes use of the relationship between the blocking volume ratio and ratio of clear reinforcement spacing to particle diameter [*Billberg, 1999b*]. However, it is not clear how to carry out the critical tests because concrete mixed with coarse aggregates and paste only is susceptible to severe segregation. Details of such methods will be discussed in Chapter 2.

It must be noted that all the proposed mix design methods are based on their locally available materials, local conditions and practice. It may not be suitable to directly adopt and apply them in a tropical area like Singapore. Thus, it is necessary to develop the proper mix design method suitable for tropical climate, which assures the workability requirements at the fresh stage and strength development at the hardened stage of SCC.

SCC is a complex mixture containing different constituents. Due to its high powder content requirements for minimizing the segregation potential, fine filler materials either inert or reactive powders, will be incorporated into ordinary Portland

cement. Chemical admixtures such as superplasticizer, air-entraining agent, viscosity agent and retarder, are also added to achieve the desired properties. Approximately 50 to 65% of the volume of SCC is occupied by various particle shapes and sizes of coarse and fine aggregate. The interaction between these various constituents will cause wide variation in workability ***[*** *Sedran and Larrard, 1999****]*****.**

The workability or flow characteristic is the most important properties, which contribute mainly to the quality of SCC. The workability or flow properties of SCC need to be well controlled in the fresh stage in order to obtain the quality in the hardened stage. Determining the rheology to ensure the desired properties of SCC by testing concrete is not always an option, particularly on site. Extensive concrete trials require a large amount of materials and labor, which are not cost effective **[***Farrais and Larrard*, *1998***].** There is, therefore, a need to predict the workability or flow properties of SCC through a simpler, theoretical approach. Unlikely, due to the complex interaction of the different constituents in SCC, a definite method has yet to be developed that can predict its desired workability from the properties of its constituents.

An analytical model is needed to be able to predict the flow of SCC from the properties of individual mix constituents. If the effect of constituents on workability is known, the desired properties of SCC can be controlled at the time of production rather than conducting extensive trials. Thus, the cost of SCC can be reduced.

To date, the slump test and the slump-flow spread test are the two common methods used to evaluate the flow properties of ordinary concrete and SCC respectively. However, flow of fresh concrete is in the domain of fluid dynamics that deals with the

mass in motion, namely time-dependent parameters. Using static measurements to predict the dynamic behavior of fresh concrete is disputed. It is generally accepted that the basic properties influencing the performance of fresh concrete in casting and compacting are its rheological behaviors [*Ho et.al, 2002b, 2003*]. The rheology of concrete is described by two parameters of Bingham model, yield stress and plastic viscosity [*Tattersall and Banfill, 1983*]. For SCC, the rheology can be characterized by low yield stress, which corresponds to the minimum shear stress required to initiate the SCC to flow, and moderate viscosity to ensure homogeneous dispersion of solid particles and retention of water as the concrete flows. To predict and ensure the desired rheology behaviors of SCC, many factors shall be taken into consideration. In this research, the factors are as classified below:

- Properties of cement (chemical reactivity and fineness, particle shape and sizes)
- Properties and content of supplementary fine powder (chemical reactivity, fineness, particle shape and size distribution)
- Properties of chemical admixtures (superplasticizer, retarder, air-entraining agent, viscosity enhancing agent)
- Water content
- Properties of fine and coarse aggregates (particle size distribution, specific gravity, surface texture and shape)
- Interaction between different components (reaction between cement and chemical or mineral admixture)

To date, various researchers reported various models which can predict the rheological properties of concrete from its constituents. However, these models are suitable only for

their local conditions and types of materials. Moreover, some of their models required specific software and equipments developed by those researchers. The details of such models will be discussed in Chapter 2. Thus, it is necessary to develop a model which can be useful and applicable in Singapore's local condition.

## 1.4 Objectives and Scopes

As discussed in section 1.3, to resolve the problems encountered in the usage of SCC technology, it is necessary to develop a proper mix design method, which can be applied and implemented in Singapore. To reduce the cost and effort, it is also necessary to develop the rheological model, which can predict the flow properties of SCC without conducting extensive concrete trials.

In order to develop the rheological model to predict the flow properties of SCC, it is helpful to think of concrete as highly concentrated suspension of solid particles (aggregate) in a viscous liquid (paste matrix). These rheological properties of mixtures can then be considered in terms of both the concentration of suspended particles and their properties. It is clear that the changes in the rheology of cement paste affect the rheology of concrete. To achieve the desired properties and workability of SCC, chemical admixture such as superplasticizer or viscosity agent can be added. These materials mainly affect the rheology of cement paste since the aggregate in concrete can be assumed as inert materials suspended in the paste matrix. On the other hand, aggregate physical properties, such as shape, size, and surface area, may only contribute to the rheological parameters of concrete. Therefore, it is possible that, by considering the surface effects of aggregates, a correlation between cement paste and concrete rheology could be determined.

The research will focus firstly on the development of a rheological model on the paste fraction of SCC. Secondly, the investigation could extend the rheology research from paste to mortar and then to concrete. A model of SCC can then be developed, which can be used to predict the desired fresh properties of concrete prior to its production. The mix design method has been proposed from flow properties of SCC, The following are the main objectives of this research, as summarized in Fig 1.2:

1. To investigate the physical characteristics and chemical properties of constituent materials and study their contributions to rheology

2. To develop a model to predict the rheological properties (especially yield stress and plastic viscosity) of the paste fraction of SCC from the properties of constituent materials.

3. To correlate the paste rheology to mortar rheology by introducing the surface effect of fine aggregate and to develop a model to predict mortar rheology

4. To develop a model to predict rheological properties of SCC from its paste fraction and mortar fraction

5. To find the possible relationship between the rheological parameters and the workability from simple physical tests.

6. To propose the mix design procedure for self-compacting concrete which not only achieve the strength requirement but also satisfy the fresh properties such as slump flow, flow retention, blocking and segregation resistance.

By linking the rheology properties of paste, mortar and concrete to their constituent materials, this research is expected to bridge the information gaps of concrete technology.

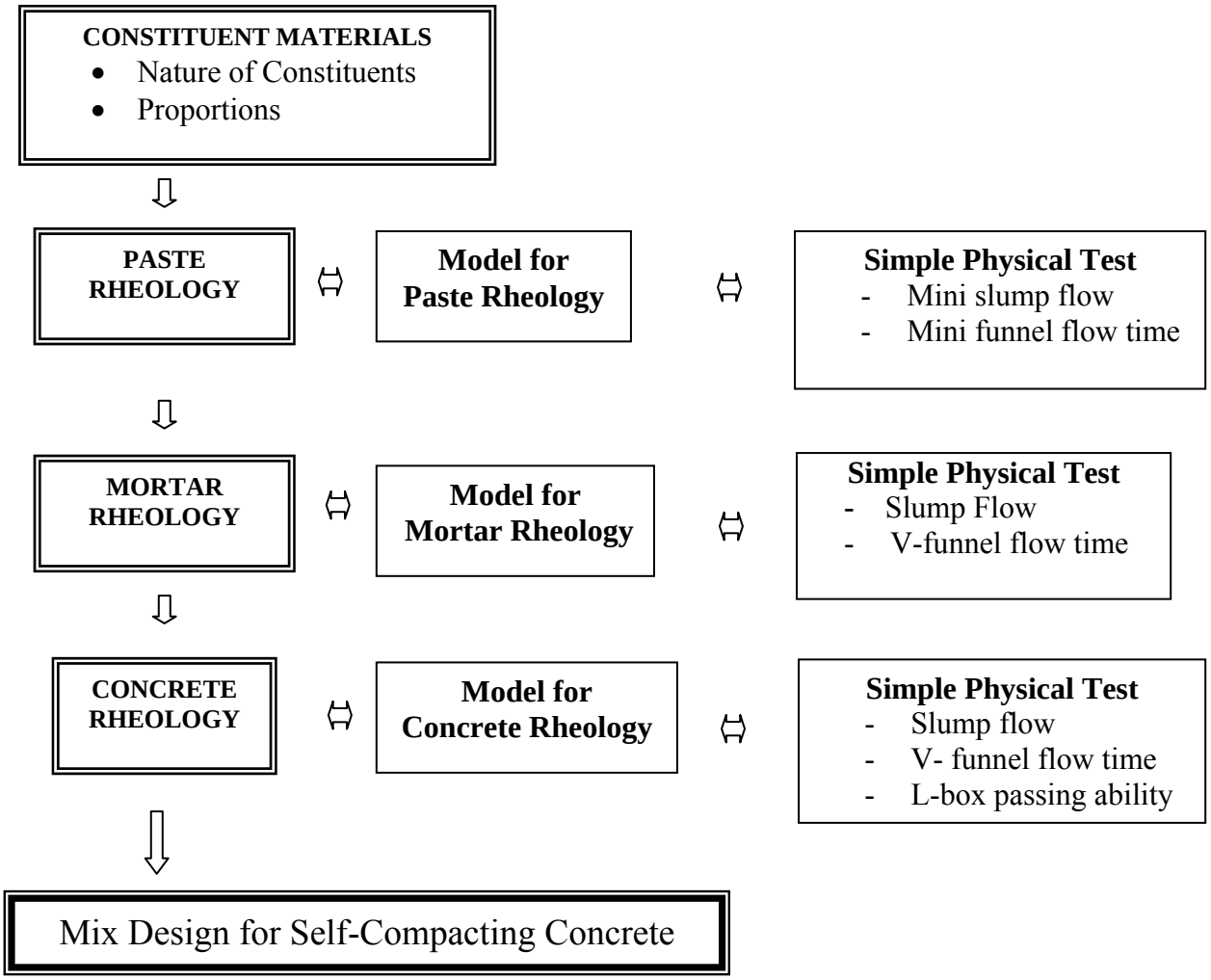


Fig. 1.2 Schematic diagram on objectives of the current research

In order to achieve the main objectives, the following research programs involving laboratory tests together with analytical and theoretical studies were carried out systematically:

- Parametric studies on the physical and chemical properties of constituent materials have been carried out to determine the suitable type of filler powders, which are available locally.
- Rheological data on paste, mortar and concrete were obtained from various mixture compositions to correlate rheological parameters for paste, mortar and concrete.
- Rheological models for paste, mortar and concrete are proposed by linking the mixture composition with rheological parameters from SCC paste, mortar and concrete.
- The possible correlation between the rheological parameters with the flow results from simple physical tests is investigated.
- The mix design method of SCC for tropical areas is proposed and the suitability of the proposed mix design will be verified by conducting trial mixes under laboratory conditions and plant conditions.

With the proposed rheological model and mix design procedure, the concrete engineer could estimate the flow properties of SCC from the properties of its constituents with minimum parametric study instead of conducting extensive trials. The model is useful in enhancing the successful application of SCC in the local construction industry.

# CHAPTER 2

# LITERATURE REVIEW

## 2.1 Mechanism of Self-Compacting Concrete

Self-Compacting Concrete is a new composite material. There is as yet no internationally well-agreed definition for SCC. EFNARC [*EFNARC, 2002*] defines self-compacting concrete as "*concrete that is able to flow under its own weight and completely filled the formwork, even in the presence of dense reinforcement, without the need of any vibration, whilst maintaining homogeneity*". Therefore to be truly self-compacting, fresh SCC must possess three key physical properties at adequate levels throughout its 'working period' [*Bartos & Grauers, 1999*]. These three key properties are:

1 ***Flowing Ability***: The concrete must be able to flow into and fill all spaces within the formwork under its own weight.

2. ***Passing Ability***: The concrete must be able to flow through all openings such as the spaces between reinforcing bars and within the formwork without blocking.

3. ***Resistance to Segregation***: The concrete must be able to fulfill items 1 & 2 without significant separation of material constituents and its composition remains uniform during flow as well as at rest after placing.

These key physical properties must remain present in SCC for at least ninety minutes, 'working period', after mixing to allow enough time for transportation and

placing. The approach to achieve these properties is shown in Figure 2.1 [*RILEM Report 23, 2000*]. A low coarse aggregate volume reduces the amount of collisions between the aggregate particles, thus providing better passing ability, and a consequent increase in paste volume. In addition, low water/powder ratio and superplasticizer provide both flowing ability and segregation resistance.

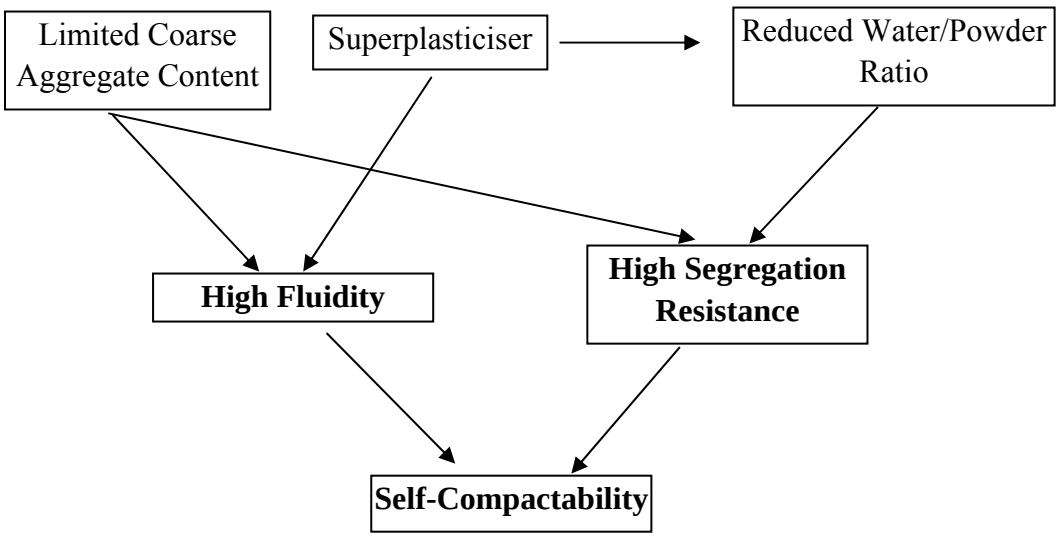


Fig 2.1 General approaches to achieve self-compacting concrete

### 2.1.1 Flowing Ability

In order to achieve adequate flowing ability, SCC mixes must possess a much higher workability than traditional vibrated concrete. The main factor affecting the workability is the water content of the mixture. It is well known that within a certain range, the greater the water/cement ratio, the higher the workability of the concrete mixture. However, the increase in water/cement ratio will tend to decrease the hardened

strength of concrete. Abrams in 1919, devised a rule where he found that the strength of concrete could be approximately calculated by the following equation;

$$f_c = K_1 / K_2^{w/c} \qquad \text{Eq. (2.1)}$$

Where $f_c$ is the strength of the hardened concrete, *w/c* is the water cement ratio of the mix (originally taken by volume), and $K_1$ and $K_2$ are empirical constants [*Neville A.M, 1995*]. Because of this relationship between water /cement ratio and strength, it is not possible to simply increase the water content within the mix in order to increase the workability [*Day K.W, 1995*].

Another important factor affecting the workability of concrete is the characteristics of aggregate and the aggregate/cement ratio of the mixture. A high ratio of surface area to volume of aggregate will increase the water demand for a given workability of the concrete mixture. Angular aggregates also require more water for a given workability [*Neville, A.M., 1995*]. Moreover, the aggregate/cement ratio affects the inter-particle friction between aggregate particles [*Ozawa et al, 1990*]. A higher aggregate/cement ratio will result to a high degree of aggregate interlocking and a stronger inter-particle friction, thus produce a concrete with low workability.

However by introducing plasticisers or superplasticisers in the mix, since the late 1960's, it is possible to produce high workability concrete with relatively low

water/cement ratios without increasing the amount of water. Therefore, SCC makes use of new superplasticiser technology and provides the mix with a high degree of workability to allow it to flow into all spaces within the formwork without segregation. The mechanism of superplasticizer performance will be discussed in the later part of this chapter.

### 2.1.2 Passing Ability

Passing ability is one of the important properties of fresh SCC and it is affected by various factors. Noguchi [*Noguchi T et.al.,1999*] summarized them:

***1) Size and characteristics of aggregate***

It is clear that the passing ability of the mixture composed of small size and round shaped aggregates are better than the mixture composed of big size and crushed aggregates.

**2)** ***Ratio between aggregate diameter and the clear spacing between reinforcing bar***

The lower the ratio of aggregate diameter to clear spacing between reinforcing bars, the better the passing ability. For the same aggregate diameter, the smaller clear spacing between reinforcing bars increases the possibility of higher formation of aggregate arching, resulting in poor passing ability of the mixture.

### *3) Volume of aggregate*

Higher aggregate volume within a SCC mixture leads to a higher risk for aggregate to collide with each other and increases the inter-particle friction, there by reducing the passing ability.

### 4) *Properties of paste and boundary conditions.*

Tangtermsirikul [*Tangtermsirikul, 1998*] reported that to avoid blocking (poor passing ability), the size and amount of large solid particles in SCC must be optimal and compatible with the clear spacing between the reinforcing bars through which the concrete can flow. He also illustrated that the mechanism of blocking could be clearly explained by using a two dimensional illustrative model of concrete flowing through an opening (Fig. 2.2).

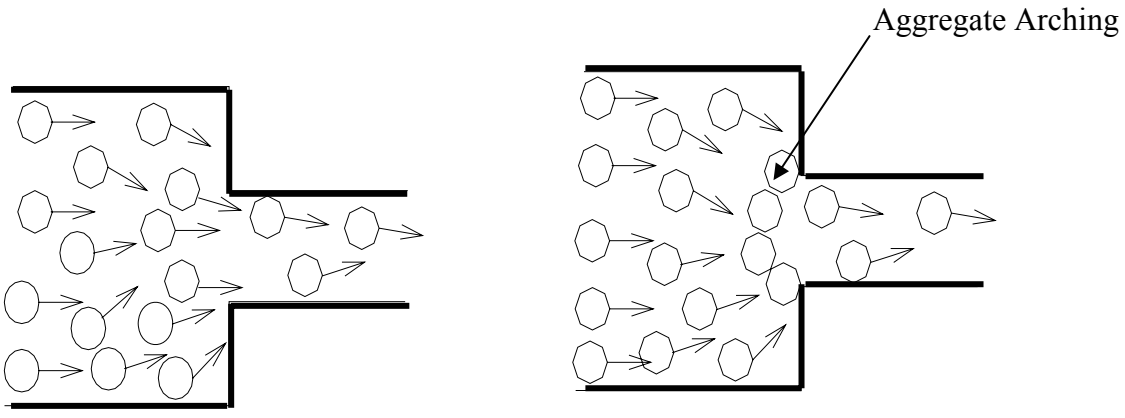


Fig 2.2 Mechanism of Particle Blockage [*Tangtermsirikul, 1998*]

To be able to flow through the opening, the coarse aggregate particles have to change their flow path while approaching the opening [Figure.2.2a]. As a result, collisions between the coarse aggregate particles occurred, creating a high level of contact among them at the opening. As a consequence of these collisions, there is a strong likelihood that some particles would form a stable arch which then blocked the flow of the remaining concrete [Figure.2.2b].

Such blockages are more likely to occur when the size of coarse aggregate is large and its content is high. The diameter of the reinforcing bars around which concrete flows also influences the passing ability of the SCC. When using SCC with a specific maximum size and content of aggregate, the use of a large diameter bar will be more susceptible to blocking, even though the clear spacing between the bars is the same. This is due to the fact that the larger diameter of reinforcing bar provided a more stable support for the arching of coarse aggregate.

Tam et.al [*Tam C.T .et.al, 2005*] developed the modified J-ring approach to assess the passing ability of SCC. The diameter of the modified J-ring was 500 mm instead of 300 mm in the standard J-ring. By varying the diameter of reinforcing bars of 10, 20 and 40 mm and selecting the number of bars used in the ring from 4 to 24 together with the different size of bars, the clear spacing between the bars can be varied from around 20 to 300 mm. The passing ability of SCC is assessed by the ratio of the flow diameter with the ring in position to that of a standard slump flow test as the Passing Ability Index. This is

an indication of the reduction in flow due to the presence of the selected configuration of bars.

Ozawa [*Ozwa et al, 1990*] reported that once the coarse aggregate arch had formed and caused a blockage, only mortar was able to flow through the spaces between the coarse particles. However, the fine aggregate within the mortar could also then cause blockages within the spaces between the coarse aggregate particles, resulting in a situation where only paste or water was able to pass through. This is the case for severe blockage.

Domone [*Domone, 1999*], reported that in order to minimize the collision between the coarse aggregate particles as they flowed through the narrow openings between steel reinforcement, and to avoid blocking, the mortar content within SCC should be higher than that of traditional vibrated concretes. This high volume of mortar helped to lubricate the coarse aggregate particles and acted as a cushion to prevent them from collision as their flow path altered from wide to narrow.

Increasing the fine components of the mix, but normally not cement, at the expense of the coarse aggregate, provides higher mortar content. Such increments of fine fillers will increase the paste content, and subsequently the mortar content, which also has an effect on segregation resistance and will be discussed further in the next section of this chapter.

### 2.1.3. Resistance to Segregation

For hardened concrete to attain maximum performance, it should have an even distribution of constituent materials, especially the coarse aggregates. However, SCC requires a high degree of flowing ability, i.e., it is more like a liquid than conventional concrete mixes. In order to achieve this fluidity, there must be a high degree of free movement among the particles within the concrete. It is obvious that to attain this free movement, there must have enough free water within the mix. Unfortunately, the viscosity and density of cement paste changes with the water content. Once the amount of water is increased, the viscosity and density will be reduced subsequently [*Bartos, 1992*]. This can be explained in simplified terms as 'a thickened paste being diluted through the introduction of water'.

Betancourt [*Betancourt, 1988*] considered segregation of fresh concrete as a phenomenon related to viscosity and density of the cement paste i.e. when the density of solid is higher than that of liquid, the solid particle tends to sink inside the liquid. Due to the increase in free water in the mix, the viscosity of cement paste is reduced and subsequent reduction in density. Once the density of overall paste is lower than the density of aggregate, it is unable to hold the aggregate particle, which then sink down or separate from the mix. This phenomenon is usually known as "Segregation"

Segregation resistance in SCC is primarily achieved by increasing the amount of inert powder material in the mix– but not the cement content. These powders help to

'thicken' the paste and provide an increase in viscosity and density. In terms of resistance to segregation, the thickened paste enables the aggregate particles to be uniformly suspended within the mortar. These mineral powders, as explained in the previous section of this chapter, also help to provide the concrete with better passing ability.

Besides the addition of powder materials, chemical viscosity agents (not used in this study) are sometimes incorporated into the mix. Chemical viscosity agents increase the water phase viscosity of the paste by means of a reaction with the water [*Ozawa et al, 1990*]. The use of these agents, also known as thickeners or stabilisers, has been shown to make mixes less sensitive to small changes in the amount of free water, and to provide consistency between batches, that is sometimes difficult to achieve using mineral powders on their own. However, viscosity modifying agents can be costly.

## 2.2 Specific Tests for Physical Properties of SCC

Different test apparatus and methods have been proposed by various researchers to assess the same or different requirements. The commonly used tests and apparatus in practice and their suggested acceptance limits for SCC are summarized in Table 2.1. [*Domone P.L.J., 2000*] It should be noted that they are intended as guidance and do not necessarily guarantee satisfactory performance in all situations.

Table 2.1 – Tests and Suggested Limits

| Test | Properties | Suggested Limits |
|---|---|---|
| **Slump Flow** | - Flowability<br>- Filling ability<br>- Segregation resistance | - Diameter > 650mm, $T_{50}$ < 12 seconds<br>- 3 to 5 seconds preferred<br>- By visual assessment |
| **L-Box** | - Filling ability<br>- Passing ability<br>- Segregation resistance | - T20 (2-3s), T40 (4-6s) and Tf (10-12s)<br>- Blocking ratio ≥ 0.75- 0.85<br>- By visual assessment |
| **U-Box** | - Filling ability<br>- Passing ability | - Filling height > 300mm<br>- Flow time: 10 to 20 seconds |
| **V-Funnel** | - Passing ability<br><br><br><br>- Segregation resistance | - Flow time: 2 to 10 seconds<br>(lower end of range for first light)<br>(upper end of range for fully empty)<br>- By visual assessment |
| **Surface Settlement** | - Segregation resistance | - Surface settlement < 0.50% |
| **Penetration Test** | - Segregation resistance | - Penetration depth < 8mm |
| **Segregation Test** | - Segregation resistance | - Segregation coefficient < 7% for 700mm column (in hardened concrete) |

## 2.3 Mix Constituents and Mix Proportions

The constituent materials used in SCC are basically the same as those used in traditional vibrated concrete. Similar to traditional vibrated concrete, SCC can be manufactured with materials from a wide variety of sources – i.e., there is no fixed mix design for SCC. Traditional vibrated concrete mixture generally consists of cement, fine aggregate, coarse aggregate, water and often chemical admixtures. SCC as mentioned includes superplasticiser and fine mineral powders. Table 2.2 presents a comparison of

mix proportion in terms of volume percentage for typical traditional vibrated concrete and SCC of a similar grade.

Table 2.2 Traditional vibrated concrete & SCC mix- proportions (% Volume) [*Sonebi et.al, 1999*]

| **Traditional Vibrated Concrete** | | **Self-Compacting Concrete** | |
|---|---|---|---|
| Cement | 10% | Cement + Fine Powder | 18% |
| Fine Aggregate | 33% | Fine Aggregate | 34% |
| Coarse Aggregate | 37% | Coarse Aggregate | 28% |
| Water | 20% | Water + Superplasticiser | 20% |

As mentioned earlier, any mix proportion for SCC must satisfy three key criteria: flowing ability, passing ability and segregation resistance. The most common method of mix design to satisfy these criteria is the "General Method" developed by various researchers at the University of Tokyo [*Ho D W S et.al, 2001a, Trägårdh J., 1999*]. Since then, many attempts have been made to modify this method to suit local conditions [*Domone, P.L.J., 2000*]

Experiences in Japan and Europe showed that there are wide variations of materials and proportions that can be used to produce satisfactory SCC, with certain key factors falling within certain limits. Ho [*Ho et al, 2001b*] presented some typical range of mix constituents commonly adopted for Singapore as shown in Table 2.3. In achieving economical mixes, the powder content should be kept to a minimum for technical and

economical reasons. The upper limit of water content should only be used if viscosity modifying agent is incorporated.

Table 2.3 Range of Mix Constituents

| **Constituents** | **By volume** | **By weight (kg/m$^3$)** |
|---|---|---|
| Coarse aggregate | 30 - 34% of concrete volume (32%) | 750 - 920 |
| Fine aggregate | 40 - 50% of mortar volume (47%) | 710 - 900 |
| Powder | - | 450 - 600 (500) |
| Water | 150 - 200 $\ell$/m$^3$ of concrete (180 $\ell$/m$^3$) | 150 - 200 |
| Paste | 34 - 40% of concrete volume (35%) | - |

To satisfy the deformability requirements, the maximum size aggregate is generally limited to 25mm. The amount of coarse aggregates also needs to be reduced, as they take up a lot of energy in moving them. Reduction in the coarse aggregate content is balanced by the increase in paste volume, which has the effect of increasing the aggregate inter-particle distance, thereby reducing the possibility of contact and lowering the aggregate-aggregate friction. It is important to realize that the amount of aggregate reduction has to be balanced with structural requirements as coarse aggregates serve a very useful purpose in controlling creep and shrinkage as well as stiffness and ductility of the hardened concrete.

Superplasticiser (SP) is needed to lower the water demand while achieving high fluidity. It is a surface-active agent causing dispersion and reducing the friction among powder materials. The common SP used is a new generation type based on

polycarboxylated polyether. In Singapore, this SP is considerably more expensive than the traditional SP used in normal concrete. This is one of the high cost items in SCC production.

For SCC to have a high segregation resistance, high powder content is often required. Powder generally refers to particles of cement and fillers with sizes less than 125 μm [*Skarendahl Å, 2000c*]. The content ranges from 450 to 600 kg/m$^3$ of concrete. Thus, SCC usually incorporates some 200 kg/m$^3$ of fillers. In Singapore, the cost of the conventional filler, limestone powder, is as high as Portland cement. Besides limestone powder, other inert or cementitious fillers can also be used. Viscosity modifying agent is sometimes incorporated to minimize the addition of expensive fillers. This admixture is similar to that used in under-water concreting. It increases the viscosity of water, therefore increasing segregation resistance.

It is obvious from the above that viscosity plays a vital role in the performance of SCC. On one hand, a lower viscosity is needed so that the concrete can deform and flow easily at a reasonable rate. However, in spite of this, SCC requires a sufficiently high viscosity to avoid segregation. The balance between these conflicting requirements becomes the art and science of SCC mix proportioning. To achieve this balance, it is important to have a fundamental understanding of the rheology of fresh concrete.

## 2.4 Rheological Properties

Rheology, defined as the science of deformation and flow [*Barnes et.al, 1989*], has been an area of serious concrete research since the 1970's [*Marrs, 1998*]. Fresh concrete can be described as a particle suspension. The rheological properties of fresh concrete are rather complex and can be time dependent due to cement hydration. In this approach, fresh concrete could be considered as coarse aggregates suspended in a liquid mortar phase, or sand particles in liquid paste. Thus the evaluation of the paste and mortar would yield useful information in the optimization of mix proportions of self-compacting concrete.

Tattersall [*Tattersall, 1991*] has proposed flow properties of concrete to be represented by the Bingham model. The two characteristic Bingham parameters are the yield stress and the plastic viscosity as shown in Figure 2.3. These are mathematical constants determined from experiments using a viscometer rather than physical properties of concrete.

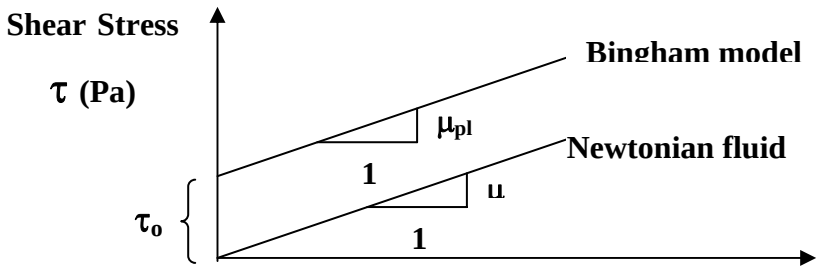


Fig 2.3 Bingham Rheology Model

According to this Bingham model (Fig.2.3), fresh concrete must overcome a limiting stress (yield stress, τo) before it can flow. Once the concrete starts to flow, shear stress increases linearly with increases in strain rate as defined by plastic viscosity, μ. Thus, one target rheological property of SCC is to reduce the yield stress to as low as possible so that it behaves like a Newtonian fluid with zero yield stress. The other target property is 'adequate' viscosity to hold all the constituents evenly.

The use of Bingham parameters is helpful in describing the behavior of fresh concrete and in understanding the influence of various mix constituents. However, there is no consensus, at least at this stage, on their limiting values appropriate for SCC. Suggested values from the use of different viscometers by various researchers [*Domone, 2000*] are presented in Table 2.4.

Table 2.4 Suggested Bingham Constants for SCC

| Equipment (source) | Yield stress (Pa) | Plastic viscosity (Pa.s) |
|---|---|---|
| BTRHEOM (France) | < 400 | < 200 |
| BML (Iceland) | < 80 | 20 – 30 |
| BML (Sweden) | < 12 | 150 - 250 |

It is obvious that appropriate Bingham rheological values depend on the materials and equipments used. Thus, to get reliable values of rheological parameters for SCC, it is important to specify the type of equipment, testing procedure and the nature of constituent materials used for the mix.

Besides the linear Bingham model, a more sophisticated Hershel-Bulkley model has been suggested with the relation between shear stress, $\tau$, and strain rate, $\gamma$, being non-linear and taking the following form;

$$\tau = \tau_o + a.\gamma^b$$

where $\tau_o$ = yield stress

a = viscosity term

b = constant.

The constant, b, can be greater or less than unity depending on whether the fluid is characterized by shear thickening or thinning. The situation is even more complicated if the fluid exhibits thixotropic behaviour.

## 2.5 Effect of Constituent Materials on Rheology of SCC

SCC is a complex composite containing different constituent of various types and contents. Those constituent materials can be generally classified into three major components:

i) Fine Powder Materials;

ii) Water Content and Superplasticizer

iii) Fine and Coarse Aggregate

This section discusses the effect and influence of those individual components on rheological properties of SCC.

### 2.5.1 Fine Powder Materials

The fine powder part of SCC consists of ordinary Portland Cement (OPC) and fillers, which can either be inert or reactive. Powder generally refers to particles of cement and fillers with sizes less than 125 μm [*Skarendahl, 2000c*].

- **Content of Fine Powder**

SCC has the ability to flow into every corner of formwork by its self-weight without the need of vibrating and compacting **[***Ozawa et. al., 1989***].** Therefore, it is important to keep its stability in order to avoid segregation. In other words, SCC should possess low yield stress to achieve better flow ability and sufficient viscosity to maintain its stability. There are two methods to keep stability at the same time achieving flowability of SCC. Adding viscosity modifying agent will increase water phase viscosity as well as yield stress, which mainly determine the flow. The other method is to increase the solid fraction of the paste phase of concrete, thereby increasing viscosity of paste phase **[***Billberg, 1999a***].**

SCC generally has higher powder content than normal concrete of a similar grade. RILEM technical committee recommended that the total powder content of somewhere between 450 to 600 kg/m$^3$ is suitable to produce SCC with desired fresh state properties **[***RILEM Report 23, 2000***].** Thermal cracking is usually the problem that arises if a large amount of heat is evolved during cement hydration when high cement content is used especially in casting massive concrete structures. This problem is a major concern for

concreting in the tropics, such as Singapore. Therefore, the use of inert fine filler as part of the powder content is essential in SCC production, not only for economic purpose but also for technical reasons. Poppe and group [*Poppe A.M, et.al, 2005*] studied the heat development during the hydration process in SCC and found that SCC generates heat more or less similar to normal concrete of similar strength range due to the incorporation of inert filler to achieve powder content in SCC.

- **Particle Fineness of Powder**

It is important to recognize that both yield stress and viscosity are dependent on particle fineness of filler. The finer the added filler, the higher both measured yield stress and plastic viscosity **[***Zhang et al., 2000, Christensen B.J. et al, 2005***].** For similar mass, the specific surface area of the materials increases by increasing the particle fineness. The greater the surface area, the more water is needed to envelope the total particle surface and subsequently there is less moveable water in the water-cement system (matrix system), which in turn leads to higher resistance when the system is sheared.

- **Particle Shape and Surface Texture of Powder**

The surface roughness and angularity of fine particles as well as their reactivity in the matrix system are other important parameters that affect rheological properties. It was observed that SCC incorporated with flaky and elongated shape granite fine powder required a higher dosage of superplasticizer than that of cubical shape limestone filler in order to have similar yield stress **[***Ho et al., 2001a***].** The rounded particle shape of fly ash

as replacement of cement at 30% resulted in excellent workability and flowability of SCC **[***Kim et al., 1996***].**

- **Chemical Reactivity of Powder**

Besides traditional filler, limestone powder, mineral admixtures **[***Nishibayashi et al., 1996, Ozawa et. al., 1989, Billberg, 1999***]** as well as rock dust **[***Ho et al., 2001a***]** and metal slag fines **[***Shoya et al., 1999***]** were successfully utilized. As in research conducted by Yahia et al. **[***Yahia et al., 1999***]** the same yield stress, use of silica fume in combination with superplasticizer can reduce the viscosity of the paste by 30% compared to the paste containing Portland cement alone with superplasticizer. The use of fly ash and blast furnace slag in SCC reduces the dosage of superplasticizer needed to obtain similar slump flow compared to concrete made with Portland cement alone. Also the use of fly ash improves rheological properties and reduces the cracking of concrete due to lower heat evolved during cement hydration **[***Kurita et. al.,* 1999**].** High slag cement is expected to provide similar lowering of heat evolved. However, the uses of these mineral admixtures reduce the early strength of concrete and this issue must be checked for specific applications [*Zukoski, et.al, 1993, Jiang W. et.al, 1992, Ho et al, 2003, 2004*]

## 2.5.2 Water Content and Superplasticizer

- **Effect of Water Content**

The addition of water reduces both the yield stress and viscosity. However, too much water can reduce the viscosity to such an extent that segregation occurs. As

mentioned earlier, segregation resistance between water and solid particles can be increased by increasing the viscosity of water through the incorporation of viscosity agents. Note that it is the 'movable' water that controls the segregation resistance and flow properties of fresh concrete. Moveable water is defined as the water in the mix, which is not absorbed into, nor adsorbed onto the surface of solid particles.

- **Effect of Superplasticizer**

Superplasticisers are water-soluble polymers which have to be synthesised, using a complex polymerisation process to produce long molecules of high molecular mass. The main action of these long molecules is to wrap themselves around the individual cement / powder particles to give them a highly negative charge in order that they can repel each other [*Neville, 1995*]. These result in deflocculation and dispersion of cement / powder particles, which releases the trapped water and increases the free water within the mix, producing a material which makes more efficient use of the water to provide a higher workability fresh concrete. Superplasticizers developed especially for use in SCC make use of steric hindrance to prevent the particles from refloccating in order to enhance the length of time or flow retention time after mixing so that the concrete can retain its high level of flowing ability. The amount of superplasticizer which can be adsorbed on to the surface of the cement / powder particles is limited by their surface area. Excessive dosage rates therefore do not cause proportionally higher workability [*Bartos, 1992*].

Generally, up to the point where the surface area of the powder material is completely coated, the greater the dosage of superplasticiser, the greater the flowing

ability of the concrete. However as reported by Ozawa [*Ozawa et al., 1990*], there must be an upper limit for the dosage of superplasticizer – if the dosage of superplasticizer is higher than the required dosage, there was excessive free water within a mix, this could be expelled from the material by normal forces, resulting in a high degree of interparticle friction amongst the solid elements of the mix. This will lead to severe segregations [*Schober I. et.al, 2005*]

The incorporation of SP reduces the yield stress but causes limited reduction in plastic viscosity. Ho. [*Ho W.S.D et. al 2001 a*] reported the effect of SP on Bingham constants in Table 2.5. The water-to-powder ratio of these pastes was maintained at 0.36 with various combinations of Portland cement and limestone. The dosage of SP was expressed as a percentage of the total powder content. As indicated, yield stress decreased drastically as the SP dosage was increased. However, the effect on plastic viscosity was relatively small.

Table 2.5 Bingham Constants for Pastes with W/P of 0.36 by weight

| Powder (%) | | Superplasticiser | Yield stress | Plastic viscosity |
|---|---|---|---|---|
| Cement | Limestone | (%) | (Pa) | (Pa.s) |
| 65 | 35 | 0.10 | 33.4 | 0.26 |
| | | 0.20 | 10.8 | 0.21 |
| | | 0.30 | 1.4 | 0.17 |
| 55 | 45 | 0.10 | 23.3 | 0.22 |
| | | 0.20 | 10.2 | 0.21 |
| | | 0.30 | 4.3 | 0.19 |
| 45 | 55 | 0.10 | 12.8 | 0.20 |
| | | 0.15 | 6.3 | 0.18 |
| | | 0.20 | 2.6 | 0.16 |

The role of superplasticizer in concrete is not only to achieve the dispersion efficiency but also to maintain important properties of SCC such as low slump loss, compatibility with other chemical admixtures such as viscosity modifying agents as well as air-entraining agents and retarders. The dosage is kept as low as possible for economic purpose. As expected, the rheology properties of SCC vary largely with the chemical admixture used. One of the variables that sometimes affect the rheological properties of SCC is an incompatible interaction between cement and superplasticizer used. The incompatibility between cement and admixture is judged by the interaction on whether the expected rheological properties of concrete are obtained by using a particular cement together with recommended dosage of the chemical admixture for SCC [*Agarwal S.K. et.al, 2000, Banfill, P.F.G., 1983, Ambroise J et.al, 1999*].

- **Suitability of Polycarboxylic Acid Base Admixture**

Polycarboxylic acid based admixture is a new generation non-ionic surface-active agent with zeta potential. The side chains of polyethylene oxide (EO) extending onto the surface of cement particles provide a high dispersibility and ease for contact with water. Hanehara **[***Hanehara et.al, 1999***]** investigated the interaction between cement with commercially available naphthalene and melamine based superplasticizer together with the polycarboxylate admixture from the viewpoint of cement hydration and paste rheology. It was found that the fluidization mechanism of cement varied with the type of admixture. Polycarboxylic acid based admixture gave the required fluidity by adding,

dosage based on total powder content, as little as 0.2% by weight of powder. Meanwhile, the cement paste prepared by using naphthalene sulfonic and melamine-based admixture had hardly changed its fluidity by adding up to 0.8% by weight of the total powder content.

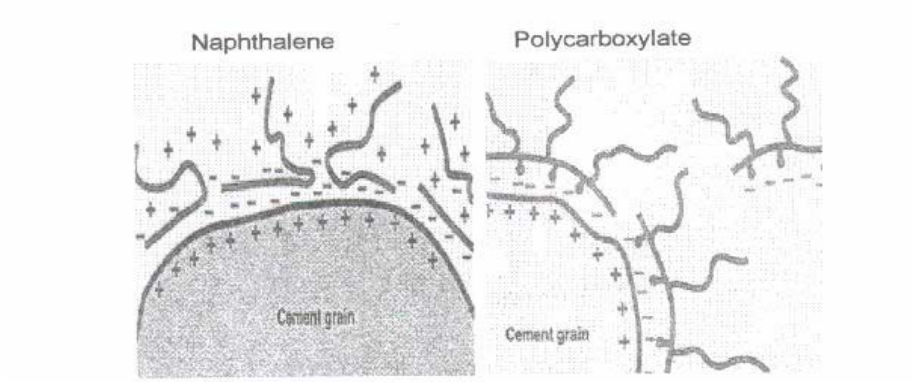


Fig. 2.4 Different repulsive actions between ordinary superplasticizer and polycarboxylic acid based admixture **[***Hanehara et.al, 1999***]**

Agarwal **[***Agarwal et.al, 2000***]** studied the compatibility of superplasticizer with different cements in terms of setting behavior and compressive strength. They found that the use of polycarboxylate type admixture increased the compressive strength of approximately 20% together with water reduction of up to 18%.

The interaction problem of polycarboxylic acid-based admixture is a phenomenon in that the amount of the chemical admixture added to cement paste varies largely according to the type of cement. Since this type of chemical admixture is meant to be used for concrete with low water to cement ratio, a slight difference in dosage of chemical admixture changes the fluidity of the system remarkably.

Yamaguchi **[***Yamaguchi et.al,1995***]** analyzed the relationship between the characteristic of cement and its rheological properties in combinations of the polycarboxylic acid-based admixture with 18 types of cement, and found that soluble alkali in cement highly correlates to the fluidity of cement. Matsuhisa **[***Matsuhisa et.al 1998***]** elucidated a detailed analysis of variance in which 80% of the variation of fluidity of cement paste prepared by the use of polycarboxylic acid-based admixture depends upon the content of alkali sulfate, one of the soluble alkalis in cement. They confirmed that the fluidity was lowered by increasing the amount of alkali sulfate in the cement tested. This phenomenon is explained by the indication that EO chains, contained in the chemical admixture as an ingredient with the dispersion action, are shrunk by using cement containing a substantial amount of sulfate ions, thereby decreasing the steric repulsion.

### 2.5.3 Fine and Coarse Aggregate

- **Volumetric Ratio of Fine Aggregate (Vs/Vm)**

In SCC, the mortar phase provides lubrication between the coarse aggregate particles and overall stability to concrete. Its required properties are similar to those of concrete itself, i.e. low yield stress to ensure the flow under its self-weight and a plastic viscosity sufficient to ensure that the concrete dose not segregate during flow. However, the high viscosity could cause problems in practice because of its slow flowability. A yield stress value between 20 Pa to 50 Pa and plasticity viscosity between 6 Pas to 12 Pas for mortar have been suggested by Domone **[***Domone, 1999***]** as suitable. To attain the

stable concrete mix with desired flowability, the volume of paste phase plays an important role since SCC usually has lower coarse aggregate content, typically 31 ~35% by volume, than normal mixes. The powder used should be as low as possible; the required solid phase is maintained by the volume fraction of fine aggregate. RILEM **[***RILEM Report 23***,** 2000**]** recommended that the volume of sand to mortar ratio, Vs/Vm should be between 0.4 and 0.5.

- **Volumetric Ratio of Coarse Aggregate (S/A)**

Besides the self-deformability of SCC, passing ability between reinforcing bars is also one of the important performance since it determines the final filling capacity, which influences the strength and durability of the hardened concrete [*Petersson, Ö., 2000b*]. Obviously, the coarse aggregate content is the major factor in determining the passing ability of SCC. As the fresh concrete flow approaching the narrow spaces, i.e., reinforcement and narrow formworks, the paste proceeds faster than the aggregate because of velocity difference caused by obstruction. The aggregate content is considered to increase locally since the new aggregate is fed from behind. For this reason, the relative viscosity (concrete viscosity/paste viscosity) of SCC is expected to become higher than the original value when passing through a narrow space. This effect was demonstrated by *Noguchi* **[***Noguchi et.al, 1999***]**. The increase in volume of aggregate to volume of mortar ratio, Vg/Vm, the V-funnel flow times as well as U-box flow time were increased. At the same time, U-box filling heights were decreased significantly **[***Urano et al., 1999***].**

## 2.6 Existing Rheological Model for SCC

For concrete engineer to design the concrete for specific application or placement method, it is necessary to predict the fresh concrete properties from the proportions of mix constituents. There are numerous tests to characterize the flow of concrete, however few gives results in fundamental units and cannot be directly compared and applied. Recently, new tests or model for characterizing concrete using more fundamental approach have been developed. A model that could predict the rheological parameters, yield stress and plastic viscosity, from the composition or from minimal laboratory tests would be beneficial. To date, various researchers reported the models which can predict the rheological properties of concrete from its constituents. Two promising models for concrete will be reviewed and discussed here; the compressible packing model (CPM) developed by De Larrard and simulation of flow of suspension developed by NIST researchers.

### 2.6.1 Compressible Packing Model (CPM)

This model was developed by De Larrard [*Larrard F.De., 1999*] from the Laboratory Central Des Ponts et Chausses (LCPC) for predicting concrete properties from its compositions. In this model, each component, i , of the mixture was defined by its closed packing density, $\Phi^*_i$, and the volumetric fraction of solid materials, $\Phi_i$. A close packing density was defined as the maximum possible value of $\Phi_i$ *with* all other $\Phi_j$. ($j \neq i$) being constant. With this assumption, the yield stress was calculated by a linear

combination of the ratios of volume fraction, $\Phi_i$, to its closed packing, $\Phi^*_i$, of the components. Therefore, yield stress, $\tau_0$, was defined as :

$$\tau_0 = f\left(\frac{\phi_1}{\phi_1^*}, \frac{\phi_2}{\phi_2^*}, \frac{\phi_3}{\phi_3^*}, \ldots\ldots, \frac{\phi_n}{\phi_n^*}\right)$$

where ***f*** is an increasing function because the yield stress will increase with increasing value of $\Phi i / \Phi^*_i$. In this model, different coefficients were calculated for concrete with and without high-range water reducing admixture (HRWRA).

**For mixtures without HRWRA,** $\tau_0 = \exp(2.537+0.540\ K'_g+0.854\ K'_s+1.134\ K'_c)$

**For mixtures with 1% HRWRA,** $\tau_0 = \exp(2.537+0.540\ K'_g+0.854\ K'_s+0.224\ K'_c)$

In these equations, $\tau_0$ was the yield stress obtained by fitting the rheometer results in accordance with the Herschel-Bulkley model. The indices *g, s* and *c* related to gravel, sand and cement, respectively. $K_x$ is equal to $(1- \Phi_x / \Phi^*_x)$.

For plasticity, the authors assumed that the flow of the fluid between the particles is laminar and that the shear resistance is proportional to the overall gradients. Based on Bingham model, the plastic viscosity was determined from the best fit equation of the rheological parameters measured by using BTRHEOM rheometer and given as.

$$\eta_0 = \exp\left[26.75\left[\left(\frac{\phi}{\phi^*}\right) - 0.7448\right]\right]$$

It is observed in these proposed models, the author used the Herschel-Bulkley model to determine the yield stress while Bingham Model is used to determine the plastic viscosity. This is contradictory and questionable as these two models approach differently in determining yield stress and plastic viscosity. Moreover, all the models are developed from the best fit equations of rheological parameters of the series of mixes which were measured by using BTRHEOM rheometer. It is well documented that different rheometer give different values of yield stress and plastic viscosity for the same concrete [*Ferraris C.F. and Martys N.S , 2003*]. Furthermore, the close packing and the volumetric fraction of each components, $\Phi_x / \Phi^*_x$, were calculated by using CPM [*Ferraris C.F. and Larrard F. de, 1998*]. Since these models are based on best fit equation of the series of mixes made with their locally available materials, their CPM software and BTRHEOM rheometer, it is not possible to directly apply those proposed models without their software and equipments. Therefore, there is a need to develop a model which is suitable for our local condition, materials as well as the available equipments.

### 2.6.2 Simulation of Flow of Suspension

The researchers from National Institute of Standard and Technology (NISC) [*Ferraris, C.F., et.al, 2001*] developed the new method which included simulation of concrete flow. In this method, they tried to link between the mixture design/cement paste rheology to concrete rheology by using the simulation model. The simulation of concrete flow was based on Dissipative Particle Dynamics (DPD), in which cellular automata ideas were blended together with molecular dynamic methods.

In this method, Ferraris and group studied the flow of suspension of spheres of equal radii under shear as a function of solid fraction and shear rate. By applying a constant rate of strain in opposite directions at the top and bottom of the system, they observed the flow behavior of spheres. From computer simulation, they first studied the effective viscosity, $\eta/\eta_0$, as a function of the solid fraction of suspension normalized by maximum random packing, $\Phi/\Phi_0$. Secondly, they examined the effect of varying the distribution of sizes of spheres by replacing 10% of spheres with smaller spheres (about one-sixth of the radius). The effect of particle shape was evaluated as ellipsoids with varying aspect ratios in DPD simulation.

From the data from simulation model, the effective viscosity, $\eta/\eta_0$, or effective yield stress, $\tau/\tau_0$, was plotted against the solid fraction of suspension normalized by maximum random packing, $\Phi/\Phi_0$. The yield stress and plastic viscosity were proposed from these best fit curves as a function of $\Phi/\Phi_0$. They aimed to produce computer software in which the input data such as cement paste rheological parameters, aggregate grading and shape are then output as concrete rheological parameters. In order to produce such software, they used their in-house program called VCCLT (The Virtual Cement and Concrete Testing Laboratory Consortium) which could obtain the relative plastic viscosity of concrete at various concentrations of aggregates if the user input the plastic viscosity of mortar.

However in order to use their model, one need to understand the basic of the DPD simulation model as well as obtain the VCCLT software. Moreover, their model is based

on the gap between the aggregate. Thus, the equipment which required measuring the rheological parameters must have the variable geometry in which the gap can be changed. In addition, they also used the specific hardware to control the shear rate during the mixing for the cement paste in their study to experience a similar shear stress in the concrete. Furthermore, they used special hardware to control the mixing temperature. Without those special equipments and hardware, it is not possible for other concrete researcher to use their procedure or model to investigate the rheological parameters of the SCC.

### 2.6.3 Overview of Existing Models

Besides the two models discussed in the previous section, the literature concerning rheological models linking mixture composition and viscosity of suspensions were examined and it was found that most authors [*Hu . et.al, 1995, Murata, J. et.al, 1992, Martys, N.S. et.al, 2003, Ferraris, C.F., et.al, 2001*] analyzed fresh concrete as a paste/aggregate composite and tried to deduce the plastic viscosity of the concrete from the plastic viscosity of the paste by multiplying it by a function that took into account the volume and nature of the granular phase. Some authors even extended this analysis to the cement paste, using the Farris approach. [*Domone P.L.J.,2000, Jiang W. and Roy D.M., 1992, Ferraris, C.F et.al, 1992,* Wüstholz T, 2005]. In order to calculate the plastic viscosity of the multi-modal suspensions, they performed an iterative calculation, the whole being made up of the suspending fluid and the finest classes being dealt with homogeneously at the scale of a given class. As elegant as they might be, these models

suffer from not taking into consideration the inter-particle interactions. In fact, most concrete mixtures have a more or less continuous size distribution, so that the division into a number of discrete classes is arbitrary. Even the distinction between cement paste and aggregate, which is pertinent in the case of hardened concrete, is difficult to justify for fresh concrete. The large particles of cement are of comparable size comparable to the finest sand particles and their respective contributions to the rheology of the whole are not of a different nature (at least as long as the hydration of the cement remains negligible). One way of attempting to link the rheology of the neat cement paste with that of concrete was to introduce another factor, i.e., the rheology of mortar. However in this approach, it is important that the paste should experience the same shear history and experimental conditions as the paste fraction in the mortar. Similarly, the mortar should have the same shear history and experimental conditions as the mortar fraction in concrete. By linking the rheology properties of paste, mortar and concrete to their constituent materials, this research is expected to bridge the information gaps of concrete technology.

## 2.7 Overview of Existing Mix Design Methods for SCC

Since the first prototype of SCC was introduced in 1988 in Japan [*Okamura et al ,1989, 1999*], a number of mix design methods for SCC have been developed based on several approaches to produce high performance of fresh and hardened SCC and reduce the testing times and works as well as the sensitivity to quality control and increase cost efficiency. However, due to the variation and availability of materials from place to place,

and a wide variety of performance requirements, it is not possible to produce any universal SCC mixture proportions.

The first mix design method, which has become known as "General Method", is a relatively simple step-by-step method and was developed at the University of Tokyo for a single set of component materials, and results in more than adequate self-compacting properties for many applications [*Ozawaa et al, 1989*]. However, "General Method" is applicable to mixes containing a limited range of Japanese materials, including coarse aggregate with a size range of 5-20mm, fine aggregate with a maximum size of 5mm, and a low heat, high belite content Portland cement without viscosity modifying agent. In this mix design method, the coarse aggregate content was set as 50% of the dry rodded weight in the concrete volume less the air content. This allows for the effect of particle shape and grading. The fine aggregate content is set as 40% of the resulting mortar volume [*Okamura et al, 2003*]. This content is considered critical, and depends to some extent on the particle shape and size distribution of the aggregate, and the properties of the cement. If the content is too high, the fine aggregate particles will interfere with each other during flow and cause blocking. If too low, the resulting higher cement and water content will be detrimental to the hardened concrete properties [*Power. T.C., 1968*]. The water/powder ratio and superplasticiser dosage will be determined by testing mortars with the spread and V-funnel tests [*Billberg P., 1999a, Domone P.L.J., 1999*]. There is no inclusion of a concrete strength requirement in the mix design process, but with Portland cement being the only binder material, the required low water/cement ratios result in adequate strengths

for most structural purposes. However, it generally leads to concrete with higher paste volume than required in the optimum mix. The induced over-cost may be unacceptable in countries where the materials cost is one of major factor in competition. In addition, due to the usage of high cement content in this mix design method, it will generate a considerable amount of heat during cement hydration and it is thus not practicable in tropical area [*Gibbs J C et.al, 1999, Mindess S. et.al, 1981*]

Another proposed SCC mix design method is the CBI method proposed by Petersson [*Petersson et al, 1996*] based on the work done by Tangtermsirikul and Van. The main target of this method is to produce an efficient mix, and it has the advantages of;

1) Considering the overall grading of the combined aggregate;

2) Being applicable to any size specification of coarse and fine aggregate;

3) Taking into account the placing conditions, including the ratio of aggregate size to the minimum gap through which the concrete has to pass.

The main difference between the CBI method and the general method is the method of determining the aggregate, and hence paste content. There are also differences in mortar and concrete tests used. In the CBI method, a blocking criterion for the solid phase is proposed and the risk of blocking is calculated. A value for coarse/total aggregate ratio at or close to for minimum voids in aggregate mixture is normally selected, then the required paste content is calculated. The water/cement ratio and the type of cement are defined by the strength and durability requirements of the hardened

concrete. The blocking behavior of the concrete is measured with the L-box and the blocking ratio (H2/H1) is suggested to be greater than 0.8. A slump flow value of about 700mm is considered appropriate with stability evaluated by observing any tendency to segregation at the outer rim. This method gives no recommendations for the design of mixes containing a viscosity modifying agent. Though this method proposes a better optimization of the contribution of aggregates but the reference curve for blocking criterion is not general and is cumbersome to obtain for each nature of aggregate. Moreover, the relationship between slump flow and packing density of the skeleton is not clearly established and needs the conduct of extensive trials.

To produce an optimal (low paste volume) mix from local materials as efficiently and simply as possible, the Laboratory Central Des Ponts et Chausses (LCPC) developed the so-called LCPC's approach. Its central feature is the use of a 'Compressible Packing Model'. Firstly, the virtual packing density of each class of solids was obtained, then the partial compaction index for each class of solid was calculated and a compaction index for the whole concrete can be summarized according to the individual partial compaction index for each size group. After having obtained the gradings, specific gravities and packing density of the constituent materials, the saturation dosage of superplasticizer and the constants for the passing ability analysis, the mix proportions can be adjusted until the values of the rheological constants and the compaction indices for the coarse aggregate and paste fractions can be calculated with the CPM. However, the LCPC approach is developed on the basis of BTRHEOM Rheometer and RENE LCPC software [*Ferraris*

*and Larrard, 1998*]. It is difficult for others to adopt their method without the equipment and their software.

There are also other design methods proposed by various researchers [*Ambroise et.al, 1999, Karam, 1992, Khayat et.al, 1999, Peter et. al, 2001*], however it can be noted from all mix design methods that all of them are based on their locally available materials, local conditions and practice. However in Singapore, these mix design methods are not only economically unsuitable due to the constraint of materials availability but also technically undesirable due to the usage of higher cement content. It is thus necessary to develop a proper mix design method suitable for tropical areas, which assures the workability requirements at fresh the stage and strength development at the hardened stage of SCC. Therefore, this research is aimed to propose a mix design concept that is suitable for Singapore with regards to economical and technical aspects.

# CHAPTER 3

# THEORETICAL INVESTIGATION

## 3.1 Fundamental of Rheology

Rheology is the study of deformation and flow of materials under the influence of an applied stress. Therefore it is concerned with the relationship between applied stress, strain, rate of strain and time **[***Tattersall G. H. et al., 1983***].**

In considering the application of rheological principles to cement paste, mortar and concrete, it is necessary to understand the fundamentals of rheological behavior by looking at the material whose behavior can be described by simple relationship. A material whose rheological behavior can be described by the simple relationship between stress and strain is a Newtonian liquid.

In Newtonian liquid, laminar motion of liquid occurs when the liquid is confined between two parallel planes, one of which is moving slowly in its own plane with respect to the other. If the shear force is applied to the system as shown in Fig 3.1, a velocity gradient occurs.

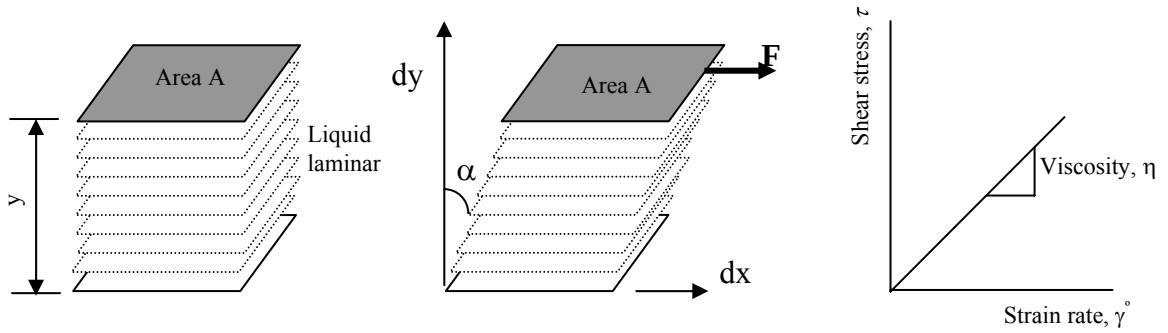


Fig. 3.1 Newton law for viscous flow

The shear stress is proportional to the distance ***y*** between two planes, which can be expressed as:

Shear stress ; $\tau = F/A$ *Eq. (3.1)*

Deformation due to shear ; $\gamma = tan\ \alpha = dx/dy$

Rate of deformation ; $\dot{\gamma} = d\gamma/dt$

Viscosity ; $\eta = \tau / \dot{\gamma}$

where $d\gamma/dt$ is the rate of deformation and can be expressed as strain rate, $\dot{\gamma}$. The proportionality factor between the shear stress and the strain rate is called viscosity. Therefore, the *Newton Law of viscous flow* or rheological behavior of Newtonian liquid can be written as:

$$F/A = \tau = \eta\dot{\gamma} \qquad \textit{Eq. (3.2)}$$

where $\eta$ = viscosity (Pa.s)

$\gamma$ = strain rate ($s^{-1}$) = $d\gamma/dt$

$\tau$ = shear stress (Pa) = $F/A$

$F$= shear force (N)

$A$= area of plane parallel to force ($m^2$)

However, many other fluid-like materials, including cement paste, mortar and concrete, are non-Newtonian [*Hattori K., 1990*]. Even casual observation indicates that concrete is not a simple Newtonian liquid. The fact that concrete can stand in a pile (eg. Slump test) indicates that there is some minimum stress necessary to initiate the flow. This minimum stress is called yield stress. The rheological behaviors of these systems can

still be described by the relation of shear stress and rate of shear or strain rate. However this relationship is not a linear straight line passing through the origin as in a Newtonian fluid. Thus for non-Newtonian materials, it is important to describe their flow properties by using at least two parameters, yield stress and plastic viscosity [*Cyr M. et.sl, 2000*]. Fig. 3.2 shows the example of how two concretes could have very different flow behaviors even if they both have one identical parameter. Therefore, it is important to use a model that will describe concrete flow by measuring (at least) both parameters [*Tattersall G. H. et.al, 1983*]

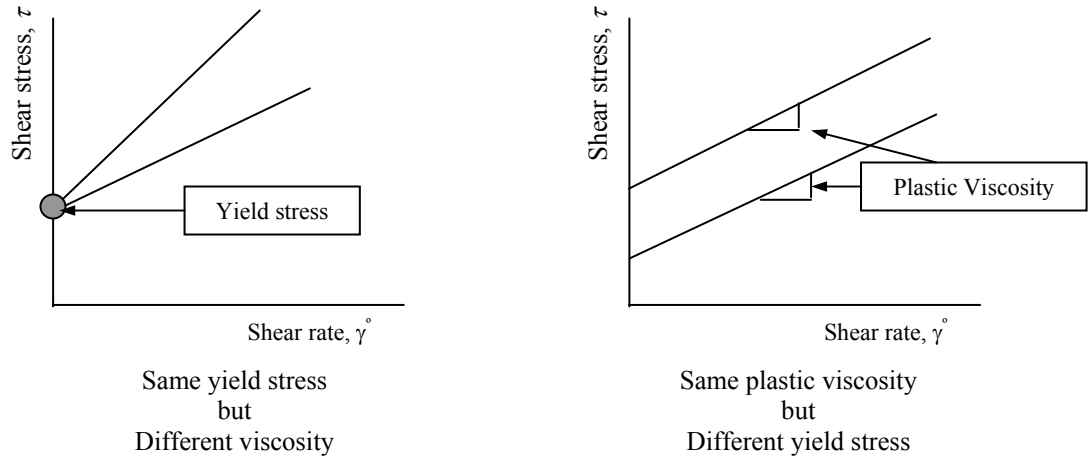


Fig. 3.2 Expressions of flow behavior of two materials

## 3.2 Bingham Model

A major thrust in rheological research has been developed the models that described the rheological behavior in terms of the relationship between stress and strain rate [*Saak W. et.al, 1999, Hattori K., 1990*]. With such models, it may be possible to determine the complex behavior of flow by the general relationship between flow behavior and material aspects.

Many materials are only elastic as long as the stress does not exceed some critical value, which is yield stress. These materials will stretch and return to their original shape when the applied stress is lower than the yield stress. However when the applied stress is higher than the yield stress, those materials will first stretch, then flow and be permanently deformed. Such materials are called 'plastic' [*Power. T.C., 1968*].

The commonly used constitutive relationship for plastic behavior is the *Bingham model* which introduces yield stress into Newton's law of viscous flow (Eq 3.2). Bingham pointed out that the flow behavior of many materials that have a yield point could be approximated on "*the rheogram*" or "*stress vs strain rate curve*" as a straight line intercepting the axis at the yield point (Fig 3.2) [*Tattersall G. H. et.al, 1983*]. Therefore, *Bingham Model* can be written as;

$$\tau = \tau_0 + \eta_p \dot{\gamma} \qquad \textit{Eq. (3.3)}$$

where $\tau_0$ is the yield stress with the unit of Pa (1 N/m$^2$ = 1 Pa) and $\eta$ in unit of Pa.s is the viscosity of the material, which is in the fluidized state, called Plastic Viscosity. $\dot{\gamma}$ is the shear rate (strain rate) with the unit of s$^{-1}$

Fig.3.3 shows some of the idealized types of curves that can be obtained when shear stress is plotted against strain rate. The simplest is the Newtonian behavior. The stress and strain relation is linear and zero stress at zero strain rate. This is the ideal fluid behavior. Many fluids exhibit plastic behavior in which the flow initiates above some level of stress (called yield stress) and once flow initiates, the relationship between stress and strain rate is linear.

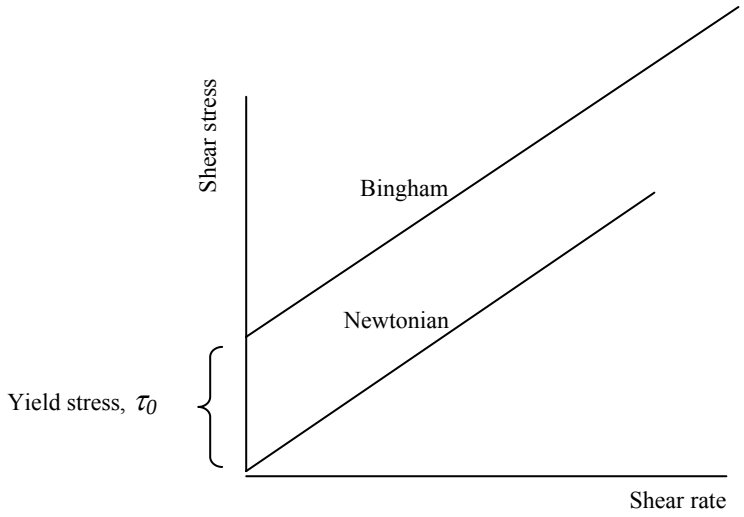


Fig. 3.3 Comparison on flow behaviors of Newtonian and Bingham Fluid

The gradual transition of flow from Newtonian behavior to Bingham behavior is often seen when the particle content of a flocculated dispersion is increased. The reason for this is that the higher concentration of particles creates a stronger structure in the dispersion with a corresponding higher yield value. The yield point of a Bingham model marks the destruction of an internal static structure, which is found in a flocculated suspension [*Ferraris, C.F. et.al, 2000*].

In the case of concentrated suspension such as concrete, yield stress exists. *Bingham equation* is the most commonly used equation to describe concrete flow, because the parameters used in that equation can be measured independently, and the flow of concretes, especially SCC, seems to follow this equation in most cases [*Tattersall G. H. et.al, 1983*].

However by studying the Bingham equation as well as other existing flow equations, it is necessary to measure the stress and strain value of the suspension with

necessary equipments. This is not practical for field applications due to poor availability of equipments and low reproducibility of results and different equipments will give different values of yield stress and plastic viscosity for the same suspension [*Tattersall G.H. et.al, 1976*]. Therefore, this study is targeted to predict rheological parameters through the properties of individual constituent materials and these values will be further verified with those calculated from the Bingham equation using the BML equipment.

## 3.3 Theories Adopted For Current Research

In order to understand the rheological behavior for cement, mortar and concrete, some assumptions are made and the theories needed are also adopted. This section discussed the adopted theories and their applications to achieve the objectives of the current research.

### 3.3.1 Suspension Theory

Suspension is the dispersion of particles in the fluid [*Russel W.B. et.al,1989*] In any type of suspension, there are two components: suspended particles and suspending medium. The properties of suspension can be described and analyzed as a function of properties of suspended particles and suspending medium [*Russel W.B. et.al,1989*]. In this study, paste, mortar and concrete will be analyzed as granular suspensions by applying the suspension theory.

In the paste mixture, the suspending medium is water in which cement grains and fine filler particles are suspended. While for the mortar mixture, the paste will be regarded as the suspending medium in which sand particles (fine aggregate) are suspended. For the concrete mixture, the mortar becomes a suspending medium

containing coarse aggregates as the suspended particles. Fig. 3.4 schematically illustrates these three suspension systems. Therefore, it is possible to consider that the rheology of cement paste is a function of cement, fine filler particles and water. Similarly, the rheology of mortar is a function of fine aggregate and paste, and finally the rheology of concrete is a function of coarse aggregate and mortar.

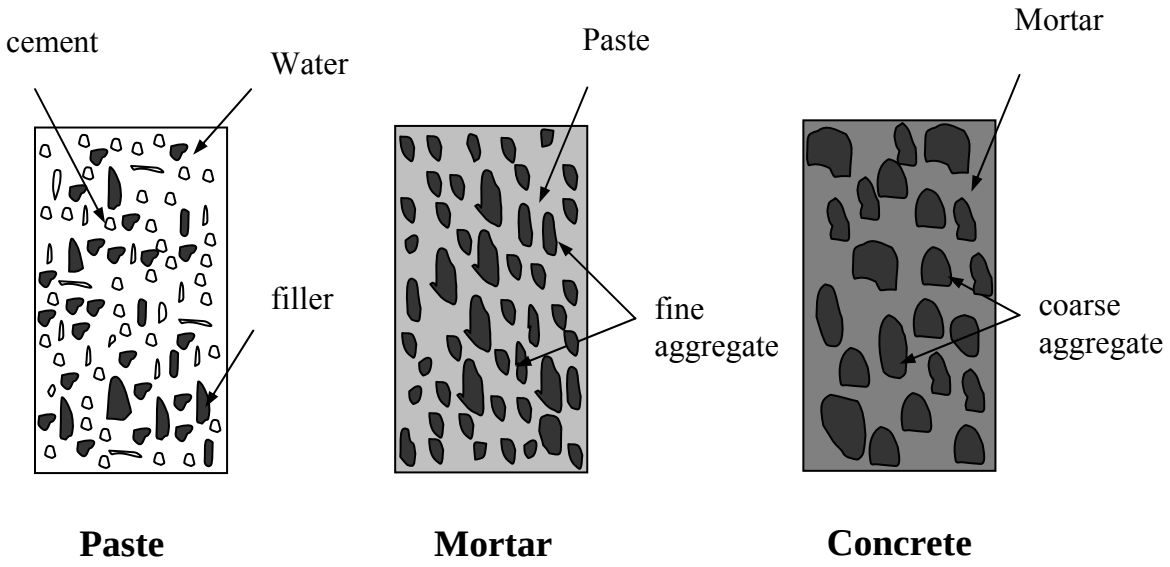


Fig. 3.4 Suspension systems for paste, mortar and concrete mixture

Generally, the following key factors will affect the rheological properties of a suspension;

1) Particle concentration (volume of suspended particles vs. total volume)
2) Particle physical properties (packing properties, particle shape, particle sizes , size distributions, and their contribution to total surface area)
3) Degree of particle flocculation

Low concentration of solid particles affects more on the viscosity than the yield stress. With low concentrations of suspended particles, the suspension continues to

behave as a Newtonian Liquid, which has slightly higher viscosity coefficient than the suspending medium. *Einstein* proposed the following relationship for the viscosity of a suspension containing spherical shape suspended particles:

$$\eta = \eta_c (1+k\phi) \qquad \textit{Eq. (3.7)}$$

where $\phi$ is the solid volume concentration of the suspension system, the detailed explanation of which will be given in Section 3.4. $\eta$ is the viscosity of the suspension and $\eta_c$ is the viscosity of the fluid phase. $k$ is the shape factor of the suspended particles and equal to 2.5 for the spherical particles.

It can be seen that the increase in solid volume concentration $(\phi)$ will lead to a considerable increase in viscosity. However, Einstein's equation is valid for the suspension with low solid volume concentration. It can be found that due to the increase in the solid volume concentration, the actual progressive increase in viscosity is higher than that predicted by Eq. 3.7, and the relation between viscosity and solid volume concentration is not linear as the relation given in Eq 3.7 [*Hattori K., 1990*]. Therefore, there is a need to develop a model in order to better describe the relationship between the wide range of solid volume concentration and viscosity.

It is recognized that the flocculation or dispersion of particles will affect mostly the yield stress. In a suspension system, flocculated particles either form the discrete aggregate or gel (a continuous three dimensional network) as shown in Fig.3.5. Since the forces between particles are often fairly weak, the bond or network between these particles can be broken by a small amount of shear stress. When applying enough stress,

the flocculated network can be easily disrupted. After the flocculated network was broken down, the suspension system begins to flow [*Russel et al, 1989*]. The stress at which such a breakdown occurred is called yield stress.

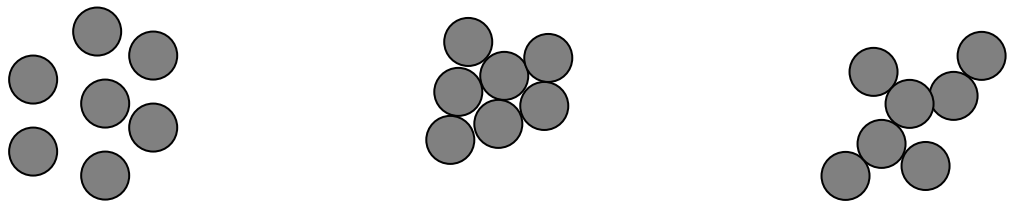

dispersed aggregated gelled

Fig. 3.5 Typical Microstructures of Suspension System

Although dispersed suspensions usually show Newtonian behavior, when the particle concentration reaches a sufficiently high level, they develop pseudoplastic behavior with a moderate yield stress. The yield stress also increases as the solid volume concentration increases. [*Karam G. N., 1992*]. This relationship can be described by using Power law.

$$\tau_0 = \phi^x \qquad \textit{Eq. (3.8)}$$

where $\tau_0$ is the yield stress of the system and $x$ is a constant lying between *2* and *4* **[***Zukoski and Struble, 1993***].** However, it should be noted that the yield stress not only depends on solid volume concentration as described in Eq 3.8 but also depends on the inter-particle potential that may lead to particle flocculation. Such inter-particle potential is influenced by the inter-particle distance in the system. Therefore, in addition to solid volume concentration, inter-particle distance is one of the important parameters that influence the yield stress of the concentrated suspension. In this study, the inter-particle distance of the suspensions: paste, mortar and concrete, will be determined according to "*excess paste theory*".

### 3.3.2 Excess Paste Theory

As discussed in section 3.3.1, Self-Compacting Concrete, SCC, will be analyzed as a granular suspension in which aggregate (fine and coarse) particles are suspended in the mortar matrix. The inter-particle distance of aggregate in SCC can be determined according to the excess paste theory.

The excess paste can be defined as the excess volume of paste left after filling the interstitial voids between the compacted aggregate binary mix. The excess paste is the major cause leading to certain dispersion of aggregate particles in the cement paste matrix. To attain a better workability, it is necessary for the concrete mixture to have enough paste to cover all the surfaces of the aggregate particles. The thicker the paste between aggregates, the lesser the friction occurs between the aggregates and the better workability. Therefore, thickness of paste on the surface of particles is one of the important parameters influencing the flow properties of SCC.

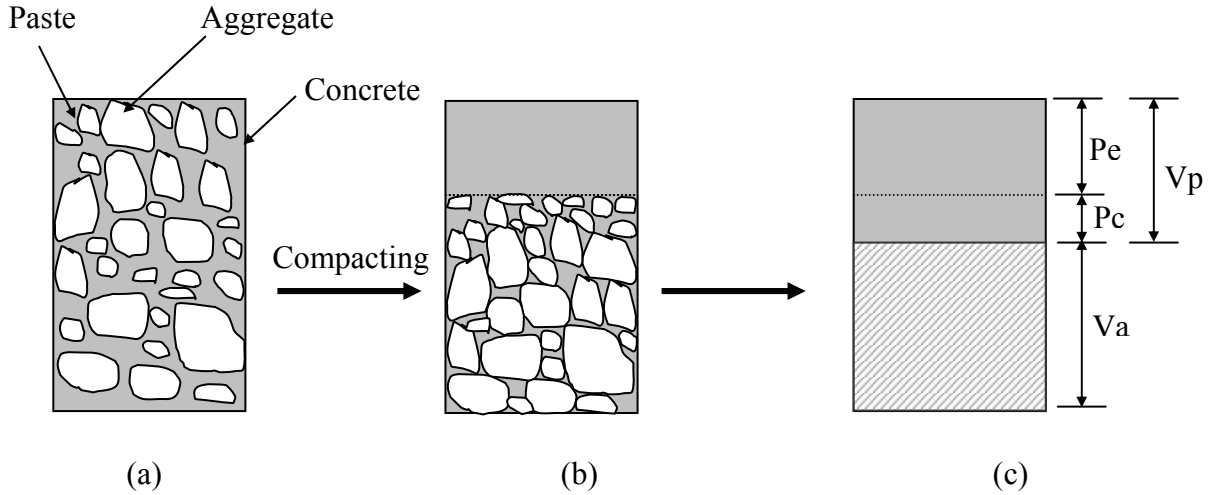


Fig. 3.6 Illustration of excess paste theory

In excess paste theory **[***Power. T.C., 1968***],** the thickness of the paste is the total volume of paste minus the volume of paste required to fill the voids of the compacted

aggregates divided by the surface area of the aggregate (Fig. 3.7). It can be calculated as follows;

$$T_p = P_e / S_{all} = (V_p - P_c) / S_{all} \qquad Eq. (3.9)$$

Where $T_p$ is the thickness of paste on the surface of aggregate, $P_e$ is the volume of excess paste, $V_p$ is the total volume of paste, $P_c$ is the volume of paste to fill the voids between the compacted aggregates and $S_{all}$ is the total surface area of aggregate.

## 3.4 Paste Rheology

The paste fraction of SCC is the most complicated constituent of SCC. As discussed in chapter 1, the paste fraction of SCC is composed of very fine particles undergoing chemical reactions. And it is obvious that the incorporation of different fillers in SCC paste will cause more complicated fresh properties due to their differences in physical and chemical properties.

The factors affecting the rheology of paste can be categorized into two groups: i.e. internal and external factors. Internal factors include the chemical and physical properties of the materials that are incorporated in the paste and external factors are related to the environmental conditions, preparation methods and testing conditions of the paste. Some important internal and external factors affecting the paste rheology are summarized below as:

1) Internal factors

- Primary Parameters
    - Water content or water/powder ratio

- Solid volume concentration
- Inter particle distance

- Secondary Parameters
  - Particle shape and size
  - Particle reactivity
  - Particle repulsivity

2) External factors

- Temperature of the paste
- Humidity or moisture content of surrounding environment
- Initial mixing conditions, such as mixing procedure, mixer speed, duration and capacity of mixer
- Shear history during the rheology test
- Testing procedure such as time since adding water to the dry mixture, test duration, measuring system

It can be observed from above the that all the external factors can be controlled by conducting the test under controlled conditions with specified testing procedures. Thus, in this research, all the external factors are kept constant and only the effects of internal factors on paste rheology are studied. In the proposed paste rheology model, yield stress and plastic viscosity are predicted from the physical and chemical properties of the constituent materials from the mix.

### 3.4.1 Primary Parameters

- **Water Content**

As discussed above, the fresh paste exhibits the characteristics of a concentrated colloidal suspension in which the whole population of particles (cement grains and fine

fillers) are suspended in water. In this analysis, the small content of entrapped air is ignored. In the case of paste rheology, water is considered as the suspending medium in which cement grains and fine filler particles are suspended.

In order to study the rheological behavior of paste suspension, it is helpful to start by looking at the system containing chemically inert particles of various shapes and sizes. When the water is added to such a system, the whole system is under a stable condition until the voids between the particles are filled with water. This required amount of water to fill the voids between the particles is called the minimum amount of water for that particular system. Once the added water content goes beyond the minimum, the water filled spacing between the particles are increased and the system is susceptible to sliding. (Fig. 3.7).

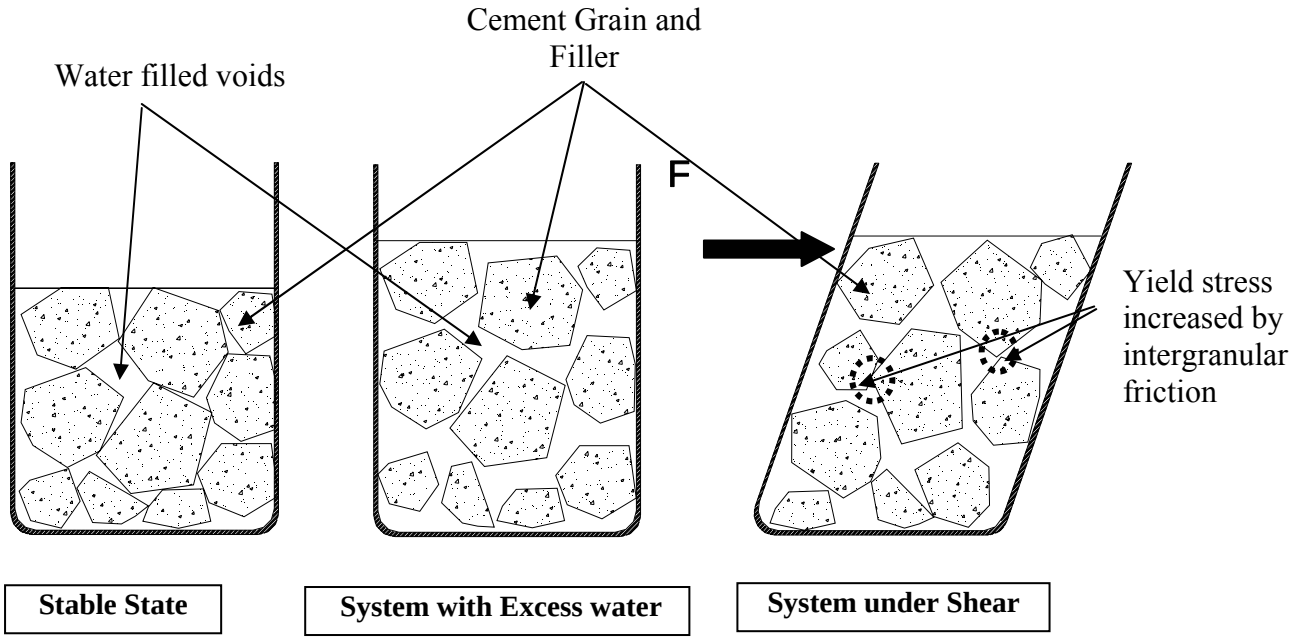


Fig. 3.7 Suspension system containing different water content

In a confined system as shown in Fig 3.7, a deformation will occur if this applied shear stress is sufficient to overcome the friction forces between the solid particles.

Therefore yield stress is the required minimum stress that initiates the system to flow [*Ferraris and Larrard, 1998*]

Tattersall and Banfill had observed that yield stress is an exponential function of the water to cement ratio [*Tattersall G. H. et.al,1983*]. In the paste fraction of SCC, it is water to powder ratio instead.

$$\tau_0 = f\,[\exp\,(w/p)] \qquad \textit{Eq. (3.10)}$$

Where $\tau_0$ *is* yield stress (Pa) and *f* is a decreasing function. Instead of describing yield stress as a function of water to powder ratio (w/p), the more acceptable relation is to present using the function of the solid volume concentration,$\phi$, which is defined in Eq. (3.11a).

$$\tau_0 = f\,[\exp\,(\phi)] \qquad \textit{Eq. (3.11)}$$

$$\phi = \frac{V_{SP}}{V_{SM} + V_{SP} - V_V} \qquad \textit{Eq. (3.11a)}$$

where $\boldsymbol{\phi}$ is the solid volume concentration of suspension. $\boldsymbol{V_{SP}}$ is the volume of suspended particles ($m^3$) and $\boldsymbol{V_{SM}}$ is the volume of suspending medium ($m^3$) and $\boldsymbol{V_v}$ is the volume of voids ($m^3$) in the system. In this relation, the small volume of entrapped air is ignored.

In the paste fraction, $\boldsymbol{V_{SP}}$ is the volume of powder particles, $V_p$ , and $V_{SM}$ is the volume of water, $V_w$

- **Solid Volume Concentration**

The yield stress term is a manifestation of the friction between solid particles. If the solid volume concentration of the suspension is increased, the contact area and friction between each particle will be increased. Hence the yield stress ($\tau_0$) also increased. *[Jiang et.al, 1992]*. By replacing Eq (3.11) to Eq (3.10), the increase in yield stress can be expressed as a function of the solid volume concentration in exponential form as shown in Eq. (3.12) in which $K_A$ and $K_B$ are constants depending on the type of powder and admixture used.

$$\tau_0 = K_A (\exp K_B \phi) \qquad \textit{Eq. (3.12)}$$

This model was successfully used for suspensions containing one type of material such as clays, clayey mud and cement together with water [*Karam, 1992*].

If the fluid remains in the laminar regime while flowing between the solid particles, its contribution to the shear resistance will remain proportional to the overall strain gradient. Thus applying the Bingham model from *Eq. (3.3),* the term $\tau_0$ is the contribution of the skeleton and the term $\eta\dot{\gamma}^{\circ}$ is the contribution of the suspending liquid. When the structure of the colloidal suspension is broken under a high enough shear stress, the suspension shows viscous behavior unlike non-colloidal concentrated suspensions in a Newtonian Liquid. It is generally accepted that the plastic viscosity of a low volume fraction of suspension can be modeled as the viscosity of a Newtonian suspension of non-interacting solid particles adjusted with their electro viscous effects and surface geometry. Einstein (1906) had proposed the first derivation for viscosity, $\eta$, of the system containing a low volume fraction of spherical shape solid particle as in Eq 3.13. Experimental study showed that the plastic viscosity of diluted suspension varies linearly with its solid

volume till the solid volume fraction of 0.5 [*Ng, C.C.,2001*]. Thus, the suspension with moderate solid concentrations can be written as

$$\eta = f(\phi) \qquad \textit{Eq. (3.13)}$$

$$\eta = (K_C + K_D \phi) \qquad \textit{Eq. (3.13a)}$$

For a high solid volume fraction of suspension, plastic viscosity appears to be controlled essentially by the ratio of solid volume to the packing density of the granular mixture. *Krieger and Dougherty* proposed the following colloidal suspension model that can be used extensively for higher solid volume fraction or concentrated paste [Barnes, H. A. et.al, 1989)

$$\eta = \eta_c \left(1 + \phi/\phi_m\right)^{-[\eta]\phi m} \qquad \textit{Eq. (3.14)}$$

where $\phi_m$ is the maximum possible volume fraction for the particular size class of particles (65% for randomly close-packed sphere). $[\eta]$ is intrinsic viscosity and can be defined as:

$$[\eta] = \lim_{\phi \to 0} \frac{\eta/\eta_c - 1}{\phi} \qquad \textit{Eq. (3.15)}$$

The intrinsic viscosity is 2.5 for spherical particles and this value is higher for non-equate shapes.

- **Inter Particle Distance**

It is clear that the higher the solid volume in the system, the larger the contact or friction occurring between particles and the bigger the yield stress and plastic viscosity. Thus, inter particle friction is the key factor affecting the initiating of flow in the system. (Fig 3.8) It is also a fact that inter-particle friction is dependent on the inter-particle

distance between each solid particle. In the system containing powder as suspended particles and water as suspending medium, the average inter-particle distance is assumed to be the thickness of water separating adjacent particles in the system (Fig 3.9). Thus, the average inter-particle distance is twice the thickness of the water film surrounding each powder particles.

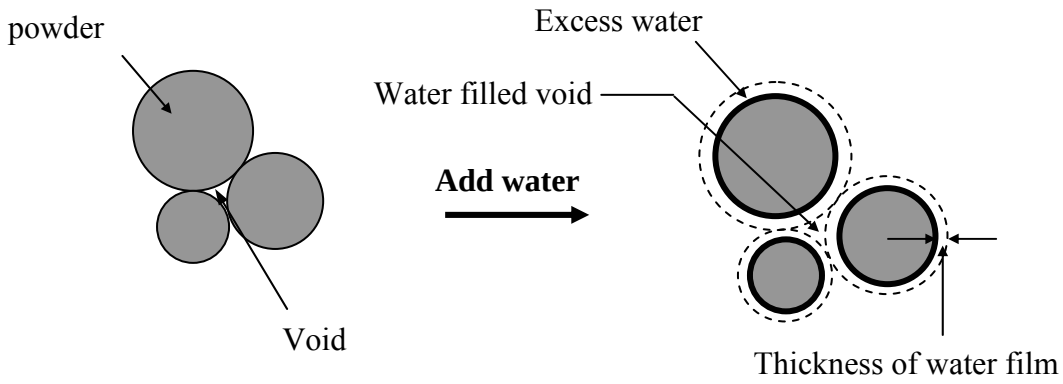


Fig. 3.8. Dispersion of compacted powder particles due to excess water

By applying the excess paste theory from Eq. (3.9), and making following assumptions;

1) All powder particles are chemically inert at initial contact with water
2) All powder particles are spherical in shape
3) The thickness of water film around each powder particles is the same regardless of their sizes
4) Boundary (wall) effects are ignored

The thickness of the water film around each powder particle can be calculated as;

$$T_w = \frac{V_w - V_V}{S_{SP}} \qquad \textit{Eq. (3.16)}$$

where $T_W$ is the thickness of water film around the powder particles (um), $V_W$ is the volume of water ($m^3$) , $V_V$ is the volume of voids in the compacted powder ($m^3$) and $S_{SP}$ is the total surface area of cement and filler ($m^2$). Therefore, the solid volume fraction, $\phi$, from Eq (3.11) can be expressed in terms of $T_W$ as;

$$\phi = \left[ \frac{1}{1 + T_W \left( S_{SP} / V_{SP} \right)} \right] \qquad \textit{Eq. (3.17)}$$

By substituting Eq. (3.16) into Eq. (3.12), Eq (3.13) and Eq (3.14), the yield stress and plastic viscosity of the system containing water and inert powders can be expressed as:

$$\tau_0 = K_A \exp \left[ K_B \frac{1}{1 + T_W \left( S_{SP} / V_{SP} \right)} \right] \qquad \textit{Eq. (3.18)}$$

For $\phi \leq 0.5$

$$\eta_p = \left[ K_C + K_D \frac{1}{1 + T_W \left( S_{SP} / V_{SP} \right)} \right] \qquad \textit{Eq. (3.19)}$$

For $\phi > 0.5$

$$\eta_p = \eta_0 \left[ 1 + \frac{K_C}{\phi_m} . \frac{1}{1 + T_w \left( S_{all} / V_{all} \right)} \right]^{\phi_m K_C} \qquad \textit{Eq. (3.20)}$$

Where $\eta_p$ is the plastic viscosity of paste. $\eta_0$ is the plastic viscosity of suspending medium (water) and $K_C$ is an empirical constant depending on the type of powders and admixture used. $T_w$ is the thickness of water film (μm), $S_{SP}$ and $V_{SP}$ are the total surface area ($m^2$) and volume ($m^3$) of cement grains and filler powders respectively.

In all cases, plastic viscosity results from the viscous dissipation due to the movement of water in the sheared materials. This research focuses only on the case of low solid volume fraction effect on plastic viscosity, since the nominal value of the solid volume fraction for paste fraction is below 0.5, (i.e w/c ≥ 0.3). The suspension with high volume fraction is not applicable in cement paste rheology and is beyond the scope of study.

### 3.4.2 Secondary Parameters

- **Effect of Powder Particle Size and Geometrical Shape**

In actual condition, the fine powder particles cannot be expected to be perfect spheres. When the particle size and surface geometry of the particles change, the number of contacts between particles and their frictions also change. Therefore, it is necessary to consider the effect of particle size and geometrical shapes in paste rheology by introducing the angularity factor.

In this study, the angularity factor is assumed to be the reciprocal of the sphericity factor modified with size ratio of particle group [*Power. T.C.,1968*]. The angularity of an irregular particle can be expressed in terms of sphericity factor defined as follows;

$$1/\psi_{Li} = [\frac{d^{v}_{0i}}{d^{s}_{0i}}]^{0.25} \qquad \textit{Eq. (3.21)}$$

where $1/\psi_{Li}$ is the angularity factor of individual suspended particle i, $d^{v}_{0i}$ and $d^{s}_{0i}$ are the diameters of the sphere of the same volume and the same surface area as irregular particle. The average angularity factor of the system containing different types of

powders can be calculated by summing up the individual angularity values with respect to their specific surface area and volume modified by their respective sizes, as shown in Eq. (3.22).

$$1/\psi_{LR} = \frac{\sum_{i=1}^{n} S_{SPi} V_{SPi} / \psi_{Li}}{\sum_{i=1}^{n} S_{SPi} V_{SPi}} \frac{d_{max}}{d_{min}} \qquad \textit{Eq. (3.22)}$$

Where $1/\psi_{LR}$ is average angularity factor of suspended particle group in the system. $S_{SPi}$, $V_{SPi}$ and $1/\psi_{Li}$ are the specific surface area ($m^2/m^3$), volume ($m^3$) and angularity factor of individual suspended particle i. $d_{max}$ and $d_{min}$ are the maximum and minimum sizes of different types of powder in the particle group.

- **Effect of Powder Reactivity**

In the paste fraction of SCC, not all the powder particles are inert. Obviously, the main component, OPC is a highly reactive powder and other types of filler powder can also be chemically reactive such as silica fumes and GGBS. During mixing, when the mixing water comes into contact with the dry powder, electro chemical forces appear between the powders and form a three-dimensional structure of the fine particles. The forces acting on them determine the physico-chemical behavior of the paste, especially in the fresh stage. If the powder is highly reactive, these forces cause them to flocculate and the flocs come in contact with one another and percolate throughout the whole volume of the mixture to create some form of continuous structure. This increases the yield stress, as well as plastic viscosity of the system. The reactivity of each type of powder will be determined experimentally and presented in Chapter 5 of this thesis.

The average reactivity factor of the system containing different types of powders can be calculated by summing up the individual reactivity factor with respect to their specific surface area and volume, as shown in Eq. (3.23).

$$\delta_R = \frac{\sum_{i=1}^{n} \delta_i S_{SPi} V_{SPi}}{\sum_{i=1}^{n} S_{SPi} V_{SPi}} \qquad \textit{Eq. (3.23)}$$

Where $\delta_R$ is the average reactivity factor of suspended particle group. $S_{SPi}$, $V_{SPi}$ and $\delta_i$ are the specific surface area ($m^2/m^3$), volume ($m^3$) and reactivity factor of individual suspended particle i. Reactivity factor, $\delta i$ is assumed to be 1 ($\delta i = 1$) for non-reactive suspended particles and greater than 1 ($\delta i > 1$) for reactive particles.

- **Effect of Powder Repulsibility**

Essentially, superplasticizer is required to be added to SCC in order to get higher flowability. When it is added to the mix, the admixture is adsorbed onto the surface of the powder particles and gives them a negative charge, which induces inter-particle repulsive force and develops steric repulsion if polycarboxylate type superplasticizer is used. This force prohibits the powder particles from approaching and flocculating with one another. At the same time, it helps to stabilize the dispersion of solid particles in the mix [*Tangtermsirikul S. et.al, 2001*]. Therefore, the repulsion factor ($\alpha_{rep}$) is introduced. Even though, every fine particle may develop a repulsive effect upon adding the admixture, it is expected that the repulsive force for highly reactive powder is much higher than that for non-reactive powder. Thus, the repulsive effect of the system is dependant on the combined effect of admixture and reactive powder.

The effect of superplasticizer is largely dependent on the particle reactivity. The yield stress is more affected by the flocculation or dispersion of particles. The average repulsion factor of the system containing different types of powders can be calculated by summing up the individual repulsion factor with respect to their specific surface area and volume, as shown in Eq. (3.24).

$$\alpha_{rep} = \frac{\sum_{i=1}^{n} \alpha_i S_{SPi} V_{SPi}}{\sum_{i=1}^{n} S_{SPi} V_{SPi}} . D_{sp} \qquad \textit{Eq. (3.24)}$$

Where $\alpha_{rep}$ is the average repulsion factor of suspended particle group. $S_{SPi}$, $V_{SPi}$ and $\alpha_i$ are the specific surface area ($m^2/m^3$), volume ($m^3$) and repulsion factor of individual suspended particle i. $D_{sp}$ is the dosage of superplasticizer in the system as a percentage of solid volume.

### 3.4.3 Proposed Rheological Model for Paste Fraction of SCC

Based on the above discussion, it is obvious that the rheological behavior of the paste fraction of SCC, described by yield stress and plastic viscosity, depends first of all on the solid volume concentration, then on the inter-particle distance which can be expressed in terms of thickness of water film around the individual powder particles. Due to the essential requirements of SCC, the introduction of different powders and chemical admixtures also contribute as a secondary parameter on rheology. Hence, it is proposed to represent the rheological parameters, yield stress and plastic viscosity in terms of the characteristics of the constituent materials as in following equations;

**Yield Stress:** $$\tau_p = K_1 . \left\{ f\left(\frac{\delta_R}{\psi_{LR}}\right) \exp\left[ \frac{K_2}{f(\psi_{LR}\alpha_{rep})} . \frac{1}{1 + T_w\left( S_{sp} / V_{sp} \right)} \right] \right\}$$ *Eq. (3.25)*

**Viscosity :** $$\eta_p = \left[ K_3 + \frac{K_4 f(\delta_R)}{f(\psi_{LR}\alpha_{rep})} . \frac{1}{1 + T_W \left( S_{SP} / V_{SP} \right)} \right] \qquad \textit{Eq. (3.26)}$$

Where $\delta_R$ is the average reactivity factor of the paste suspension. $1/\psi_{LR}$ is the average angularity factor from the combined shape effect of the powders in the paste suspension. $\alpha_{rep}$ is the average repulsion factor of the system due to the addition of chemical admixture. $T_W$ is the thickness of water film (um) around the powder particles in the system. $S_{SP}$ and $V_{SP}$ are the total surface area ($m^2$) and volume ($m^3$) of powder particles in the paste suspension. $K_1$, $K_2$, $K_3$, $K_4$ are empirical constants.

## 3.5 Proposed Rheological Model for Mortar Fraction of SCC

The model described herein is basically to predict the rheological parameters of mortar from those of paste, which has an identical mix proportion as the paste fraction of the mortar. It is assumed that the whole population of fine aggregate is suspended in the paste, which is regarded as a suspending medium. Therefore, the rheology of mortar is controlled by the rheology of the suspending medium (paste) and the inter-particle distance between the fine aggregate particles. In which, the inter-particle distance between fine aggregate particles are determined by the thickness of the excess paste around each particle. It is assumed that in this case, the thickness of excess paste around the sand particle is the same for different sizes since the sand particles are uniformly dispersed in the paste and the distance between each particle is constant. Thus, the general form for the rheological parameter for mortar can be deduced as:

For Yield Stress of Mortar: $\tau_m = \tau_p \left[ A + KT_P \right]$ *Eq (3.27)*

For Plastic Viscosity of Mortar: $\eta_m = \eta_p \left[ B + KT_P \right]$ *Eq. (3.28)*

where $\tau_m$ *(Pa)* , $\eta_m$ *(Pa-s)*are the yield stress and plastic viscosity of mortar. $\tau_p$ and $\eta_p$ are the yield stress and plasticity viscosity of the corresponding paste K is the slope of the best fit line. A and B are empirical constants dependent on the angularity factor and the surface modulus of the fine aggregate used in the mix. $T_p$ (um) is the thickness of the excess paste which can be expressed as:

$$T_p = (1\text{-}V_s/G_s \times 100) \times 10^4 / \sigma_s \times V_s \qquad \textit{Eq. (3.29a)}$$

Where $G_s$ is the solid volume percentage of sand (%), $V_s$ is the volume ratio of sand with respect to the total volume of mortar and $\sigma_s$ is the specific surface area of sand. It is quite difficult in reality to calculate or even to predict the total surface area of aggregate. Many researchers proposed different methods to attain such value. In this research, the calculated method will be based on sieve analysis proposed by Power. **[***Power. T.C., 1968***]**

$$\sigma_s = (5.58 / \psi_L)\, SM \qquad \textit{Eq. (3.29b)}$$

$$1/\psi_L = 1 + 4.44(\epsilon - 0.42) \qquad \textit{Eq. (3.29c)}$$

where $\sigma_s$ is specific surface area of sand per unit solid volume, $cm^2/cm^3$, $1/\psi_L$ is angularity factor which can be calculated from Eq (3.29c) in which $\epsilon$ is the void content (%) [*Power. T.C., 1968*]. *SM* is the surface modulus. Surface modulus is defined as the

number of particles proportional to the surface area and can be determined from sieve analysis as shown in Eq (3.29d). **[***Talbot, 1919***]**

$$SM = 100\,(p_1 + 1/2p_2 + 1/4p_3 + 1/8p_4 + 1/16p_5 + 1/32p_6) \qquad Eq.\ (3.29d)$$

Where $p_i$ is the weight fraction of individual group.

## 3.6 Proposed Rheological Model for SCC

Aside from measuring the flow of concrete, rheology is concerned with the prediction of flow from properties of the components (i.e. cement paste, mortar) or from the mix proportion (i.e. w/b ratio, type of filler, admixture dosage). Attempts to develop a prediction model has not yet been successful. One difficulty comes from the fact that the size range of particles is very wide (micrometer to tens of millimeter). Also, the factors influencing the flow properties of concrete are more than those of paste. There is no simple relationship between rheological parameters of cement paste and those of concrete. The main reason is the distance between aggregate, which varies with the volume of paste content. Also, the rheological behavior of the material depends on the condition of experiments such as shear rates, temperature and mixing energy. Therefore it is important that the cement paste must be measured at the same condition that it will experience in concrete.

It is considered that concrete rheology is a function of mortar rheology, assuming that the coarse aggregate particles are suspended in the mortar; suspended media. By introducing the surface geometry of coarse aggregate, the general form for rheological parameter can be deduced as:

For Yield Stress of SCC: $\tau_c = \tau_m\left[C + KT_m\right]$ *Eq (3.30)*

For Plastic Viscosity of SCC: $\eta_c = \eta_m\left[D + KT_m\right]$ *Eq. (3.31)*

where $\tau_c$ , $\eta_c$ are the yield stress and plastic viscosity of concrete and $\tau_m$ , $\eta_m$ are the yield stress and plasticity viscosity of the corresponding mortar. $T_m$ is the thickness of excess mortar. K is the slope of the best fit line. C and D are empirical constants dependent on the angularity factor and surface modulus of coarse aggregate used in the mix. Similarly, the same assumptions and calculation procedure are applied to predict the thickness of excess mortar surrounding the coarse aggregate particles.

$$T_m = (1-V_g/G_g \times 100) \times 10^4/ \sigma_g \times V_g \qquad \textit{Eq. (3.32a)}$$

Where $G_g$ is the solid volume percentage of coarse aggregate (%), $V_g$ is the volume ratio of aggregate with respect to the total volume of concrete and $\sigma_g$ is the specific surface area of the aggregate.

Similar procedure is applied as in fine aggregate (Sand), the specific surface area of the coarse aggregate will be calculated as follows;

$$\sigma_g = (5.58 / \psi_L)\, SM \qquad \textit{Eq. (3.32b)}$$

$$1/\psi_L = 1+4.44(\in -0.42) \qquad \textit{Eq. (3.32c)}$$

where $\sigma_g$ is the specific surface area of the coarse aggregate per unit solid volume, $cm^2/cm^3$, $1/\psi_L$ is the angularity factor which can also be calculated from Eq (3.29c). *SM* is the surface modulus and can be determined from sieve analysis. **[***Talbot, 1919***]**

$$SM = 100\ (1/64p_7 + 1/128p_8 + 1/256p_9) \qquad Eq.\ (3.32d)$$

Where $p_i$ is the weight fraction of individual group.

## 3.6 Concluding Remarks

Due to its complex nature and sensitivity to proportion and quality control of the constituent materials, determining the rheology to ensure the desired properties of SCC by conducting concrete trail tests are not advisable due to the high material cost and labors. This chapter proposed a correlation between the rheological parameters of paste, mortar to concrete. With this proposed correlation, the concrete engineer can estimate the rheological or flow properties of SCC by conducting rheological tests on the paste fraction which required much lesser amount of materials and work. By introducing the contributing effect of fine and coarse aggregates, the flow properties of SCC can be predicted with a minimum number of trials.

# CHAPTER 4

# PARAMETRIC STUDY ON CONSTITUENT MATERIALS

SCC is a complex mixture containing different constituents. Due to its high powder content requirements for minimizing the segregation potential, fine filler materials, either inert or reactive powder, are incorporated into ordinary Portland cement. Chemical admixtures such as superplasticizers, air-entraining agents, viscosity modifying agents and retarders, are also added to achieve desired properties. Approximately 50 to 65% of the volume of SCC is occupied with various particle shapes and sizes of coarse and fine aggregates. It is important to characterize the constituent materials before they are incorporated into SCC.

## 4.1 Source of Materials

### 4.1.1 Powder Materials

In general, powder is referred to as materials with particle sizes less than 0.125 mm [*K.H.Khayat, 1999*] and these include cementitious materials and inert fillers. According to Billberg [*P. Billberg, 2001*], the rheology of concrete is mainly controlled by the fine powder phase, which is composed of particles less than 0.250 mm. In this research, there are five types of powder materials used besides Ordinary Portland Cement. They are Granite Dust (GR), two types of Copper Slag Fines, [Cyclone slag (CY) and Dust collector slag (DC)], Limestone Powder (LS) and Ground Granulated Blast furnace Slag (GGBS).

Ordinary Portland cement (OPC) Type 1 was used throughout the project.

The granite dust (GR) is generally referred to as quarry dust, which is derived from the crushing of rock into different fractions of concrete aggregate. The size of these 'dust' can range upto 300 um. Depending on the quality of this material and market circumstances, these 'dust' may or may not be saleable. In many quarries, there are unwanted stockpiles of thousands of tonnage.

Two types of copper slag fines (Cyclone Slag, CY and Dust Collector slag, DC) were used in this study. Copper slag is a type of inert abrasive blast material, which is generated from the ship building industry during removal of paints, coatings and antifouling compounds by blasting with copper slag. Such blasting process generates a large amount of used blast materials that need to be disposed off properly. For example, it is not unusual to produce 10 to 12 pounds of used abrasives per square foot of hull area treated. With the sand blasting activities in Singapore, it is found that an abundant supply of abrasive blast materials, copper slag, is fast becoming a disposal problem. In the processing plant, copper slag is dried using a Fluidized-bed Dryer and sieved into different sizes. In the process of recovering the coarser fraction from used copper slag, copper slag fines are collected as cyclone slag (CY), most of the particle size is finer than 0.6mm, was flew to the top of dryer and collected by Cyclone. The dust collector collected the dust portion from the top of cyclone, which is called dust collector slag (DC), most of the particles size is finer than 0.3mm. Copper slag is generally less elongated in particle shape than granite dust and has comparatively lower processing cost.

All these types of powder materials can and do present a serious disposal problem in Singapore. Thus, it is required to find means of environmentally acceptable disposal, or, ideally, economic usage for them. Attempts have been made, with varying degrees of

success to use this material for various purposes in the construction industry (e.g. dust as partial replacement of sand) and elsewhere (e.g. artificial soils), but there is always a surplus. Environmental legislation requires that the air borne dust that is inevitably generated should be prevented from escaping into the atmosphere. Thus, this research studies the feasibility of such fine powder in SCC. The possible utilization of these dusts in SCC may not only solve the disposal problems but also help bring down the material cost of SCC.

Two types of traditionally used filler, Limestone powder (LS) and Ground Granulated Blast Furnace Slag (GGBS), were also used for comparison with recently introduced fillers in this research. These two fillers were supplied by Ssangyong Cement Company, Singapore.

### 4.1.2 Fine Aggregate

Natural sand is used as fine aggregate in mortar and concrete mixtures. The natural sand is air dried till the surface is dry and stored in clean and dry plastic containers which were tightly sealed with plastic sheets to maintain the constant moisture condition till the day of the tests.

### 4.1.3 Coarse Aggregate

Crushed granite aggregate is used as coarse aggregate in SCC mix. The aggregates were first washed thoroughly to remove all impurities and contaminants, and dried under in-door conditions for 1 day. These surface dried aggregates were then subsequently

stored separately in the containers that were covered and sealed tightly with plastic sheets in order to control the constant moisture condition until the day of the tests.

### 4.1.4 Chemical Admixture

Two types of superplasticizer (ADVA 108 and ADVA 109) were used in this research and they were supplied by WR Grace (Singapore) Pte. Ltd. Both admixtures are Polycarboxylate and polyether type. The difference between these two admixtures is that ADVA 108 contains retarder while ADVA109 does not. Therefore, in this research, ADVA 108 is used when flow retention of SCC is required and ADVA 109 is used when early strength is required. The details of the materials used and their sources are listed in Table 4.1.

Table 4.1 Material used and their source of supply

| Materials Used | Source of Supply |
|---|---|
| **Powder materials** | |
| Ordinary Portland Cement (OPC) | RDC Concrete |
| Granite Powder | Eng Seng Construction Pte. Ltd |
| Copper Slag (CY slag and DC slag) | JPL Industries Pte. Ltd |
| Limestone Powder (LS) | Ssangyong Cement Pte. Ltd |
| Ground Granulated Blast Furnace Slag (GGBS) | Ssangyong Cement Pte. Ltd |
| **Aggregates** | |
| Coarse Aggregate | RDC concrete |
| Fine Aggregate | RDC Concrete |
| **Chemical Admixture** | |
| Superplasticizer (ADVA 108 & ADVA 109) | WR Grace (Singapore) Pte Ltd |

## 4.2 Properties of Powder Materials

In this section, different types of powder were studied in terms of their physical characteristics and chemical compositions.

### 4.2.1 Physical Appearance

The physical appearances of powders influence the color of the concrete product. For example, the concrete containing white colored limestone powder appears to be of a lighter color than ordinary concrete. Similarly, incorporation of black color copper slag will result in concrete of a darker color. Thus, it is necessary to take note of the color of these powder incorporated in SCC if such concrete products are used for aesthetic purposes.


**OPC**


**GGBS**


**LS**


**GR**


**DC Slag**

Fig. 4.1 Physical appearance of each type of powder used in this research

### 4.2.2 Particle Shape and Surface Texture

The shape and surface texture of those fillers are also important factors affecting the workability of SCC in the fresh stage. The physical shapes of the powders are examined by the use of Scanning Electron Microscope (SEM) and some SEM photos are presented in figure 4.2. It was observed that most of the particles of the granite dust (GR) powder are flaky, elongated and irregular. The shape of particles of the limestone and DC slag are more or less rectangular. For the OPC and GGBS, the particles are smaller, of similar cubical shape and evenly distributed (Fig. 4.2).

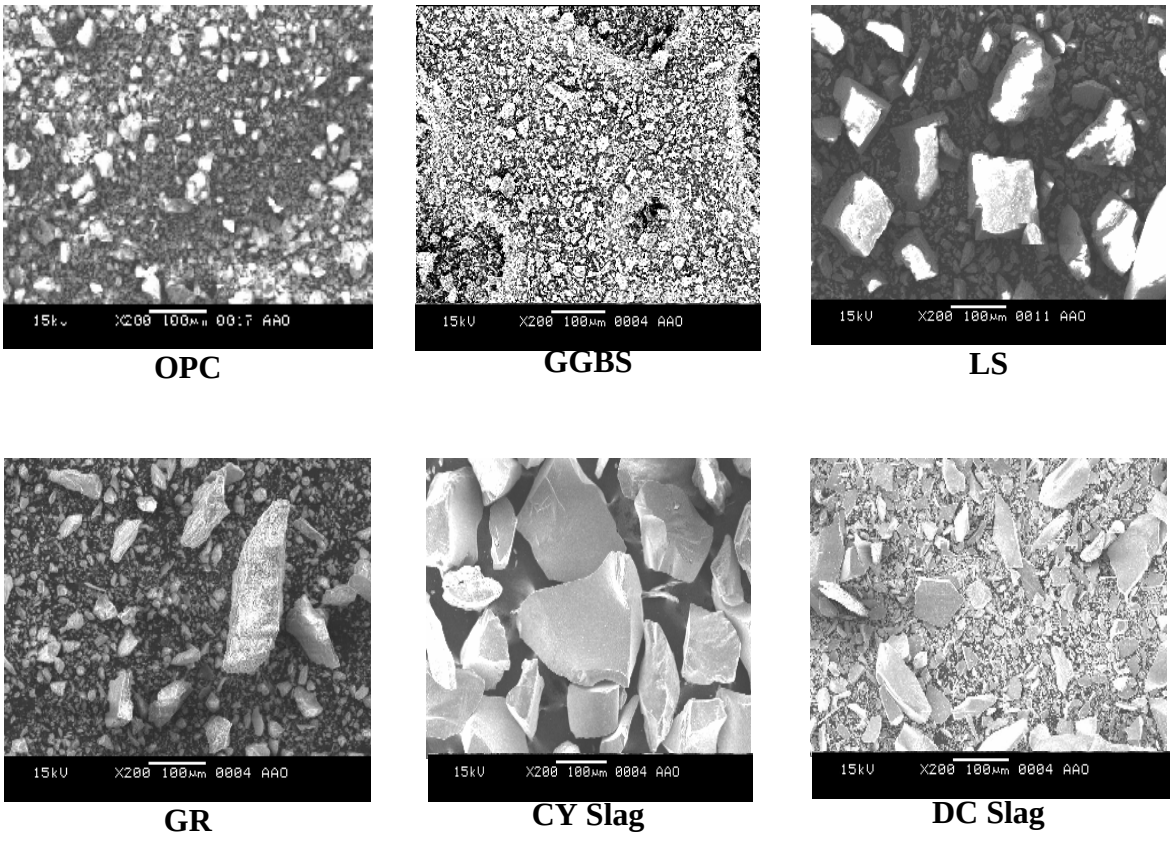


Fig 4.2 Physical shapes of each powder (SEM photographs)

### 4.2.3 Particle Size and Size Distribution

Laser Scattering Particle Size Analyzer, the Malvern Mastersizer (Fig. 4.3) was used to determine the particle size distribution of each type of powders and Micro V2.17 software was used to analyze the particle characteristics. This equipment can detect the particle sizes ranges from 0.3 um to 300 um. Since the maximum particle size of powder suitable to incorporate in SCC is 125 um, this equipment is suitable for this purpose. For simplicity, it was assumed that the irregular particle shape of powders as sphere to calculate the surface area and distribution.


Fig. 4.3 Laser Scattering Particle Size Analyzer (Malvern Instrument)

The sample preparation for the particle size analysis is critical as the sample required for analysis is very small compared to the whole lot of received powders. The sample taken from each type of powder must be a representative sample of that type of powder. Before conduct of the test, the selected powder sample was stirred to make sure that the particles were uniformly distributed. The typical dispersant used was water if the tested powder was ascertained to be inert. As for the powder, which may react with water, either carefully selected dispersant or recommended dispersant was used to assure there was no chemical reaction during the test process. The type of dispersant used for different

powders are presented in Table 4.2. Ultrasonic bath (about 2 min) was used to achieve the total dispersion of powder in the dispersant during the test process.

The particle size distributions of each type of powders are shown in Fig. 4.4. It can be seen that except of the cyclone slag (CY), the size distribution of all other powders falls between the acceptable ranges for incorporation in SCC. The particle sizes of cyclone slag are far beyond the acceptable range and thus, in consideration of this aspect, cyclone slag is not suited to incorporate as filler in SCC. Physical characteristics of different powder materials are presented in Table 4.2. The specific gravity of cement and power are determined according to ASTM C150-84. It can be observed that the specific gravity values of both types of copper slag are significantly higher than all other types of powders. This is because these two copper slag powders contain heavy ferric oxide. It may be noted that the heavy particle copper slag powders tend to increase the segregation potential of SCC if a higher amount of such powder is used. The filler GR has similar specific gravity as traditionally used LS powder but its average particle size is smaller.

Table 4.2 Physical characteristics of different powder materials and dispersant used

| **Designation** | **Color** | **Dispersant** | **Specific gravity** | **Surface Area ($m^2/\ell$)** | **Mean Dia (um)** | **Sizes below (um)** | | |
|---|---|---|---|---|---|---|---|---|
| | | | | | | **10%** | **50%** | **90%** |
| OPC | Dark Gray | Acetone | 3.15 | 836 | 20 | 1 | 14 | 45 |
| GGBS | White | Acetone | 2.90 | 839 | 17 | 1 | 11 | 40 |
| GR | Light Gray | Water | 2.65 | 674 | 59 | 2 | 33 | 159 |
| LS | White | Ethanol | 2.70 | 595 | 76 | 3 | 54 | 184 |
| DC slag | Black | Water | 3.60 | 612 | 70 | 5 | 52 | 164 |
| CY slag | Black | Water | 3.60 | 235 | 138 | 30 | 148 | 248 |

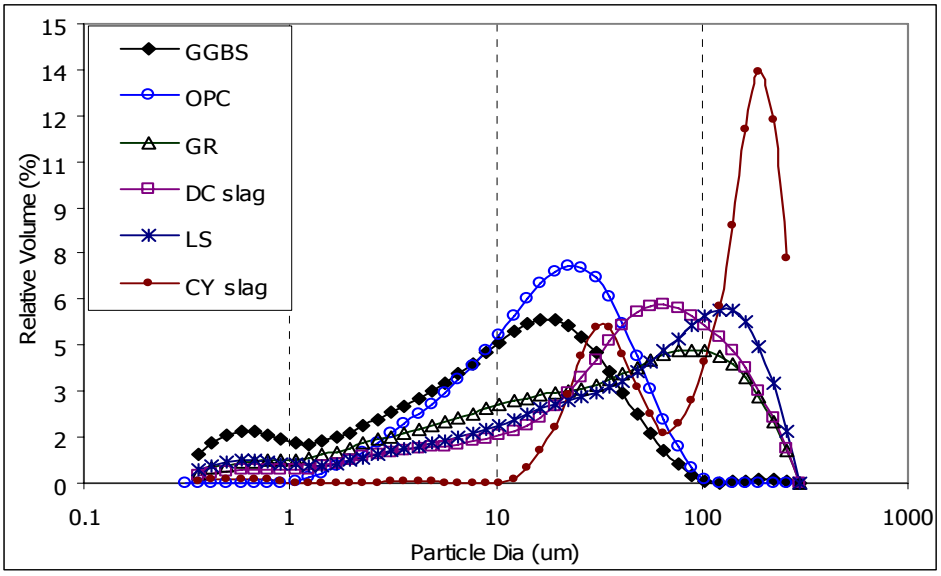


**(a)**

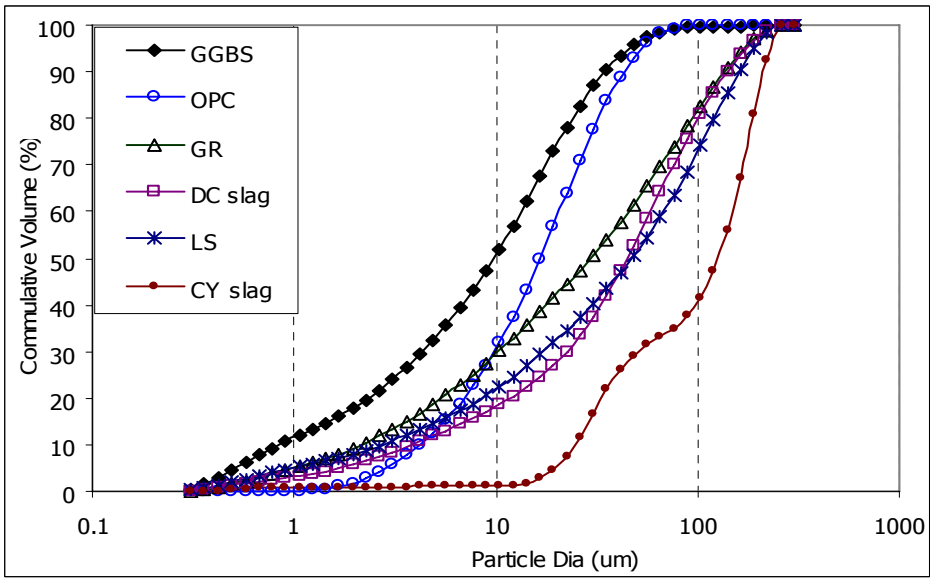


**(b)**

Fig. 4.4 Particle size distribution of different powder materials

### 4.2.4 Chemical Compositions of Fine Powder

Since the chemical composition of powders influence not only the workability of SCC at fresh stage but also the durability in hardened stage. It is important to identify the feasibility of powders in SCC in terms of chemical acceptance. The chemical composition of each types of powder was determined by using XRF analysis and ASTM C114-83b or EN 196 specified test methods and their chemical components are listed in Table 4.3 and 4.4

Table 4.3: Chemical composition of powders *(By XRF and ASTM C114-83b* or *EN 196: Part 2: 1995)*

| Element | Content (%) | | | | | |
|---|---|---|---|---|---|---|
| | OPC | GGBS | LS | GR$^+$ | DC Slag | CY Slag |
| $SO_3$ | 2.1 | | | 2.1 | 1.05 | 1.17 |
| CaO | 63.7 | 34.0 | 28 | | 2.09 | 2.65 |
| $CaCO_3$ | | | 98 | | | |
| MgO | 2.0 | 12.0 | 19 | | 1.03 | 1.26 |
| $MgSO_4$ | | | | | - | - |
| $Na_2O$ | *0.19* | | | | | |
| $K_2O$ | 0.35 | 0.8 | | | | |
| $Al_2O_3$ | 5.8 | 14.0 | | | 5.58 | 6.48 |
| $SiO_2$ | 20.5 | 37 | | 4.2 | 27.97 | 35.34 |
| ZnO | | | | | | |
| Br | | | | | | |
| $Fe_2O_3$ | 2.6 | 0.5 | | | 58.58 | 50.0 |
| PbO | | | | | | |
| $Sb_2O_3$ | | | | | | |
| $SnO_2$ | | | | | | |
| CuO | | | | | | |
| $C_3A$ | 10.9 | | | | | |
| **IR** | **0.1** | | | | | |
| **LOI** | **2.5** | | | 0.6 | -4.6* | -3.6* |

Note: "*" negative value indicates that sample weight is increased after heating up at 925°C for 1 hour. It is possibly due to the oxidation of sample during heating process.

"+" for GR, limited analysis results provided from independent testing company

Table 4.4: Chloride content in powders *(By EN 196: Part 21: 1992)*

| Element | Content (%) | | | | | | | |
|---|---|---|---|---|---|---|---|---|
| | OPC | GGBS | LS | GR | DC Slag | CY Slag | EP Ash | FF Ash |
| ***Cl$^-$*** | ***<0.02*** | ***<0.01*** | ***<0.01*** | ***<0.02*** | ***<0.02*** | ***<0.02*** | ***5.62*** | ***17.58*** |
| $CaCl_2$ | | | | | | | 4.43 | 13.87 |

## 4.3 Properties of Fine and Coarse Aggregates

### 4.3.1 Grading of Aggregates (Sieve Analysis)

Reasonably consistent grading is necessary for aggregates to ensure practical control of SCC mixes. ASTM C136 (*ASTM 1996d*), Standard Test Method for Sieve Analysis of Fine and Coarse Aggregates, was employed for the determination of the particle size distribution of fine and coarse aggregates. Sieves conforming to ASTM E11 (*ASTM, 1995e*), Standard Specification for Wire-Cloth Sieves for Testing Purposes, were used for all ASTM C136 grading analyses. (Fig 4.5a). Mechanical sieving machine (Fig 4.5b) was used to obtain the grading of aggregates.

(a)

(b)

Fig. 4.5 Wire Cloths sieves and mechanical sieving machine used to determine the grading of aggregate

The results of sieve analysis of coarse and fine aggregate are given in Table 4.5 and Table 4.6 and the grading curves are presented in Fig. 4.6 and Fig 4.7 respectively.

Table 4.5 Sieve analysis results of coarse aggregate

| Sieve size (mm) | Cumulative % passing | | | | ASTM C33-97 | |
|---|---|---|---|---|---|---|
| | CA 1 | CA 2 | CA 3 | CA 4 | Upper limit | Lower limit |
| **37.5** | 100 | 100 | 100 | 100 | 100 | 100 |
| **19** | 82 | 100 | 72 | 77 | 100 | 85 |
| **12.5** | 22 | 25 | 23 | 53 | 70 | 0 |
| **10.0** | 8 | 0 | 8 | 19 | 25 | 0 |
| **4.75** | 1 | 0 | 1 | 4 | 5 | 0 |
| **Fineness Modulus** | *7.87* | *7.75* | *7.97* | *7.64* | *7.00* | *8.15* |

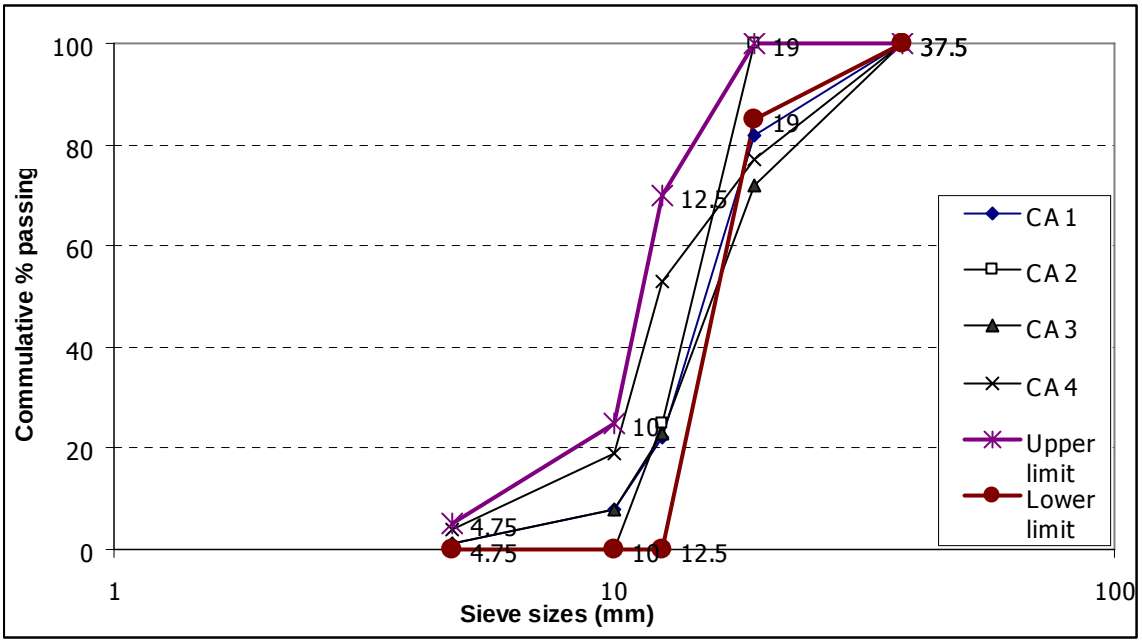


Fig 4.6 Grading curves of coarse aggregate

It can be observed from Table 4.6 and Fig. 4.6 that except for Batch 2, more than 10% of the particles in other batches of aggregates are larger than the size limit of 20 mm suggested by ASTM C33-97.

Table 4.6 Sieve analysis results of fine aggregate

| Sieve size (mm) | Cumulative % passing | | | | ASTM C33-97 | |
|---|---|---|---|---|---|---|
| | FA 1 | FA 2 | FA 3 | FA 4 | Upper limit | Lower limit |
| **10.0** | 100 | 100 | 100 | 100 | 100 | 100 |
| **4.75** | 99 | 97 | 95 | 99 | 100 | 89 |
| **2.36** | 96 | 85 | 89 | 91 | 100 | 60 |
| **1.18** | 65 | 56 | 65 | 70 | 100 | 30 |
| **0.60** | 39 | 27 | 32 | 44 | 100 | 15 |
| **0.30** | 18 | 8 | 5 | 4 | 70 | 5 |
| **0.15** | 4 | 2 | 3 | 1 | 15 | 0 |
| **Fineness Modulus** | *2.78* | *3.25* | *3.11* | *2.91* | *1.15* | *4.01* |

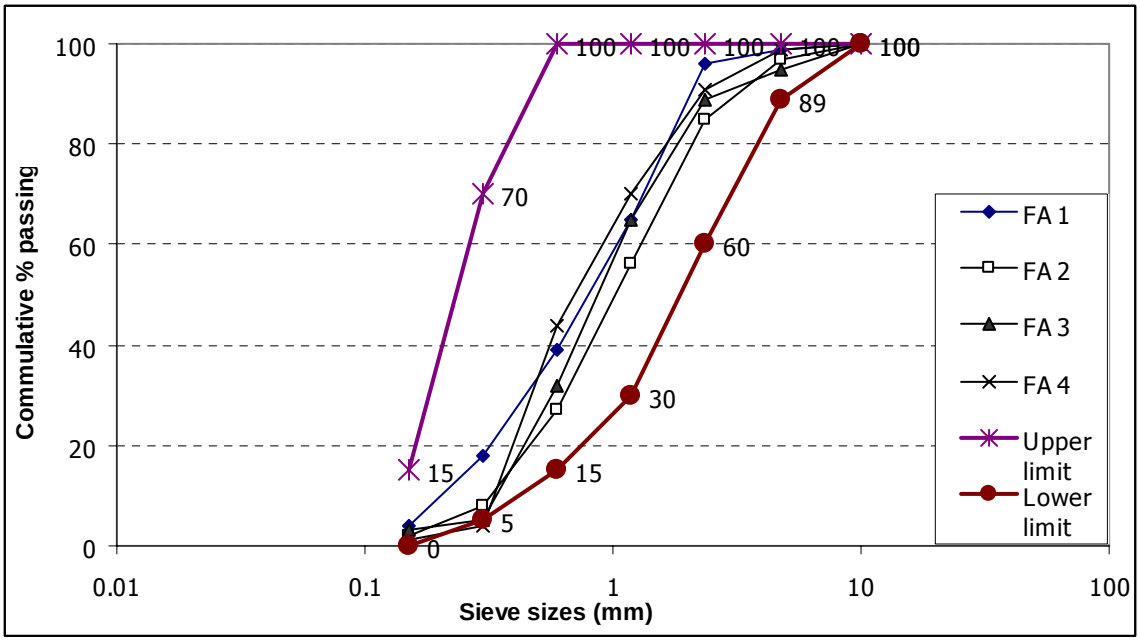


Fig 4.7 Grading curves of fine aggregate

It can be seen from the data that the size distribution of all batches of sand falls between the upper and lower limit of particle sizes recommended by ASTM C33-97. The fineness moduli of the fine aggregates varied between 2.78 to 3.25.

### 4.3.2 Specific Gravity of Fine and Coarse Aggregates

Specific gravity values of coarse and fine aggregates are important since it can be used to determine the quantity of aggregates required for the given volume of concrete. Specific gravity is indeed derived from the mineralogical properties of aggregates as this value generally depends on the specific gravity of the minerals of which the aggregate is composed and on the amount of voids in the aggregates [*Neville, 1995*]. Because of the presence of permeable and impermeable pores in the aggregate, the definition of specific gravity needs to be carefully defined. There are indeed several types of specific gravity. However in this research, only the apparent specific gravity values in oven-dried condition and saturated surface dry condition are determined according to following ASTM standards.

- ASTM C127 (*ASTM 1988*): Standard Test Method for Specific Gravity and Absorption of Coarse Aggregate
- ASTM C128 (*ASTM 1993*): Standard Test Method for Specific Gravity and Absorption of Fine Aggregate

*Apparent specific gravity (oven dry condition)* is the volume of the solid, which includes the impermeable pores but not the capillary [*Neville, 1995*]. Therefore, the oven dried apparent specific gravity is the ratio of the mass of aggregate dried in the oven at 100 to 110 °C for 24 hours to the mass of water occupying a volume equal to that of the solid including the impermeable pores.

*Apparent specific gravity (saturated surface dry condition)* is the volume of the solid, which includes both impermeable and capillary pores because the water contained in all pores in the aggregate does not take part in the chemical reactions of cement

[*Neville, 1995*]. The saturated surface dry apparent specific gravity is the ratio of the mass of aggregates, which were soaked in water for 24 hours and surface water had been removed, to the mass of water occupying a volume equal to that of the solid This specific gravity value is usually used to calculate the quality of aggregate required for a given volume of concrete.

Eq 4.1 and Eq 4.2 show the calculation of specific gravity values on an oven dry and saturated surface dry basis. The values of the specific gravity of coarse and fine aggregate at both oven dry condition and SSD condition are presented in Table 4.7 and Table 4.8.

Apparent Specific Gravity (Oven-Dry Basis) = A / (B + A - C) *Eq. (4.1)*

Apparent Specific Gravity (Saturated Surface-Dry Basis) = S / (B + A - C) *Eq (4.2)*

Where:

A : weight of oven-dry specimen in air, g

B : weight of pycnometer filled with water, g

S : weight of saturated-surface dry specimen, g

C : weight of pycnometer with specimen and water to calibration mark, g

### 4.3.3 Absorption of Coarse and Fine Aggregate

All of the aggregate particles contain internal pores, which may vary in size over a wide range. Due to the presence of those pores, the aggregate shows absorption upon contact with water. If dry aggregates are used in the concrete mix, those aggregates will tend to absorb the water, resulting in a substantial reduction of the free water left for the

entire mix. Thus, the presence of internal pores in the aggregate and the characteristics of these pores are important in the study of aggregate properties. Although there is no clear-cut relation between the strength of concrete and the water absorption of aggregate used, the pores at the surface of the aggregate particle affect the bond between the cement paste and the aggregate itself, and may thus exert some influence on the strength of concrete [*Neville, 1995*].

The water absorption of aggregate is determined by measuring the increased in mass of an oven-dry sample, when immersed in water for 24 hours (the surface water being removed). The ratio of the mass increase in the surface dried sample to the mass of oven dry sample, expressed as a percentage, is termed *Absorption.* The absorption of aggregate can be calculation from Eq 4.3 [*ASTM C127, C128*]. Table 4.7 and Table 4.8 report the absorption values of the coarse and fine aggregates in different batches.

Absorption, % = [(S - A) / A] x 100 *Eq. (4.3)*

Where:

A : weight of oven-dry specimen in air, g

S : weight of saturated-surface dry specimen, g

Table 4.7 Specific gravity and Absorption of coarse aggregate

| **Designation** | **Apparent Specific Gravity** | | **Absorption** |
|---|---|---|---|
| | **Oven Dry** | **SSD** | **(%)** |
| **Coarse Aggregate** | | | |
| CA 1 | 2.79 | 2.80 | 0.60 |
| CA 2 | 2.78 | 2.79 | 0.71 |
| CA 3 | 2.79 | 2.80 | 0.65 |
| CA 4 | 2.78 | 2.80 | 0.75 |
| *Mean* | 2.79 | 2.80 | 0.88 |
| *Std. Deviation* | 0.006 | 0.005 | 0.066 |

Table 4.8 Specific gravity and Absorption of fine aggregate

| Designation | Apparent Specific Gravity | | Absorption (%) |
|---|---|---|---|
| | Oven Dry | SSD | |
| **Fine Aggregate** | | | |
| FA 1 | 2.68 | 2.70 | 0.90 |
| FA 2 | 2.68 | 2.69 | 0.95 |
| FA 3 | 2.68 | 2.70 | 0.98 |
| FA 4 | 2.67 | 2.90 | 1.00 |
| *Mean* | 2.68 | 2.75 | 0.96 |
| *Std. Deviation* | 0.005 | 0.102 | 0.043 |

### 4.3.4 Bulk Density and Void Content of Fine and Coarse Aggregate

The bulk density clearly depends on how densely the aggregate is packed, and it follows that, for a material of a given specific gravity, the bulk density mainly depends on the size distribution and shape of the particles [*Neville, 1995*]. All the particles of one single size can be packed to a limited extent, but smaller particles can be added in the voids between the larger ones, thus increasing the bulk density of the packed materials. The shape of the particle greatly affects the closeness of the particles. For coarse aggregate of a given specific gravity, a higher bulk density means that there are fewer voids to be filled by fine aggregate and cement. Thus the bulk density test was one of the indications on the size and shape of the aggregate particles.

The actual bulk density of the aggregate depends not only on the various characteristics of materials which determine the potential degree of packing, but also on the actual compaction achieved in a given case. Thus for test purposes, the degree of compaction has to be specified. According to ASTM C29 and BS 812: Part 2: 1975, two degrees of compaction, loose (uncompacted) and compacted, can be categorized.

For determination of loose bulk density, the dry aggregate is gently placed in the container to over flowing and leveled by rolling a rod across the top of container. In order to find the compacted bulk density, the container is filled in three stages, each third of the volume being tamped a prescribed number of times with a 16 mm diameter round-nose rod. Again, the overflow is removed. The net mass of the aggregate in the container is divided by its volume, represents the bulk density for either degree of compaction (Eq 4.4 & 4.5).

Bulk density (compacted), $M_C = (GC - T) / V$ *Eq. (4.4)*

Bulk Density (uncompacted) $M_L = (GL - T) / V$ *Eq. (4.5)*

Where:

M : unit weight of aggregate, kg / $m^3$

$G_C$ : mass of compacted aggregate plus measure, kg

$G_L$ : mass of loose aggregate plus measure, kg

T : mass of the measure, kg

V : volume of the measure, $m^3$

Knowing the apparent specific gravity for saturated and surface dry condition of aggregate, the void content can be calculated from Eq (4.6) and Eq (4.7). Table 4.9 and Table 4.10 report the bulk density and void content of coarse and fine aggregate in different batches.

% Voids (compacted) = $100 [(S \times W) - M_C] / (S \times W)$ *Eq. (4.6)*

% Voids (Loose) = $100 [(S \times W) - M_L] / (S \times W)$ *Eq. (4.7)*

Where:

S : Bulk Specific Gravity (SSD Basis)

W : Density of Water, 998 kg / $m^3$

Table 4.9 Bulk density and Void content in different batches of coarse aggregates

| Designation | Bulk Density | | Void Content (%) | |
|---|---|---|---|---|
| | Loose | Compacted | Loose | Compacted |
| **Coarse Aggregate** | | | | |
| CA 1 | 1355.6 | 1492.4 | 50.4 | 45.4 |
| CA 2 | 1324.2 | 1451.8 | 51.4 | 46.9 |
| CA 3 | 1300.2 | 1456.6 | 52.4 | 46.7 |
| CA 4 | 1331.6 | 1481.5 | 51.5 | 46.0 |
| *Mean* | 1328.0 | 1470.6 | 51.4 | 46.3 |
| *Std. Deviation* | 22.7 | 19.5 | 0.8 | 0.7 |

Table 4.10 Bulk density and Void content in different batches of fine aggregates

| **Fine Aggregate** | | | | |
|---|---|---|---|---|
| FA 1 | 1580.2 | 1619.3 | 40.0 | 35.8 |
| FA 2 | 1575.5 | 1623.5 | 41.3 | 36.2 |
| FA 3 | 1578.2 | 1625.4 | 45.5 | 40.0 |
| FA 4 | 1573.4 | 1622.8 | 46.3 | 41.2 |
| *Mean* | 1576.8 | 1622.8 | 43.2 | 38.3 |
| *Std. Deviation* | 3.0 | 2.5 | 0.1 | 0.2 |

## 4.4 Concluding Remarks on Properties of Materials

Based on the properties of powders presented, it can be seen that the particle sizes of all powders except Cyclone Copper Slag (CY) are less than 0.125 mm. Thus, all powder except CY can be used as a filler or part of powder content in the production of SCC.

It can be seen from Table 4.1 to 4.5, all batches of supplied aggregates have similar physical properties except for the particle size distributions of coarse aggregate, a small percentage which is bigger than 20 mm. In terms of mineralogy of supplied aggregates, it

can be concluded from their respective specific gravity and absorption values that all batches of aggregate come from the same sources and they can then be considered to have similar chemical properties. With some modification of workability assessing test methods, both coarse and fine aggregate as supplied can be incorporated in production of SCC.

# CHAPTER 5

# RHEOLOGICAL STUDY ON PASTE FRACTION OF SCC

In this chapter, the stress-strain relationship of SCC pastes was measured with rheometer and experimental values of yield stress and plastic viscosity were determined by applying the Bingham equation. Through the possible influencing factors from mix constituents, the values of yield stress and plastic viscosity were investigated and the rheological model for paste fraction was proposed as a function of the constituent materials.

## 5.1 Experimental Program

### 5.1.1 Materials

As discussed in Chapter 3, the rheological properties of SCC paste fraction are influenced by physical and chemical characteristics of its constituent materials. Therefore, the experimental program was carefully designed to investigate the characteristics of individual constituents and their possible contributions on paste rheology.

The powder materials used in this study were Ordinary Portland Cement (OPC) together with four types of filler powder, namely Granite dust (GR), Limestone powder (LS), Dust Collector copper slag (DC), and Ground Granulated Blast Furnace Slag (GGBS). According to their reactivity, those powders can be classified into three groups, such as reactive powder, non-reactive powder and partially reactive powder. It is assumed that for reactive powder, paste rheology will be affected by both physical and chemical characteristics of powders. Where-as for a non-reactive powder, only physical characteristics will affect paste rheology.

Among five types of powders, OPC is obviously the most reactive powder, thus in this study, OPC is identified as reactive powder. GR and LS are identified as non-reactive powder in this study since these powders are the by-products in the production of concrete aggregates during the crushing process of rock. Similarly, DC slag is a type of inert abrasive blast material, which is generated from the ship building industry. The chemical compositions of DC slag (Table 4.7) confirmed that there is no significant chemical component that may alter the rheological properties of the tested paste. Therefore, DC slag is also identified as non-reactive powder. However for GGBS, although this powder is not as reactive as OPC but its contributions to concrete properties such as strength, durability, etc are well documented [*Ferraris, C.F. et. al, 2000, Gibbs J C et. al, 1999*]. Thus, in this study, GGBS is identified as partially reactive powder.

### 5.1.2 Sample Preparations

Hobart Mixer shown in Fig 5.1 was used to prepare the paste samples for all the tests. In this study, a mixing procedure stipulated in ASTM 305-99 was modified to suit the initial mixing condition of the paste. The mixing duration should be long enough to achieve the homogeneity of the paste. Research has shown that the mixing duration of about 4 to 5 minutes gave a better workability and stability for cement paste [*Peter A.C. et. al, 2001*]. Thus in this study, the total mixing duration of the paste was fixed at 4 minutes (240 sec).The following mixing procedure is adopted for all the tested samples.

**Paste sample without Superplasticizer;**

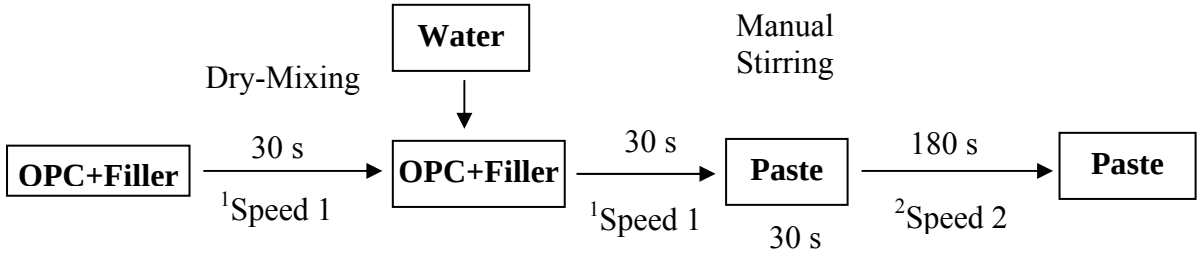


**Paste sample with Superplasticizer;**

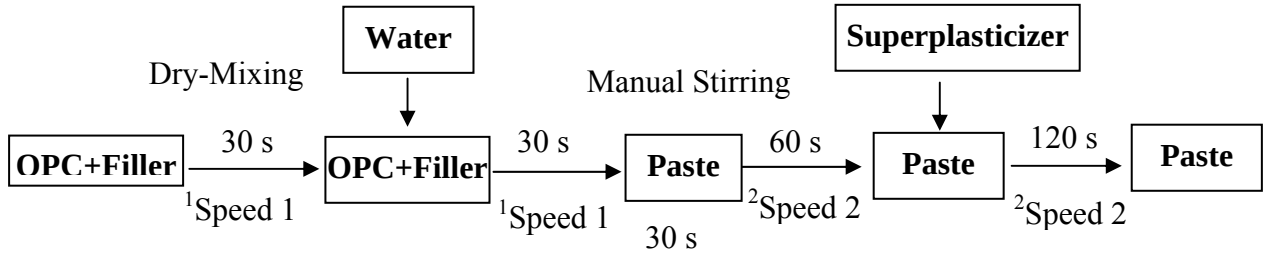


*Note: [1] Mixer Speed 1 = 60 rpm, [2] Mixer Speed 2 = 90 rpm*

Fig. 5.1 Hobart Mixer to prepare the paste sample

Immediately after mixing, a small amount of paste sample was placed in the measuring container of the rheometer for testing. To ensure the constant volume of the

paste sample, the height of the paste sample was maintained at 4 cm in the container for all tests.

### 5.1.3 Testing Procedure

As discussed earlier, the difference in testing procedures and testing equipments will lead to a difference in the yield stress and plastic viscosity values for the same paste sample. In order to minimize the influences of external factors, the testing program was carefully designed in such a way that all the samples were experienced the same shear history and all the tests were conducted at the same environmental condition under controlled temperature. The test samples were prepared inside the room with a constant temperature of 28°C and Relative Humidity (RH) of 70%.

The rheological characteristics based on strain-stress relationship of the pastes were investigated by the use of coaxial –cylinder rheometer (Haake Rotovisco 1) with the measuring head Z38 interior sensor (Fig. 5.2).

In this study, all the measured paste samples were given a constant ramp-up shear rate of 100/s over a time interval of 150 seconds followed by a ramp-down shear rate of 100/s over the next 150 seconds time interval. The total measuring time for all samples was kept at 300 seconds. This shear sequence was repeated three times on each tested sample for rheological measurement (Fig. 5.3-a). The first up and down curves function as pre-shearing process of the sample. Pre-shearing is used to break down the flocs or aggregate which is often formed during the mixing and shearing process [*Billberg P, 1999*]. Theoretically, an equilibrium curve is obtained after some up and down curves. It is obvious in Fig. 5.2 (b) that the paste had yet to reach a homogeneous and stable

condition under the first ramp-up and down curve. Therefore, the first measured data was ignored. The evaluations of the rheological parameters (yield stress and plastic viscosity) were made by performing regression on the ramp down curves of second and third measurements (Fig. 5.3-b) and the average value was recorded. The temperature during testing was set at 30°C to simulate the actual casting temperature in tropical areas.

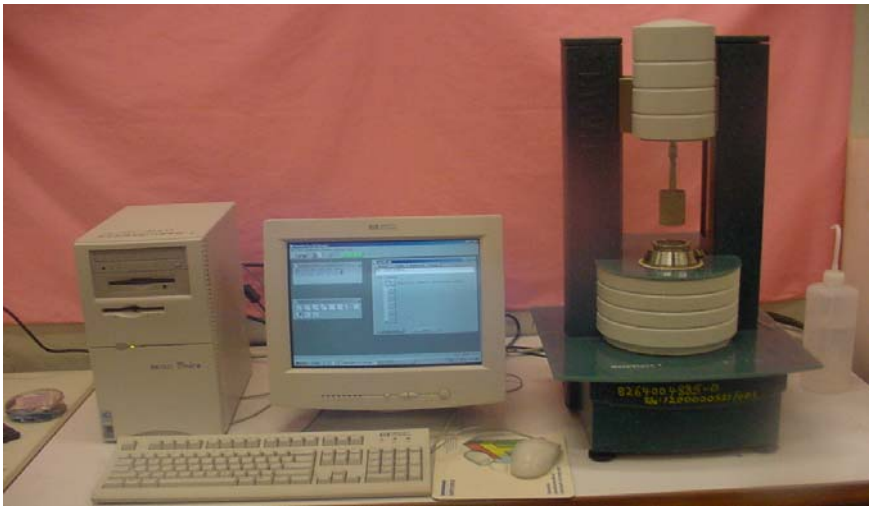

Fig. 5.2 Co-axial cylinder Rheometer for paste rheology measurement

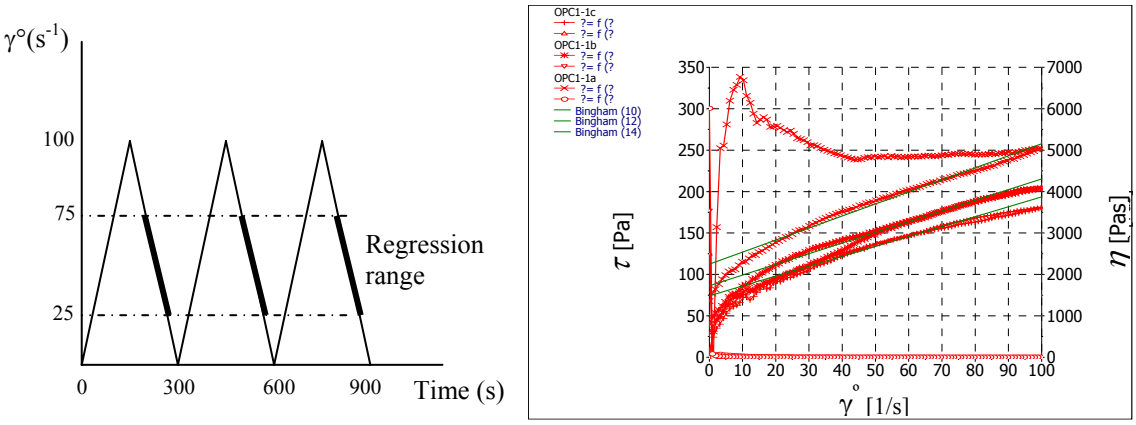


(a) (b)

Fig. 5.3 Shear history of paste and regression performed on typical flow curve

The characteristics of three up and down curves also indicate whether any particle segregation occurs during shearing process. When the particles sink to the bottom of the container during shearing, a vertical concentration gradient of the system will be formed. Once this sediment layer eventually reaches the bob, a much higher value of torque is recorded. Thus, the increase in measured shear stress was recorded for every up and down curve [*Billberg P., 1999a*]. This is one of the indications that segregation has occurred during the shearing process of the testing sample.

It is recognized that the shear thinning behavior of cement paste during rheological measurement. However in this research, the Bingham Model was used to analyze the flow behavior of SCC due to following reasons;

- The flow of concrete, especially SCC, seems to follow Bingham equation in most cases due to high flowability.
- The complex flow behavior of SCC can be simplified into two parameters of Bingham Model, yield stress and plastic viscosity measured independently from stress vs strain curve.

In paste rheological study, the strain rate used was carefully selected (75 to 25 $s^{-1}$) in the ramp down curve for regression analysis in order to minimize the shear thining behavior of cement paste under applied stress.

## 5.2 Rheological Investigation

The fresh paste exhibits the characteristics of a concentrated colloidal suspension in which the whole population of particles (cement grains and fine fillers) are suspended in water. According to the suspension theory, it is possible to consider water as the suspending medium in which cement grains and fine fillers are suspended as the

suspended particles. In the paste suspension system, as discussed in Chapter 3, the free water content or water to powder ratio (w/p), solid volume concentration and water film thickness are the primary parameters controlling the paste rheology. Besides these primary parameters, the powder particle shape and size, powder reactivity as well as the powder repulsibility due to addition of chemical admixture will affect the paste rheology as secondary parameters.

### 5.2.1 Primary Parameters

#### (a) Effect of Free Water Content or Water to Powder Ratio (w/p)

It is elucidated that the amount of free water in the mix is the basic factor influencing the workability of the paste. Within a certain range, the increase in free water content in the mix will lead to an increase in workability which can be defined quantitatively by rheological parameters, yield stress and plastic viscosity. The water content in the paste mixture can be described as the water to powder ratio. In order to analyze the influence of water content on rheological parameters of the paste suspension, a series of experiments were conducted under the following conditions. One of the detailed mix proportions of the series with similar total surface area are presented in Table 5.1.

1) By varying the filler powder content, similar total surface area of powders ($m^2$) were used in the mix to minimize the effect due to different sizes of powder.
2) For blended GR, LS, DC and GGBS mixtures, a fixed amount of reactive powder (OPC) was used to maintain similar reactivity of each mix.
3) Water to powder ratios, by volume, were varied from 1.0 to 2.0.

Table 5.1 Mix proportions of pastes containing different powders

| Mixture Type | Cement | | Filler | | Total Weight (g) | Total Volume ($m^3$) | Total Surface ($m^2$) |
|---|---|---|---|---|---|---|---|
| | Weight (g) | Volume ($m^3$) | Weight (g) | Volume ($m^3$) | | | |
| **OPC** | 900 | 0.29 | - | - | 900 | 0.29 | 239 |
| **GR** | 200 | 0.06 | 700 | 0.26 | 900 | 0.32 | 231 |
| **LS** | 200 | 0.06 | 850 | 0.31 | 1050 | 0.37 | 240 |
| **DC** | 200 | 0.06 | 1100 | 0.31 | 1300 | 0.37 | 240 |
| **GGBS** | 200 | 0.06 | 620 | 0.22 | 820 | 0.28 | 239 |

Different functional equations presented in Table 5.2 were applied to investigate the possible co-relation between rheological parameters and w/p. The actual data from rheological test was plotted against the values calculated using different equations and possible co-relation was determined from the correlation value, $R^2$.

Table 5.2 Different functional equations for yield stress and plastic viscosity.

| Functions | Yield Stress (Pa) | Plastic Viscosity (Pa.s) |
|---|---|---|
| Exponential Function | $\tau_0 = f\{ exp\ (w/p)\}$ | $\eta_0 = K_{e2}\ exp(w/p)$ |
| Linear Function | $\tau_0 = f\ (w/p)$ | $\eta_0 = K_{L2}\ (w/p)$ |
| Log Function | $\tau_0 = f\{log\ (w/p)\}$ | $\eta_0 = K_{g2}\ log(w/p)$ |
| Power Function | $\tau_0 = K_{p1}\ (w/p)^x$ | $\eta_0 = K_{p2}\ (w/p)^x$ |

The detail analysis plots of different co-relationship coefficient ($R^2$) for the different relationship between the yield stress and water to powder ratio for all the investigated mixtures are presented in Fig.5.4 and 5.5.

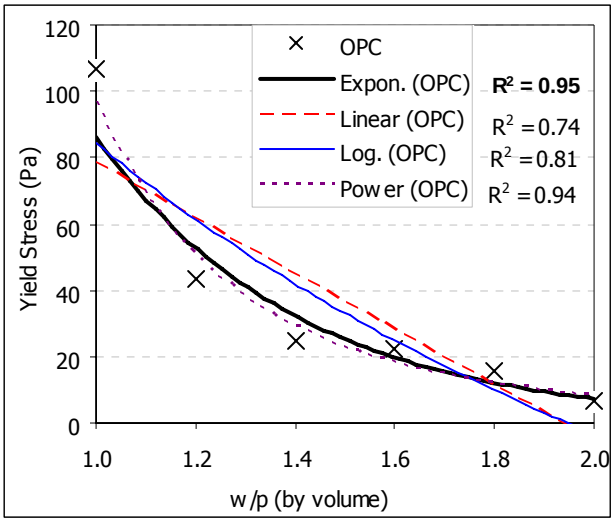


**(a) OPC Series**

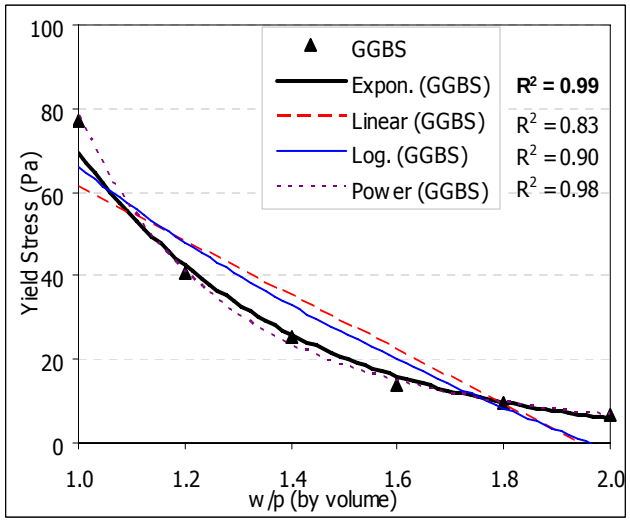


**(b) GGBS Series**

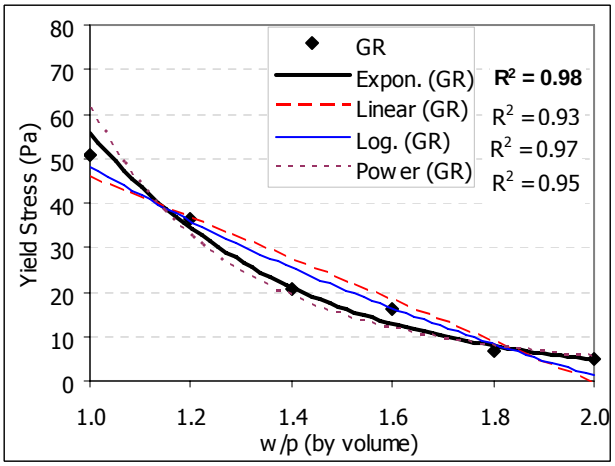


**(c ) GR Series**

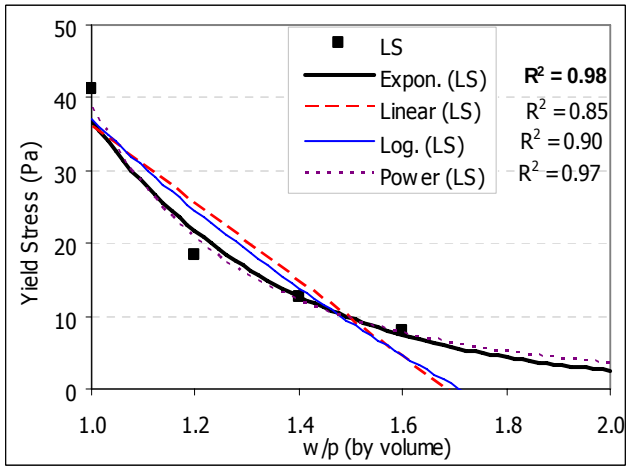


**(d) LS Series**

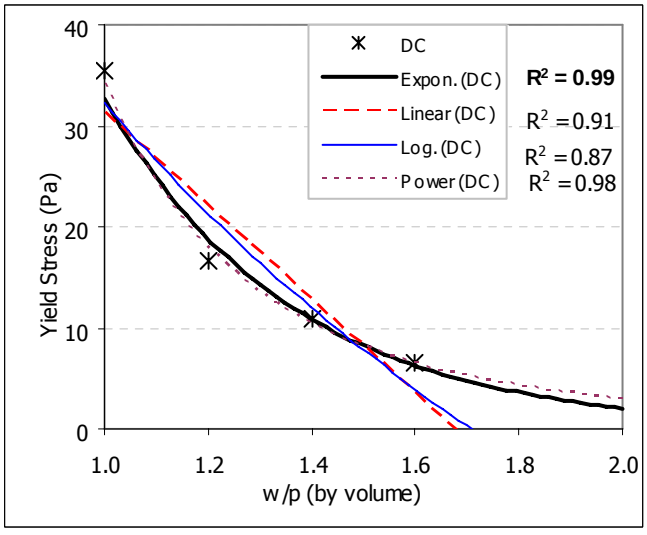


**(e) DC Series**

Fig 5.4. Relationship between yield stress and w/p with respect to different Functional Equations

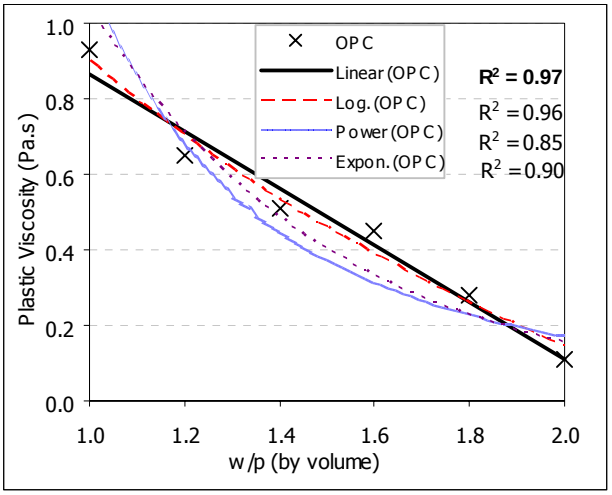


**(a) OPC Series**

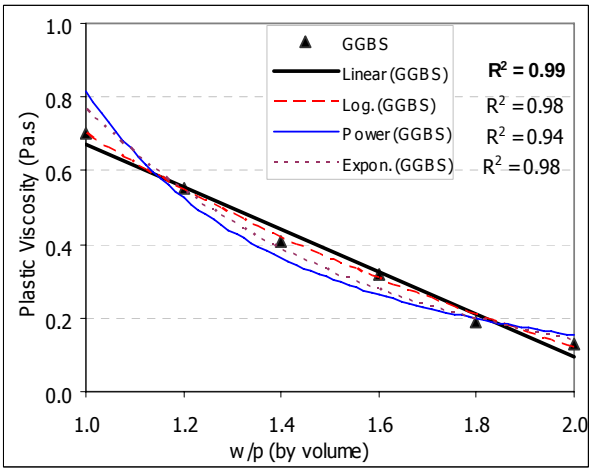


**(b) GGBS Series**

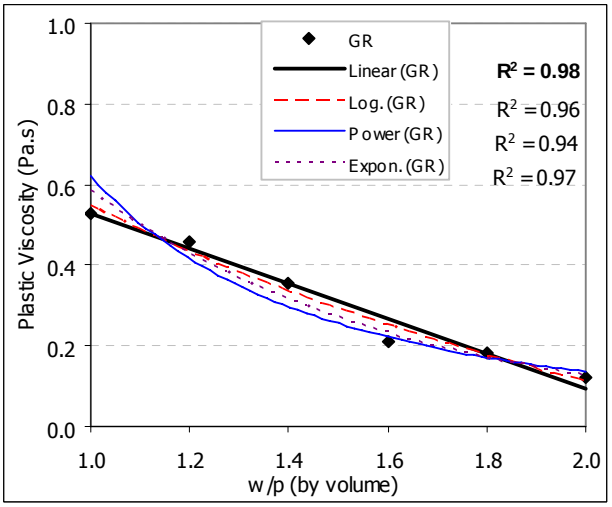


**(c ) GR Series**

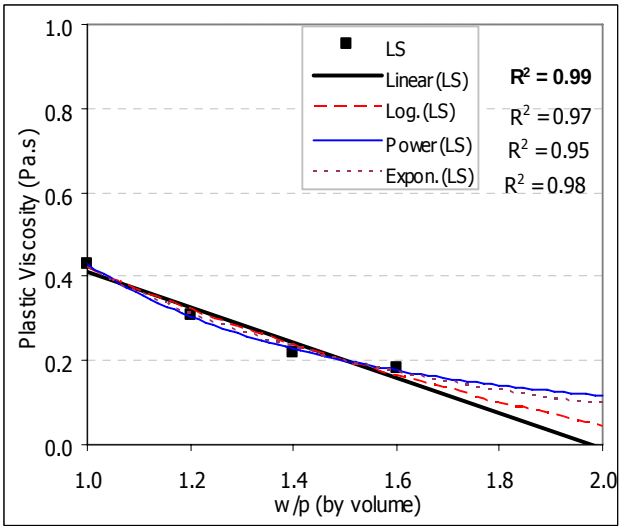


**(d) LS Series**

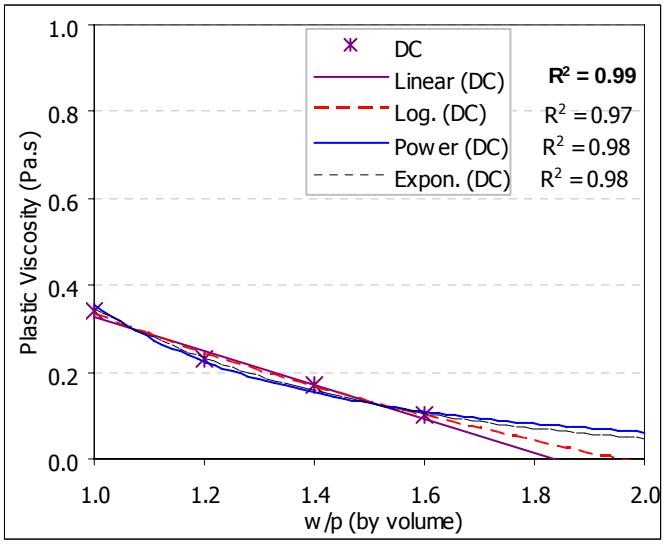


**(d) DC Series**

Fig 5.5. Relationship between plastic viscosity and w/p with respective to different Functional Equations

Among all the possible relationship, it is observed that the exponential function seems to yield the best-fit correlation between yield stress and w/p. As shown in Fig 5.6a, yield stress of the paste containing different types of powder decreased exponentially [$R^2$ = 0.94~0.99] with an increase in the water to powder ratio by volume from 1.0 to 2.0. This finding agreed well with Eq 3.10 proposed by Tattersall G. H. and Banfill P. F. G. (1983).

However, a linear relation is observed between plastic viscosity and water to powder ratio with a best-fit co-relation, $R^2$, of between 0.93~0.99. (Fig 5.6 b) Among all the types of paste sample, the OPC paste sample shows the highest yield stress and plastic viscosity while DC paste has the lowest yield stress and plastic viscosity at the same level of water to powder ratio. These two types of functional relationship have been adopted in this study.

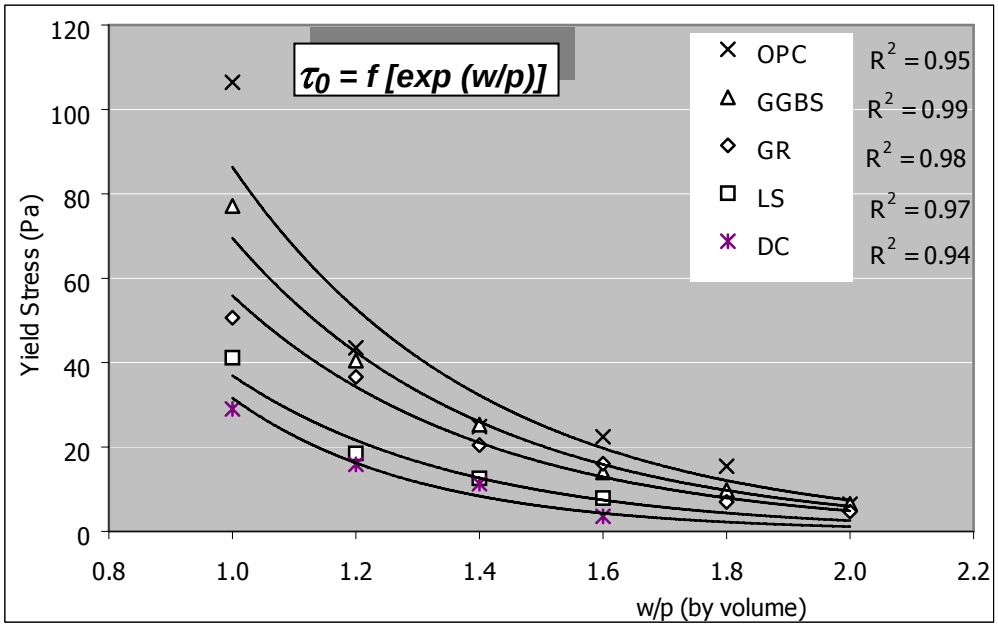


(a) Variation of Yield Stress

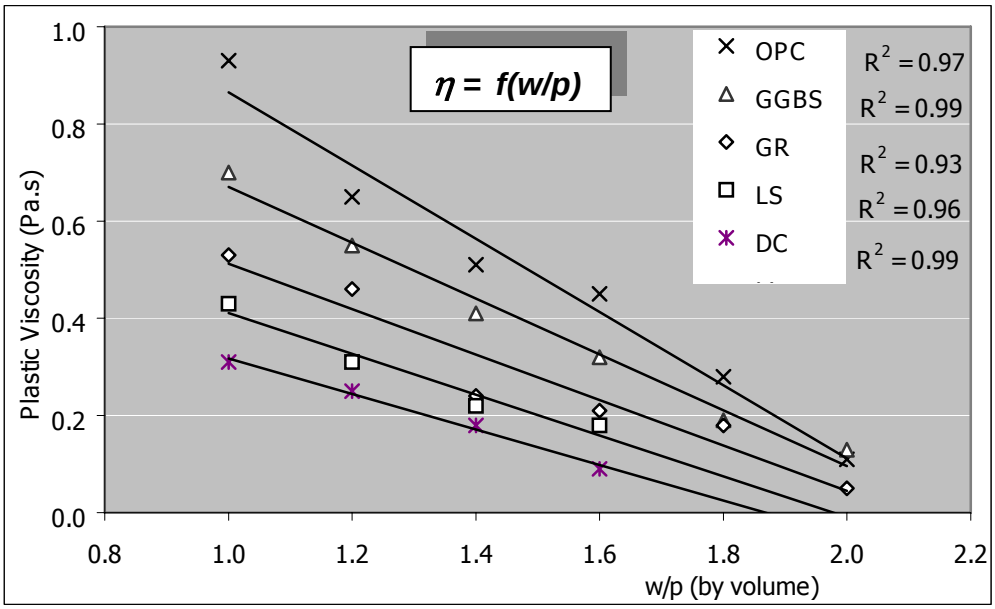


(b) Variation of Plastic Viscosity

Fig. 5.6 Relationship between rheological parameters and water/powder ratio by volume

## (b) Effect of Solid Volume Concentration

As discussed in Chapter 3, water to powder ratio can be described specifically as a form of solid volume concentration of the system.

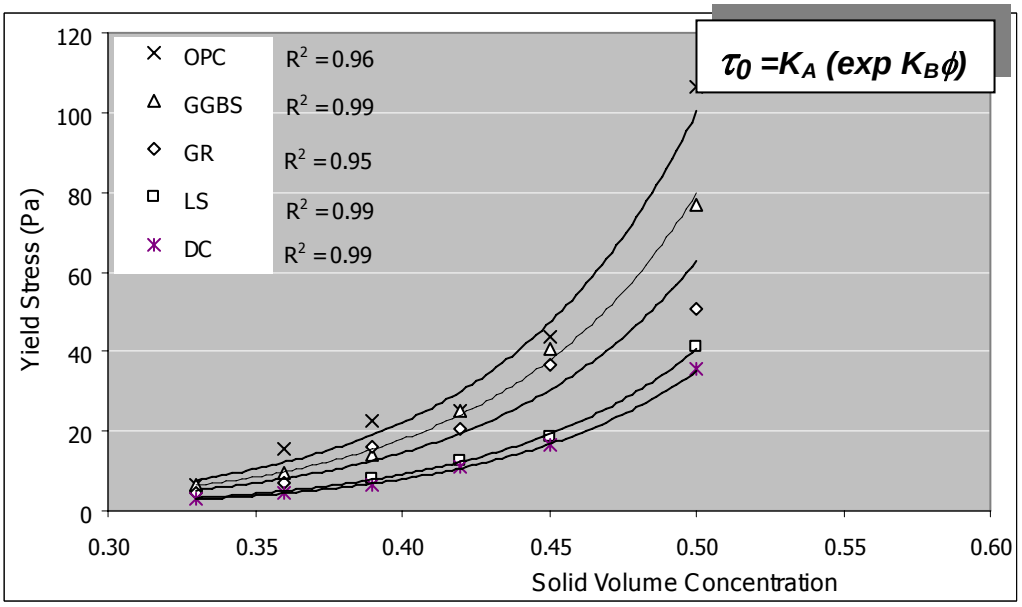


(a) Variation of Yield Stress

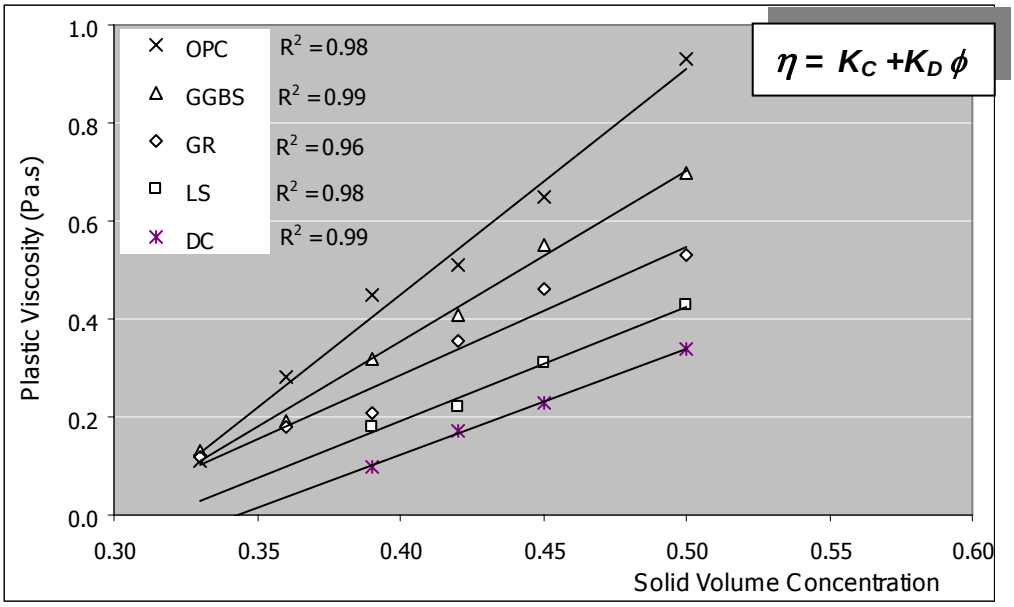


(b) Variation of Viscosity

Fig 5.7. Relationship between rheological parameters of paste and solid volume concentration

As shown in Fig 5.7 (a), the yield stress of the paste, as expected, increases exponentially with the solid volume concentration. The linear relation of increment between plastic viscosity and solid volume concentration is still observed for solid volume fractions up to 0.5 [Fig 5.7 (b)]. The solid volume concentration beyond 0.5 is not considered in this study since the nominal value of solid volume concentration in the paste mixture is below 0.5, (i.e w/c $\geq$ 0.3).

In these series of paste mixture, the mix proportions of each type of paste were carefully designed in such a way that all the mixtures contained a similar surface area of powder and equal amount of reactive powder OPC. It was also assumed that all powder particles were inert and spherical in shape. If such assumption was correct, the similar volume concentration of paste should have been given similar value of yield stress and plastic viscosity regardless of the type of powder. However it can be observed from Fig 5.7 that rheological parameters for the different paste series are not the same. The factors

contributing to such differences are particle geometry and reactivity of the powder since superplasticizer is not added to those mixes.

Among all types of powders, the paste containing pure OPC powder shows the highest yield stress and plastic viscosity while the DC paste gives the lowest yield stress and plastic viscosity at the same level of solid volume concentration. It might be that the higher rheological parameters of OPC paste are due to the effect of its high reactivity. Therefore, it can also be observed that the partially reactive powder GGBS paste gives the next level of rheological parameters. While comparing the inert fillers, the GR paste shows a higher yield stress and plastic viscosity than that of LS and DC. It might be due to the effect of the flaky and elongated particle shape of granite powder, which creates a larger contact area and higher inter-particle friction force while the paste system is sheared, resulting in higher values of yield stress and plastic viscosity. DC has much smaller size particles than LS and its angularity factor is closer to unity.

Table 5.3 summarizes the respective constants for yield stress and plastic viscosity of the different types of paste sample.

.

Table 5.3 Tabulation of respective constants for yield stress and plastic viscosity

| **Designation** | **$K_A$** | **$K_B$** | **$K_C$** | **$K_D$** |
|---|---|---|---|---|
| OPC | *0.0544* | *15.036* | *4.605* | *-1.392* |
| GGBS | *0.0458* | *14.927* | *3.491* | *-1.042* |
| GR | *0.0424* | *14.605* | *2.616* | *-0.759* |
| LS | *0.0235* | *14.905* | *2.349* | *-0.748* |
| DC | *0.0219* | *14.755* | *2.167* | *-0.743* |

From Table 5.3, the constant value of $K_A$, $K_B$, $K_C$ and $K_D$ are assumed as the function of particle geometry and reactivity of powder in each series. It is observed in the yield stress; $K_B$ values for non-reactive powder (GR, LS, DC) or reactive powder (OPC, GGBS) are more or less similar. It indicates that there is little or no influence of reactivity effect on constant $K_B$ since all the paste series contain a similar amount of reactive powder, OPC. However for $K_A$, the paste with the reactive powder OPC gives a significantly higher value than among all the types of paste series. This finding indicates that reactivity of powder or reactivity factor contributes to the different $K_A$ values of the different paste sample. Comparisons between non-reactive powders, $K_A$ value of GR series give the highest of all paste series (GR, LS, DC). It might be due to the fact that the angularity factor for irregular particle shape of GR powder is higher than those of LS and DC. From these observations, it is assumed that $K_B$ is a function of particle geometry or angularity of powder while $K_A$ is a function of both reactivity and angularity of the powder.

Similarly for plastic viscosity, it is observed that both values of $K_C$ and $K_D$ for non-reactive powders (GR, LS, DC) are much lower than those of reactive powders (OPC, GGBS). Therefore, it is assumed that both $K_C$ and $K_D$ can be described as a function of both reactivity and angularity of the powder.

It can be deduced from the above data that the particle reactivity and particle shape of powders determine the variations in paste rheology. Thus, beyond a solid volume concentration of 0.35 or water to powder ratio of 2.0 (by volume), both rheological parameters seems to converge to a single level indicating the minor effect of reactivity and shape of powders. This phenomenon can be explained by the fact that the

higher water content in the paste system leads to the formation of a thicker water film around the particles and reduces the surface interference effect. Thus, the thickness of the water film around each powder particle is an important contributing factor on the behavior of rheological parameters of the paste.

## (c) Effect of Thickness of Water Film

Fig 5.8 presents the variation of rheological parameters with the thickness of water film around the particle.

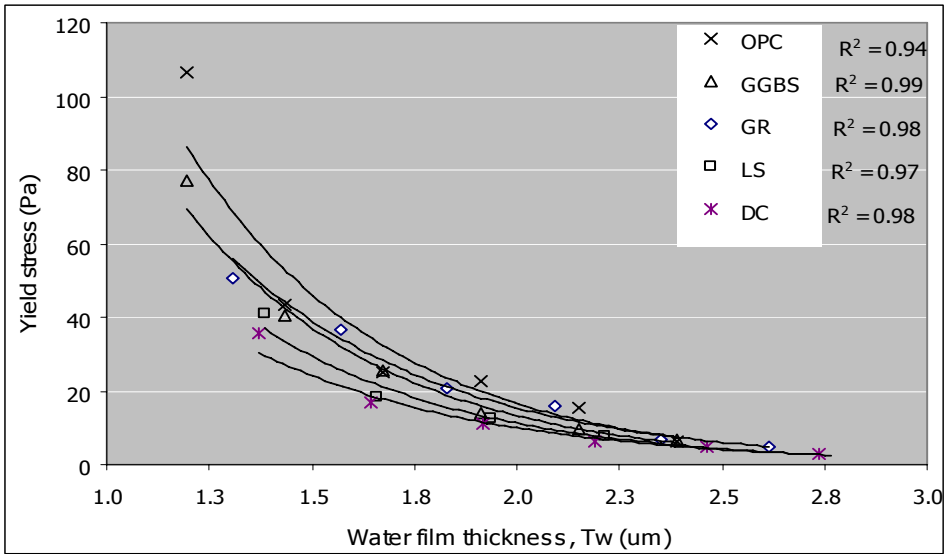


(a) Variation of Yield Stress

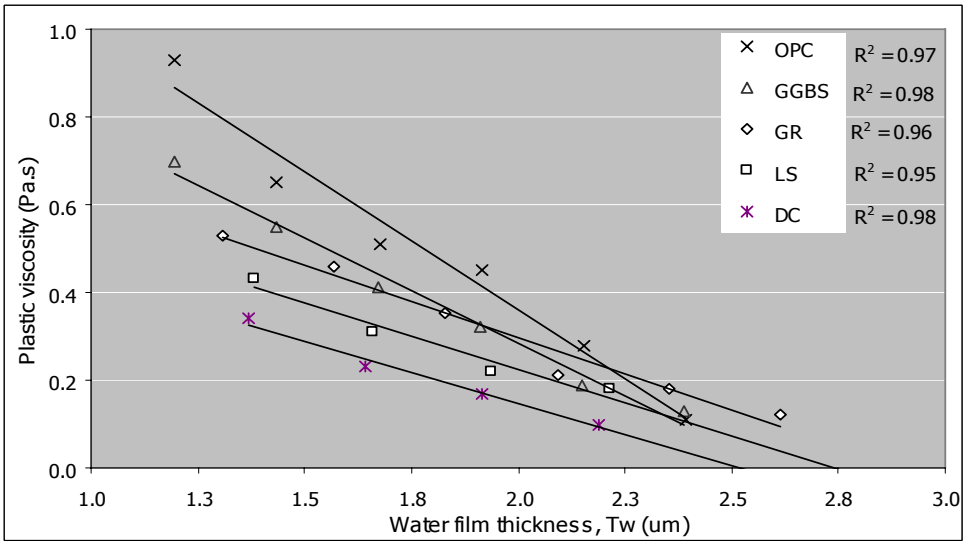


(a) Variation of Plastic Viscosity

Fig 5.8 Relationship between rheological parameters of paste and water film thickness

Table 5.4 Functional equation for best fit line of yield stress and plastic viscosity of mixes

| Designation | Yield Stress, $\tau_0$ (Pa) | Plastic Viscosity, $\eta_0$ (Pa.s) |
|---|---|---|
| OPC | $\tau_0=1008.91e^{-2.05Tw}$ | $\eta_0$=1.62-0.63Tw |
| GGBS | $\tau_0=812.849e^{-2.05Tw}$ | $\eta_0$=1.24-0.48Tw |
| GR | $\tau_0=641.31e^{-1.87Tw}$ | $\eta_0$=0.96-0.33Tw |
| LS | $\tau_0=534.63e^{-1.93Tw}$ | $\eta_0$=0.83-0.31Tw |
| DC | $\tau_0=342.54e^{-1.77Tw}$ | $\eta_0$=0.72-0.28Tw |

It is possible that for non-reactive spherical shape particle, the same thickness of water film or similar inter-particle distance around the particle will give similar yield stress and plastic viscosity values regardless of the type of powder because inter-particle potential, which leads to particle flocculation, is dependent on inter-particle distance. However it is observed in Fig 5.8 that the yield stresses as well as the plastic viscosity of the different types of paste are not the same even if they are assumed to have the same water film thickness. The secondary parameters that cause the difference in the rheological parameters of the paste fraction containing different types of powder are the particle shape and particle reactivity of these powders.

## 5.2.2 Secondary Parameters

As discussed in Section 5.2.1, the rheological parameters of paste fraction mainly depend on the solid volume concentration of the mix. However it can be observed from Fig 5.5 and 5.6 that the surface geometry or particle shape and particle reactivity of powders are also reasons that cause the difference in rheological parameters of the paste

which has similar solid volume concentration. Therefore, this section investigates the secondary parameters which affect the rheological parameters of the paste.

## (a) Angularity Factor

The surface geometry or particle shape of different powders will be described in this study as "Angularity Factor". The angularity factor of each type of powders was investigated by applying Micro V2.17 software to the respective particle size distribution of powder. Laser Scattering Particle Size Analyzer, the Malvern Mastersizer (Fig. 4.1) was used to determine the particle size distribution of each type of powders. Every powder sample was analyzed three times and the tests procedure for one test sample is repeated three times. A total of nine tests were conducted for each powder in order to obtain the reliable data. The angularity factor for each type of powder was calculated from Eq 3.21 and the average angularity of the system containing different types of powder was calculated from Eq 3.22. Tables 5.2 to 5.6 present the analysis data and angularity factor for each type of powder.

Table 5.5 Summary of Angularity Factor for OPC powder from particle analysis

| Designation | Volume Dia (um) $d_{0i}^{v}$ | Surface Dia (um) $d_{0i}^{sp}$ | $d_{0i}^{sp} / d_{0i}^{v}$ | $d_{0i}^{v}\alpha / d_{0i}^{sp}$ | Sphericity Factor $\psi_{Li}$ | Angularity Factor $1/\psi_{Li}$ |
|---|---|---|---|---|---|---|
| TEST 1 | 20.84 | 3.85 | 0.18 | 5.41 | 0.66 | 1.53 |
| | 20.17 | 3.74 | 0.19 | 5.39 | 0.66 | 1.52 |
| | 20.35 | 3.71 | 0.18 | 5.49 | 0.65 | 1.53 |
| | *20.45* | *3.77* | *0.18* | *5.43* | *0.66* | *1.53* |
| TEST 2 | 20.69 | 2.64 | 0.13 | 7.84 | 0.60 | 1.67 |
| | 19.86 | 2.85 | 0.14 | 6.97 | 0.62 | 1.62 |
| | 20.24 | 2.55 | 0.13 | 7.94 | 0.60 | 1.68 |
| | *20.26* | *2.68* | *0.13* | *7.58* | *0.60* | *1.66* |
| TEST 3 | 19.04 | 2.13 | 0.11 | 8.93 | 0.58 | 1.73 |
| | 19.71 | 2.22 | 0.11 | 10.69 | 0.58 | 1.73 |
| | 20.06 | 2.15 | 0.14 | 10.13 | 0.57 | 1.75 |
| | *19.67* | *2.34* | *0.12* | *9.91* | *0.59* | *1.70* |
| **Average** | **20.15** | **2.94** | **0.15** | **7.64** | **0.61** | **1.63** |

Table 5.6 Summary of Angularity Factor for GGBS powder from particle analysis

| Designation | Volume Dia (um) $d_{0i}^{v}$ | Surface Dia (um) $d_{0i}^{sp}$ | $d_{0i}^{sp} / d_{0i}^{v}$ | $d_{0i}^{v\alpha} / d_{0i}^{sp}$ | Sphericity Factor $\psi_{Li}$ | Angularity Factor $1/\psi_{Li}$ |
|---|---|---|---|---|---|---|
| TEST 1 | 18.21 | 3.28 | 0.18 | 5.55 | 0.65 | 1.54 |
| | 17.01 | 3.54 | 0.21 | 4.81 | 0.68 | 1.48 |
| | 17.21 | 3.53 | 0.21 | 4.88 | 0.67 | 1.49 |
| | *17.48* | *3.45* | *0.20* | *5.08* | *0.67* | *1.50* |
| TEST 2 | 17.06 | 3.05 | 0.18 | 5.59 | 0.65 | 1.54 |
| | 17.02 | 3.10 | 0.18 | 5.49 | 0.65 | 1.53 |
| | 16.88 | 3.02 | 0.18 | 5.59 | 0.65 | 1.54 |
| | *16.99* | *3.06* | *0.18* | *5.56* | *0.15* | *1.54* |
| TEST 3 | 16.98 | 3.23 | 0.19 | 5.26 | 0.66 | 1.51 |
| | 16.83 | 3.22 | 0.19 | 5.23 | 0.66 | 1.51 |
| | 17.02 | 3.23 | 0.19 | 5.27 | 0.66 | 1.51 |
| | *16.94* | *3.23* | *0.19* | *5.25* | *0.66* | *1.51* |
| **Average** | **17.14** | **3.24** | **0.19** | **5.3** | **0.66** | **1.52** |

Table 5.7 Summary of Angularity Factor for GR powder from particle analysis

| Designation | Volume Dia (um) $d_{0i}^{v}$ | Surface Dia (um) $d_{0i}^{sp}$ | $d_{0i}^{sp} / d_{0i}^{v}$ | $d_{0i}^{v\alpha} / d_{0i}^{sp}$ | Sphericity Factor $\psi_{Li}$ | Angularity Factor $1/\psi_{Li}$ |
|---|---|---|---|---|---|---|
| TEST 1 | 59.81 | 2.78 | 0.05 | 21.51 | 0.46 | 2.15 |
| | 61.62 | 2.81 | 0.05 | 22.04 | 0.46 | 2.17 |
| | 58.09 | 2.75 | 0.05 | 21.12 | 0.47 | 2.14 |
| | *59.94* | *2.75* | *0.05* | *21.56* | *0.46* | 2.15 |
| TEST 2 | 59.91 | 2.32 | 0.04 | 28.52 | 0.44 | 2.25 |
| | 60.51 | 2.55 | 0.04 | 23.73 | 0.45 | 2.21 |
| | 58.27 | 2.15 | 0.04 | 27.10 | 0.44 | 2.28 |
| | *59.56* | *2.34* | *0.04* | *25.55* | *0.44* | 2.25 |
| TEST 3 | 59.29 | 3.68 | 0.06 | 16.11 | 0.50 | 2.00 |
| | 59.29 | 3.75 | 0.06 | 15.81 | 0.50 | 1.99 |
| | 59.88 | 3.66 | 0.06 | 16.36 | 0.50 | 2.01 |
| | *59.49* | *3.70* | *0.06* | *16.09* | *0.50* | 2.00 |
| **Average** | **59.66** | **2.94** | **0.05** | **21.07** | **0.47** | **2.14** |

Table 5.8 Summary of Angularity Factor for LS powder from particle analysis

| Designation | Volume Dia (um) $d_{0i}^{v}$ | Surface Dia (um) $d_{0i}^{sp}$ | $d_{0i}^{sp} / d_{0i}^{v}$ | $d_{0i}^{v}\alpha / d_{0i}^{sp}$ | Sphericity Factor $\psi_{Li}$ | Angularity Factor $1/\psi_{Li}$ |
|---|---|---|---|---|---|---|
| TEST 1 | 79.29 | 6.20 | 0.08 | 12.79 | 0.53 | 1.89 |
| | 76.20 | 6.05 | 0.08 | 12.6 | 0.53 | 1.88 |
| | 77.40 | 6.11 | 0.08 | 12.67 | 0.53 | 1.89 |
| | *77.63* | *6.12* | *0.08* | *12.68* | *0.53* | 1.89 |
| TEST 2 | 75.72 | 6.55 | 0.09 | 11.56 | 0.54 | 1.84 |
| | 74.38 | 6.34 | 0.09 | 11.73 | 0.54 | 1.85 |
| | 76.28 | 6.49 | 0.09 | 11.75 | 0.54 | 1.85 |
| | *75.46* | *6.46* | *0.09* | *11.68* | *0.54* | 1.85 |
| TEST 3 | 74.85 | 5.89 | 0.08 | 12.71 | 0.53 | 1.89 |
| | 75.96 | 5.73 | 0.08 | 13.26 | 0.52 | 1.91 |
| | 74.96 | 5.67 | 0.08 | 13.22 | 0.52 | 1.91 |
| | *75.26* | *5.76* | *0.08* | *13.06* | *0.53* | 1.90 |
| **Average** | **76.12** | **6.11** | **0.08** | **12.48** | **0.53** | **1.88** |

Table 5.9 Summary of Angularity Factor for DC powder from particle analysis

| Designation | Volume Dia (um) $d_{0i}^{v}$ | Surface Dia (um) $d_{0i}^{sp}$ | $d_{0i}^{sp} / d_{0i}^{v}$ | $d_{0i}^{v}\alpha / d_{0i}^{sp}$ | Sphericity Factor $\psi_{Li}$ | Angularity Factor $1/\psi_{Li}$ |
|---|---|---|---|---|---|---|
| TEST 1 | 70.81 | 7.36 | 0.10 | 9.62 | 0.57 | 1.76 |
| | 71.25 | 7.48 | 0.10 | 9.53 | 0.57 | 1.76 |
| | 70.12 | 7.68 | 0.11 | 9.13 | 0.58 | 1.74 |
| | *70.73* | *7.51* | *0.11* | *9.43* | *0.57* | 1.75 |
| TEST 2 | 69.91 | 6.32 | 0.09 | 11.06 | 0.55 | 1.82 |
| | 70.51 | 6.25 | 0.09 | 11.28 | 0.55 | 1.83 |
| | 70.26 | 6.15 | 0.09 | 11.42 | 0.54 | 1.84 |
| | *70.23* | *6.24* | *0.09* | *11.26* | *0.55* | 1.83 |
| TEST 3 | 69.29 | 6.01 | 0.09 | 11.53 | 0.54 | 1.84 |
| | 69.71 | 6.03 | 0.09 | 11.56 | 0.54 | 1.84 |
| | 72.14 | 6.06 | 0.08 | 11.90 | 0.54 | 1.86 |
| | *70.38* | *6.03* | *0.09* | *11.66* | *0.54* | 1.85 |
| **Average** | **70.45** | **6.64** | **0.09** | **10.70** | **0.55** | **1.81** |

### (b) Reactivity Factor

A paste is a dense suspension of cement and filler particles in water. As the mean size of these particles is of the order of 10 μm, inter-particle forces and gravity are forces that play an important role concerning the macroscopic characteristic of such suspensions. The higher the reactiveness of the particle, the stronger the force induced between particle groups and the result is a state of strongeer flocculation.

At a given rate of flow in a given system, the inter-particle forces between the particles are directly proportional to the zeta potential [*Power. T.C., 1968*]. Therefore in this study, the inter-particle forces or reactivity of the powder will be described as a function of the change in zeta potential.

The simplest way of observing the relative strength of inter-particle forces among particles due to a change in zeta potential in the suspension is to measure the volume of sediment of a given quantity of suspended materials [*Power. T.C., 1968*]. It is the fact that the stronger the inter-particle force, the greater the specific volume of the sediment or sedimentation volume.

The experiment was conducted using about 50 ml of fluid was placed inside a 150 ml capacity glass test tube and about 20g of powder sample was added into it. The test tube containing the fluid and powder sample was shaken briefly and allowed to rest for about 5 min. Then it was shaken again vigorously by hand for another 1 min and placed in the rack for 48 hours. After the designated settlement time was reached, the volume of settlement was measured and recorded as the volume of settlement per unit volume of solid.

In order to investigate the reactiveness of the powder, the fluid was prepared with various proportions of water and ethyl alcohol, the mixture ranging from pure water to pure ethyl alcohol. Ethyl alcohol was chosen as a type of fluid because the reactive powders in this study, OPC and GGBS, showed minimum reaction with this liquid.

The test results are presented in Fig. 5.9. At ordinate zero, the sedimentation volume is that of powder in pure water. It can be observed from the figure that the sedimentation volume of OPC and GGBS powder increased with an increased in ethyl alcohol percentage of up to 50%. Beyond 50% of alcohol, a significant decrease in sedimentation volumes are observed. Similar sedimentation volumes for all tested powder (inert or reactive) are found in pure ethyl alcohol solution. These findings indicate that no chemical reaction occurred between the powder particles when they are fully immersed in ethyl alcohol solution.

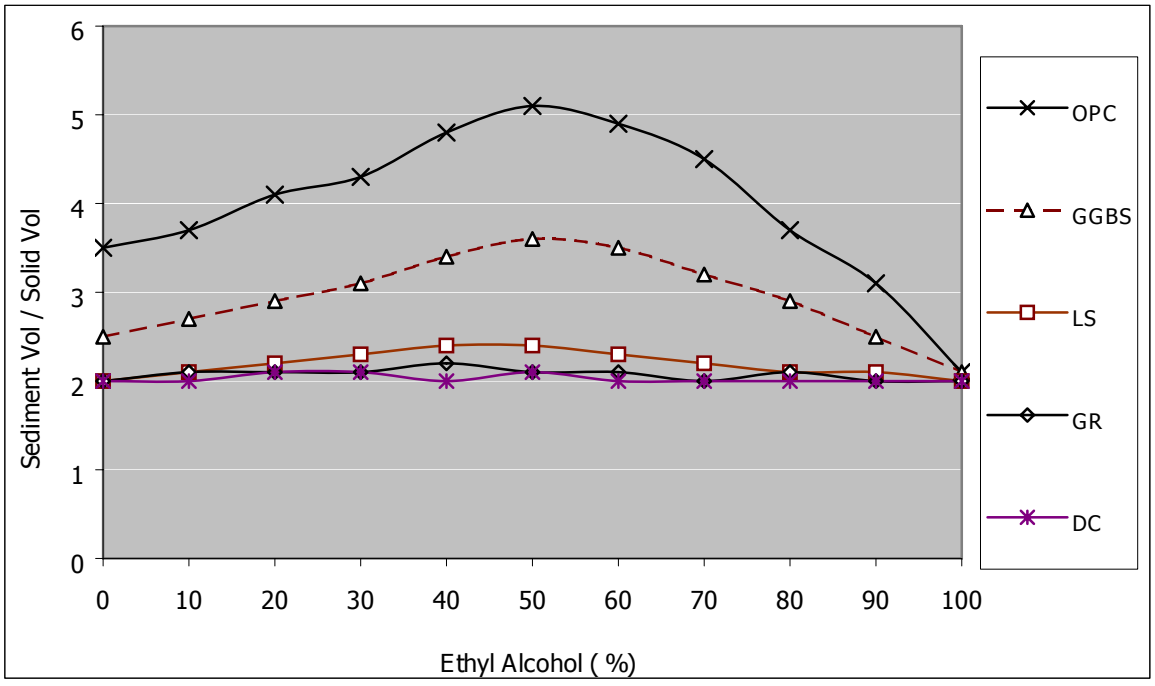


Fig 5.9. Relationship between sedimentation volume and proportions of water and ethyl alcohol

The net inter-particle attractions of OPC and GGBS particles in water are indicated not only by sedimentation volume but also by the fact that during and after settlement, the water above the sediment remains clear, that is, free from cloudy appearance caused by small particles. This means that the small and larger particles stick together and fall to the bottom.

The properties of a suspension of OPC and GGBS in water are due mainly to the electrolytically controlled zeta potential and to the strongly adhering films of water. When ethyl alcohol was substituted for some of the water, sedimentation volume increased as shown in the figure, signifying an increase in cohesive strength. This might be due to the fact that ethyl alcohol tends to dissolve the layer of adsorbed water molecules and was itself adsorbed on the surface of particles. Since the reaction product, calcium hydroxide of OPC and GGBS powder is less soluble in ethyl alcohol than in water, calcium ion concentration diminished and the positive electrostatic charge due to adsorbed calcium ions correspondingly diminished as ethyl alcohol was substituted with water. After the concentration of adsorbed positive ions decreased to a certain level, the positive charges on the surface of the particle just offset the intrinsic negative charges. [*Power. T.C., 1968*]. Thus the rise of the curve up the point representing about 50% ethyl alcohol is indicative of the effect of removing electrostatic repulsion between particles.

With a further increase in the percentage of ethyl alcohol, there was a corresponding further decrease in calcium ion concentration and the surface charge of particle become progressively more negative. The repulsive forces between the particles become dominant when the ethyl alcohol percentage increased. The charge finally

reached a maximum negative value when the point representing pure alcohol was reached. Thus, minimum sedimentation volume is observed at that point.

Slight or no volume change of LS, GR and DC powders are observed when those powders are immersed in pure water or pure ethyl alcohol. The smallest particles of those powders were observed to remain suspended for a relatively long period after the coarser ones had settled down. Similar findings were also observed in OPC and GGBS powders in 100% pure ethyl alcohol solution. These findings confirmed that LS, GR and DC powders are non-reactive powders whose inter-particle attraction or zeta-potentials are significantly lower compared to the reactive powders OPC and GGBS.

Therefore in this study, the reactivity factor for each type of powders was calculated as the ratio of sediment volume in pure water to that in pure alcohol as shown in Table 5.10.

Table 5.10 Reactivity Factor for different types of powder, δ

| Designation | Sediment Volume in Water (ml) | Sediment Volume in Alcohol (ml) | Reactivity Factor, δ |
|---|---|---|---|
| **OPC 1** | 22.3 | 13.3 | 1.68 |
| **GGBS 1** | 17.25 | 14.5 | 1.2 |
| **LS 1** | 14.8 | 14.8 | 1.0 |
| **GR 1** | 15.4 | 15.4 | 1.0 |
| **DC 1** | 11.1 | 11.1 | 1.0 |

## (c ) Repulsivity Factor

It is obvious that the suspensions have good flowing properties when repulsive inter-particle forces are greater then attractive Van der Waals forces. By adding the

superplasticizer to the system, the surface electric charges occurred on each particle and enhance the dominance of the repulsive inter-particle forces [Banfill, P.F.G.1983].

The same principle as reactivity factor was applied to determined repulsivity of the powders. However in this experiment, superplasticizer (ADVA108) was used as a fluid instead of ethyl alcohol, the mixture ranging from pure water to pure superplasticizer. DAVA 108 was chosen in this case because it contains a retarder that can enhance the setting time of the cement and allow the particle to settle in the solution for a longer time. Its retardation effect also makes it a suitable type of superplasticizer in most applications a tropical areas like Singapore.

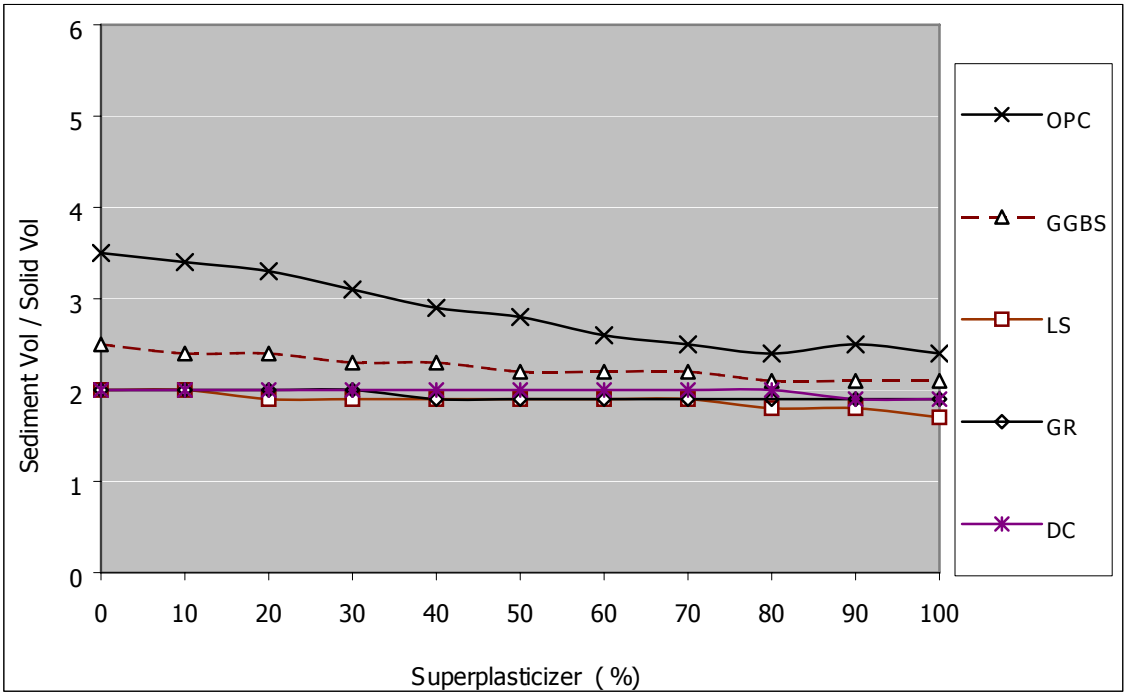


Fig 5.10 Relationship between sedimentation volume and various proportions of water and superplasticizer

The test results are presented in Fig. 5.10. The sedimentation volume of OPC and GGBS reduce significantly with an increase in superplasticizer content up to a certain level, about 60%. Beyond that level, the sedimentation volume seems constant regardless of the increased in superplasticizer content. These findings indicate that there is a maximum repulsion effect of superplasticizer on the powder up to a particular level. Beyond that level, superplasticizer contributes little or no repulsion effect on the powder. It is also observed that for LS, GR and DC powders, the changes in sedimentation volume are not significant when those powders are immersed in pure water or pure superplasticizer.

Therefore in this study, the reactivity factor for each type of powders was calculated as the ratio of sediment volume in pure water to that in the particular level of superplasticizer in which the minimum volume of sedimentation volume was observed as shown in Table 5.11. Though repulsivity factor for LS and GR in this experiments are marginally above 1, which may be due to experimental uncertainties, it is assumed that the repulsivity factor for all the inter filler in this study, LS, GR, DC are more likely to be 1.0, meaning that there is no significant influence on the repulsion effect for these powders when superplasticizer is added to the mix.

Table 5.11 Repulsivity Factor for different types of powder, $\alpha_{rep}$

| Designation | Sediment Volume in Water (ml) | Sediment Volume in Alcohol (ml) | Repulsivity Factor $\alpha_{rep}$ |
|---|---|---|---|
| **OPC 1** | 22.3 | 15.88 | 1.40 |
| **GGBS 1** | 17.25 | 15.18 | 1.14 |
| **LS 1** | 14.8 | 14.06 | 1.05* |
| **GR 1** | 15.4 | 14.63 | 1.05* |
| **DC 1** | 11.1 | 11.1 | 1.0 |

* value taken as 1.o for inert powder

## 5.3 Verification of Proposed Model

In order to verify the paste rheological model presented in Chapter 3, a series of tests was conducted under the following conditions and examined the variation of the rheological parameters with reference to angularity, reactivity and repulsivity factors of particles under different water film thicknesses.

### 5.3.1 SERIES 1 (no repulsivity factor is considered)

a) To minimize the size effect of particle, the total surface area of all powders in the paste was fixed to (217 ± 2) $m^2$

b) To maintain the reactiveness of the paste, OPC content in the mix was fixed at 500 g. The filler content was varied to achieve the designated total surface area.

c) Water to powder ratio by volume was varied from 1.0 to 2.0.

d) No chemical admixture was added to the mix. (no repulsivity factor)

The detail mix proportions for different paste are presented in Table 5.12.

As discussed in section 5.1.1, the usage of reactive powder OPC and GGBS contribute to the reactiveness of the paste system in addition to their particle shape. Based on the mix proportion presented in Table 5.12, the angularity factor and reactivity factor of the paste containing different types of powder are summarized in Table 5.13.

Table 5.12- Mix proportions for different types of paste (w/o chemical admixture) to verify Angularity and Reactivity Factor

0

| Designation | w/p | water | Cement | | Filler | | Total powder | | SURFACE AREA | | | Film Thickness |
|---|---|---|---|---|---|---|---|---|---|---|---|---|
| | (by Vol) | (g) | weight (g) | volume (lit) | weight (g) | volume (lit) | T. weight (g) | T. voulme (lit) | OPC (m2) | filler(m2) | Total Area | Tw (um) |
| OPC 1-1 | 1.0 | 260 | 820 | 0.26 | 0 | 0.00 | 820 | 0.26 | 218 | 0 | 218 | 1.20 |
| OPC 1-2 | 1.2 | 312 | 820 | 0.26 | 0 | 0.00 | 820 | 0.26 | 218 | 0 | 218 | 1.44 |
| OPC 1-3 | 1.4 | 364 | 820 | 0.26 | 0 | 0.00 | 820 | 0.26 | 218 | 0 | 218 | 1.67 |
| OPC 1-4 | 1.6 | 417 | 820 | 0.26 | 0 | 0.00 | 820 | 0.26 | 218 | 0 | 218 | 1.91 |
| OPC 1-5 | 1.8 | 469 | 820 | 0.26 | 0 | 0.00 | 820 | 0.26 | 218 | 0 | 218 | 2.15 |
| OPC 1-6 | 2.0 | 521 | 820 | 0.26 | 0 | 0.00 | 820 | 0.26 | 218 | 0 | 218 | 2.39 |
| GGBS 1-1 | 1.0 | 260 | 500 | 0.16 | 290 | 0.10 | 790 | 0.26 | 133 | 85 | 218 | 1.19 |
| GGBS 1-2 | 1.2 | 313 | 500 | 0.16 | 290 | 0.10 | 790 | 0.26 | 133 | 85 | 218 | 1.43 |
| GGBS 1-3 | 1.4 | 365 | 500 | 0.16 | 290 | 0.10 | 790 | 0.26 | 133 | 85 | 218 | 1.67 |
| GGBS 1-4 | 1.6 | 417 | 500 | 0.16 | 290 | 0.10 | 790 | 0.26 | 133 | 85 | 218 | 1.91 |
| GGBS 1-5 | 1.8 | 469 | 500 | 0.16 | 290 | 0.10 | 790 | 0.26 | 133 | 85 | 218 | 2.15 |
| GGBS 1-6 | 2.0 | 521 | 500 | 0.16 | 290 | 0.10 | 790 | 0.26 | 133 | 85 | 218 | 2.39 |
| GR 1-1 | 1.0 | 283 | 500 | 0.16 | 330 | 0.12 | 830 | 0.28 | 133 | 84 | 217 | 1.31 |
| GR 1-2 | 1.2 | 340 | 500 | 0.16 | 330 | 0.12 | 830 | 0.28 | 133 | 84 | 217 | 1.57 |
| GR 1-3 | 1.4 | 397 | 500 | 0.16 | 330 | 0.12 | 830 | 0.28 | 133 | 84 | 217 | 1.83 |
| GR 1-4 | 1.6 | 453 | 500 | 0.16 | 330 | 0.12 | 830 | 0.28 | 133 | 84 | 217 | 2.09 |
| GR 1-5 | 1.8 | 510 | 500 | 0.16 | 330 | 0.12 | 830 | 0.28 | 133 | 84 | 217 | 2.35 |
| GR 1-6 | 2.0 | 567 | 500 | 0.16 | 330 | 0.12 | 830 | 0.28 | 133 | 84 | 217 | 2.62 |
| LS 1-1 | 1.0 | 299 | 500 | 0.16 | 380 | 0.14 | 880 | 0.30 | 133 | 84 | 216 | 1.38 |
| LS 1-2 | 1.2 | 359 | 500 | 0.16 | 380 | 0.14 | 880 | 0.30 | 133 | 84 | 216 | 1.66 |
| LS 1-3 | 1.4 | 419 | 500 | 0.16 | 380 | 0.14 | 880 | 0.30 | 133 | 84 | 216 | 1.94 |
| LS 1-4 | 1.6 | 479 | 500 | 0.16 | 380 | 0.14 | 880 | 0.30 | 133 | 84 | 216 | 2.21 |
| LS 1-5 | 1.8 | 539 | 500 | 0.16 | 380 | 0.14 | 880 | 0.30 | 133 | 84 | 216 | 2.49 |
| LS 1-6 | 2.0 | 599 | 500 | 0.16 | 380 | 0.14 | 880 | 0.30 | 133 | 84 | 216 | 2.77 |
| DC 1-1 | 1.0 | 300 | 500 | 0.16 | 510 | 0.14 | 1010 | 0.30 | 133 | 87 | 219 | 1.37 |
| DC 1-2 | 1.2 | 360 | 500 | 0.16 | 510 | 0.14 | 1010 | 0.30 | 133 | 87 | 219 | 1.64 |
| DC 1-3 | 1.4 | 421 | 500 | 0.16 | 510 | 0.14 | 1010 | 0.30 | 133 | 87 | 219 | 1.92 |
| DC 1-4 | 1.6 | 481 | 500 | 0.16 | 510 | 0.14 | 1010 | 0.30 | 133 | 87 | 219 | 2.19 |
| DC 1-5 | 1.8 | 541 | 500 | 0.16 | 510 | 0.14 | 1010 | 0.30 | 133 | 87 | 219 | 2.46 |
| DC 1-6 | 2.0 | 601 | 500 | 0.16 | 510 | 0.14 | 1010 | 0.30 | 133 | 87 | 219 | 2.74 |

Table 5.13 Angularity and Reactivity Factor for different types of paste sample

| Designation | Powder Type | | Size Factor | | | Angularity Factor | | | Reactivity Factor | | |
|---|---|---|---|---|---|---|---|---|---|---|---|
| | OPC | Filler | $d_{max}$ | $d_{min}$ | $d_{max}/d_{min}$ | $1/\psi_{opc}$ | $1/\psi_{filler}$ | $1/\psi_R$ | $\delta_{opc}$ | $\delta_{filler}$ | $\delta_R$ |
| **OPC 1** | OPC | - | 20 | 20 | 1.00 | 1.63 | - | 1.63 | 1.68 | - | 1.68 |
| **GGBS 1** | OPC | GGBS | 20 | 17 | 1.18 | 1.63 | 1.52 | 1.82 | 1.68 | 1.20 | 1.49 |
| **LS 1** | OPC | LS | 76 | 20 | 3.80 | 1.63 | 1.88 | 6.92 | 1.68 | 1.0 | 1.41 |
| **GR 1** | OPC | GR | 59 | 20 | 2.95 | 1.63 | 2.14 | 5.96 | 1.68 | 1.0 | 1.41 |
| **DC 1** | OPC | DC | 70 | 20 | 3.50 | 1.63 | 1.81 | 6.16 | 1.68 | 1.0 | 1.41 |

Under this controlled condition, the yield stress, $\tau_p$ , and plastic viscosity, $\eta_p$, of the paste system containing different types of powder can be calculated by applying proposed equations given in Chapter 3. The repulsivity in the mix was ignored as the mixes were designed in such a way that no chemical admixture is incorporated ($\alpha_{rep}=1.0$). Thus, Eq 3.25 and 3.26 presented in Chapter 3 are modified as .

**Yield Stress:** $$\tau_p = K_1 \frac{\delta_R}{\psi_{LR}} \exp\left[\frac{K_2}{\psi_{LR}} . \frac{1}{1 + T_W\left(S_P / V_W\right)}\right] \qquad \textit{Eq. (5.1)}$$

**Viscosity :** $$\eta_p = \left[K_3 + \frac{K_4 \delta_R}{\psi_{LR}} . \frac{1}{1 + T_W\left(S_P / V_W\right)}\right] \qquad \textit{Eq. (5.2)}$$

Where $\delta_R$ is the average reactivity factor of the paste suspension, which is mainly contributed by the OPC in GR, LS and DC paste. $1/\psi_{LR}$ is the average angularity factor from the combined shape effect of powders in the paste suspension. $T_W$ is the thickness of water film (um) around the powder particles in the system. $S_P$ and $V_W$ are the total surface area ($m^2$) and volume ($m^3$) of powder particles in the paste suspension. $K_1$, $K_2$, $K_3$, $K_4$ are empirical constants which were determined by using least square

exponential method from the equations of different paste mixture with the input value of $\tau_p$, $\eta_p$. As it is mentioned in this study, these are purely empirical constants derived from experimental data. In order to specify those empirical constants, five types of powders with different in physical and chemical natures were used to study the rheological characteristic of paste. Thus, the values of $K_1$ to $K_4$ are valid for five types of powders studied.

Fig 5.11 to 5.15 shows a comparison of the rheological parameters between experimental and calculated results from Eq. 5.1 and 5.2 by substituting angularity factor and reactivity factor presented in Table 5.10. It can be observed from these figures that the rheological parameters, yield stress and plastic viscosity, calculated from the proposed models are closed to the experimental values measured using the Rheometer. Test 1,2,3 and Avg test shown in those figures refer to the value used for angularity factor presented in Tables 5.2 to 5.6 for each type of powder.

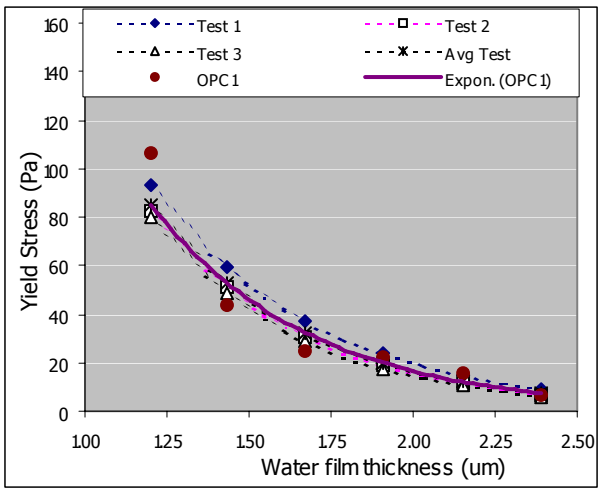


(a) Yield Stress

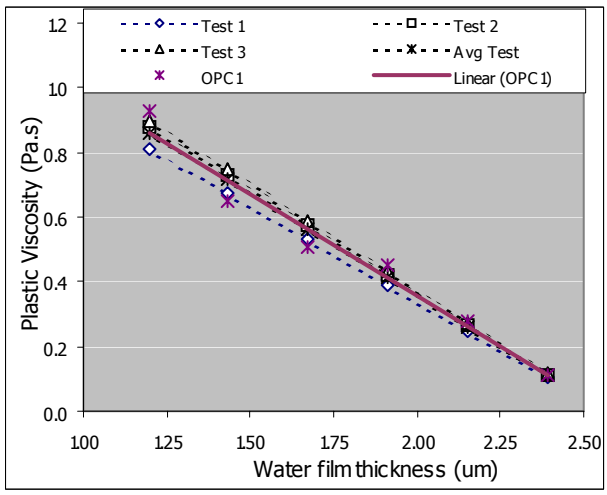


(b) Plastic Viscosity

Fig 5.11 Comparison of experimental and calculated rheological parameters (OPC series)

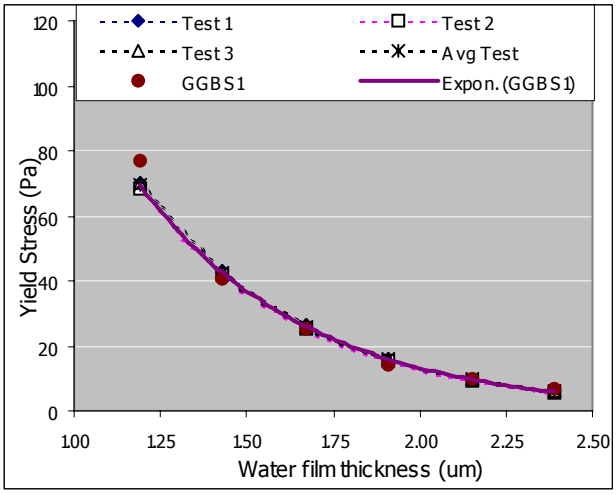


(a)

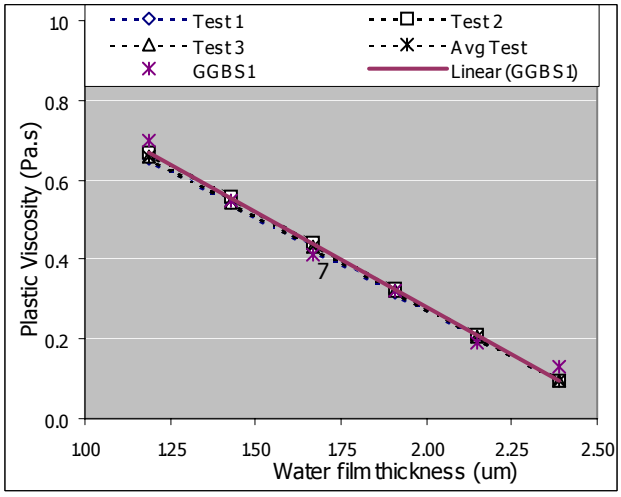


(b

(a) Yield Stress Plastic Viscosity

Fig 5.12 Comparison of experimental and calculated rheological parameters (GGBS series)

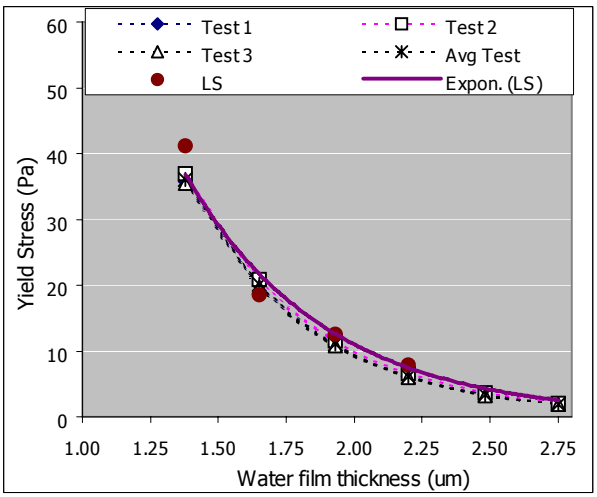


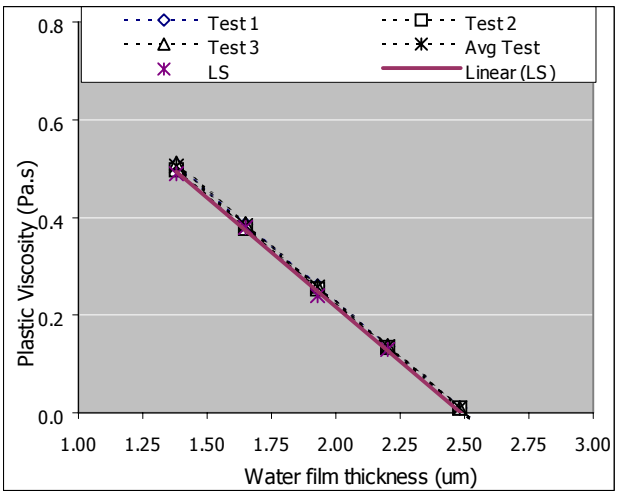


(a) Yield Stress (b) Plastic Viscosity

Fig 5.13 Comparison of experimental and calculated rheological parameters (LS series)

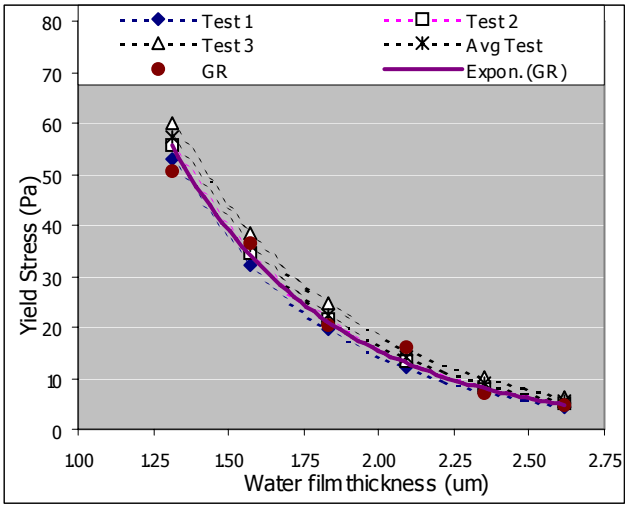


(a) Yield Stress

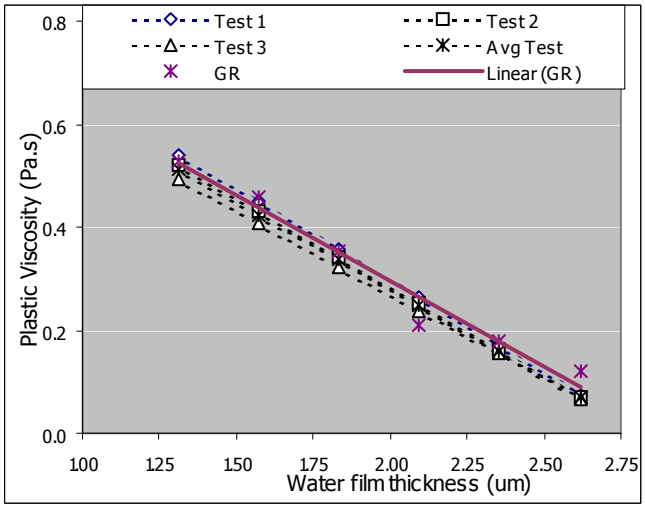


(b) Plastic Viscosity

Fig 5.14 Comparison of experimental and calculated rheological parameters (GR series)

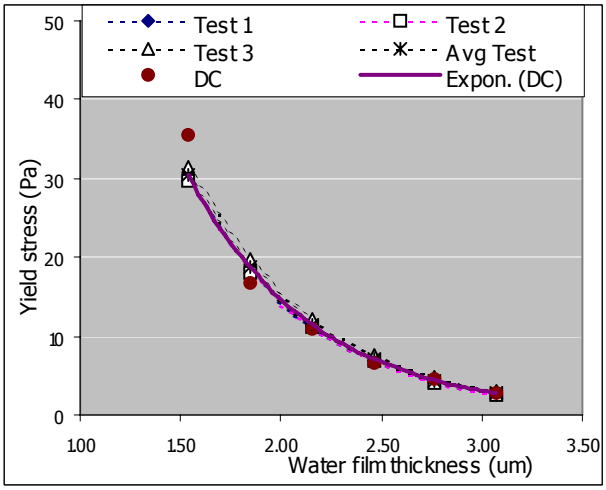


(a) Yield Stress

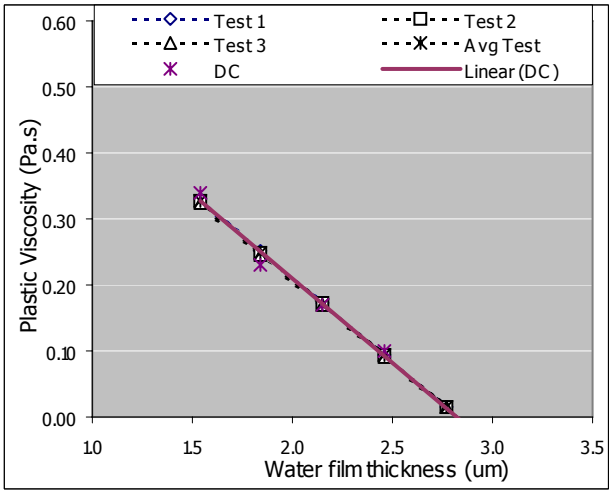


(b) Plastic Viscosity

Fig 5.15 Comparison of experimental and calculated rheological parameters (DC series)

### 5.3.2 SERIES 2 (including repulsivity factor)

In order to understand the influence of Superplasticizer on paste rheology, the various dosage of superplasticizer, ADVA 108, were added to selected pastes with similar mix proportion as in Table 5.12. Brief detail mix proportions of different types of paste are presented in Table 5.14.

Table 5.14- Mix proportions for different types of paste (w chemical admixture) to verify Replusivity Factor

| Designation | w/p | water | Cement | | Filler | | Total powder | | SURFACE AREA | | | Film Thickness |
|---|---|---|---|---|---|---|---|---|---|---|---|---|
| | (by Vol) | (g) | weight (g) | volume (m3) | weight (g) | volume (m3) | T. weight (g) | T. voulme (m3) | OPC (m2) | filler(m2) | Total Area | Tw (um) |
| OPC 1-1 | 1.0 | 260 | 820 | 0.26 | 0 | 0.00 | 820 | 0.26 | 218 | 0 | 218 | 1.20 |
| OPC 1-2 | 1.2 | 312 | 820 | 0.26 | 0 | 0.00 | 820 | 0.26 | 218 | 0 | 218 | 1.44 |
| OPC 1-3 | 1.4 | 364 | 820 | 0.26 | 0 | 0.00 | 820 | 0.26 | 218 | 0 | 218 | 1.67 |
| GGBS 1-1 | 1.0 | 260 | 500 | 0.16 | 290 | 0.10 | 790 | 0.26 | 133 | 85 | 218 | 1.19 |
| GGBS 1-2 | 1.2 | 313 | 500 | 0.16 | 290 | 0.10 | 790 | 0.26 | 133 | 85 | 218 | 1.43 |
| GGBS 1-3 | 1.4 | 365 | 500 | 0.16 | 290 | 0.10 | 790 | 0.26 | 133 | 85 | 218 | 1.67 |
| GR 1-1 | 1.0 | 283 | 500 | 0.16 | 330 | 0.12 | 830 | 0.28 | 133 | 84 | 217 | 1.31 |
| GR 1-2 | 1.2 | 340 | 500 | 0.16 | 330 | 0.12 | 830 | 0.28 | 133 | 84 | 217 | 1.57 |
| GR 1-3 | 1.4 | 397 | 500 | 0.16 | 330 | 0.12 | 830 | 0.28 | 133 | 84 | 217 | 1.83 |
| LS 1-1 | 1.0 | 299 | 500 | 0.16 | 380 | 0.14 | 880 | 0.30 | 133 | 84 | 216 | 1.38 |
| LS 1-2 | 1.2 | 359 | 500 | 0.16 | 380 | 0.14 | 880 | 0.30 | 133 | 84 | 216 | 1.66 |
| LS 1-3 | 1.4 | 419 | 500 | 0.16 | 380 | 0.14 | 880 | 0.30 | 133 | 84 | 216 | 1.94 |
| DC 1-1 | 1.0 | 300 | 500 | 0.16 | 510 | 0.14 | 1010 | 0.30 | 133 | 87 | 219 | 1.37 |
| DC 1-2 | 1.2 | 360 | 500 | 0.16 | 510 | 0.14 | 1010 | 0.30 | 133 | 87 | 219 | 1.64 |
| DC 1-3 | 1.4 | 421 | 500 | 0.16 | 510 | 0.14 | 1010 | 0.30 | 133 | 87 | 219 | 1.92 |

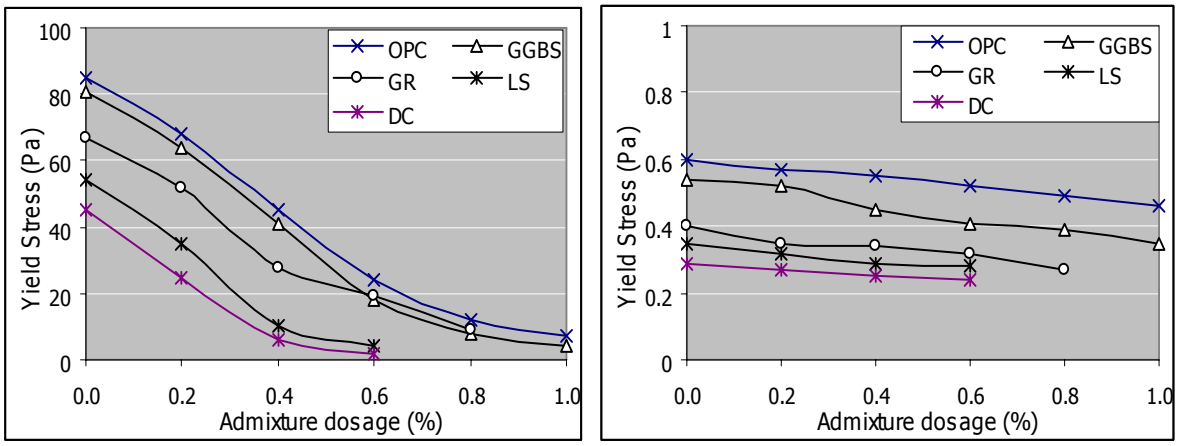


Fig. 5.16 Relation between rheological parameters and dosage of admixture (w/p = 1.2)

Fig 5.16 presents a typical graph of variation of rheological parameters under a wide range of admixture dosages. It is obvious that the suspensions have good flowing properties when the repulsive inter-particle forces are greater then the attractive Van der Waals forces. By adding the superplasticizer to the system, the surface electric charges occurred on each particle and enhance the dominance of the repulsive inter-particle forces [*Banfill, P.F.G.,1983*]. The effect of superplasticizer is largely dependent on the particle reactivity. The yield stress is more affected by the flocculation or dispersion of particles. The addition of superplasticizer leads to a reduction in yield stress more than the plastic viscosity when the total surface area of the paste is kept constant (Fig. 5.16 a & b). It is the result of an accumulation of contributions of each granular class. These contributions involve the size and roughness of the particles and their affinity for superplasticizer [*Tanigawa Y.,et.al, 1990*].

Though the affinity of superplasticizer is more dependent on powder reactivity, it can also observed from Fig 5.16 that, between the inert filler, flaky and elongated powder particle composed of GR paste shows a higher yield stress and viscosity than LS paste, which is composed of rectangular particles, at the same dosage level of admixture.

Tables 5.15 to 5.19 present the detail analysis of the different factors for the individual mixes given in Table 5.14. By substituting the respective factors in the proposed model (Eq 3.25 and 3.26), the rheological parameters; yield stress and plastic viscosity; of the paste samples of the different mixes can be calculated according to the modified equation 5.3 and 5.4. Fig 5.15 (a) and (b) shows a graph of rheological parameters calculated using proposed model and those measured with Rheometer.

**Yield Stress:** $$\tau_p = 3\left(\frac{\delta_R}{\psi_{LR}}\right)^{7/2} \exp\left[\frac{1.28}{(\psi_{LR})^{1/6}\alpha_{rep}} \cdot \frac{1}{1 + T_W\left(S_{SP}/V_{SP}\right)}\right] \quad \textit{Eq. (5.3)}$$

**Plastic Viscosity :** $$\eta_p = \left[-0.0573 + \frac{2(\delta_R)^{1/2}}{(\psi_{LR})^{1/6}\alpha_{rep}} \cdot \frac{1}{1 + T_W\left(S_{SP}/V_{SP}\right)}\right] \quad \textit{Eq. (5.4)}$$

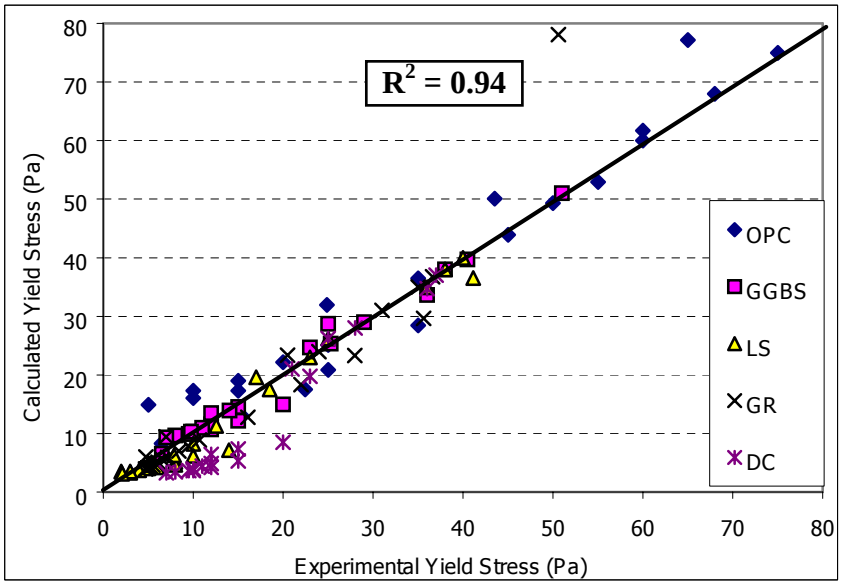


(a) Analysis of Yield Stress

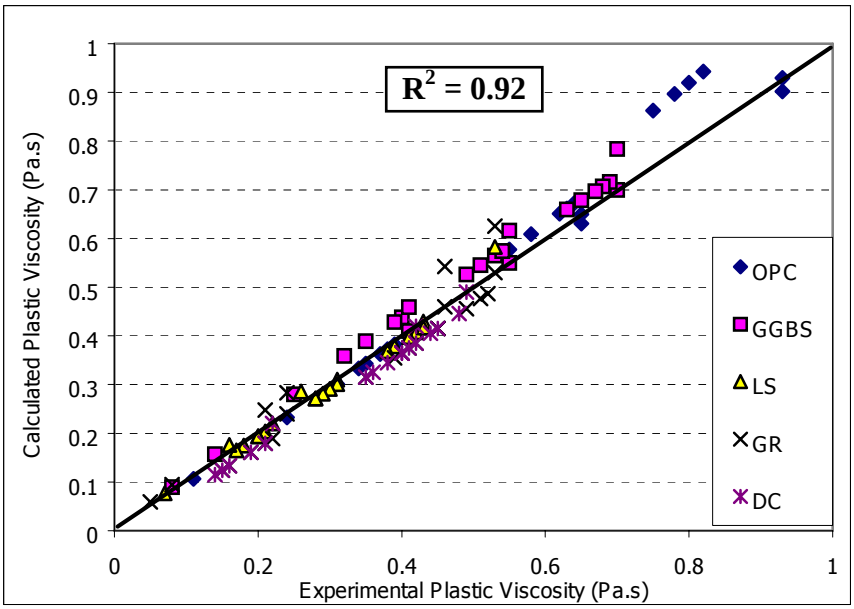


(b) Analysis of Plasticity Viscosity

Fig..5.17 Relation between the calculated and experimental rheological parameters of SCC paste fraction

The verification in Fig. 5.17 shows that the proposed model can be used to predict the rheological parameters, yield stress and plastic viscosity of the SCC paste fraction satisfactorily with a $R^2$ value (based on best fit linear y=kx) of more than 0.9.

## 5.4 CONCLUDING REMARKS

Rheological property of SCC paste fraction is very complex due to a combination of the different powders interaction between chemical reaction and physical effect. With regards to the internal factors, extensive work in the paste study shows that rheological properties of the paste fraction of SCC depend mainly not only on the solid volume fraction but also on the physical and chemical characteristic of powders. An experimental program has been specifically designed to take into account the factors indicated in the study.

Based on the proposed model and verification results, the following conclusions can be drawn:

1. The rheological parameters, yield stress and plastic viscosity of the paste fraction of SCC, are dependent on not only the solid volume fraction of the system but also on the physical and chemical characteristics of the powder materials used.
2. The inter-particle distance, presented as thickness of water film around the powder particle, was found to be the primary controlling factor. By taking into account the physical and chemical effect of the powder (angularity factor and reactivity factor), and the type of chemical admixture used (repulsion factor), both yield stress and plastic viscosity of the paste can be predicted by conducting a minimum number of rheology tests for a given set of materials intended for use in SCC.
3. According to the verification results, it seems that the proposed rheological model is suitable to predict the yield stress and plastic viscosity of paste fraction of SCC satisfactorily ($R^2$ = 0.94 and 0.92 respectively).

With the understanding of the factors of paste rheology, there is a potential to predict the workability of SCC from its paste fraction by combining it with the additional physical effect of aggregate. However, it may need ptimization the mix proportions of SCC through trial mixing before actual production.

Table 5.15- Mix proportions for OPC paste (w chemical admixture) to verify Proposedf Model

| Designation | ADVA 108 | Size Factor | | | Angularity Factor | | | Reactivity Factor | | | Replusivity factor | | |
|---|---|---|---|---|---|---|---|---|---|---|---|---|---|
| | (%) | $d_{max}$ | $d_{min}$ | $d_{max}/d_{min}$ | $1/\psi_{opc}$ | $1/\psi_{filler}$ | $1/\psi_{R}$ | $\delta_{opc}$ | $\delta_{filler}$ | $\delta_{R}$ | $\alpha_{opc}$ | $\alpha_{filler}$ | $\alpha_{rep.}D_{sp}$ |
| OPC 1-1a | 0.2 | 20 | 20 | 1.00 | 1.63 | 1.63 | 1.63 | 1.68 | 1.68 | 1.68 | 1.40 | 1.40 | 0.28 |
| OPC 1-1b | 0.4 | 20 | 20 | 1.00 | 1.63 | 1.63 | 1.63 | 1.68 | 1.68 | 1.68 | 1.40 | 1.40 | 0.56 |
| OPC 1-1c | 0.6 | 20 | 20 | 1.00 | 1.63 | 1.63 | 1.63 | 1.68 | 1.68 | 1.68 | 1.40 | 1.40 | 0.84 |
| OPC 1-1d | 0.8 | 20 | 20 | 1.00 | 1.63 | 1.63 | 1.63 | 1.68 | 1.68 | 1.68 | 1.40 | 1.40 | 1.12 |
| OPC 1-1e | 1.0 | 20 | 20 | 1.00 | 1.63 | 1.63 | 1.63 | 1.68 | 1.68 | 1.68 | 1.40 | 1.40 | 1.40 |
| OPC 1-2a | 0.2 | 20 | 20 | 1.00 | 1.63 | 1.63 | 1.63 | 1.68 | 1.68 | 1.68 | 1.40 | 1.40 | 0.28 |
| OPC 1-2b | 0.4 | 20 | 20 | 1.00 | 1.63 | 1.63 | 1.63 | 1.68 | 1.68 | 1.68 | 1.40 | 1.40 | 0.56 |
| OPC 1-2c | 0.6 | 20 | 20 | 1.00 | 1.63 | 1.63 | 1.63 | 1.68 | 1.68 | 1.68 | 1.40 | 1.40 | 0.84 |
| OPC 1-2d | 0.8 | 20 | 20 | 1.00 | 1.63 | 1.63 | 1.63 | 1.68 | 1.68 | 1.68 | 1.40 | 1.40 | 1.12 |
| OPC 1-2e | 1.0 | 20 | 20 | 1.00 | 1.63 | 1.63 | 1.63 | 1.68 | 1.68 | 1.68 | 1.40 | 1.40 | 1.40 |
| OPC 1-3a | 0.2 | 20 | 20 | 1.00 | 1.63 | 1.63 | 1.63 | 1.68 | 1.68 | 1.68 | 1.40 | 1.40 | 0.28 |
| OPC 1-3b | 0.4 | 20 | 20 | 1.00 | 1.63 | 1.63 | 1.63 | 1.68 | 1.68 | 1.68 | 1.40 | 1.40 | 0.56 |
| OPC 1-3c | 0.6 | 20 | 20 | 1.00 | 1.63 | 1.63 | 1.63 | 1.68 | 1.68 | 1.68 | 1.40 | 1.40 | 0.84 |
| OPC 1-3d | 0.8 | 20 | 20 | 1.00 | 1.63 | 1.63 | 1.63 | 1.68 | 1.68 | 1.68 | 1.40 | 1.40 | 1.12 |
| OPC 1-3e | 1.0 | 20 | 20 | 1.00 | 1.63 | 1.63 | 1.63 | 1.68 | 1.68 | 1.68 | 1.40 | 1.40 | 1.40 |

Table 5.16- Mix proportions for GGBS paste (w chemical admixture) to verify Proposedf Model

| Designation | ADVA 108 | Size Factor | | | Angularity Factor | | | Reactivity Factor | | | Replusivity factor | | |
|---|---|---|---|---|---|---|---|---|---|---|---|---|---|
| | (%) | $d_{max}$ | $d_{min}$ | $d_{max}/d_{min}$ | $1/\psi_{opc}$ | $1/\psi_{filler}$ | $1/\psi_{R}$ | $\delta_{opc}$ | $\delta_{filler}$ | $\delta_{R}$ | $\alpha_{opc}$ | $\alpha_{filler}$ | $\alpha_{rep.}D_{sp}$ |
| GGBS 1-1a | 0.2 | 20 | 17 | 1.18 | 1.63 | 1.52 | 1.60 | 1.68 | 1.20 | 1.54 | 1.40 | 1.14 | 0.27 |
| GGBS 1-1b | 0.4 | 20 | 17 | 1.18 | 1.63 | 1.52 | 1.60 | 1.68 | 1.20 | 1.54 | 1.40 | 1.41 | 0.56 |
| GGBS 1-1c | 0.6 | 20 | 17 | 1.18 | 1.63 | 1.52 | 1.60 | 1.68 | 1.20 | 1.54 | 1.40 | 1.14 | 0.80 |
| GGBS 1-1d | 0.8 | 20 | 17 | 1.18 | 1.63 | 1.52 | 1.60 | 1.68 | 1.20 | 1.54 | 1.40 | 1.14 | 1.06 |
| GGBS 1-1e | 1.0 | 20 | 17 | 1.18 | 1.63 | 1.52 | 1.60 | 1.68 | 1.20 | 1.54 | 1.40 | 1.14 | 1.33 |
| GGBS 1-2a | 0.2 | 20 | 17 | 1.18 | 1.63 | 1.52 | 1.60 | 1.68 | 1.20 | 1.54 | 1.40 | 1.14 | 0.27 |
| GGBS 1-2b | 0.4 | 20 | 17 | 1.18 | 1.63 | 1.52 | 1.60 | 1.68 | 1.20 | 1.54 | 1.40 | 1.14 | 0.53 |
| GGBS 1-2c | 0.6 | 20 | 17 | 1.18 | 1.63 | 1.52 | 1.60 | 1.68 | 1.20 | 1.54 | 1.40 | 1.14 | 0.80 |
| GGBS 1-2d | 0.8 | 20 | 17 | 1.18 | 1.63 | 1.52 | 1.60 | 1.68 | 1.20 | 1.54 | 1.40 | 1.14 | 1.06 |
| GGBS 1-2e | 1.0 | 20 | 17 | 1.18 | 1.63 | 1.52 | 1.60 | 1.68 | 1.20 | 1.54 | 1.40 | 1.14 | 1.33 |
| GGBS 1-3a | 0.2 | 20 | 17 | 1.18 | 1.63 | 1.52 | 1.60 | 1.68 | 1.20 | 1.54 | 1.40 | 1.14 | 0.27 |
| GGBS 1-3b | 0.4 | 20 | 17 | 1.18 | 1.63 | 1.52 | 1.60 | 1.68 | 1.20 | 1.54 | 1.40 | 1.14 | 0.53 |
| GGBS 1-3c | 0.6 | 20 | 17 | 1.18 | 1.63 | 1.52 | 1.60 | 1.68 | 1.20 | 1.54 | 1.40 | 1.14 | 0.80 |
| GGBS 1-3d | 0.8 | 20 | 17 | 1.18 | 1.63 | 1.52 | 1.60 | 1.68 | 1.20 | 1.54 | 1.40 | 1.14 | 1.06 |
| GGBS 1-3e | 1.0 | 20 | 17 | 1.18 | 1.63 | 1.52 | 1.60 | 1.68 | 1.20 | 1.54 | 1.40 | 1.14 | 1.33 |

Table 5.17- Mix proportions for GR paste (w chemical admixture) to verify Proposedf Model

| Designation | ADVA 108 | Size Factor | | | Angularity Factor | | | Reactivity Factor | | | Replusivity factor | | |
|---|---|---|---|---|---|---|---|---|---|---|---|---|---|
| | (%) | $d_{max}$ | $d_{min}$ | $d_{max}/d_{min}$ | $1/\psi_{opc}$ | $1/\psi_{filler}$ | $1/\psi_{R}$ | $\delta_{opc}$ | $\delta_{filler}$ | $\delta_{R}$ | $\alpha_{opc}$ | $\alpha_{filler}$ | $\alpha_{rep.}D_{sp}$ |
| GR 1-1a | 0.2 | 59 | 20 | 2.95 | 1.63 | 2.14 | 1.79 | 1.68 | 1.00 | 1.46 | 1.40 | 1.00 | 0.25 |
| GR 1-1b | 0.4 | 59 | 20 | 2.95 | 1.63 | 2.14 | 1.79 | 1.68 | 1.00 | 1.46 | 1.40 | 1.00 | 0.51 |
| GR 1-1c | 0.6 | 59 | 20 | 2.95 | 1.63 | 2.14 | 1.79 | 1.68 | 1.00 | 1.46 | 1.40 | 1.00 | 0.76 |
| GR 1-1d | 0.8 | 59 | 20 | 2.95 | 1.63 | 2.14 | 1.79 | 1.68 | 1.00 | 1.46 | 1.40 | 1.00 | 1.02 |
| GR 1-1e | 1.0 | 59 | 20 | 2.95 | 1.63 | 2.14 | 1.79 | 1.68 | 1.00 | 1.46 | 1.40 | 1.00 | 1.27 |
| GR 1-2a | 0.2 | 59 | 20 | 2.95 | 1.63 | 2.14 | 1.79 | 1.68 | 1.00 | 1.46 | 1.40 | 1.00 | 0.25 |
| GR 1-2b | 0.4 | 59 | 20 | 2.95 | 1.63 | 2.14 | 1.79 | 1.68 | 1.00 | 1.46 | 1.40 | 1.00 | 0.51 |
| GR 1-2c | 0.6 | 59 | 20 | 2.95 | 1.63 | 2.14 | 1.79 | 1.68 | 1.00 | 1.46 | 1.40 | 1.00 | 0.76 |
| GR 1-2d | 0.8 | 59 | 20 | 2.95 | 1.63 | 2.14 | 1.79 | 1.68 | 1.00 | 1.46 | 1.40 | 1.00 | 1.02 |
| GR 1-2e | 1.0 | 59 | 20 | 2.95 | 1.63 | 2.14 | 1.79 | 1.68 | 1.00 | 1.46 | 1.40 | 1.00 | 1.27 |
| GR 1-3a | 0.2 | 59 | 20 | 2.95 | 1.63 | 2.14 | 1.79 | 1.68 | 1.00 | 1.46 | 1.40 | 1.00 | 0.25 |
| GR 1-3b | 0.4 | 59 | 20 | 2.95 | 1.63 | 2.14 | 1.79 | 1.68 | 1.00 | 1.46 | 1.40 | 1.00 | 0.51 |
| GR 1-3c | 0.6 | 59 | 20 | 2.95 | 1.63 | 2.14 | 1.79 | 1.68 | 1.00 | 1.46 | 1.40 | 1.00 | 0.76 |
| GR 1-3d | 0.8 | 59 | 20 | 2.95 | 1.63 | 2.14 | 1.79 | 1.68 | 1.00 | 1.46 | 1.40 | 1.00 | 1.02 |
| GR 1-3e | 1.0 | 59 | 20 | 2.95 | 1.63 | 2.14 | 1.79 | 1.68 | 1.00 | 1.46 | 1.40 | 1.00 | 1.27 |

Table 5.18- Mix proportions for LS paste (w chemical admixture) to verify Proposedf Model

| Designation | ADVA 108 | Size Factor | | | Angularity Factor | | | Reactivity Factor | | | Replusivity factor | | |
|---|---|---|---|---|---|---|---|---|---|---|---|---|---|
| | (%) | $d_{max}$ | $d_{min}$ | $d_{max}/d_{min}$ | $1/\psi_{opc}$ | $1/\psi_{filler}$ | $1/\psi_{R}$ | $\delta_{opc}$ | $\delta_{filler}$ | $\delta_{R}$ | $\alpha_{opc}$ | $\alpha_{filler}$ | $\alpha_{rep.} D_{sp}$ |
| LS 1-1a | 0.2 | 76 | 20 | 3.80 | 1.63 | 1.88 | 1.72 | 1.68 | 1.00 | 1.44 | 1.40 | 1.00 | 0.25 |
| LS 1-1b | 0.4 | 76 | 20 | 3.80 | 1.63 | 1.88 | 1.72 | 1.68 | 1.00 | 1.44 | 1.40 | 1.00 | 0.50 |
| LS 1-1c | 0.6 | 76 | 20 | 3.80 | 1.63 | 1.88 | 1.72 | 1.68 | 1.00 | 1.44 | 1.40 | 1.00 | 0.75 |
| LS 1-1d | 0.8 | 76 | 20 | 3.80 | 1.63 | 1.88 | 1.72 | 1.68 | 1.00 | 1.44 | 1.40 | 1.00 | 1.01 |
| LS 1-1e | 1.0 | 76 | 20 | 3.80 | 1.63 | 1.88 | 1.72 | 1.68 | 1.00 | 1.44 | 1.40 | 1.00 | 1.26 |
| LS 1-2a | 0.2 | 76 | 20 | 3.80 | 1.63 | 1.88 | 1.72 | 1.68 | 1.00 | 1.44 | 1.40 | 1.00 | 0.25 |
| LS 1-2b | 0.4 | 76 | 20 | 3.80 | 1.63 | 1.88 | 1.72 | 1.68 | 1.00 | 1.44 | 1.40 | 1.00 | 0.50 |
| LS 1-2c | 0.6 | 76 | 20 | 3.80 | 1.63 | 1.88 | 1.72 | 1.68 | 1.00 | 1.44 | 1.40 | 1.00 | 0.75 |
| LS 1-2d | 0.8 | 76 | 20 | 3.80 | 1.63 | 1.88 | 1.72 | 1.68 | 1.00 | 1.44 | 1.40 | 1.00 | 1.01 |
| LS 1-2e | 1.0 | 76 | 20 | 3.80 | 1.63 | 1.88 | 1.72 | 1.68 | 1.00 | 1.44 | 1.40 | 1.00 | 1.26 |
| LS 1-3a | 0.2 | 76 | 20 | 3.80 | 1.63 | 1.88 | 1.72 | 1.68 | 1.00 | 1.44 | 1.40 | 1.00 | 0.25 |
| LS 1-3b | 0.4 | 76 | 20 | 3.80 | 1.63 | 1.88 | 1.72 | 1.68 | 1.00 | 1.44 | 1.40 | 1.00 | 0.50 |
| LS 1-3c | 0.6 | 76 | 20 | 3.80 | 1.63 | 1.88 | 1.72 | 1.68 | 1.00 | 1.44 | 1.40 | 1.00 | 0.75 |
| LS 1-3d | 0.8 | 76 | 20 | 3.80 | 1.63 | 1.88 | 1.72 | 1.68 | 1.00 | 1.44 | 1.40 | 1.00 | 1.01 |
| LS 1-3e | 1.0 | 76 | 20 | 3.80 | 1.63 | 1.88 | 1.72 | 1.68 | 1.00 | 1.44 | 1.40 | 1.00 | 1.26 |

Table 5.19- Mix proportions for DC paste (w chemical admixture) to verify Proposed Model

| Designation | ADVA 108 | Size Factor | | | Angularity Factor | | | Reactivity Factor | | | Replusivity factor | | |
|---|---|---|---|---|---|---|---|---|---|---|---|---|---|
| | (%) | $d_{max}$ | $d_{min}$ | $d_{max}/d_{min}$ | $1/\psi_{opc}$ | $1/\psi_{filler}$ | $1/\psi_{R}$ | $\delta_{opc}$ | $\delta_{filler}$ | $\delta_{R}$ | $\alpha_{opc}$ | $\alpha_{filler}$ | $\alpha_{rep.} D_{sp}$ |
| LS 1-1a | 0.2 | 70 | 20 | 3.50 | 1.63 | 1.81 | 1.70 | 1.68 | 1.00 | 1.43 | 1.40 | 1.00 | 0.25 |
| LS 1-1b | 0.4 | 70 | 20 | 3.50 | 1.63 | 1.81 | 1.70 | 1.68 | 1.00 | 1.43 | 1.40 | 1.00 | 0.50 |
| LS 1-1c | 0.6 | 70 | 20 | 3.50 | 1.63 | 1.81 | 1.70 | 1.68 | 1.00 | 1.43 | 1.40 | 1.00 | 0.75 |
| LS 1-1d | 0.8 | 70 | 20 | 3.50 | 1.63 | 1.81 | 1.70 | 1.68 | 1.00 | 1.43 | 1.40 | 1.00 | 1.00 |
| LS 1-1e | 1.0 | 70 | 20 | 3.50 | 1.63 | 1.81 | 1.70 | 1.68 | 1.00 | 1.43 | 1.40 | 1.00 | 1.25 |
| LS 1-2a | 0.2 | 70 | 20 | 3.50 | 1.63 | 1.81 | 1.70 | 1.68 | 1.00 | 1.43 | 1.40 | 1.00 | 0.25 |
| LS 1-2b | 0.4 | 70 | 20 | 3.50 | 1.63 | 1.81 | 1.70 | 1.68 | 1.00 | 1.43 | 1.40 | 1.00 | 0.50 |
| LS 1-2c | 0.6 | 70 | 20 | 3.50 | 1.63 | 1.81 | 1.70 | 1.68 | 1.00 | 1.43 | 1.40 | 1.00 | 0.75 |
| LS 1-2d | 0.8 | 70 | 20 | 3.50 | 1.63 | 1.81 | 1.70 | 1.68 | 1.00 | 1.43 | 1.40 | 1.00 | 1.00 |
| LS 1-2e | 1.0 | 70 | 20 | 3.50 | 1.63 | 1.81 | 1.70 | 1.68 | 1.00 | 1.43 | 1.40 | 1.00 | 1.25 |
| LS 1-3a | 0.2 | 70 | 20 | 3.50 | 1.63 | 1.81 | 1.70 | 1.68 | 1.00 | 1.43 | 1.40 | 1.00 | 0.25 |
| LS 1-3b | 0.4 | 70 | 20 | 3.50 | 1.63 | 1.81 | 1.70 | 1.68 | 1.00 | 1.43 | 1.40 | 1.00 | 0.50 |
| LS 1-3c | 0.6 | 70 | 20 | 3.50 | 1.63 | 1.81 | 1.70 | 1.68 | 1.00 | 1.43 | 1.40 | 1.00 | 0.75 |
| LS 1-3d | 0.8 | 70 | 20 | 3.50 | 1.63 | 1.81 | 1.70 | 1.68 | 1.00 | 1.43 | 1.40 | 1.00 | 1.00 |
| LS 1-3e | 1.0 | 70 | 20 | 3.50 | 1.63 | 1.81 | 1.70 | 1.68 | 1.00 | 1.43 | 1.40 | 1.00 | 1.25 |

# CHAPTER 6

# RHEOLOGICAL STUDY ON MORTAR FRACTION OF SCC

## 6.1 Introduction

To reach the optimum mix design of Self-Compacting Concrete, it is important to attain the right combination of cement and filler, amount and type as well as the most efficient superplasticizer. By using rheological measurement, the optimization for the paste fraction of SCC can be established as discussed in Chapter 5. However, due to a wide range particle sizes, it is generally not possible to correlate the rheology of SCC with the rheology of its paste fraction. Therefore, rheological study on the mortar fraction of SCC, which has a closer particle size range with cement paste, is required to bridge this information gap. It can be considered that the only difference between the mortar and its paste fraction is the addition of sand particles (fine aggregate), which ranges from 5 mm to 150 um.

In this chapter, a rheological study on the mortar fraction of SCC is first presented and the correlation between the paste and mortar fraction of SCC is investigated. The correlation described herein is intended to predict the rheological parameters of the mortar using those of the paste, which has a similar mix proportion as the paste fraction of the mortar.

## 6.2 Experimental Program

### 6.2.1 Materials and Mix Proportions

Natural sand with four types of grading was used as fine aggregate to produce the mortar mixes. The physical properties of each grading of sand such as specific gravity, absorption, bulk density and voids ratios had been presented in Chapter 4.

The different mortar samples investigated in this study were prepared by adding constant amount to sand to the paste mixtures which had a similar composition as the paste fraction which had been investigated in Chapter 5. Although constant amount of sand was added in the mix, the relative volume of the sand in the mortars was different for different mixtures.

### 6.2.2 Sample Preparations

A Hobart mixer with a maximum capacity of 15 liters (Fig. 6.1) was used to carry out the mechanical mixing of the mortar. A digital stopwatch with an accuracy of up to 0.1 seconds was also used to record the time that elapsed after the addition of water to the materials. It is important that the paste fraction in the mortar must experience a similar shear history as the paste tested for the investigation of the paste rheology. The following mixing procedure was adopted:

**Mortar sample without Superplasticizer;**

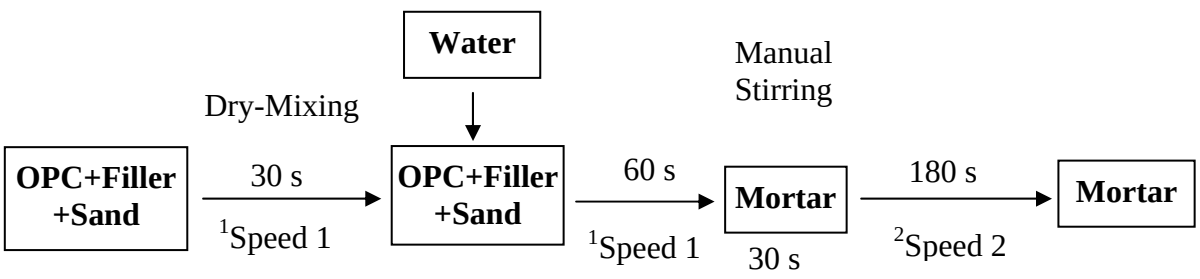

**Mortar sample with Superplasticizer;**

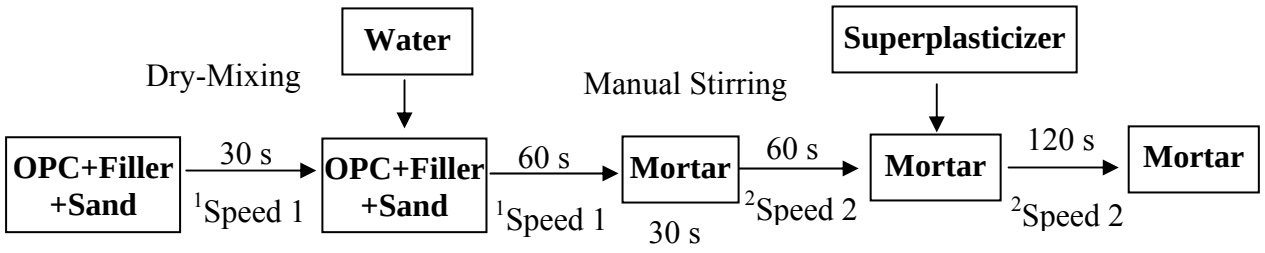


*Note: [1] Mixer Speed 1 = 60 rpm, [2] Mixer Speed 2 = 90 rpm*


Fig. 6.1 Hobart Mixer to prepare the mortar sample

### 6.2.3 Testing Procedure

- **Equipment**

The rheological characteristics of the SCC mortar fraction were conducted with a BML rheometer. (Fig. 6.2) The testing principle is basically the same as that of the paste rheology measurement. The outer cylinder was filled with the test sample; fresh mortar; and rotation started once the inner cylinder was lowered down to the specified location. While the outer cylinder rotated at different rotational speeds, the torque was recorded simultaneously. The samples were shared starting from a lower to higher rotational speed, then, decreased back to zero to get the ramp up and down curve with the resulting relationship being rotation versus torque. Taking the actual geometry into consideration facilitates re-calculation of these parameters to obtain the fundamental shear rate and shear stress; and the results were verified according to Bingham model.

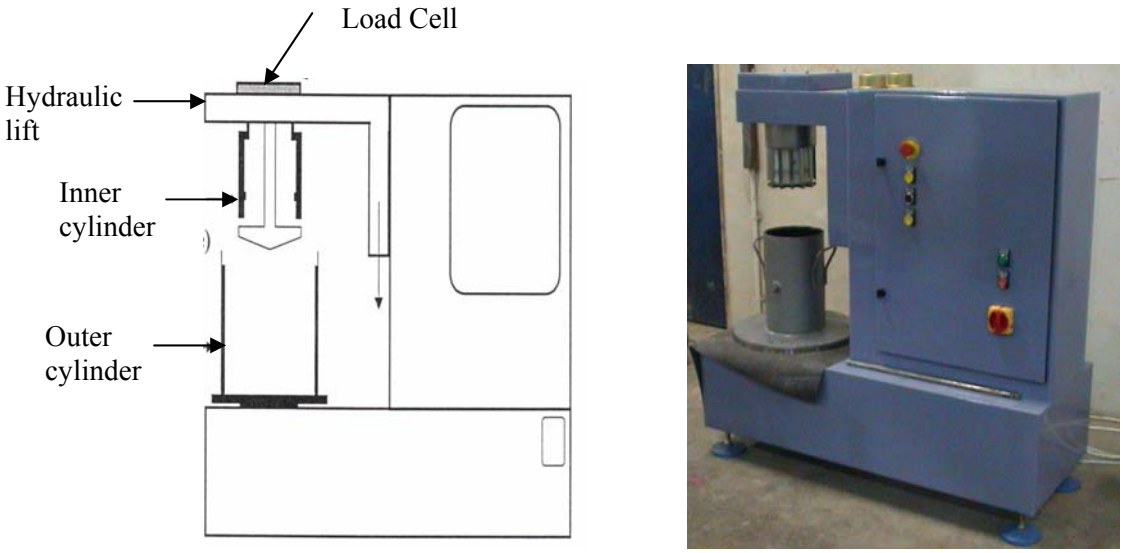


(a) Schematic diagram of BML Rheometer

(b) Outer cylinder (container) and inner cylinder (blades) used for mortar rheology test

Fig. 6.2 BML Rheometer and its component for mortar rheology test

- **Methods & Conditions of Testing**

A fresh batch of mortar was prepared for each rheological test series. After 3.5 minutes of mixing, the mortar sample was placed into the outer cylinder (container) up to the indicated level on the test cylinder. The mortar sample was then tested by rotating the outer cylinder of the rheometer. The angular velocity of the outer cylinder decreased steadily from 0.60 rps to 0.10 rps in decrements of 0.04 rps. After that, a further reading was taken at 0.40 rps in order to check for segregation of the mortar. The graph of resistance [T/Nm] against velocity [rps/N] was plotted from the data points. The yield stress and plastic viscosity of the mortar were then derived from the graph by applying the Bingham Model.

The change in the yield stress and plastic viscosity of the mortar was monitored over a time period of 90 minutes. The time period of 90 minutes was chosen because this is the estimated arrival time taken by a mixer truck to travel from the concrete batching plant to the construction site. Thus, the mix should maintain its workability for a

minimum of 90 minutes. The rheological properties of the mortar were measured at the interval of 9 minutes, 30 minutes, 60 minutes and 90 minutes. In the study, the rheological characteristics of the mortar containing copper slag (CS) was not investigated because the usage of such powder in concrete products was limited by the Ministry of Environment in Singapore, due to concern on the leaching of heavy metal to the ground water supply system. The comparatively low allowable usage in concrete, 10% by weight of fine aggregate, is not a meaningful utilization of CS in SCC.

## 6.3 Experimental Results and Discussions

### 6.3.1 Effect of Water to Powder Ratio at Different Time Interval

The results obtained from the experiments are graphically presented in Fig 6.3 and 6.4. The detail mix proportions for different mortar samples are given in Table 6.1. The change in yield stress at different water/powder ratios (w/p) for different time intervals is shown in Fig 6.3 and the change in plastic viscosity at different w/p for different time intervals are presented in Fig 6.4.

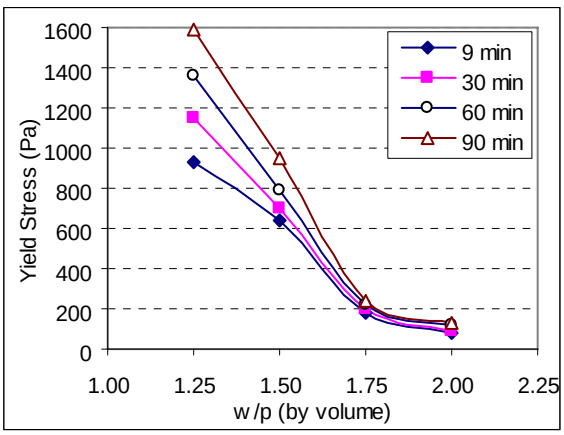


**(a) OPC Series**

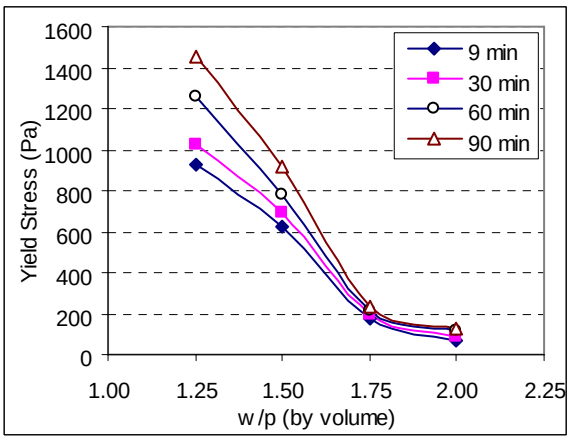


**(b) GGBS Series**

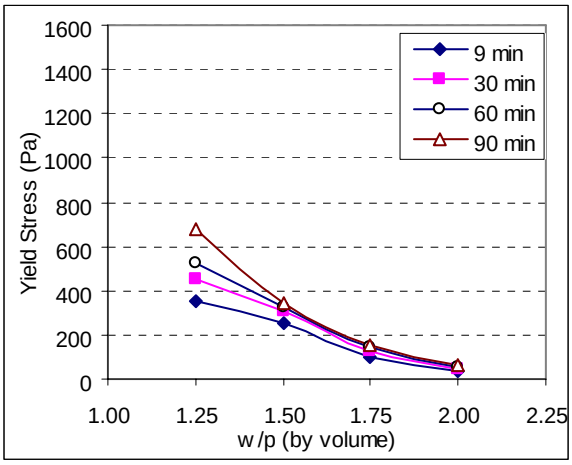


**(c) GR Series**

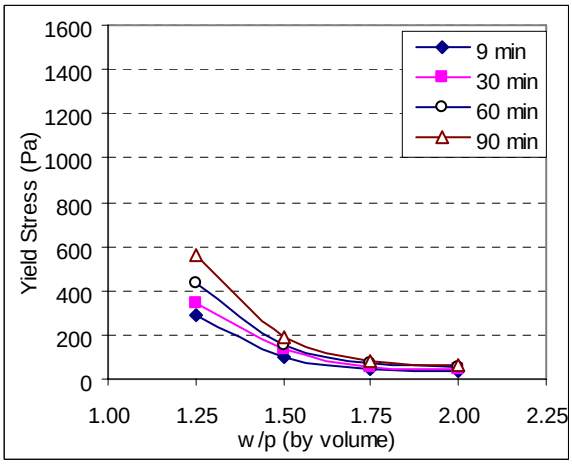


**(d) LS Series**

Fig 6.3: Relationship between yield stress and water/powder ratio at different time intervals

It can be seen from Figs 6.3 and 6.4, both the plastic viscosity and yield stress decrease with an increase in water/powder ratio. It is also observed that the changes in yield stress and plastic viscosity with respect to time was greater at lower w/p. Conversely, there was little or no change in the rheological properties at higher w/p within the time duration of 90 minutes. This is because the yield stress and plastic viscosity of the mortar depends on the amount of free water present in the system. At lower w/p, there was little free water present in the mix and this free water was significantly reduced over the 90 minutes period due to the formation of hydration products and evaporation. This caused an increase in inter-particle friction, which led to a greater force required to initiate the flow in the system. As a result, the yield stress and plastic viscosity increased greatly over time at lower w/p. However at higher w/p, the amount of free water in the system was relatively higher compare to the reduction amount over the time resulting in very little change in the yield stress and plastic viscosity over the 90 minutes time interval.

Table 6.1- Mix proportions for different types of Mortar (w/o chemical admixture)

| Designation | W/P | WATER | CEMENT | | FILLER | | TOTAL POWDER | | SURFACE AREA | | | FINE AGGREGATE | |
|---|---|---|---|---|---|---|---|---|---|---|---|---|---|
| | (by Vol) | (g) | weight (g) | volume (lit) | weight (g) | volume (lit) | weight (g) | volume (lit) | OPC (m2) | Filler (m2) | Total Area (m2) | weight (g) | volume (lit) |
| OPC 1-1 | 1.25 | 1190 | 3000 | 0.95 | 0 | 0.00 | 3000 | 0.95 | 796 | 0 | 796 | 6000 | 2.22 |
| OPC 1-2 | 1.50 | 1429 | 3000 | 0.95 | 0 | 0.00 | 3000 | 0.95 | 796 | 0 | 796 | 6000 | 2.22 |
| OPC 1-3 | 1.75 | 1667 | 3000 | 0.95 | 0 | 0.00 | 3000 | 0.95 | 796 | 0 | 796 | 6000 | 2.22 |
| OPC 1-4 | 2.00 | 1905 | 3000 | 0.95 | 0 | 0.00 | 3000 | 0.95 | 796 | 0 | 796 | 6000 | 2.22 |
| GGBS 1-1 | 1.25 | 1187 | 1830 | 0.58 | 1050 | 0.37 | 2880 | 0.95 | 486 | 309 | 795 | 6000 | 2.22 |
| GGBS 1-2 | 1.50 | 1424 | 1830 | 0.58 | 1050 | 0.37 | 2880 | 0.95 | 486 | 309 | 795 | 6000 | 2.22 |
| GGBS 1-3 | 1.75 | 1661 | 1830 | 0.58 | 1050 | 0.37 | 2880 | 0.95 | 486 | 309 | 795 | 6000 | 2.22 |
| GGBS 1-4 | 2.00 | 1899 | 1830 | 0.58 | 1050 | 0.37 | 2880 | 0.95 | 486 | 309 | 795 | 6000 | 2.22 |
| GR 1-1 | 1.25 | 1304 | 1830 | 0.58 | 1225 | 0.46 | 3055 | 1.04 | 486 | 312 | 797 | 6000 | 2.22 |
| GR 1-2 | 1.50 | 1565 | 1830 | 0.58 | 1225 | 0.46 | 3055 | 1.04 | 486 | 312 | 797 | 6000 | 2.22 |
| GR 1-3 | 1.75 | 1826 | 1830 | 0.58 | 1225 | 0.46 | 3055 | 1.04 | 486 | 312 | 797 | 6000 | 2.22 |
| GR 1-4 | 2.00 | 2086 | 1830 | 0.58 | 1225 | 0.46 | 3055 | 1.04 | 486 | 312 | 797 | 6000 | 2.22 |
| LS 1-1 | 1.25 | 1374 | 1830 | 0.58 | 1400 | 0.52 | 3230 | 1.10 | 486 | 309 | 794 | 6000 | 2.22 |
| LS 1-2 | 1.50 | 1649 | 1830 | 0.58 | 1400 | 0.52 | 3230 | 1.10 | 486 | 309 | 794 | 6000 | 2.22 |
| LS 1-3 | 1.75 | 1924 | 1830 | 0.58 | 1400 | 0.52 | 3230 | 1.10 | 486 | 309 | 794 | 6000 | 2.22 |
| LS 1-4 | 2.00 | 2199 | 1830 | 0.58 | 1400 | 0.52 | 3230 | 1.10 | 486 | 309 | 794 | 6000 | 2.22 |

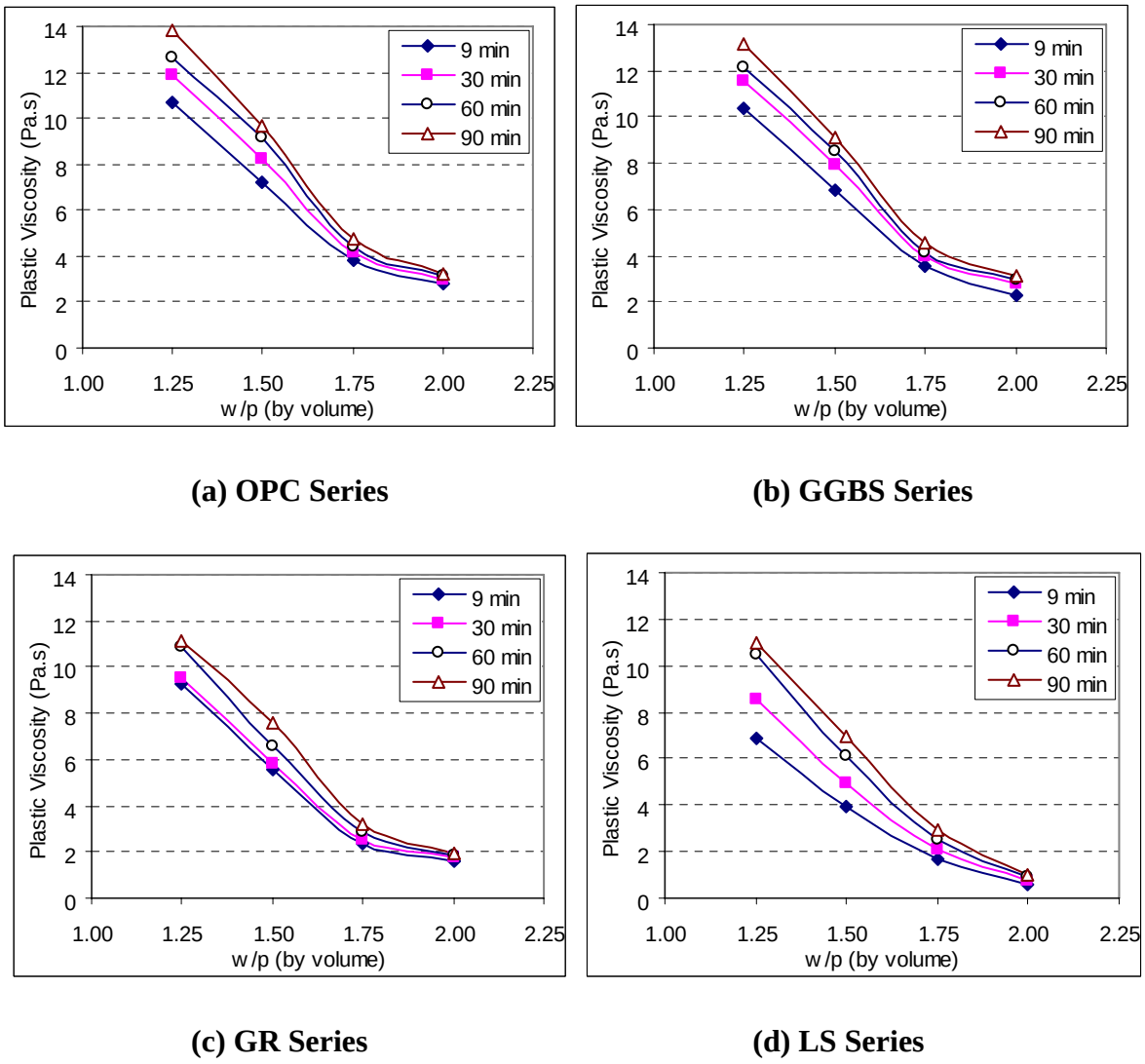


**(a) OPC Series** **(b) GGBS Series**

**(c) GR Series** **(d) LS Series**

Fig 6.4: Relationship between plastic viscosity and water/powder ratio at different time intervals

Therefore, it is obvious from the experimental results that as w/p increases, the effects of the time on changes in both the yield stress and the plastic viscosity of SCC mortar decrease significantly.

### 6.3.2 Effect of Different Dosage of Admixture (Superplasticizer)

The results obtained from the experiments are graphically presented in Fig 6.5 and 6.6. The w/p was fixed at 1.25 by volume for all the test series in order to investigate all the mixes with a similar water content.

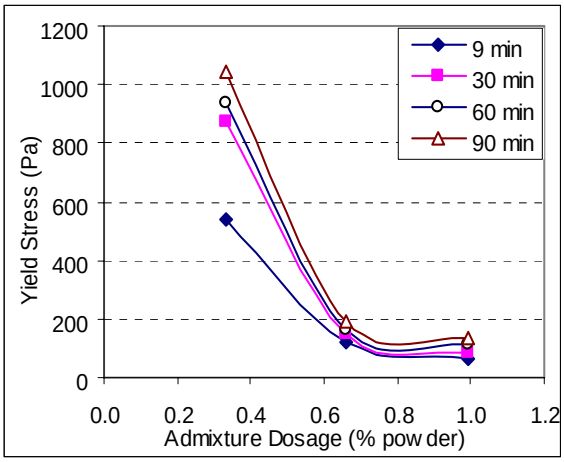


**(a) OPC Series**

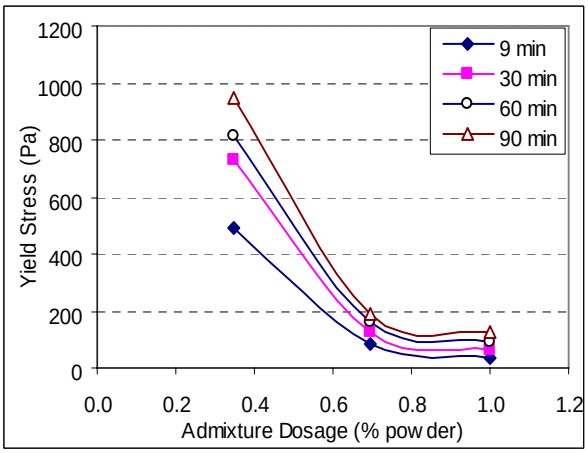


**(b) GGBS Series**

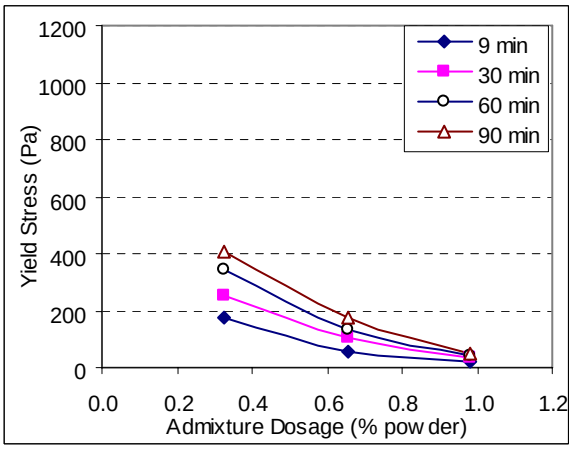


**(c) GR Series**

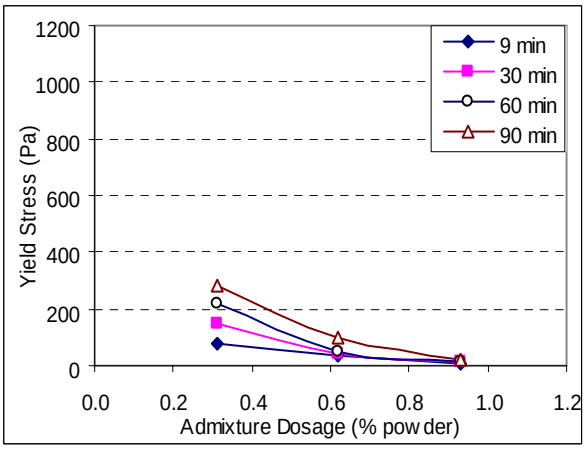


**(d) LS Series**

Fig 6.5: Relationship between yield stress and admixture dosage at different time intervals (w/p = 1.25)

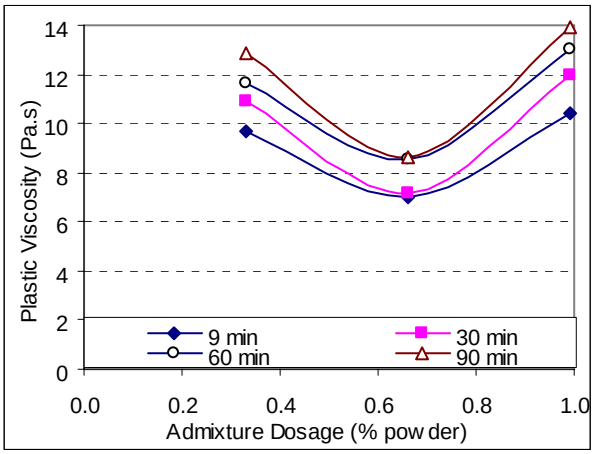


**(a) OPC Series**

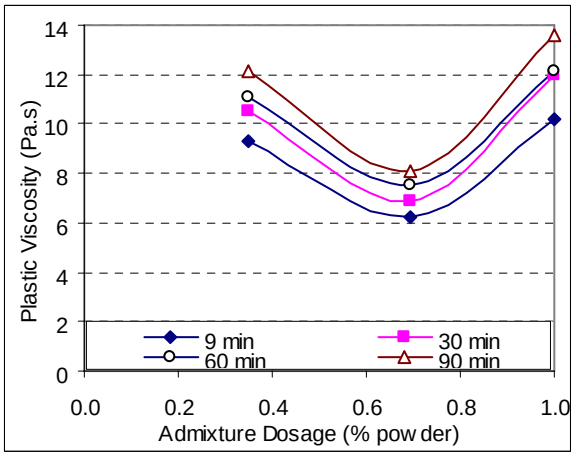


**(b) GGBS Series**

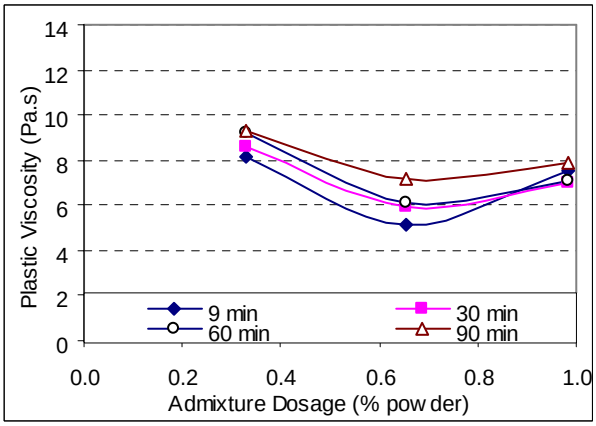


**(c) GR Series**

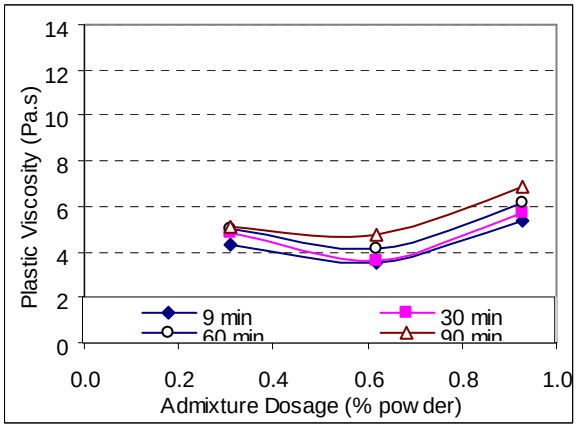


**(d) LS Series**

Fig 6.6: Relationship between plastic viscosity and admixture dosage at different time intervals (w/p = 1.25)

From Fig 6.5, it is clear that as the admixture dosage increased, the change in the yield stress with respect to time decreased. This was due to the physical and chemical interactions that took place when the Adva 108 (superplasticizer) molecules were adsorbed on the cement particle surfaces [*Betancourt, G. H., 1988*]. The thin layer of admixture on the powder particles provided a negative charge, causing repulsive forces between the particles. These repulsive forces helped to bring about deflocculation of the powder particles in the fresh mortar, hence releasing more free water in the mix. Therefore, as the admixture dosage increased, the amount of free water in the system

increased, and the inter-particle friction or inter-particle forces between the systems decreased. As a result, the change in yield stress with respect to time decreased, with an increase in dosage of superplasticizer.

From Fig 6.6, it can be observed that the decrease in plastic viscosity with respect to time is quite minimal at different dosages of Adva 108. Hence the change in plastic viscosity is not as significant as the change in yield stress due to the increased dosage of superplasticizer.

However, an unusual phenomenon was noted in the change in plastic viscosity of the SCC mortar at higher dosages of superplasticizer, Adva 108. Generally, the plastic viscosity of the system decreased with an increase in dosage of superplasticizer. On the contrary in this study, it was noticed that the plastic viscosity values measured with the BLM viscometer increased with an increase in dosage of superplasticizer. In addition, large amounts of the fine aggregate particles were found to be deposited at the bottom of the inner cylinder at the end of each rheology test.

A possible explanation for this unusual trend in the change in plastic viscosity is that when the admixture dosage increased up to certain level, the decrease in the inter-particle friction due to dispersion of cement particles in the system, resulted in a decrease in plastic viscosity. However, as the admixture dosage increased beyond this level, the excessive decreased in overall plastic viscosity of the system failed to hold the fine aggregate particles which may have resulted in the segregation of the SCC mortar. Therefore, a large quantity of the fine aggregate was found at the bottom of the inner cylinder.

This phenomenon suggested that there is an optimum value of dosage of superplasticizer for each specific mix to obtain an acceptable flowability with sufficient plastic viscosity. Such a dosage of superplasticizer is regarded as the optimum dosage which gives the best performance in terms of workability for that particular type of mix.

### 6.3.3 Influence of Different Types of Filler Materials

- **SCC Mortar Without Superplasticizer**

The results of the yield stress and plastic viscosity of SCC mortar containing different filler materials are graphically presented in Fig 6.7 and Fig 6.8. Fig 6.7 shows the change in the rheological parameters with respect to time, while Fig 6.8 shows the change in rheological parameters with respect to w/p. The w/p was fixed at 1.75 in Fig 6.7 and the time was fixed at 60 min in Fig 6.8 so that a comparison could be made regarding the influence of each type of filler material on the rheological properties of SCC mortar.

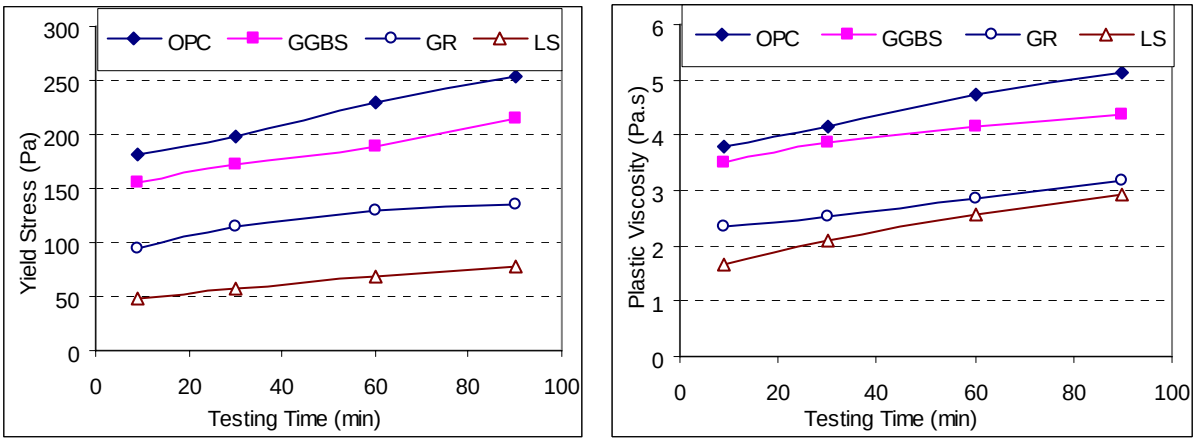


(a) Yield Stress (b) Plastic Viscosity

Fig 6.7: Relationship between yield stress and plastic viscosity with time for different types of filler (No chemical admixture, w/p = 1.75)

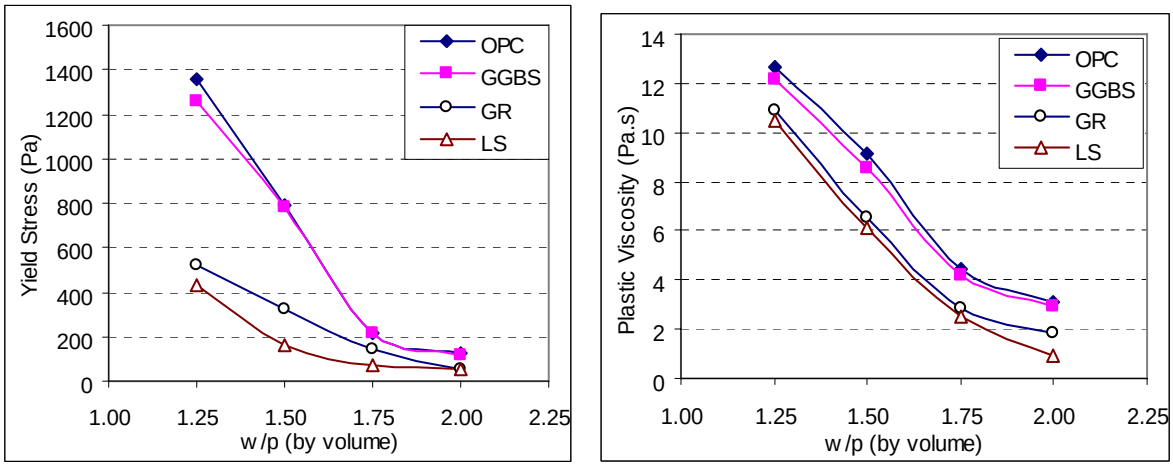


Fig 6.8: Relationship between yield stress and plastic viscosity with w/p for different types of filler (No chemical admixture, Testing time = 60 min)

From the graphs presented above, it can be seen that the mortar containing OPC showed the greatest change in yield stress and plastic viscosity with respect to time, while the mortar containing LS showed the lowest changes. This result can be explained by the reactivity and the particle shape of the different filler materials [*Day, K. W., 1995*]. By considering the hydration properties of all powders, as explain in Chapter 4, OPC is the most reactive powder, GGBS is partially reactive, while GR and LS are non-reactive. In terms of particle shape, OPC and GGBS are small and evenly distributed about the mean size, GR is flaky and elongated, while LS is cubical.

Therefore, the mortar containing OPC showed the greatest change in rheology due to its high reactivity, which caused the free water present in the system to be used up more quickly due to the hydration process than in the case of mortars containing the inert fillers GR and LS. When comparisons were made between the inert fillers, the mortar containing GR showed a greater change in yield stress and plastic viscosity with respect time than that of LS. This was because the flaky and elongated shape of GR allowed for a greater surface area of contact than the cubical shape of LS. Thus, when the system was

sheared, the internal frictional force in GR was greater than that in LS resulting in higher yield stress and plastic viscosity at the same time interval and similar w/p.

Therefore, it can be concluded from the above findings that the reactivity and the shape of the particles in the different filler materials are the two key factors influencing the change with respect to time in the rheological properties of the SCC mortar under various w/p.

- **SCC Mortar with Superplasticizer**

The results of the comparison of yield stress and plastic viscosity of SCC mortar containing Adva 108 and different filler materials are graphically presented in Fig 6.9 and Fig 6.10. Fig 6.9 shows the change in the rheological parameters with respect to time, while Fig 6.10 shows the change in the rheological parameters with respect to the dosage of superplasticizer. In order to investigate the effect of time, Adva 108 dosage was fixed at 0.6% for powder content in the mix proportion given in Table 6.1 and the w/p was fixed at 1.75 in Fig 6.9. For the effect of dosage of superplasticizer on the rheological parameters, the time was fixed at 60 min and the w/p was fixed at 1.25 in Fig 6.10.

From Fig 6.9, it is observed that among all the mortar mixtures, the mortar contained reactive powder OPC and partially reactive powder GGBS show significantly higher yield stress and plastic viscosity compared to that of the inert filler LS and GR at any testing time interval.

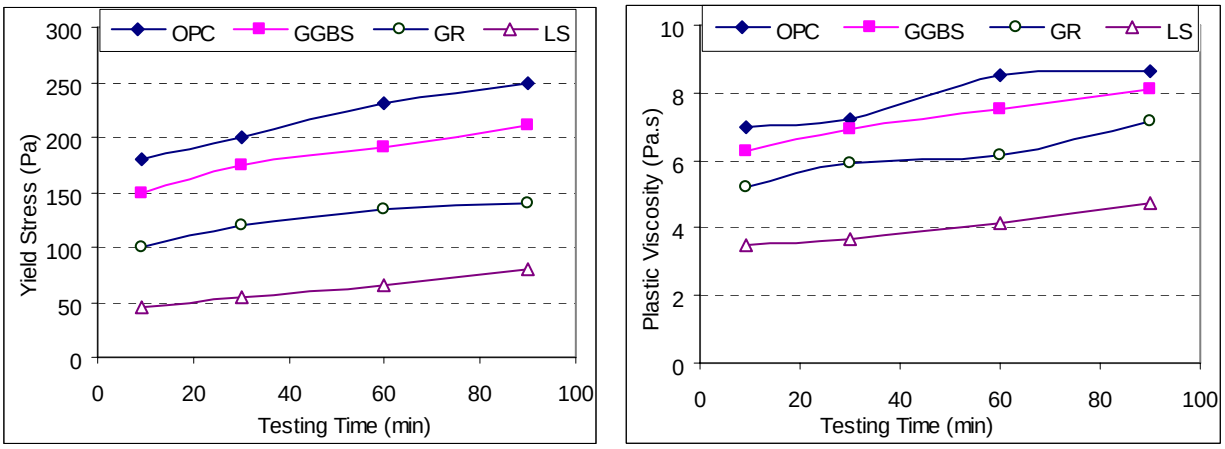


Fig 6.9: Relationship between yield stress and plastic viscosity with time for different types of filler (Admixture Dosage = 0.65% powder, w/p = 1.25)

Similarly, the changes in the yield stress and the plastic viscosity of mortar containing GGBS powder were more significant than those of LS and GR mortar at similar period of time and fixed w/p (Fig 6.10).

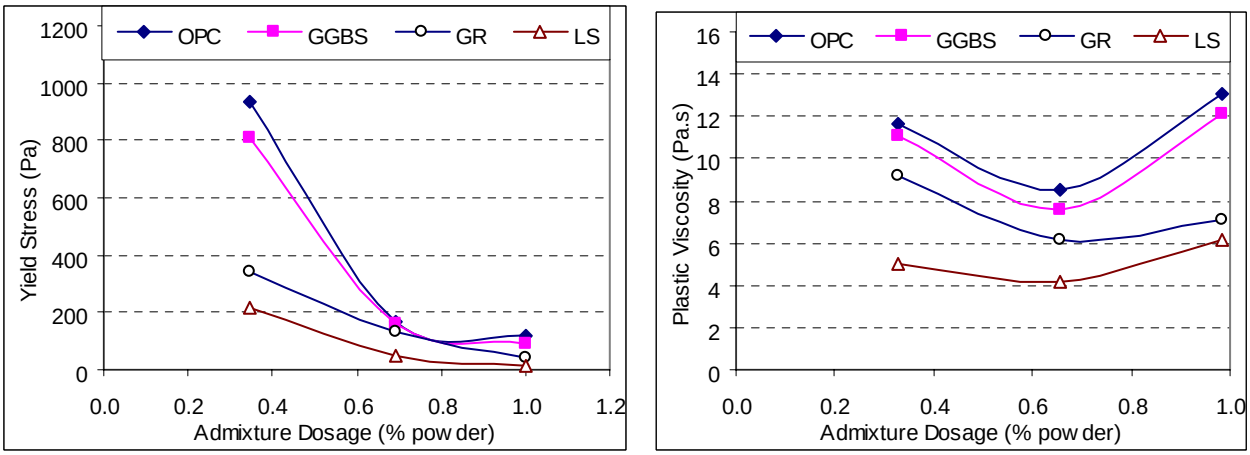


Fig 6.10: Relationship between yield stress and plastic viscosity with admixture dosage for different types of filler
(Testing time = 60 min, w/p = 1.25)

Thus, it can be concluded that the reactivity of the filler particles is the key factor determining the change in rheological parameters either with respect to time at a similar

dosage of admixture and w/p or with respect to dosage of superplasticizer at a similar period of time and fixed w/p.

## 6.4 Summary of Experimental Results

From the series of experiments conducted on SCC mortar, it can be summarized that:

(i) With an increase in w/p, the changes in the rheological properties of the SCC mortar with respect to time become minimal. Hence, the effect of time becomes less and less significant at higher w/p.

(ii) For a fixed w/p, the change with respect to time of both the yield stress and the plastic viscosity decrease as the admixture dosage increases. However, at a high admixture dosage, segregation may take place and this will then lead to an increase in plastic viscosity due to segregation.

(iii) SCC mortar containing reactive fillers exhibit a greater change with respect to time in their rheological properties than those containing inert fillers. The effect of admixture dosage is also more pronounced in SCC mortar containing reactive fillers.

## 6.5 Correlation between Mortar Rheology and Paste Rheology

In the previous section, the influence of water to powder ratio, dosage of superplasticizer, the type of powder and the time factor on change in the rheological properties of mortar had already been discussed. In this section, the possible correlations between the rheological properties of mortar and its paste fraction are investigated.

In order to investigate the correlation, it is assumed that the whole population of fine aggregate is suspended in the paste, which is regarded as the suspending medium.

Therefore, the rheology of mortar is controlled by the rheology of the suspending medium rheology (paste) and inter-particle distance between the fine aggregate particles. The mortar sample was prepared with fine aggregate with four grading in order to investigate the particle shape and size distribution of fine aggregate on the rheological parameters of mortar.

Fig 6.11 presents the variation in the yield stress and the plastic viscosity of mortar varies with solid volume concentration. Similar to the phenomenon in the paste study, both rheological parameters increased exponentially with an increase in the solid volume concentration regardless of the type of fine aggregate. It is noted that unlike cement paste, no linear relation was found between the solid volume concentration and the plastic viscosity. (Fig. 6.11 b). This might be due to the fact that the mortar contained fine aggregate particles in addition to fine powders; such incorporation of fine aggregate particles increased the solid volume concentration of mortar compared to its paste fraction. Therefore, unlike paste rheology, there is no simple linear relation to be found between the plastic viscosity and the solid volume fraction of mortar.

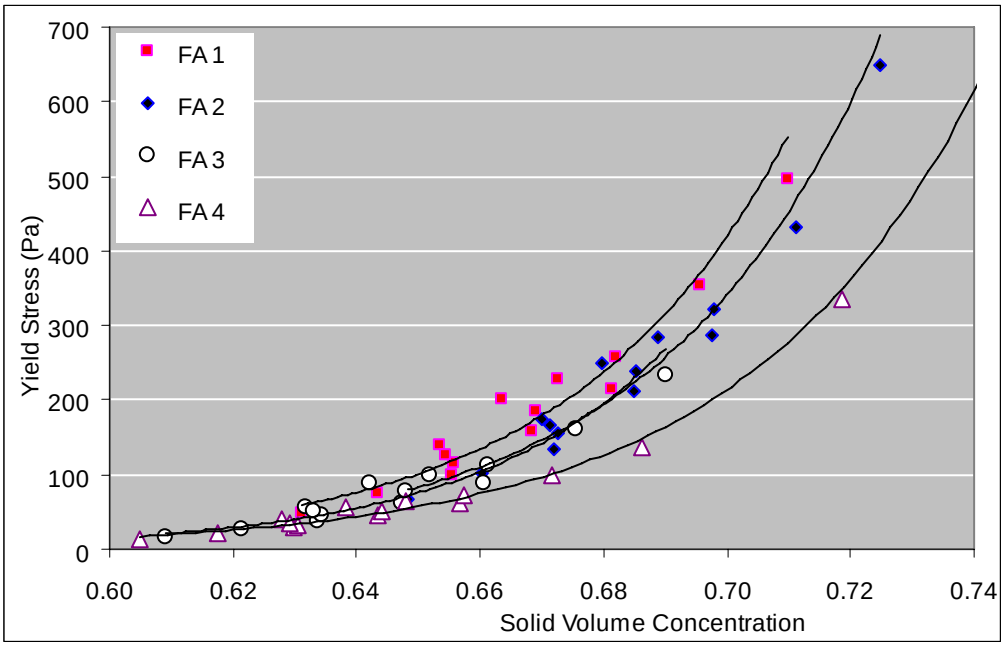


(a) Variation of Yield Stress

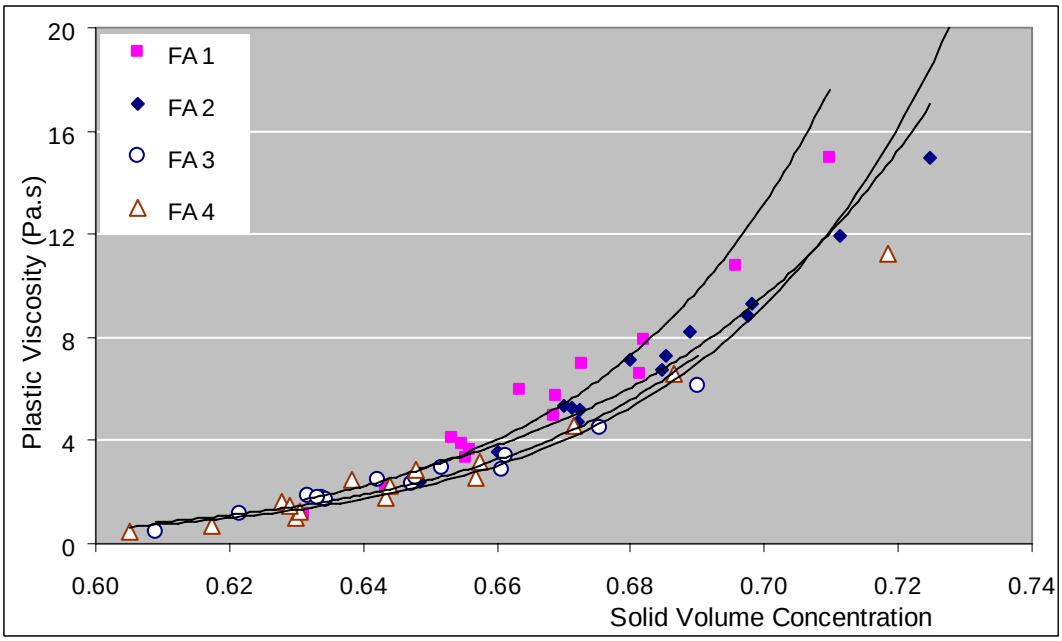


(b) Variation of Plastic Viscosity

Fig.6.11 Relationship between solid volume concentration and rheological parameters of Mortar

In this study, the inter-particle distance between the fine aggregate particles are determined as the thickness of the excess paste (*Tp*) around each particle, which was calculated from *Eq. 3.29a.* Fine aggregate with four grading had been used in this study. The specific surface area ($\sigma_g$) and the angularity factor ($1/\psi_L$) of the different graded fine aggregates were calculated using their respective size ranges obtained from sieve analysis (*Eq. 3.29b & 3.29c)* and the results are presented in Table 6.2.

Table 6.2 Specific surface modulus, angularity factor and specific surface area of different graded fine aggregate

| **Designation** | **Surface Modulus, SM** | **Angularity Factor, $1/\psi_L$** | **Specific Surface Area, $\sigma_s$ ($cm^2/cm^3$)** |
|---|---|---|---|
| **FA 1** | 24.23 | 0.73 | 186.56 |
| **FA 2** | 28.38 | 0.74 | 213.29 |
| **FA 3** | 27.71 | 0.91 | 160.32 |
| **FA 4** | 29.45 | 0.96 | 180.35 |

Similar trends are observed as in the paste study; both the yield stress and the plastic viscosity of mortar decreased exponentially with the thickness of the excess paste, Tp. (Fig 6.12)

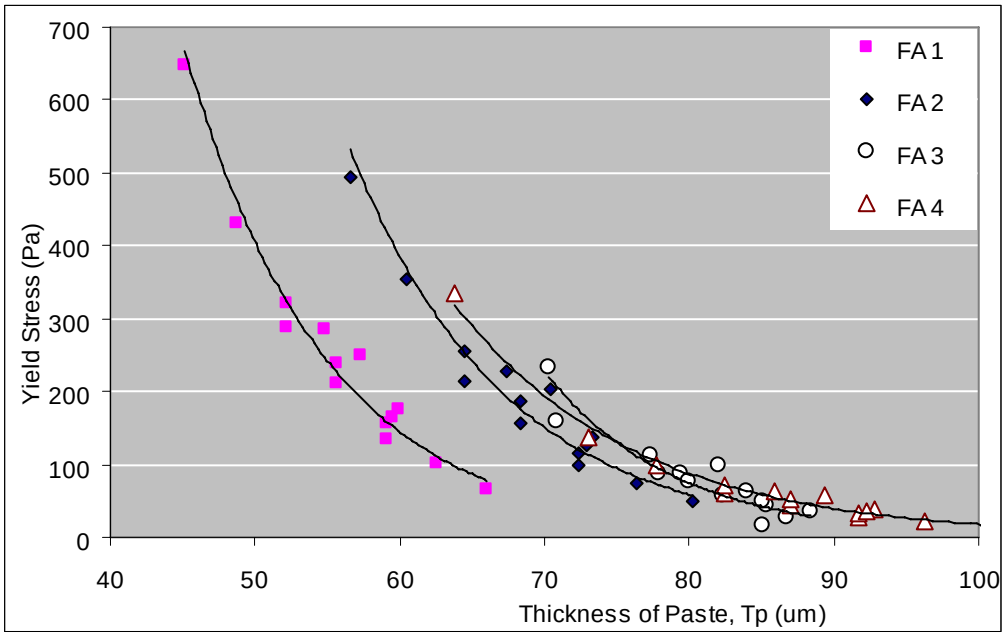


(a) Variation of Yield Stress

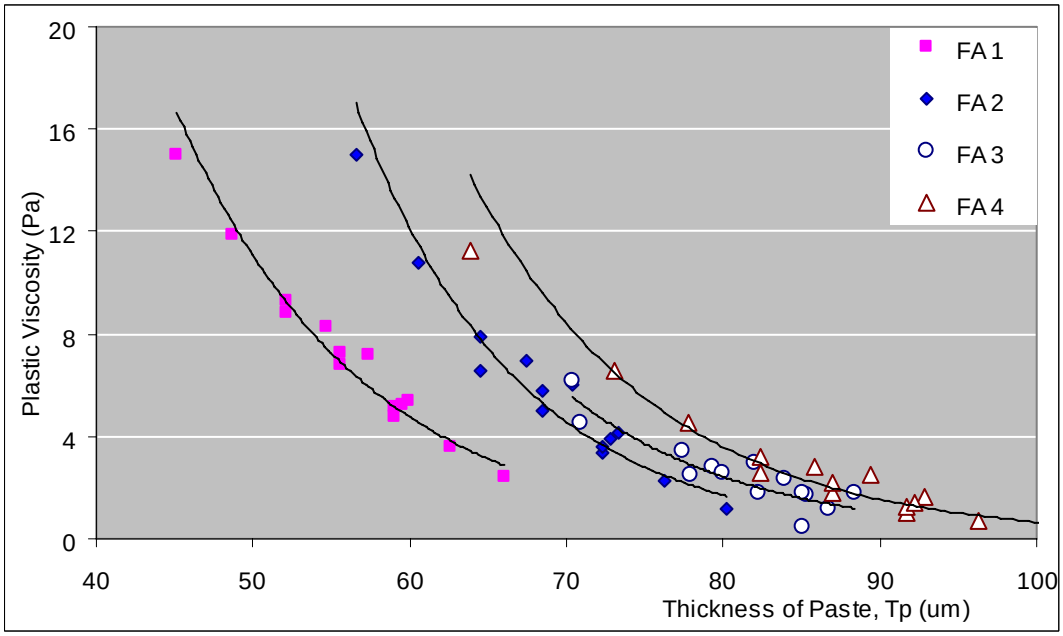


(b) Variation of Plastic Viscosity

Fig.6.12 Relationship between thickness of excess paste and rheological parameters of Mortar

In order to correlate the mortar rheology to the rheology of its paste fraction, it is necessary to understand the differences between their respective rheological parameters. In this study, the relative yield stress and relative plastic viscosity are used instead of the

actual yield stress and plastic viscosity itself. The relative rheological parameters mentioned here are defined as the ratio of the rheological parameters of the mortar to those of the respective paste.

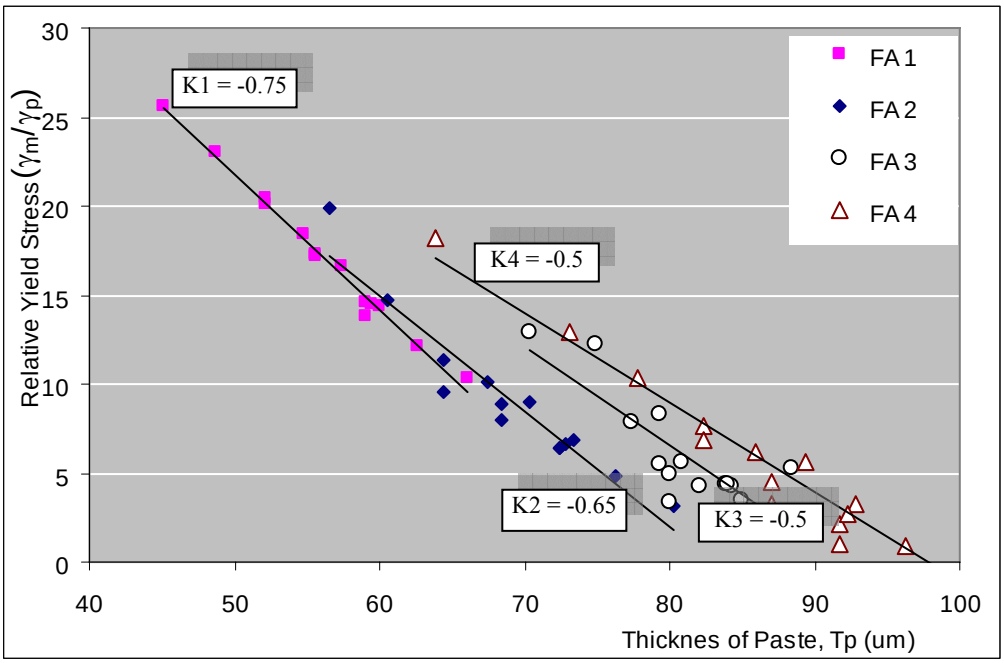


(a) Variation of Relative Yield Stress

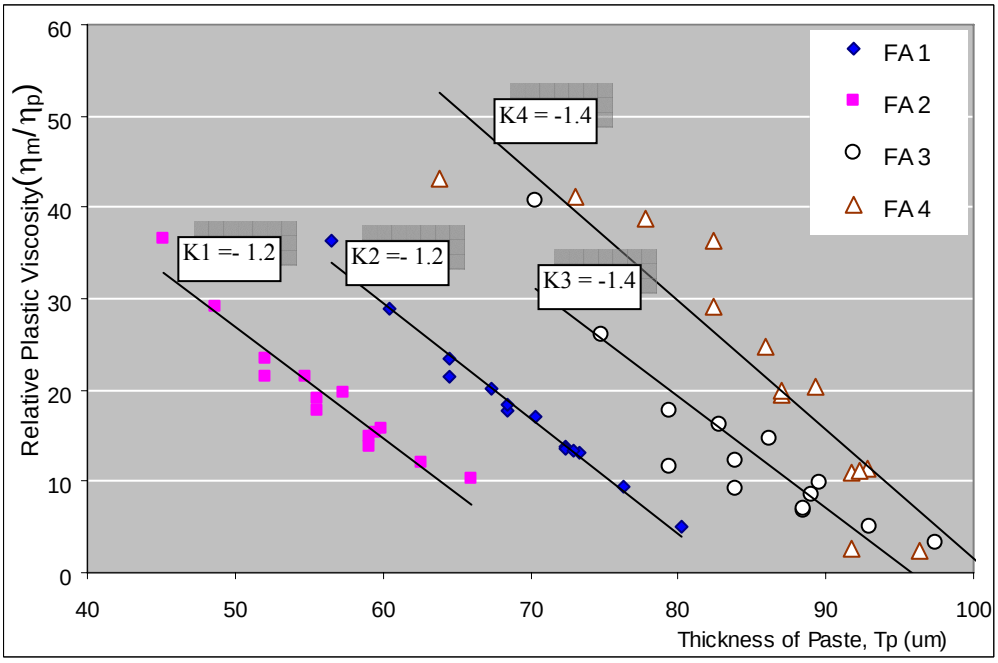


(b) Variation of Relative Plastic Viscosity

Fig. 6.13 Relation between thickness of excess paste and relative rheological parameters

It can be seen from Fig. 6.13 (a & b) that linear relations are observed between both the relative rheological parameters; which are the ratio of the yield stress and the plastic viscosity of the mortar to those of the respective paste, with the thickness of excess paste. Therefore, the proposed model for yield stress of the mortar given in Eq 3.27 and Eq 3.28 can be written as;

For Yield Stress of Mortar: $$\tau_m = \tau_p \left[1.6 SM\ \psi_L + K_{m\tau} T_P\right] \quad \text{Eq (6.1)}$$

For Plastic Viscosity of mortar: $$\eta_m = \eta_p \left[5 \frac{SM}{\psi_L} + K_{m\pi} T_P\right] \quad \text{Eq. (6.2)}$$

where $\tau_m (Pa)$ , $\eta_m (Pa\text{-}s)$are the yield stress and plastic viscosity of the mortar. $\tau_p$, $\eta_p$ are the yield stress and plasticity viscosity of the corresponding paste and $T_p$ (um) is the thickness of excess paste. $K_{\tau m}$ and $K_{\eta m}$ are the slope of the best fit line. $1/\psi_L$ and $SM$ are the angularity factor and surface modulus of the fine aggregate used in the mix and the values are given in Table 6.2.

It can be concluded from the above findings that the rheological parameters, yield stress and plastic viscosity of the mortar can be estimated from its respective paste fraction by introducing the physical effect contributed by the fine aggregate.

# CHAPTER 7

# RHEOLOGICAL STUDY ON SELF-COMPACTING CONCRETE

## 7.1 Introduction

As discussed in the previous section, the composition of the cement paste significantly governed the flow behavior of concrete such as workability, slump loss and other phenomena in the fresh stage. In addition, the paste phase also provides the cohesion necessary for mechanical integrity and durability of the concrete. Therefore, the optimization of the composition of concrete could, therefore, be based on the design of the paste phase. However, due to the large difference in particle sizes involved in the paste and the concrete, it is difficult to correlate the rheology of the paste directly to the rheology of concrete. Thus in the previous chapter, correlation between the paste fraction and the mortar fraction of SCC had been discussed. Sufficient deformability of the mortar phase is required so that concrete can be compacted into structures by its self-weight without the need for compaction by vibrators. In addition, moderate viscosity as well as deformability of the mortar phase is necessary to enhance segregation resistance of the mixture when the concrete flows through obstacles especially closely spaced reinforcing bars [*Okamur H., Ouchi M., 2003*]

The difference between a concrete and its mortar fraction is the addition of coarse aggregate particles which sometimes ranges form 5 mm to 20 ~40 mm. (max size of aggregate used in this study was 20 mm). Thus, considering the physical effect contributed by the fine and coarse aggregate particles, the correlation between flow properties of paste, mortar and concrete could be established. Concrete rheology can be optimized only if the rheology of its mortar fraction is optimal [*Westerholm M., 2006*].

In this chapter, a rheological study on SCC is first presented and the correlation between SCC and its mortar fraction is investigated. The correlation described herein is basically to predict the rheological parameters of SCC from those of the mortar, which has a similar mix proportion as the mortar fraction of corresponding SCC.

## 7.2 Experimental Program

### 7.2.1 Materials and Mix Proportions

Coarse aggregate with four types of grading was used to produce concrete mixes. The physical properties of each grading of aggregate such as sieve analysis, specific gravity, absorption, bulk density and voids ratios had been presented in Chapter 4.

The different concrete investigated in this study were prepared by adding a constant amount of coarse aggregate to the mortar which had the similar composition as the mortar fraction which had been investigated in Chapter 6. However, in order to achieve a volume of 1 $m^3$ (1000 liter), the amount of coarse aggregate to be added in the mix was adjusted based on their respective volume or specific gravity. In the series of SCC mixes, superplasticizer is required to be used as one of the essential components which can reduce the water demand while achieving the mix with high fluidity and better cohesiveness. In this research, both types of superplasticizer, ADVA 108 and ADVA 109 were used. The combined dosage of both types of admixtures was introduced in the mixes because SCC is required to maintain sufficient flowability up to a reasonable retention time (targeted retention time in this research was 90 min) as well as to achievethe necessary early strength for demoulding (targeted 1 Day strength is 10 MPa). Therefore, usage of ADVA 108, which contains a retarder, will maintain the flowability of the mix

and at the same time, usage of ADAV 109, which does not have a retarder, will promote the early strength development.

### 7.2.2 Sample Preparations

SCC is a complex mixture. Care must be taken not only to select suitable mix constituents and their proportions but also a proper mixing sequence and mixing procedure to achieve the desired flow properties. Extensive laboratory trials had been conducted to justify the mixing sequence and mixing procedure, which can be applied both in the laboratory and in actual production at a concrete batching plant. A pan mixer with a maximum capacity of 100 liters (Fig. 7.1) was used to carry out the mechanical mixing of SCC. A digital stopwatch with an accuracy of up to 0.1 seconds was also used to record the time elapsed after the addition of water to the materials. It is important that the mortar fraction in concrete must experience a similar shear history as the mortar tested for investigation of the mortar rheology. The following mixing procedure has been found to be appropriate and is adopted through out this research.

Table 7.1 Mixing procedures adopted for SCC mixes

| Steps | Time | Action |
|---|---|---|
| 1 | 0 min | Place all of dry materials (CA + Sand + Powder + OPC) |
| 2 | 0 min | Dry mix for about 15 to 20 sec. |
| 3 | 0 min | Pour all amounts of (100 % water + 100% required dosage of ADVA 109) while the mixer is running. Mix the materials for 2 min. |
| 4 | 2 min | Add 100% required dosage of ADVA 108. |
| 5 | 6 min | Observe the mix and make suitable adjustments. |
| 6 | 8 min | Discharged |

Fig. 7.1 Pan Mixer (100 Liter Capacity) used for SCC mixes

### 7.2.3 Testing Procedure

- **Equipment and Measurement Procedure**

The rheological characteristic of SCC was conducted with a BML rheometer. (Fig. 7.2) The testing principle is basically the same as mortar rheology measurement. Measurements were performed by placing the concrete between an outer and inner cylinder. The outer cylinder was then rotated at a known speed and the torque transferred through the concrete to inner cylinder was measured. In this measurement procedure, the shear stress of the concrete sample was tested under five different speeds. Using linear regression in accordance with the Bingham model, the value of the shear stress corresponding to zero shear rates was extrapolated. This value was recorded as "Yield Stress" of the concrete sample. The slope of the regression line in which the shear stress increased with increasing rotational speed was recorded as "Plastic Viscosity".

Though the Bingham model assumed a linear correlation between shear stress and strain rate, it was found in the test that BML rheometer has an upper limit beyond which the plastic viscosity does not increase with increasing values of yield stress or increasing time. This might be due to the fact that when the concrete becomes stiff, the inner

cylinder rotates with the concrete plug, which separates from the outer part of concrete with only a thin layer of paste. Therefore, the concrete sample with less than a slump value of 80 mm was not a suitable sample on which to perform the rheological measurement using the BML rheometer.

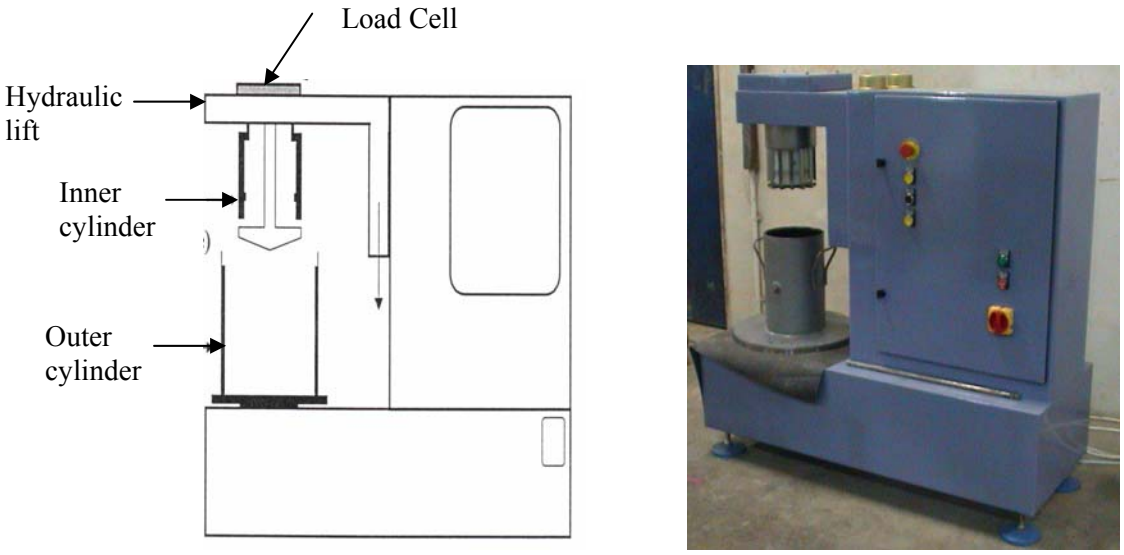


(a) Schematic diagram of BML Rheometer

(b) Outer cylinder (container) and Inner cylinder (blades) used for Concrete Rheology test

Fig. 7.2 BML Rheometer and its component for concrete rheology test

## o Methods & Conditions of Testing

The method and condition of testing for rheological measurements for concrete were similar as those for the mortar fraction because it is important that the mortar fraction in concrete sample should experience the same shear history as the mortar reported in the previous section, Chapter 6.

A fresh batch of concrete sample was prepared for each rheological test series. After 8 minutes of mixing, the concrete sample was placed into the outer cylinder (container) upto the indicated level on the test cylinder. The sample was then tested by rotating the outer cylinder of the rheometer. The angular velocity of the outer cylinder decreased steadily from 0.60 rps to 0.10 rps in decrements of 0.04 rps. After that, a further reading was taken at 0.40 rps in order to check for possible segregation of the sample. The graph of resistance [T/Nm] against velocity [rps/N] was plotted from the data points. The yield stress and plastic viscosity of the concrete were then derived from the graph by adopting the Bingham Model.

The change in the yield stress and plastic viscosity of the concrete sample was monitored over a time period of 90 minutes. A time period of 90 minutes was chosen because this is the estimated time taken by a mixer truck to travel from the concrete batching plant to the construction site. Thus, the mix should maintain its workability for a minimum of 90 minutes. The rheological properties of the concrete were measured at the time intervals of 9 minutes, 30 minutes, 60 minutes and 90 minutes. The detail proportions for the different mixes were presented in Table 7.1.

Table 7.2- Mix proportions for different types of Concrete (w chemical admixture)

| Designation | w/p | Water | Cement | | Filler | | Total Powder | | SURFACE AREA | | | FINE AGG | | COARSE AGG | |
|---|---|---|---|---|---|---|---|---|---|---|---|---|---|---|---|
| | (by Vol) | (kg) | weight (kg) | volume (lit) | weight (kg) | volume (lit) | weight (kg) | volume (lit) | OPC (m2) | Filler (m2) | Total Area (m2) | Weight (kg) | Volume (lit) | Weight (kg) | Volume (lit) |
| OPC 1-1 | 1.25 | 167 | 420 | 133.33 | 0 | 0.00 | 420 | 133.33 | 111467 | 0 | 111467 | 800 | 296.30 | 1100 | 407.41 |
| OPC 1-2 | 1.50 | 200 | 420 | 133.33 | 0 | 0.00 | 420 | 133.33 | 111467 | 0 | 111467 | 800 | 296.30 | 1000 | 370.37 |
| OPC 1-3 | 1.75 | 233 | 420 | 133.33 | 0 | 0.00 | 420 | 133.33 | 111467 | 0 | 111467 | 800 | 296.30 | 920 | 340.74 |
| OPC 1-4 | 2.00 | 267 | 420 | 133.33 | 0 | 0.00 | 420 | 133.33 | 111467 | 0 | 111467 | 800 | 296.30 | 825 | 305.56 |
| GGBS 1-1 | 1.25 | 167 | 260 | 82.54 | 145 | 50.88 | 405 | 133.42 | 69003 | 42686 | 111689 | 800 | 296.30 | 1100 | 407.41 |
| GGBS 1-2 | 1.50 | 200 | 260 | 82.54 | 145 | 50.88 | 405 | 133.42 | 69003 | 42686 | 111689 | 800 | 296.30 | 1000 | 370.37 |
| GGBS 1-3 | 1.75 | 233 | 260 | 82.54 | 145 | 50.88 | 405 | 133.42 | 69003 | 42686 | 111689 | 800 | 296.30 | 920 | 340.74 |
| GGBS 1-4 | 2.00 | 267 | 260 | 82.54 | 145 | 50.88 | 405 | 133.42 | 69003 | 42686 | 111689 | 800 | 296.30 | 825 | 305.56 |
| GR 1-1 | 1.25 | 182 | 260 | 82.54 | 180 | 63.16 | 440 | 145.70 | 69003 | 42568 | 111572 | 800 | 296.30 | 1015 | 375.93 |
| GR 1-2 | 1.50 | 219 | 260 | 82.54 | 180 | 63.16 | 440 | 145.70 | 69003 | 42568 | 111572 | 800 | 296.30 | 920 | 340.74 |
| GR 1-3 | 1.75 | 255 | 260 | 82.54 | 180 | 63.16 | 440 | 145.70 | 69003 | 42568 | 111572 | 800 | 296.30 | 830 | 307.41 |
| GR 1-4 | 2.00 | 291 | 260 | 82.54 | 180 | 63.16 | 440 | 145.70 | 69003 | 42568 | 111572 | 800 | 296.30 | 740 | 274.07 |
| LS 1-1 | 1.25 | 193 | 260 | 82.54 | 204 | 71.58 | 464 | 154.12 | 69003 | 42589 | 111593 | 800 | 296.30 | 970 | 359.26 |
| LS 1-2 | 1.50 | 231 | 260 | 82.54 | 204 | 71.58 | 464 | 154.12 | 69003 | 42589 | 111593 | 800 | 296.30 | 860 | 318.52 |
| LS 1-3 | 1.75 | 270 | 260 | 82.54 | 204 | 71.58 | 464 | 154.12 | 69003 | 42589 | 111593 | 800 | 296.30 | 760 | 281.48 |
| LS 1-4 | 2.00 | 308 | 260 | 82.54 | 204 | 71.58 | 464 | 154.12 | 69003 | 42589 | 111593 | 800 | 296.30 | 655 | 242.59 |

## 7.3 Experimental Results and Discussions

### 7.3.1 Determination of Required Dosage of Superplasticizer, $D_{SP}$

Generally, superplasticizer is used to reduce the amount of water in the concrete. As a result of the lower water to cement ratio, better concrete properties are obtained. Moreover, superplasticizer is one of the essential components for SCC which requires a higher flowability with better segregation resistance. However, over dosage of superplasticizer tends to increase the risk of segregation. For a concrete to be stable, the initial stage of the concrete must be stable. Suitable aggregate content as well as the amount of fines must be selected. The required dosage of superplasticizer is different for different water content in the mix. Superplasticizers are normally dosed in percent by weight of the cement. However in this research, the required dosage of the superplasticizer for the mix was calculated as percent by weight of the total powder, comprising cement plus fine filler.

For traditional concrete, the recommended dosage obtained from the manufacturer was used in most of the cases. Increases in the doses over and above the normal recommended ranges can, in certain cases, result in negative effects such as the segregation of fresh concrete or prolonged retardation of concrete. There is no specific method to determine the required dosage of superplasticizer for a particular mix. Therefore in this research, the possible required dosage of superplasticizer was determined by testing the pastes to reach its saturation point. Saturation point of the paste is the point in which the consistency of the paste did not change with further increase in dosage of the superplasticizer. The dosage of the superplasticizer corresponding to such a saturation point was regarded as the required dosage of the superplasticizer for that particular mix.

Saturation point of the mix was determined by using the V-funnel flow test on paste sample which comprises the paste fraction of the concrete mixes given in Table 7.1. Fig 7.3 (a) to (d) presents the saturation point of the series of mixes with different filler powders.

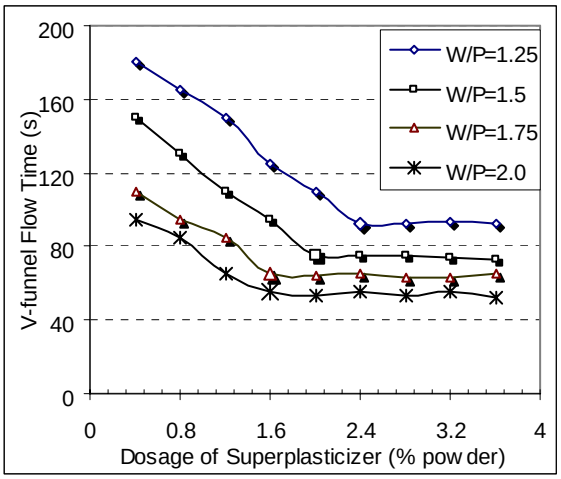


**(a) OPC Series**

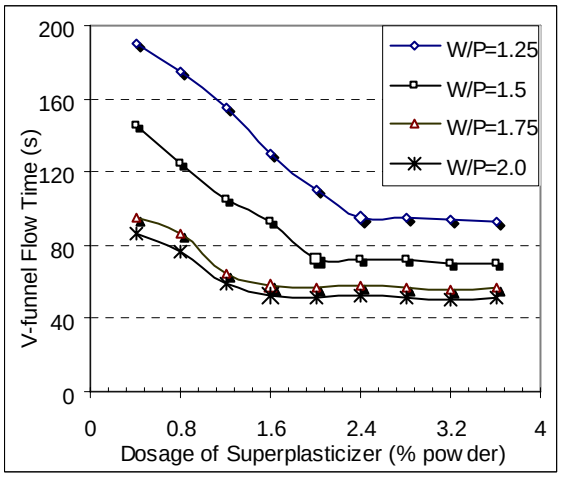


**(b) GGBS Series**

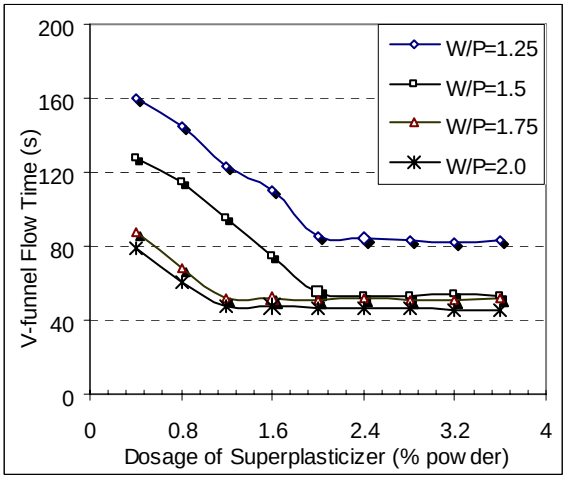


**(c) LS Series**

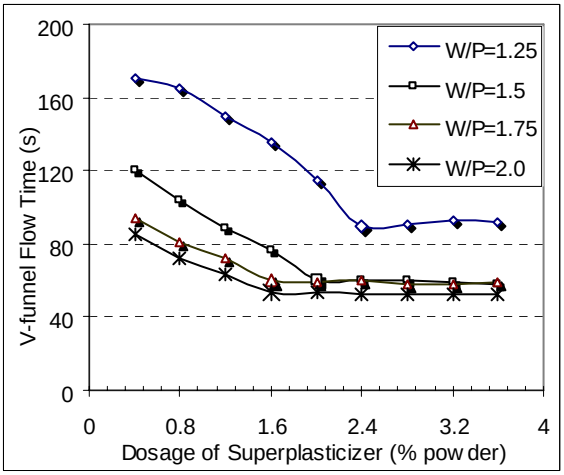


**(d) GR Series**

Fig 7.3 Relationship between flow time and admixture dosage for mixes with different w/p and different type of filler powder

It can be seen from Fig 7.3 that the V-funnel flow times of the paste mixes decrease with an increase in dosage of the superplasticizer up to a certain dosage. Beyond this dosage, there is no or little change in flow time regardless of the increase in dosage of

superplasticizer. It is also observed from figure that the saturation point of the paste mixes depends not only on the water content or water-powder ratio but also on the type of filler powder used in the mix. For the same water-powder ratio, the paste with LS powder required a lower dosage of superplasticizer to reach its saturation point than those with other filler powder. Table 7.2 summarizes the V-funnel flow time and dosage of superplasticizer at the saturation point of the different mixes with respect to water-powder ratio.

Table 7.2 Dosage of superplasticizer and corresponding flow time for different type of mixes at Saturation Point

| Designation | W/P | Saturation Point | |
|---|---|---|---|
| | (by vol) | Flow Time (s) | $D_{SP}$ (% powder) |
| OPC 1-1 | 1.25 | 92 | 2.4 |
| GGBS 1-1 | 1.25 | 95 | 2.4 |
| LS 1-1 | 1.25 | 85 | 2.0 |
| GR 1-1 | 1.25 | 90 | 2.4 |
| OPC 1-2 | 1.50 | 75 | 2.0 |
| GGBS 1-2 | 1.50 | 72 | 2.0 |
| LS 1-2 | 1.50 | 55 | 2.0 |
| GR 1-2 | 1.50 | 60 | 2.0 |
| OPC 1-3 | 1.75 | 65 | 1.6 |
| GGBS 1-3 | 1.75 | 58 | 1.6 |
| LS 1-3 | 1.75 | 52 | 1.4 |
| GR 1-3 | 1.75 | 60 | 1.6 |
| OPC 1-4 | 2.00 | 55 | 1.6 |
| GGBS 1-4 | 2.00 | 52 | 1.6 |
| LS 1-4 | 2.00 | 48 | 1.2 |
| GR 1-4 | 2.00 | 54 | 1.6 |

### 7.3.2 Effect of Water to Powder Ratio at Different Time Interval

Basically, the amount of water in the mix influences the strength of the concrete at the hardened stage. Thus, SCC with different strength requirements can be prepared by varying the water content of the mix without changing the other mix constituents. This section discusses the influence of water content on the rheological characteristic of SCC with respect to time interval after mixing with water. The dosage of the superplasticizer used for the different mixes was based on the dosage at the saturation point of the corresponding paste mixes given in Table 7.2.

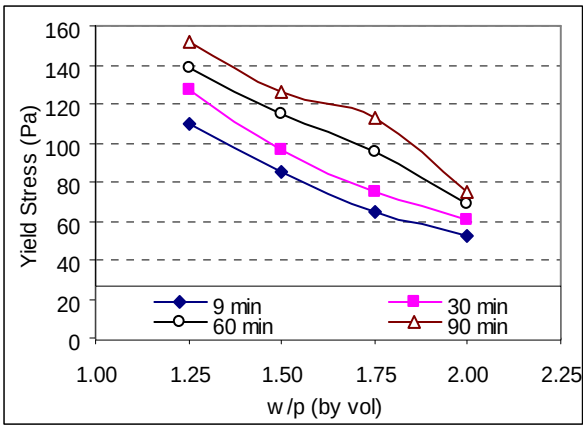


**(a) OPC Series**

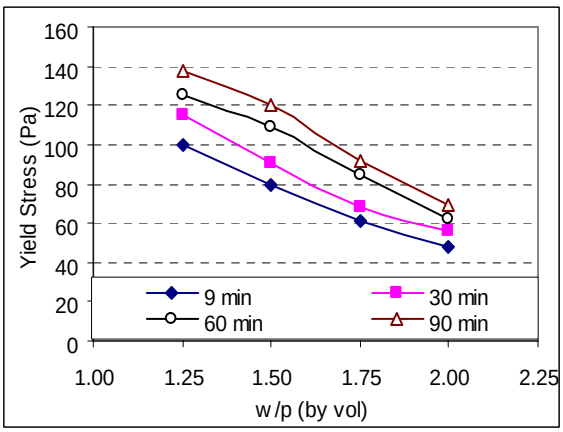


**(b) GGBS Series**

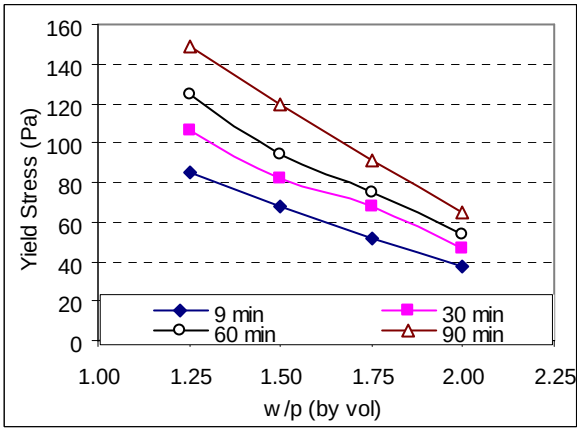


**(c) GR Series**

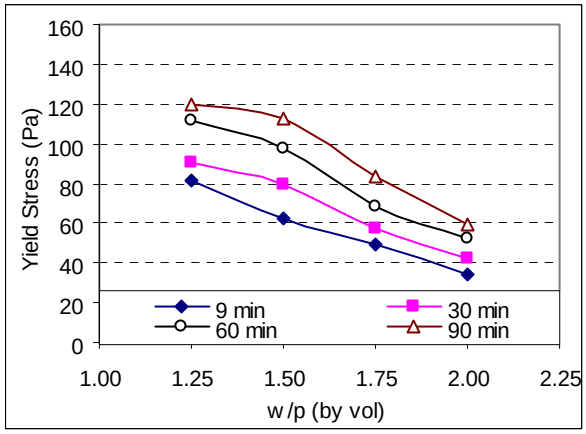


**(d) LS Series**

Fig 7.4: Relationship between yield stress and water/powder ratio at different time intervals

The graphical presentation of the change in yield stress at different water/powder ratios (w/p) for different time intervals is shown in Fig 7.4 and the change in viscosity at different w/p for different time interval is presented in Fig 7.5.

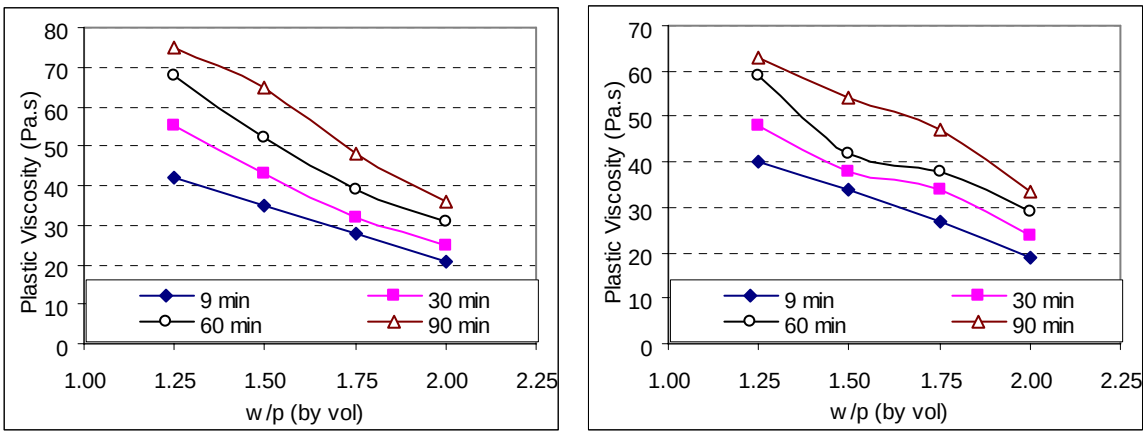


**(a) OPC Series** **(b) GGBS Series**

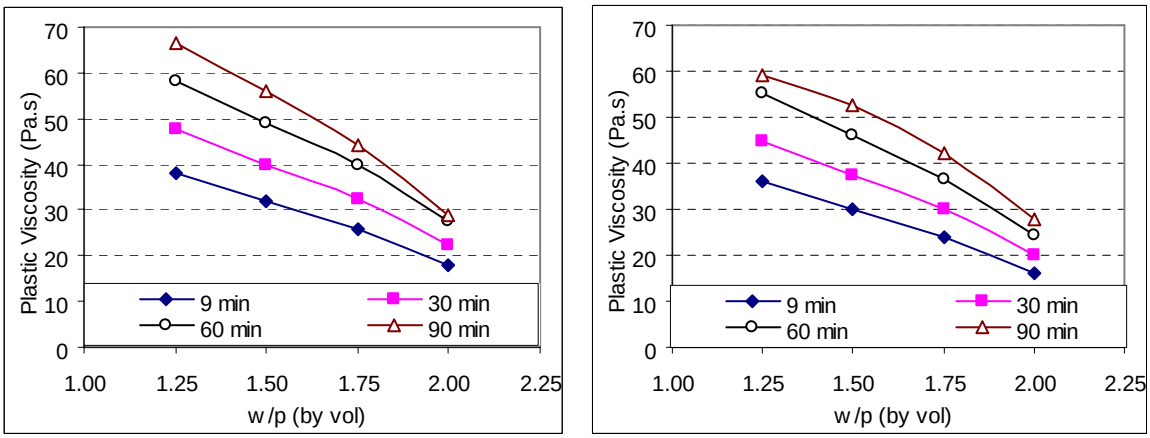


**(c) GR Series** **(d) LS Series**

Fig 7.5: Relationship between plastic viscosity and water/powder ratio at different time intervals

It can be seen from Figs 7.4 and 7.5, both the plastic viscosity and the an yield stress decrease with an increase in water/powder ratio. At a lower level of w/p (e.g w/p= 1.25), both the yield stress and the plastic viscosity increased significantly with testing time. Conversely, there was little or no changes in the rheological properties at higher w/p

within ta time duration of 90 minutes. This phenomenon is similar to that of mortar rheology and a similar explanation can be applied.

This is because the yield stress and plastic viscosity of the SCC depends on the amount of free water present in the system. At higher w/p of the mix, there was a higher amount of free water in the mix for the time duration up to 90 minutes. Thus, the excess amount of such water prolongs the retention time of the mix and therefore there is little change in the rheological parameters within the testing duration. However at lower w/p, there is less free water present in the mix as this free water is partially used up over the 90 minutes period due to the formation of hydration products. This phenomenon results an increase in the inter-particle friction, which led to greater forces required to initiate flow in the system. As a result, the yield stress and plastic viscosity increased significantly over the same time interval at lower w/p.

It can also be observed that in the mixes with higher w/p, both the yield stress and the plastic viscosity values are still within the acceptable limits for SCC (yield stress< 80 Pa and plastic viscosity < 36 Pa.s). It means that these mixes maintain their workability over a time interval of up to 90 minutes.

### 7.3.3 Influence of Different Types of Filler Materials

As discussed in the earlier section, the powder used in SCC was composed of Ordinary Portland Cement (OPC) and filler powder. Therefore it is possible that different filler powder in the mix will behave differently in the respective mixes. The results of the

yield stress of SCC containing different filler materials are graphically presented in Fig 7.6.

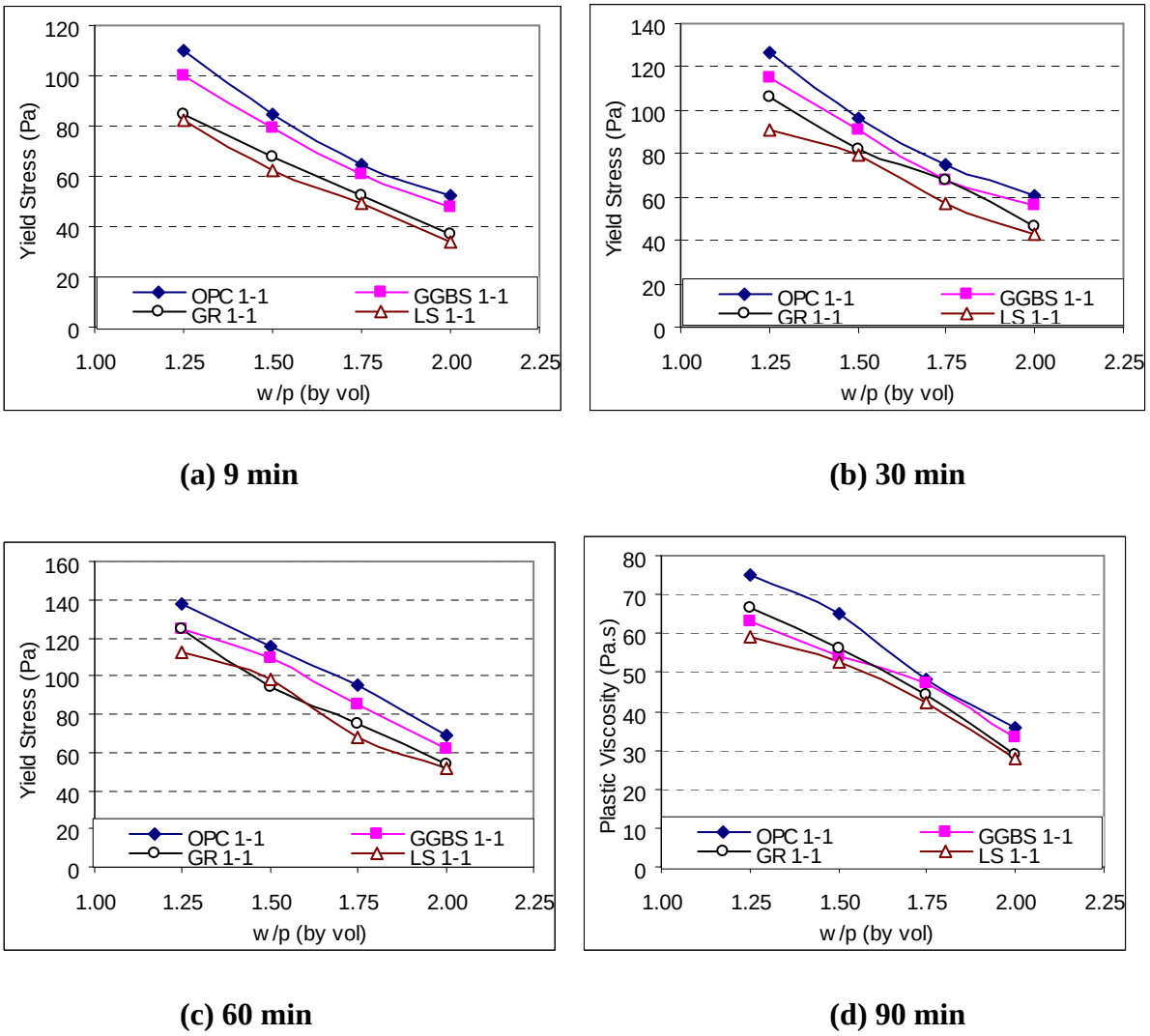


Fig 7.6: Relationship between yield stress and testing time for different types of filler

It can be observed from the above figure; SCC mixes with pure OPC powder shows a higher yield stress than the mixes with the other types of powder regardless of w/p and testing time. Comparing the other types of powder beside OPC, higher yield stress was observed in the mixes with GGBS powder and the lowest was in the mixes with LS powder for different levels of w/p and testing time.

The variation of plastic viscosity of SCC containing different filler materials are graphically presented in Fig 7.7.

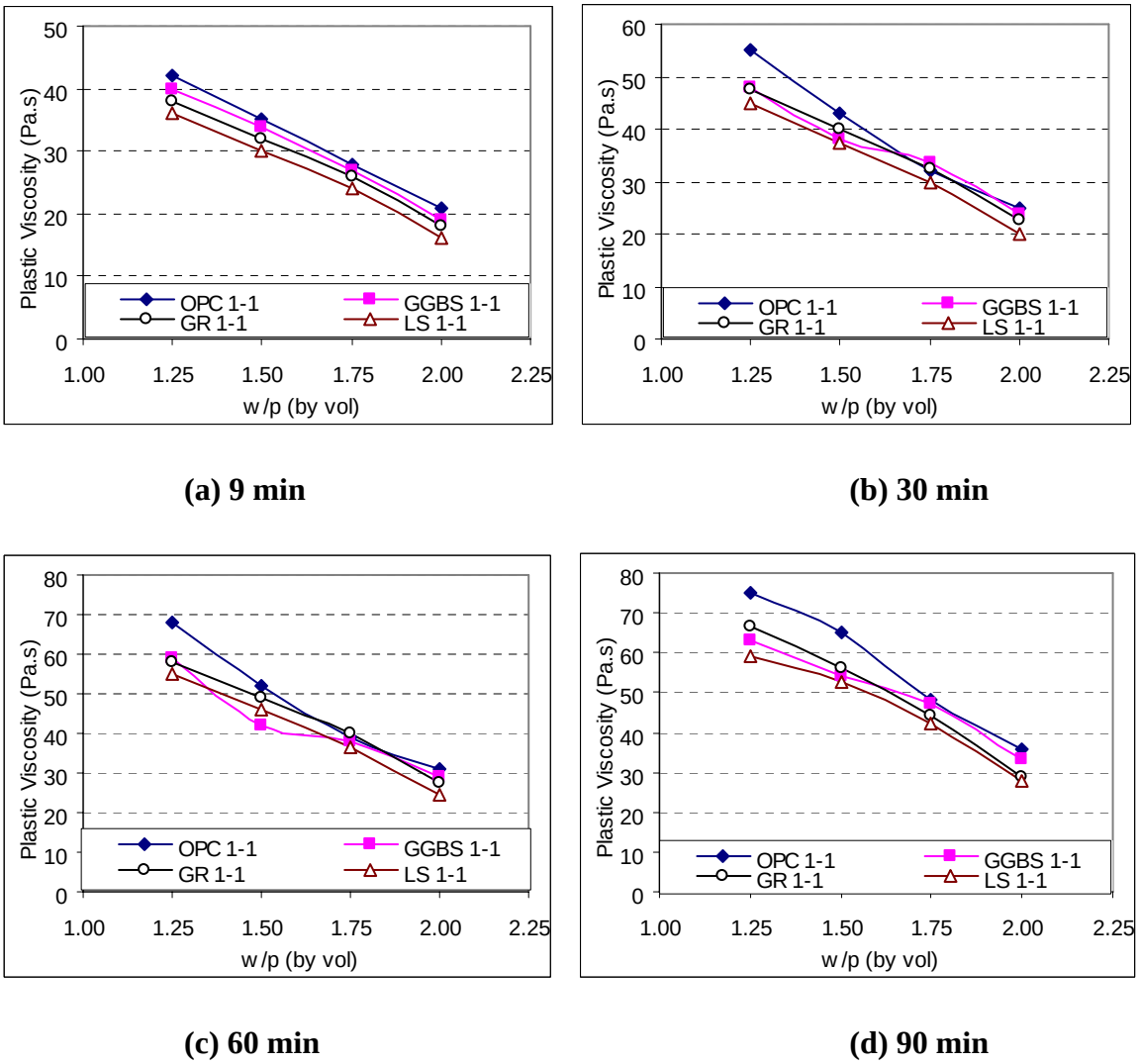


Fig 7.7: Relationship between plastic viscosity and testing time for different types of filler

From the graphs presented above, a similar phenomenon was found as in the case of yield stress. It can be seen that SCC mix containing pure OPC showed the greatest change in viscosity with respect to time, while the mix containing LS showed the lowest changes. This result can be explained by the reactivity and the particle shape of the different filler materials.

The mixes with the highly reactive pure OPC powder enhance the hydration process which required more water in the mix than those mixes with less reactive powder. Thus, less free water was available in the system to contribute towards the workability of the mix.

When comparisons were made between the inert fillers, the mortar containing GR showed a greater change in the yield stress and the plastic viscosity with respect time than that of LS. This is because the flaky and elongated shape of GR leads to a greater surface area of contact with the mortar than the cubical shape of LS. Thus, when the system is sheared, the internal frictional force in GR is higher than that in LS resulting in a higher yield stress and plastic viscosity at the same time interval and similar w/p.

Therefore, it can be concluded from above findings that the reactivity and the shape of the particles in the different filler materials are the two key factors influencing the change with respect to time of the rheological properties of SCC with various w/p.

## 7.4 Summary of Experimental Results

From the series of experiments conducted on SCC, the results can be summarized as follows;

(i) The required dosage of superplasticizer for the different mix proportions of SCC can be determined by testing its paste fraction to reach its saturation point. The saturation dose of admixture is dependent not only on the water-powder ratio or water content but also on the type of filler powder used in the mix.

(ii) The dosage of superplasticizer at the saturation point can be regarded as the optimal dosage required for the corresponding SCC.

(iii) SCC showed similar rheological characteristics as its mortar fraction. The changes in the rheological parameters of SCC with testing time are minimal when the mix had a higher water-powder ratio or higher water content.

(iv) SCC containing reactive powder showed higher rheological parameters than those with non-reactive fillers regardless of the water-powder ratio or testing time. Comparing between the non-reactive fillers, the particle shape or surface geometry of the powder influences the rheological parameters.

(v) The reactivity and surface geometry of filler used in the SCC mixes are the main controlling factors for the differences in the rheological parameters.

## 7.5 Correlation between Concrete Rheology and Mortar Rheology

In the previous section, it was found that the rheological characteristics of SCC were similar to that of mortar which had a similar mix proportions as the SCC except for the incorporation of coarse aggregates. Therefore, it is possible that there might be some correlation between SCC and its corresponding mortar fraction. In this section, the possible correlations between the rheological properties of SCC and its mortar fraction are investigated.

In order to investigate the correlation, it is assumed that the whole population of coarse aggregate in concrete is suspended in the mortar, which is regarded as suspending medium. Therefore, the rheology of the concrete is controlled by the rheology of the suspending medium (mortar) and the inter-particle distance between the coarse aggregate particles.

Fig 7.8 presents the variation of yield stress and plastic viscosity of concrete with solid volume concentration. Similar phenomenon as mortar rheological study, both rheological parameters increased exponentially with an increase in the solid volume concentration. Concrete samples were prepared with coarse aggregate of four grading types.

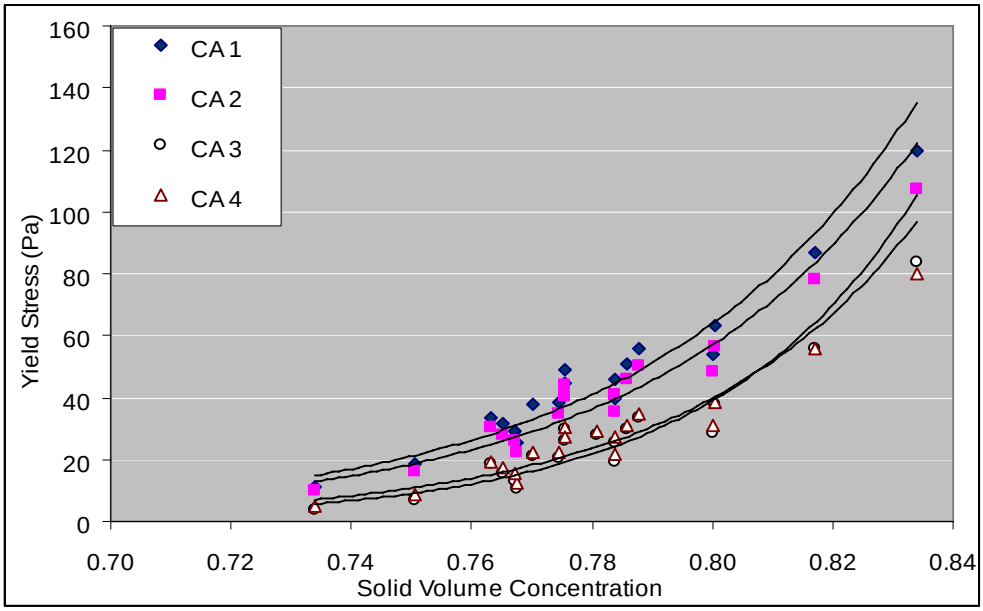


(a) Yield Stress

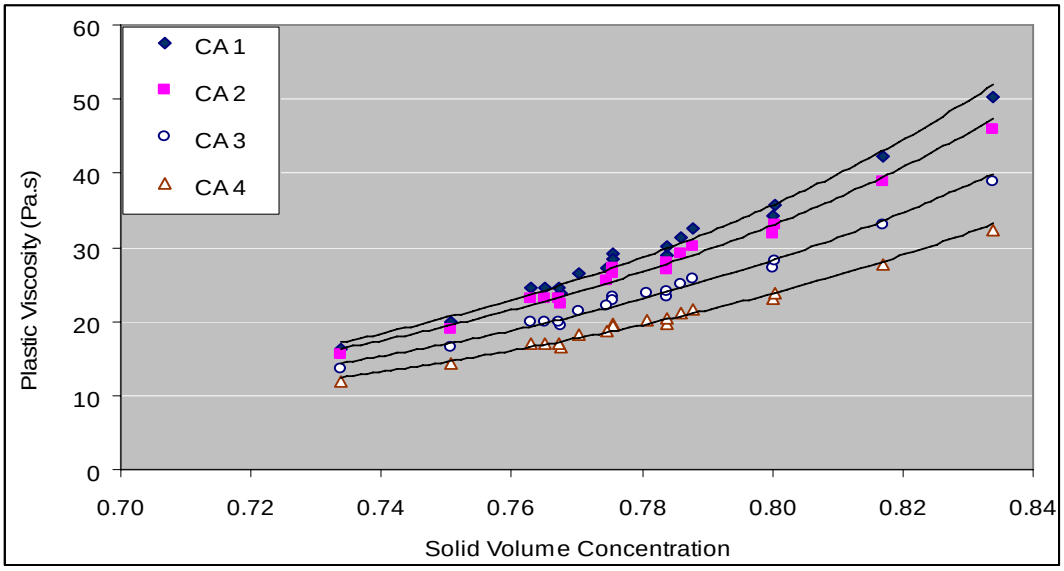


(b) Plastic Viscosity

Fig.7.8 Relationship between solid volume concentration and rheological parameters of SCC

Similar to the mortar rheological study, the inter-particle distance between the coarse aggregate particles is determined as the thickness of the mortar (*Tm*) around each particle, as calculated from *Eq. 3.32a.* Coarse aggregate with the four types of grading had been used in this study. The specific surface area ($\sigma_g$) and the angularity factor ($1/\psi_L$) of the different graded aggregates were calculated from their respective size ranges obtained from sieve analysis (*Eq. 3.32b & 3.32c)* and presented in Table 7.3.

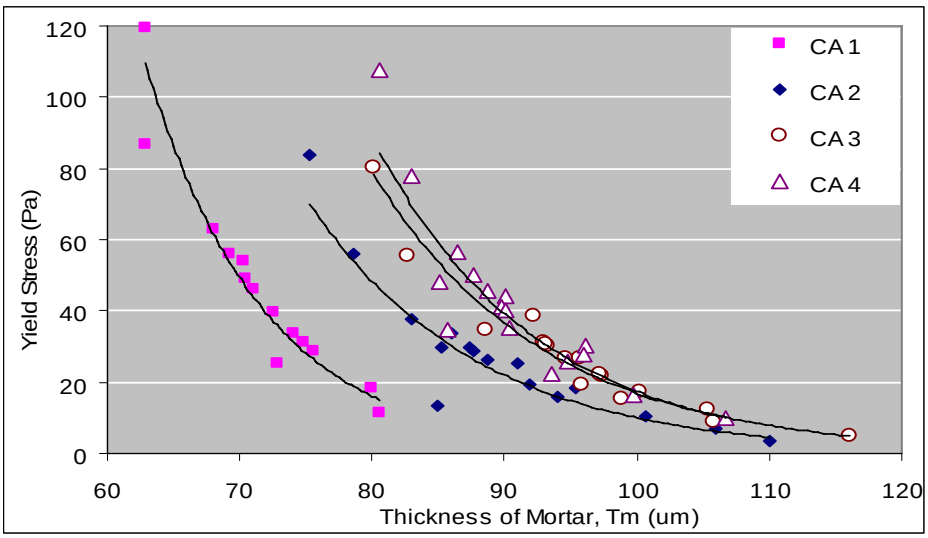


(a) Yield Stress

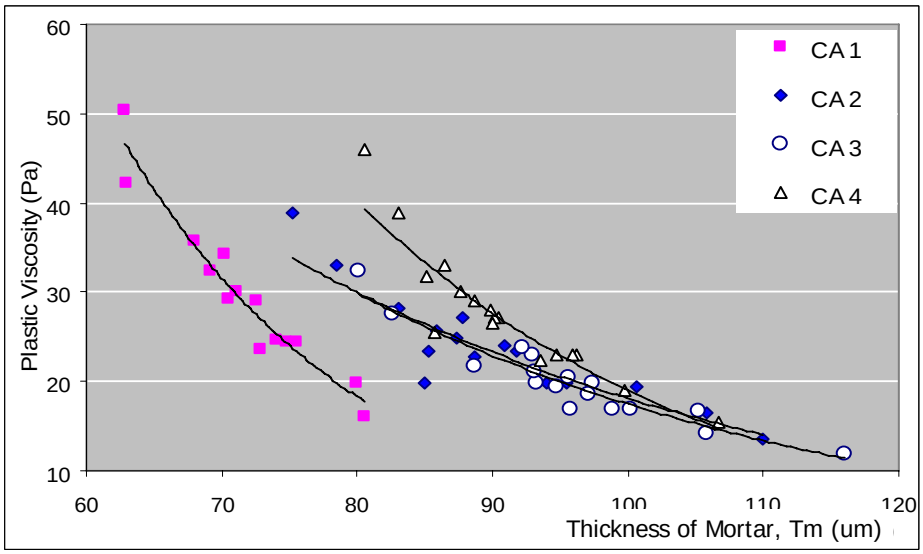


(b) Plastic Viscosity

Fig.7.9 Relationship between thickness of excess paste and rheological parameters of SCC

Similar trends observed in the mortar study; both the yield stress and the plastic viscosity of SCC decreased exponentially with the thickness of excess mortar, Tm. (Fig7.9)

Table 7.2 Specific surface modulus, angularity factor and specific surface area of different graded coarse aggregate

| Designation | Surface Modulus, SM | Angularity Factor, $1/\psi_L$ | Specific Surface Area, $\sigma_s$ ($cm^2/cm^3$) |
|---|---|---|---|
| **CA 1** | 18.5 | 1.15 | 118.81 |
| **CA 2** | 21.2 | 1.22 | 144.03 |
| **CA 3** | 23.7 | 1.21 | 159.84 |
| **CA 4** | 25.5 | 1.18 | 167.56 |

In order to correlate the rheological parameters of concrete to those of its mortar fraction, the relative yield stress and relative viscosity are used. Relative rheological parameters are defined as the ratio of each rheological parameter of the concrete to that of its corresponding mortar of the same mix proportions as the mortar fraction in concrete.

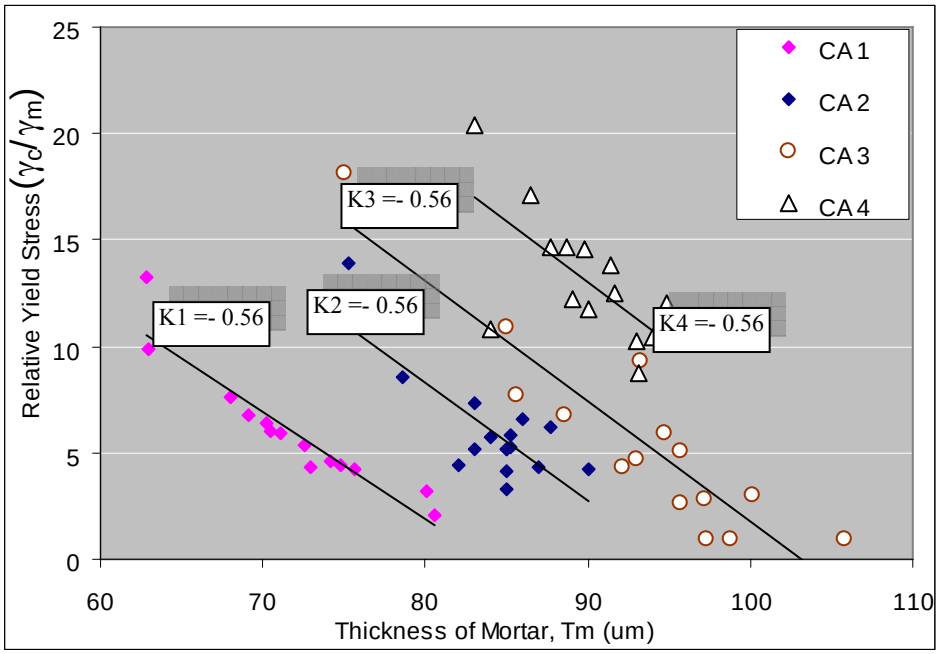


(a) Relative Yield Stress

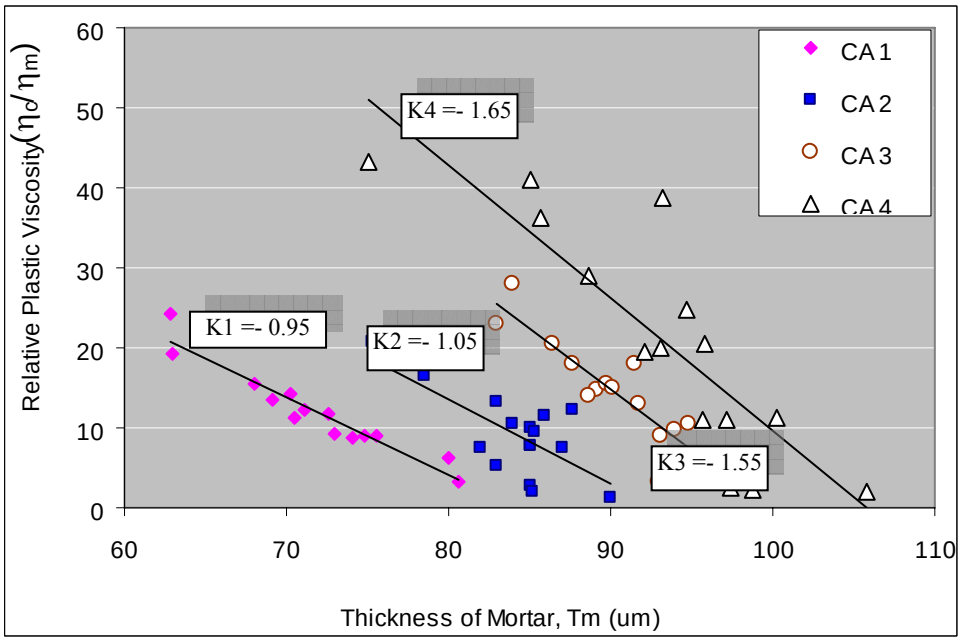


(b) Relative Plastic Viscosity

Fig. 7.10 Relationship between thickness of excess mortar and relative rheological parameters

It can be seen from Fig. 7.10 (a & b) that linear relations are observed between both the relative rheological parameters; which are the ratio of the yield stress and the

plastic viscosity of concrete to those of its corresponding mortar, with the thickness of mortar. Therefore, the proposed model for yield stress and plastic viscosity of concrete given in Eq 3.30 and Eq 3.31 can be written as;

For Yield Stress of SCC: $$\tau_c = \tau_m \left[ 2.0 \frac{SM}{\psi_L} + K_{c\tau} T_m \right]$$ Eq (7.1)

For Plastic Viscosity of SCC: $$\eta_c = \eta_m \left[ 4.7 \frac{SM}{\psi_L} + K_{c\eta} T_m \right]$$ Eq. (7.2)

where $\tau_C$ *(Pa)* , $\eta_C$ *(Pa-s)*are the yield stress and plastic viscosity of concrete. $\tau_m$ , $\eta_m$ are the yield stress and the plastic viscosity of the corresponding mortar. $K_{\tau c}$ and $K_{\eta c}$ are the slope of the best fit line. *Tm* (um) is the thickness of the excess mortar. $1/\psi_L$ and *SM* are the angularity factor and surface modulus of the coarse aggregate used in the mix and the value are given in Table 7.2.

Comparing Eq. 6.1 of mortar rheology with above Eq. 7.1 of concrete rheology, the constant ("A" in Eq 3.27 and "C" in Eq 3.30) which is the function of surface modulus and angularity of fine and coarse aggregate are not the same. It might be because in mortar, the suspending medium is paste in which fine aggregate particles are suspended. However in concrete, the suspending medium is the mortar containing fine aggregate particles which physical properties might somehow effect the empirical constant" C" in addition to physical properties of coarse aggregate. Therefore, the function of Angularity Factor and SM for constant "A" in mortar is different from those for constant" C" in concrete.

# CHAPTER 8

# RELATION BETWEEN RHEOLOGICAL PARAMETERS AND SIMPLE PHYSICAL TEST

## 8.1 Introduction

As concrete construction applications become more demanding and self-compacting concrete becomes more widely accepted, there is increasing demand by engineers to ensure high workability while at the same time maintaining the structural properties necessary to meet design specifications. For advancements to be made in the understanding and controlling the workability of SCC in the fresh stage, testing procedures and industrial standards must move to a more fundamental quantitative level. Accordingly, workability should be defined in terms of established measurable rheological parameters such as yield stress and viscosity.

Several authors have acknowledged the need for a more quantitative measure of the fluidity of fresh concrete [*Tattersall G.H et.al, 1983*]. However, measuring the fundamental rheological properties of SCC is experimentally challenging due to the large particle size of the aggregates. Furthermore, the equipment used for field-testing must be relatively inexpensive, easy to use, and sufficiently small to be of practical use at construction sites. For these reasons, there is renewed interest in understanding how the simple physical tests can correlate to the rheological properties of fresh SCC. A better understanding of the flow properties of concrete is needed to be able to predict the flow of concrete from the properties of the components. The objective of this chapter is to investigate the relationship between the rheological parameters and simple physical tests which are easier to handle than a rheological test at the construction site. With this correlation, the concrete engineer will be able to select the fundamental flow properties

of paste, mortar and concrete based on their respective physical tests without the need to conduct the rheological tests.

## 8.2 Correlation of Paste Rheology with Simple Physical Test

The flow properties of different samples of paste had been accessed by simple physical tests prior to the rheological measurement conducted on the same sample.

The main varying parameters for paste sample prepared were;

- Different types of filler powder
- Different ratio of OPC to filler powder
- Different dosage of superplasticizer
- Different water to powder ratio or water content

The detail mix proportions of the different paste samples are presented in Chapter 3.

### 8.2.1 Simple Physical Test Methods for Paste

This section discusses different types of physical tests and their test procedures to assess the flow properties of paste sample.

#### o Mini Flow Cone Test for Paste

The workability of the paste fraction of SCC incorporated with different powders was investigated by the mini slump cone test (Fig.8.1). The fresh paste was poured into the mini cone immediately after the mixing and the flow test was conducted by lifting up the cone. The final spread diameter and the time needed to reach the maximum spread were recorded. The test was repeated three times for each sample and the average value was used to evaluate the flow characteristic.

The yield stress is related to the spread diameter while the flow time is influenced by the paste viscosity. However, it is difficult to record the flow time as the amount of paste tested for the mini cone is small and the flow distance is short. P-Type funnel is introduced to measure the flow time which can be correlated to viscosity.

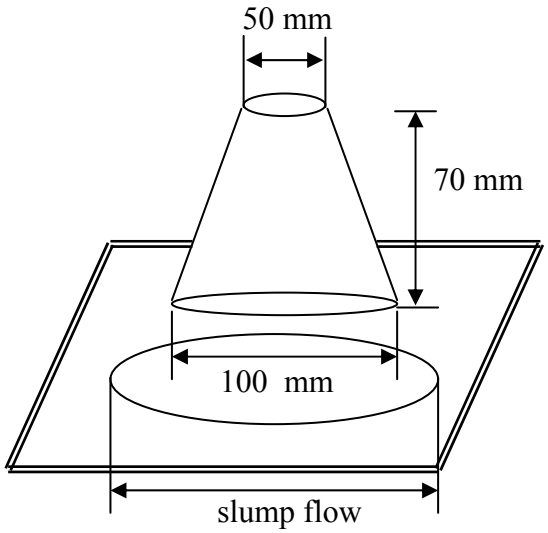


Fig. 8.1 Mini flow cone test

## o P-Type Funnel

P-type funnel test was used to measure the efflux time (flow time) for all types of paste (Fig. 8.2). Immediately after mixing, the paste of a constant volume was put into the funnel with the outlet shut. Then, the paste was allowed to flow out by opening the outlet. The efflux time was recorded once the light was seen through the bottom of orifice when looking down through the funnel. Simultaneously, the flow behavior was observed visually. The test was repeated three times for each sample and the average value was used to evaluate the flow characteristic.

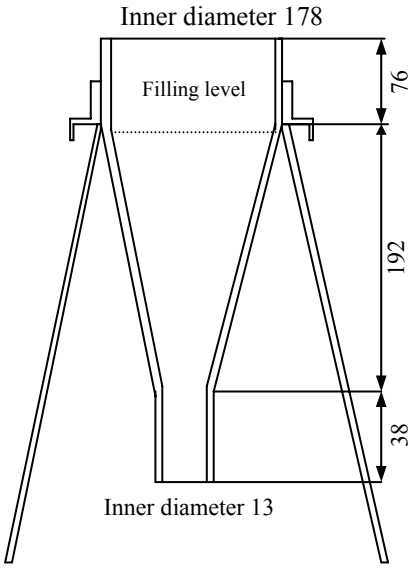


Fig. 8.2 P-Type funnel

## 8.2.2 Correlation of Mini Flow Diameter with Yield Stress

As soon as the mixing was completed, the mini-flow cone test was conducted and the flow diameter was measured. This test was done three times for each paste sample and the average of three tests was recorded as the mini-flow diameter of that particular paste. Then, the rheological measurement was conducted on the same paste sample. The correlation between mini-flow diameter and respective yield stress for the different types of paste samples are presented in Fig 8.3 (a) to (d). It can be observed from these figures that there is a liner relation between the mini-flow diameters of the paste with their respective yield stress values. A higher flow diameter corresponds to a lower yield stress of the paste samples. In other words, the paste samples with a lower yield stress can flow a longer distance than those with a higher yield stress.

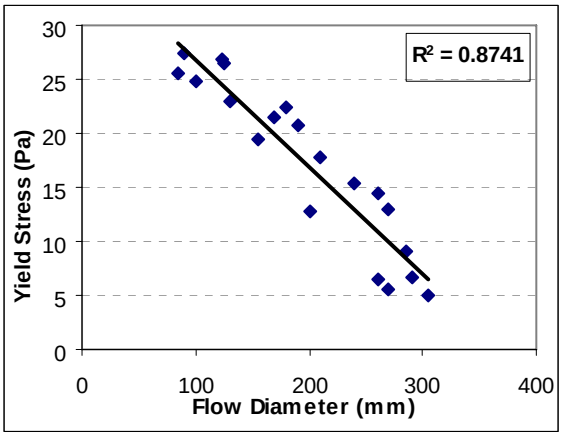


**(a) OPC Series**

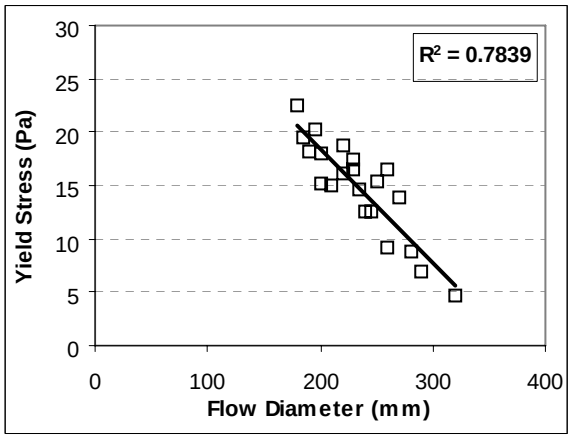


**(b) GR Series**

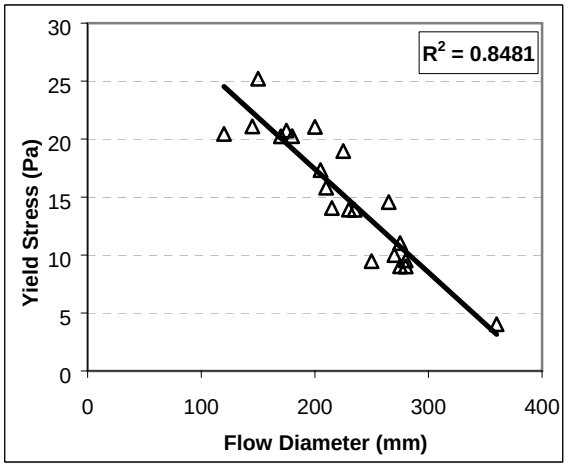


**(c) LS Series**

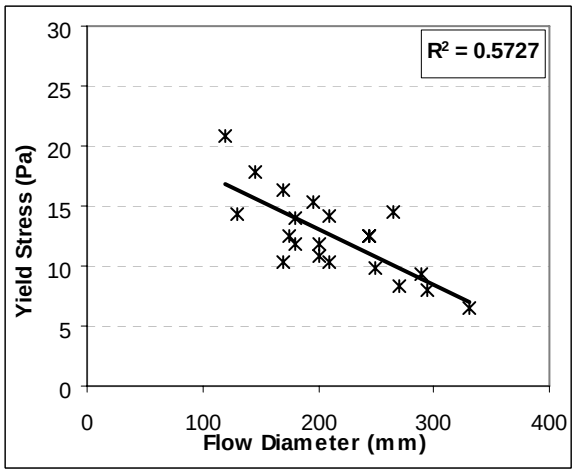


**(d) GGBS Series**

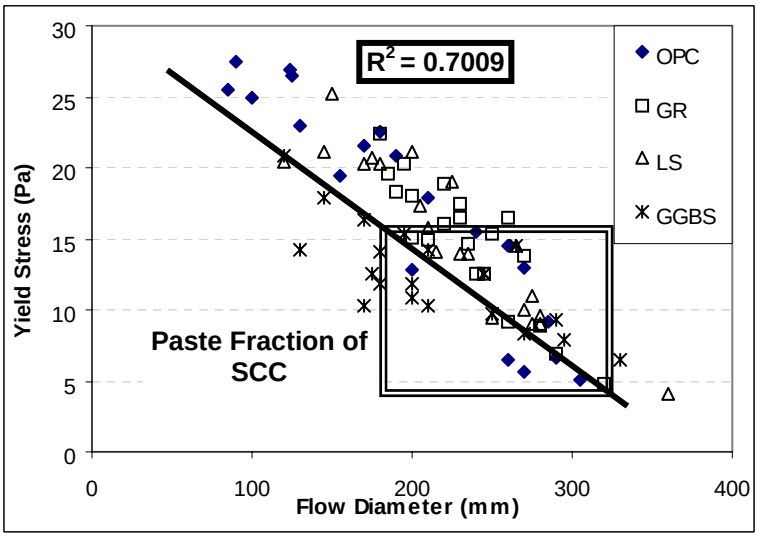


**(e) All Series**

Fig. 8.3 Correlations between Mini-Slump Cone Flow Diameter and Yield Stress of the paste containing different types of filler powder

Fig 8.3 (e) presents the correlation between the mini-flow diameters with the respective yield stress for all the paste samplestested. Despite some scatter, it can be seen that there is a reasonable relation (correlation factor, $R^2 = 0.7$) between yield stress and mini-flow diameter regardless of the type and proportion of paste samples. There is less scatter of data observed in the region within the range of flow values between 180 to 310 mm and yield stress values between 5 to 17 Pa. That region corresponds to the paste sample that is suitable for Self-Compaction Concrete or Paste-Fraction of SCC. Therefore, the yield stress value of a SCC paste fraction can be obtained approximately from the mini-flow value.

### 8.2.3 Correlation of P-Funnel Flow Time with Plastic Viscosity

P-Funnel test was conducted consecutively with the mini-flow cone test on the same paste sample. The tests were conducted three times for each paste sample and the average was recorded as the flow time for that particular paste sample. The correlation between the funnel flow time and the respective plastic viscosity for different types of paste sample are presented in Fig 8.4 (a) to (d). Similar to the correlation between yield stress and flow diameter, a linear relation between plastic viscosity and funnel flow time was observed for all series of paste sample. A higher plastic viscosity of paste sample resulted in a longer funnel flow time.

Fig 8.4 (e) presents the correlation between plastic viscosity and funnel flow time of all series of the paste sample. Although there is scatter, a linear relation (correlation factor, $R^2 = 0.7499$) can still be observed regardless of the type and proportions of paste samples. The data show more scatter for the paste samples at the higher plastic viscosity values. The linear relationship fitted better for the paste fraction of SCC with a lower plastic viscosity between, 0.02~0.42 Pa.s, and flow time between 8~22 second.

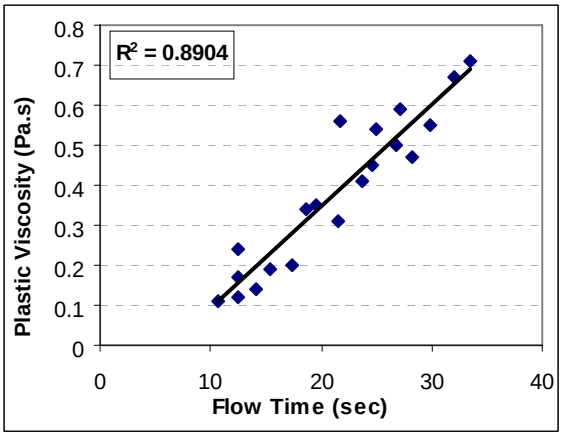


(a) OPC Series

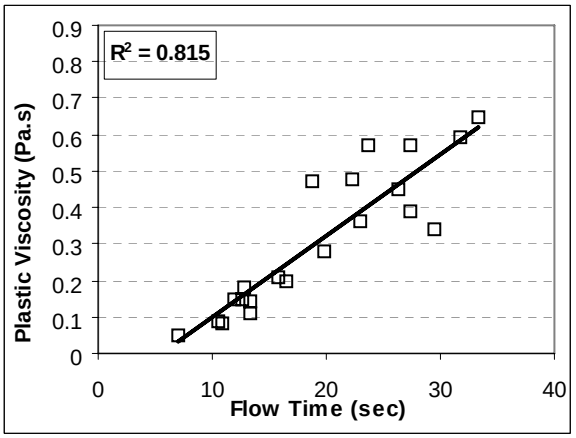


(b) GR Series

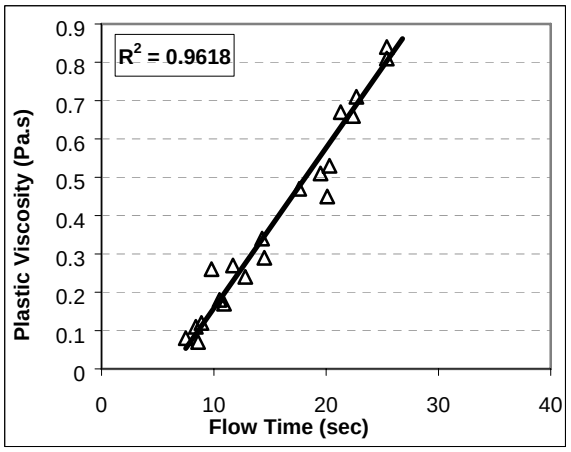


(c) LS Series

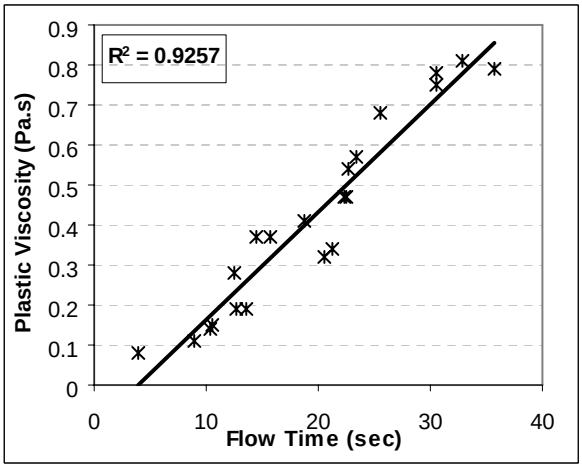


(b) GGBS Series

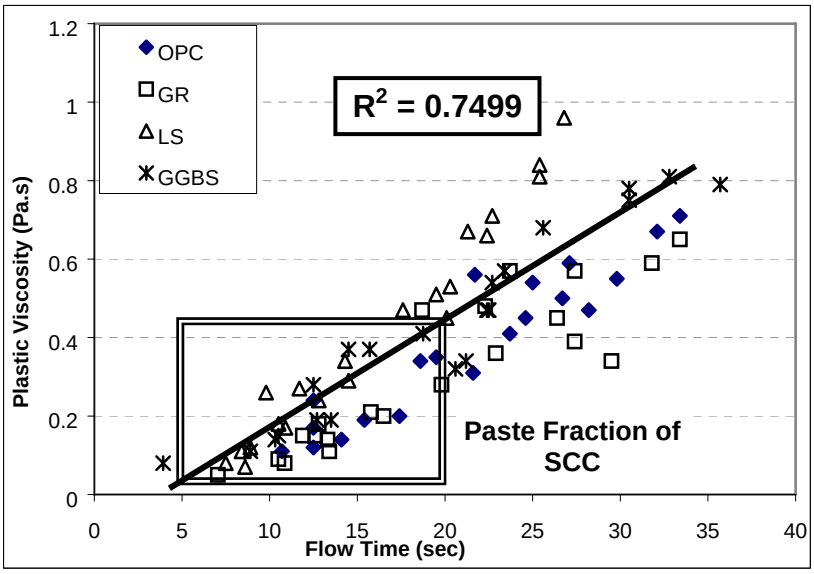


(e) All Series

Fig. 8.4 Correlations between P-Funnel Flow Time and Plastic Viscosity of the paste containing different types of filler powder

## 8.3 Correlation of Concrete Rheology with Simple Physical Test

Several simple physical tests were conducted on the same sample of concrete before the respective rheological tests.

The main varying parameters to prepare the concrete samples were:

- Different types of filler powder
- Saturation Dosage of superplasticizer for the corresponding mix
- Different water to powder ratio or water content
- The maximum size of aggregate (10 mm and 20 mm)
- Coarse aggregate with 4 types of grading

### 8.3.1 Simple Physical Test Methods for Concrete

The following section discusses the physical test methods and procedures used to assess the flow properties of the concrete to satisfy the self-compatibility without segregation of SCC.

#### o Slump Flow Test for Concrete

Slump-flow test was used to evaluate the flowability and stability of concrete. The slump flow test is a popular testing method as the procedure and apparatus are relatively simple. An ordinary slump cone was placed in the center of a metal plate (Fig. 8.5). The metal plate, of relatively smooth surface, also had a circle of 500 mm diameter drawn on the surface of the plate. After it was ensured that the plate was placed on a flat, level and firm ground, the slump cone was filled with the test sample (concrete) without any consolidation by rodding or vibrating. The top of the placed sample was leveled with the rim of the cone. The placement of sample was done within a 2 minutes duration for all the samples.

Immediately after the leveling the top surface, the slump cone was then removed by lifting it carefully in a continuously vertical direction. The time was recorded for the concrete diameter to reach 500 mm ($T_{50}$, s). When the concrete stopped flowing, the final flow diameters in two orthogonal directions of spread (D1 & D2) were measured and the time that the flow stopped completely was recorded ($T_{final}$). see Fig 8.5 and 8.6. The slump flow value, $D_{final}$, was then calculated by averaging the value of D1 and D2. A higher $D_{final}$ value reflected a more flowable concrete. In other words, the final diameter of the slump flow value, $D_{final}$, described the yield stress and the $T_{50}$ value described the plastic viscosity. Logically, a lower yield stress results in a larger flow diameter and the $T_{50}$ value represents the inverse of the fluidity since fluidity by definition is the reciprocal of dynamic viscosity **[***Tattersall et. al., 1983***].**

Fig. 8.5 Slump flow test and measurement of the ultimate slump flow diameter

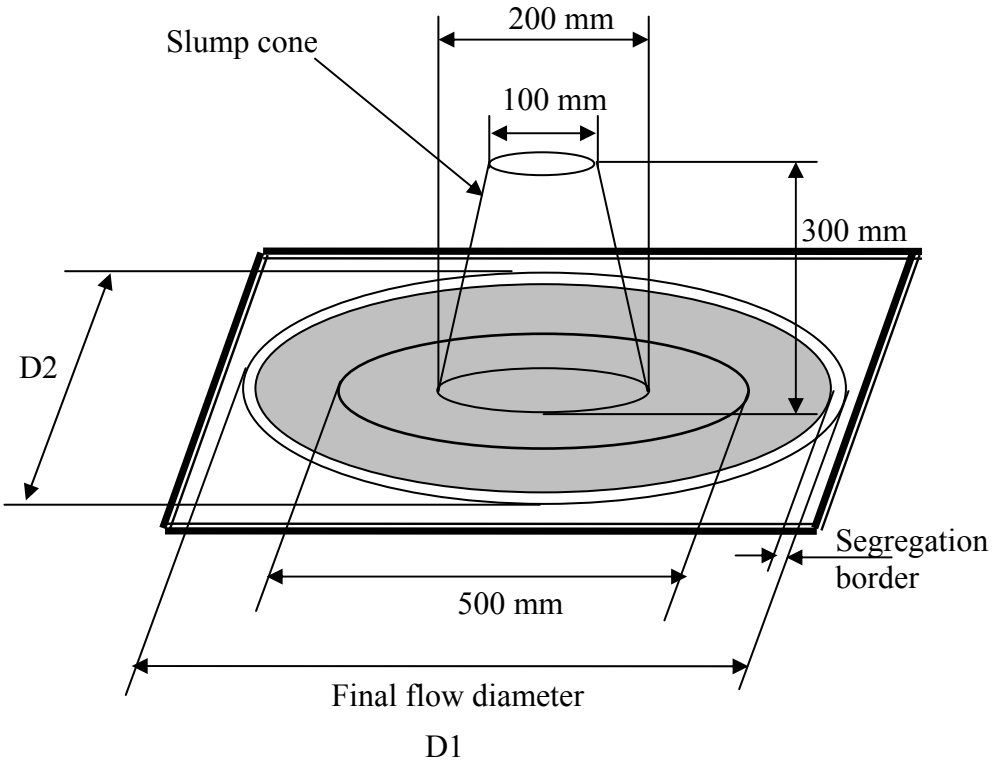


Fig. 8.6 Schematic diagram for slump flow test

The stability of the mix was evaluated by observing the coarser particles distribution and segregation border of water at the very periphery. The resistance to segregation was evaluated by visual observation, because coarse aggregates tend to stay at the center when there is insufficient resistance or viscosity as shown in Fig 8.7.

Fig 8.7: Observation of segregation by visual inspection

## o V-Funnel Test for Concrete

The narrow opening passability of concrete samples was observed by V-funnel test (Fig. 8.8). The freshly mixed sample (concrete) was filled into the funnel without rodding or vibrating. The top surface of the placed sample was leveled with the rim of the funnel using a straightedge. The bottom cover of the funnel was then opened and allowed the sample to flow through the opening. The flow time was recorded when the light was seen through the bottom orifice when looking down through the funnel. The funnel flow time t (sec) or the relative funnel speed Rc (=10/t) is the main information obtained by this test. The funnel flow time is related to the viscosity and also used in the evaluation of the segregation resistance.

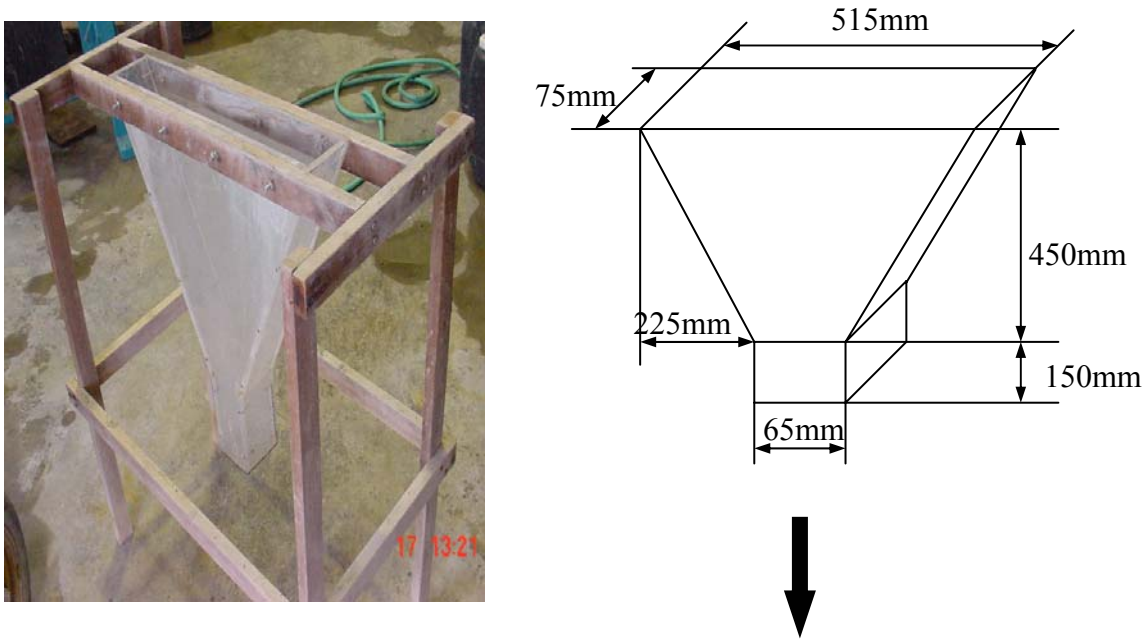


Fig. 8.8 Schematic diagram of V-funnel apparatus

In case the amount and size of coarse aggregate are sufficiently small relative to the size of the opening in V-funnel, the collision and interaction among coarse aggregate particles are supposed to be negligible for the funnel flowing characteristics of the fresh concrete. Under such a condition, the funnel flow time (t) or relative funnel speed (Rc) can be considered as the

indexes representing the viscosity of the mixture. A longer funnel flow time represents a higher viscosity of the mixture and better segregation resistance.

In case the amount and size of aggregate are relatively large for the size of opening, the collision and the interaction among the coarse aggregate particles are dominant for the funnel flowing characteristic of fresh concrete. Under such conditions, the V-funnel test is useful to evaluate the narrow opening passing ability of SCC. A shorter funnel flow time (t) or larger relative funnel speed (Rc), mostly represents a better narrow opening passing ability. It should be noted that the deformation capacity (slump flow), the size distribution of aggregate and the amount and shape of aggregates are also influential factors in the V-funnel test.

### o L-box Test for Concrete

The flowability, blocking and segregation of concrete were investigated by the L-box test (Fig. 8.9). The L-box test is carried out simultaneously with the slump test

Approximately 12.7 lit of fresh concrete was filled to the vertical section of the L-box and allowed to reste for 1 minute to display whether it was stable or segregated. Then, the sliding gate was lifted and concrete was allowed to flow out from the vertical section into the horizontal section passing through by a set of reinforcing bars at the gate, as shown in Fig 8.10. The time for the flow to reach 200 mm ($T_{200}$) and 500 mm ($T_{500}$) were recorded. When the concrete stopped, the heights of the concrete at the back and front of the L-box are also measured, denoted as H1 and H2, as shown in Fig 7.8. The blocking ratio, $H_{br}$ = H2/H1 is then calculated. A higher $H_{br}$ value would represent a concrete mix with higher passing and filling ability. The acceptable value of the so called blocking ratio, $H2/H_1$ was > 0.8.

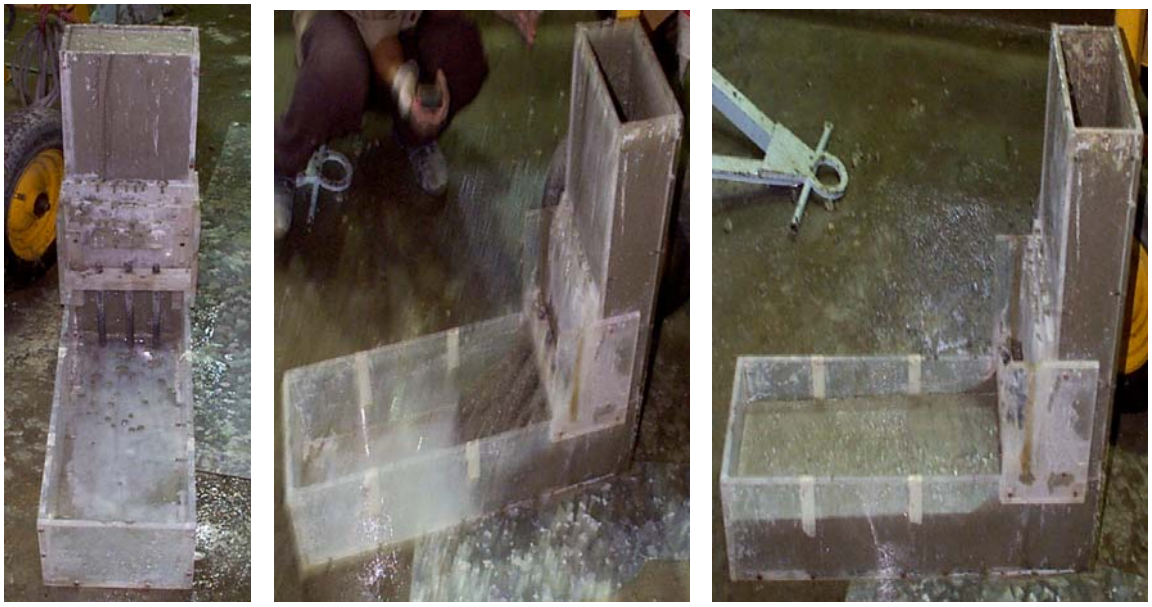

(a) (b) (c)

Fig 8.9 Testing of SCC in L-Box

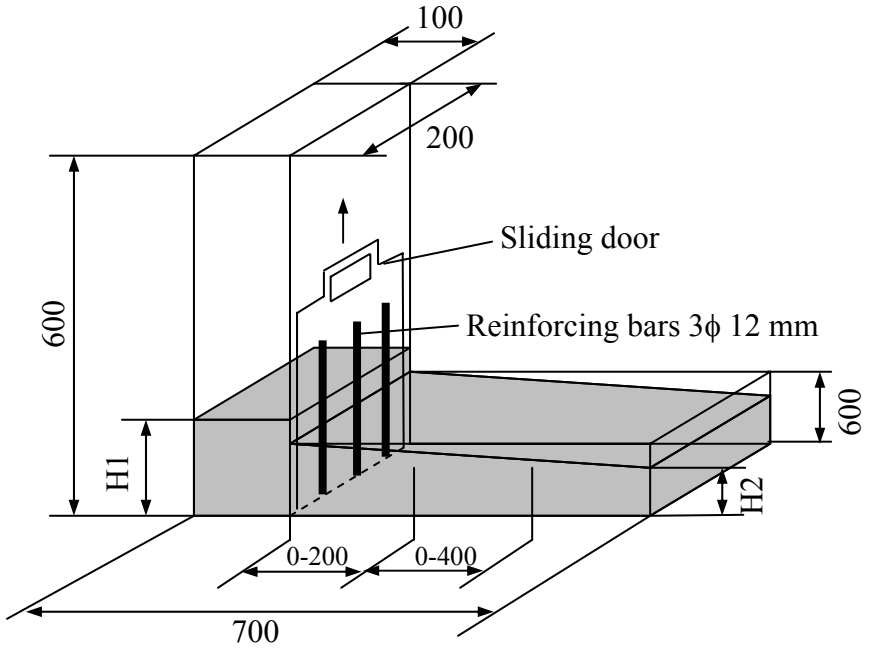


Fig 8.10: Determination of blocking ratio, $H_{br}$

If the concrete builds a plateau behind the reinforcements, the concrete has either been blocked or segregated. Usually, blocking is displayed by the gathering of coarse aggregates behind the reinforcement bars. If coarse aggregates are observed on the concrete surface all the

way to the end of the horizontal part, the concrete can be regarded as being stable and having sufficient resistance to segregation.

### 8.3.2 Correlation of Rheological Parameter of SCC with Slump Flow

- **Yield Stress with Flow Diameter**

The correlation between slump flow and yield stress obtained in this study was plotted in Fig. 8.11.

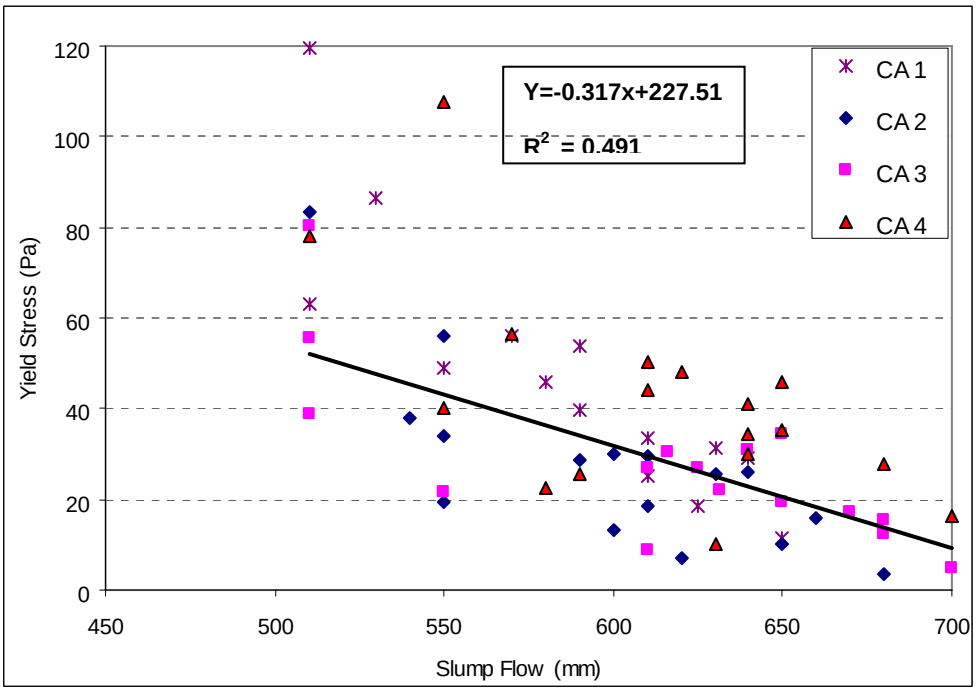


Fig 8.11: Correlations between slump flow and yield stress

Although yield stress seems to have an unclear relationship with slump flow ($R^2 = 0.49$), there is a possible linear relationship between them. Instead of slump flow, various researchers made several attempts to determine an equation to relate yield stress with slump. Tattersall and Banfill [*Tattersall G. H. and Banfill P. F. G.,1983*) were the first to report that a linear relation exits between yield stress and slump. Some of the equations reported are based on finite element simulations of the slump cone tests [*Hu, C., et.al, 1996, Kurokawa, Y., et.al, 1994*] while others

are based on the fitting of sets of data [*Ferraris C.F. et.al,1998, Sedran R., 1999*]. Only two equations developed by Hu et al. [*Hu, C., et.al, 1996*] and Kurokawa [ *Kurokawa, Y., et.al, 1994*] will be compared with current data in this study. They all have the common form:

$$\tau_0 = \frac{\rho(A - S)}{B} + C \qquad \text{Eq. (8.1)}$$

Where S is the slump in mm, $\tau_0$ is the shear yield stress in Pa, $\rho$ is density in kg/m$^3$. *A, B, C* are constants to be determined either by fitting data or by simulation. In these cases the constants are: Hu's constants: A = 300; B = 270 and C = 0. Kurakawa's constants: A = 300; B = 303 and C = 0.These constants were deduced from the finite-element calculations based on the equilibrium of the concrete sample at the end of the slump test, and not on a fit of the experimental data.

It is observed from Eq 8.1 that the yield stress is calculated based only on the slump value which is unlikely to be suitable for SCC whose slump flow is more important indication than its slump. It seems that these equations are on the high end of the data obtained in this study. [*Chidiac S.E et.al, 2006*] had studied the various models reported by numerous researchers on correlation between yield stress and slump. Most of the models were applicable only for slumps less than 150 mm. Thus he proposed the following equation which included slump and slump flow to estimate yield stress of the system.

$$\tau_y = \rho\{1.85(0.3 - S_1) + \frac{0.0198}{S_f^2}\} \qquad \text{Eq. (8.2)}$$

where $\tau_y$ is the yield stress of concrete (Pa), $\rho$ is the density of concrete (kg/m$^3$), $S_1$ and $S_f$ are slump (m) and slump flow (m) of the concrete respectively. However, all proposed equations are valid only for yield stress values measured with the BTHREOM concrete rheometer. In order to compare the yield stress measured with BML rheometer in current study,

the following equation proposed by Banfill and his group of researchers [*Banfill P.F.G., et.al, 2000*] will be used.

$$\text{BML Yield stress} = 0.50 * (\text{BTRHEOM Yield stress}) - 122.0 \qquad \text{Eq. (8.3)}$$

Figure 8.12 shows the data obtained in this study compared with the Hu, Kurokawa and Chidiac equations.

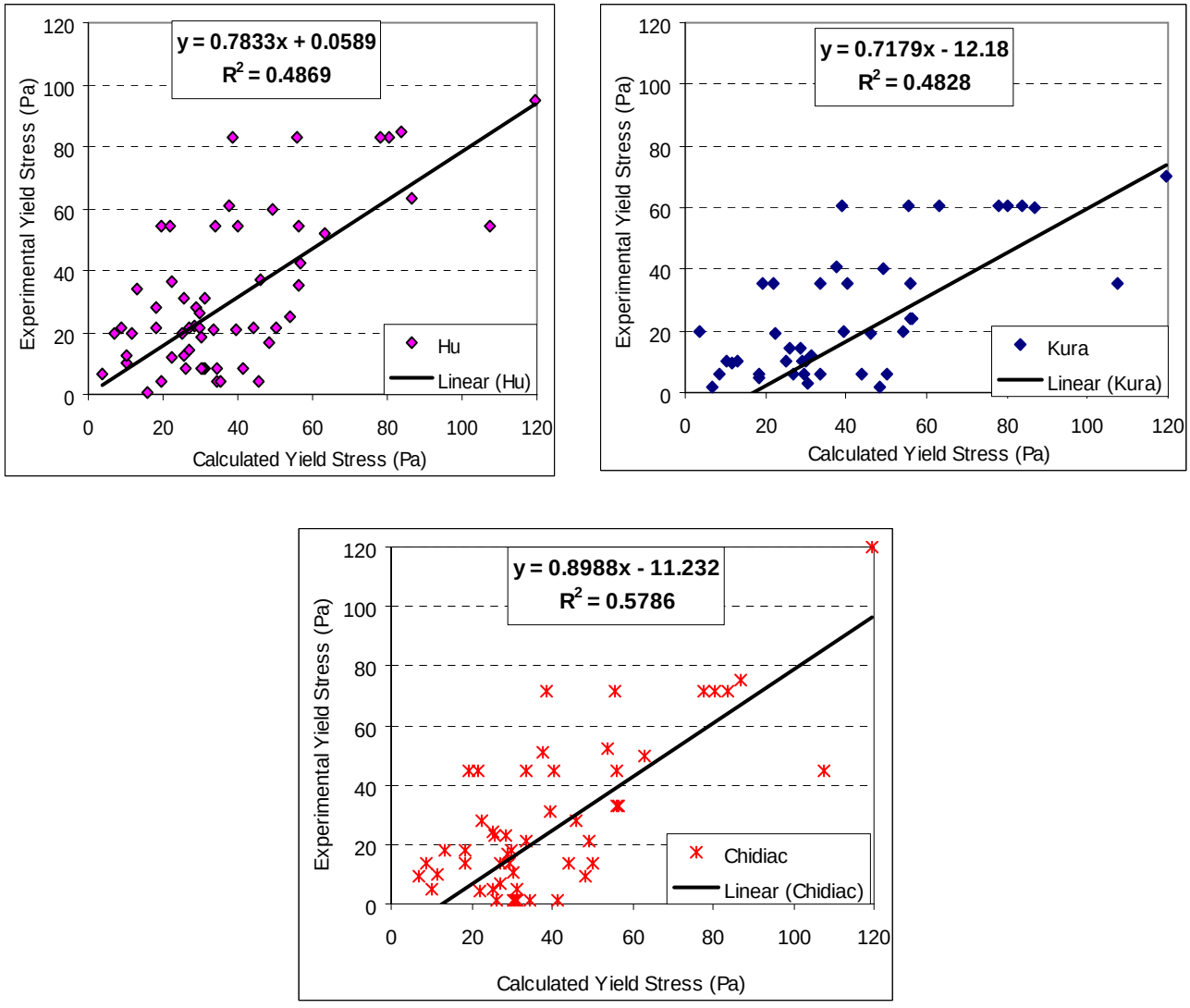


Fig. 8.12 Comparison between the experimental data with different equations

Among all three equations proposed by the different researchers, it can be seen from Figure 8.12 that Chidiac's equation seems to be a better estimation of the yield stress. Thus, it is possible that the yield stress of SCC can be roughly estimated from the value of its slump and slump flow.

- **Plastic Viscosity with Flow Time**

Correlation between the T50 value and the measured plastic viscosity is shown in Fig. 8.13. The relationship in this case is unclear.

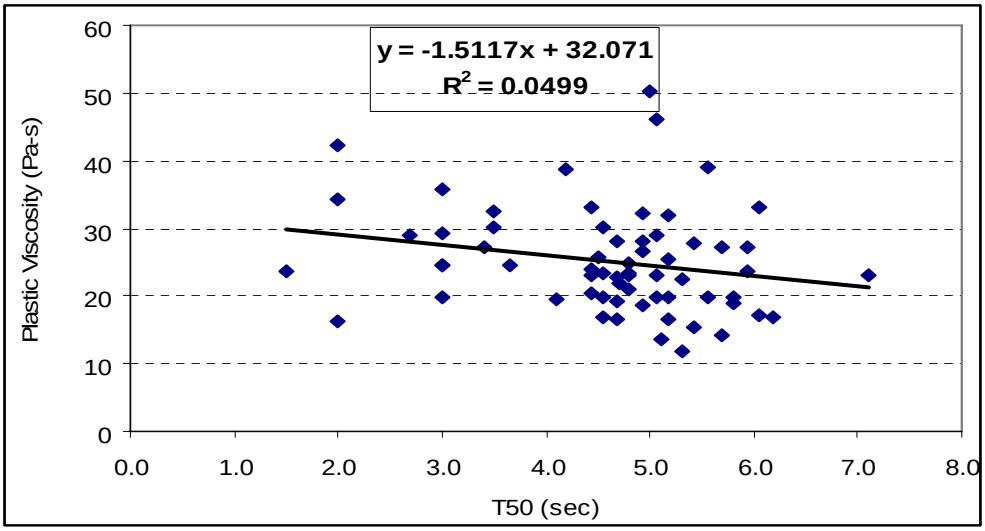


Fig. 8.13 Correlation between T50 and Plastic Viscosity

## 8.3.5 Correlation of Plastic Viscosity of Concrete with V-funnel Flow Time

The correlation between the v-funnel flow time and the measured plastic viscosity obtained in this study was plotted Fig. 8.14. Similarly, the plastic viscosity value measured with BML seems to have a relationship with V-funnel flow time even though their relationship is not as strong as that of slump flow and yield stress. However, it is also observed that the higher the plastic viscosity, the higher the V-funnel flow time.

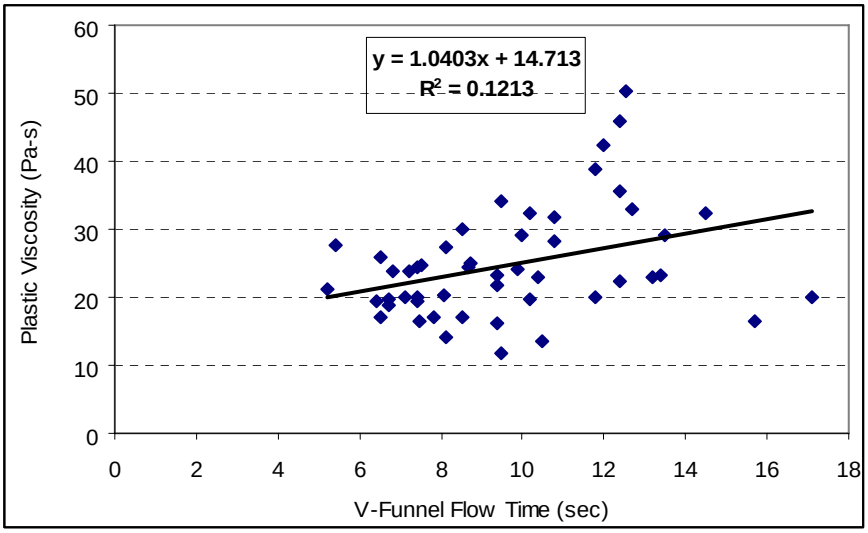


Fig. 8.14 Relation between V-funnel flow time and Plastic Viscosity

The scattering of these data may be partially explained by uncertainties occurring when conducting the slump flow test with the Abrams cone and the rheological measurement with the BML viscometer. Some possible explanation of the scattering might be:

- Separation present in the concrete while conducting rheology test
- Operation and human errors in the measured values of T50 as the flow time was measured such a short flow distance of only 200 mm. This might be difficult to judge especially if the tested concrete does not flow radially into a perfect ring shape.
- Uncertainty in the BML measurement because the penetration of blades of the BML viscometer might bring the suspended coarse aggregate down to the bottom of the container and cause segregation even when the concrete shows sufficient cohesiveness during conducting the test for slump flow and T50 value.
- The results from this test series show that the slump flow value of 650 mm or more together with a T50 value of about 4 sec may be the target value for “Good” SCC with better flowability with segregation resistance. However, some uncertainty in the T50 measurement should also be taken into account.

# CHAPTER 9

# PROPOSED MIX DESIGN CONCEPT FOR SCC

## 9.1 Introduction

The proposed mix design concept intends to produce a mix proportion for SCC that can lead to low costs together with desired hardened properties. In order to achieve such objectives, the paste, which is composed of the most expensive raw materials which leads to a higher cost of the SCC, must be reduced to its optimal volume by taking into account the satisfactory requirements of fresh and hardened properties.

Since the workability of SCC in the fresh stage plays an important role, consideration must be taken to choose the raw materials and their proportions in order to achieve the SCC with the desired fresh properties. Thus, it is important to understand the following characteristics while designing the mix proportion for SCC.

a) The filling capacity of SCC is governed by the deformability and segregation resistance of the fresh concrete. For low slump concrete, the filling capacity is controlled mainly by the deformability, while for high slump concrete, it is controlled mainly by segregation resistance.
b) The amount of free water in the concrete is one of the important factors for the deformation and segregation behavior of fresh concrete.
c) Segregation between the solid particles and the liquid phase around the narrow opening system proved to be highly affected by the boundary condition and the liquid phase viscosity which is controlled by the particle contact condition. Such particle

contact condition also controls the deformability of system. In a particle arrangement with close contact condition, relative movement of the particles is restricted by the mutual interaction between the particles, which will increase the contact stress in the particles and promote segregation.

d) The flowability of fresh mortar and concrete through narrow openings are controlled not only by the deformability, but also by the segregation resistance which is related to blocking. Both properties depend on the properties of the liquid phase. Shear transfer mechanism of the paste between the solid particles depends on the water to powder ratio. For the shear resisting mechanism of the paste with an appropriate amount of free water, frictional mechanism is controlled by the size, shape and grading of powder materials. This means that by selecting the appropriate paste mixture, the aspect of frictional mechanism arising in the aggregate interaction can then be minimized.

e) The role of chemical admixtures such as superplasticizer and viscosity modifying agent on the deformation and segregation behavior of fresh concrete is one of the most important factors for developing SCC with high filling capacity. There is a need to choose for the optimum dosage of superplasticizer and viscosity agent in order to gain the SCC with higher flowability and segregation resistance.

This research aims to propose a mix design concept with the view of good economic efficiency, durability and user friendly mix design steps. With this proposed mix design concept, the concrete engineer can determine the mix proportion of SCC from the properties of its mix constituents with the aid of minimal parametric study instead of conducting extensive trials. The mix design is important in enhancing the successful application of SCC by the industry.

## 9.2 Optimization of Solid Phase

The solid phase (also can be called as aggregate skeleton) within the SCC consists of coarse and fine aggregates. As discussed earlier, to find an optimum binary mix, which requires as lowest paste volume as possible, the void content and the inter-particle distance shall be optimized. In this section, the void content and void model are firstly formulated and then the average inter particle distance Dss is calculated.

### 9.2.1 Aggregate Binary Mix

Different ratios of coarse to fine aggregate result in different void contents in combined grading and total surface area of aggregate binary mix. An optimum coarse-fine aggregate ratio must lead to less required paste volume that can meet the satisfactory requirements of fresh concrete with better deformability and harden properties. The paste volume ($V_{pw}$) is needed not only to fill all voids between aggregate particles but also to envelop all surface areas of aggregate particles. Thus, it is required to consider not only the void content but also total surface area of aggregate binary mix. Although two types of aggregate may have the same volume, they can be of different total surface area. Thus the paste volume required to cover the aggregate particle will be different. In other words, for the same paste quality, the higher aggregate surface area requires the larger covering paste volume in order to maintain the same flowing and filling ability. It has often been mentioned that the specific surface area of aggregate is one of the factors influencing the deformability and the occurrence of particle interface for conventional concrete.

It is clearly known that when two different size groups are mixed together, the void content in the combined aggregate is less than that of either group alone. It means that the binary mixes of fine and coarse aggregate always have a smaller void content than that of

separated fine and coarse aggregate itself. For grading within a given size range and having a ratio of coarse to fine within a usual range, particle shape has a larger effect on void content than those of grading. When angular particles of given size group are mixed with various proportions to the rounded particles of the same size group, the void content of the binary mixture is reduced about in proportion of rounded materials. This shows that geometric similarity always indicates equality in the void content but geometric dissimilarity does not necessarily indicate unequal void contents.

Though relationships between void content and composition tend to be nonlinear, by choosing certain functions of voids content and composition, these relationships can be handled with least difficulty. In this research, analysis of these relationships of binary mixture is divided into two portions according to minimum void contents. These are "Fine aggregate dominant" and "Coarse aggregate dominant" (Fig. 9.1) [*Larrard F.De.,1999*]

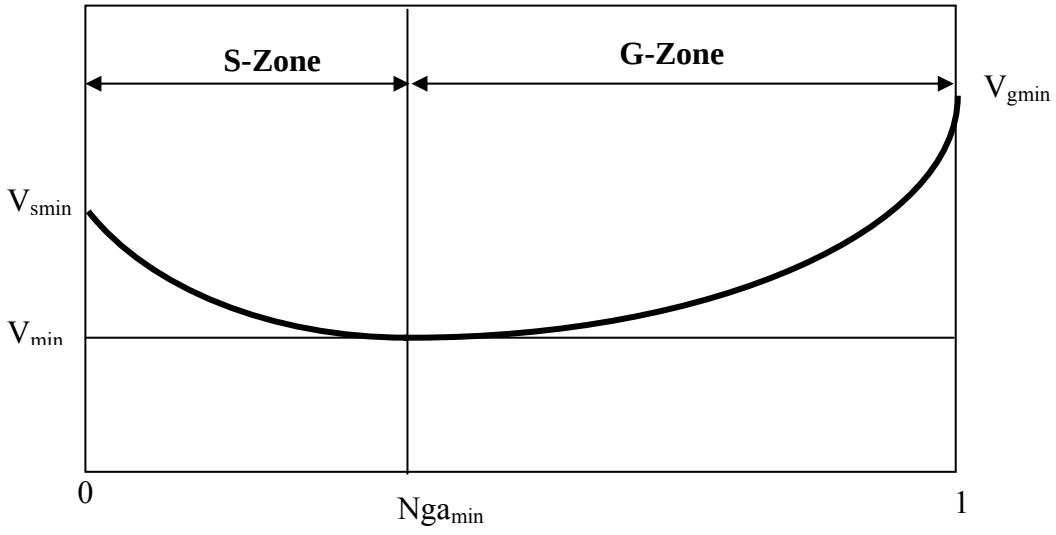


Fig. 9.1 Relationship between void content and coarse-total aggregate ratio of binary aggregate mixture

- **Fine Aggregate Dominant**

For the mixture of fine aggregate dominant (S-Zone), the effect of incorporation of coarse aggregate can be expressed in terms of the decrease in void content of fine aggregate. This phenomenon is due to the results of replacing some fine aggregate particles with a bigger size of coarse aggregate particles. When the quantity of coarse aggregate becomes larger, the mixture encounters particle interference, which is expressed by non-linearity of void curve.

- **Coarse Aggregate Dominant**

For the mixture having coarse aggregate dominant (G-Zone), the reduction of void content is not accomplished by simply filling voids between coarse aggregate with adding sand particles, because some of the voids in compacted coarse aggregate are usually too small to contain all sizes of fine aggregate. Thus, the reduction of void content cannot be considered as linear relation by adding an amount of fine aggregate to the mixture.

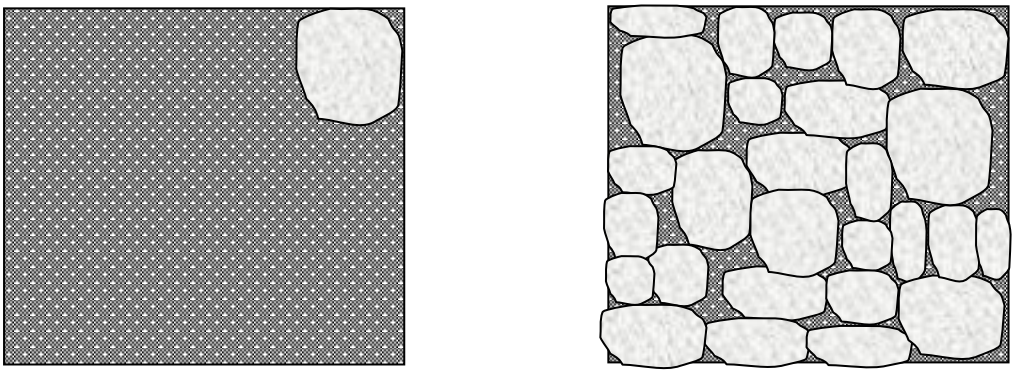

(a) Fine Aggregate Dominant (b) Coarse Aggregate Dominant

Fig 9.2 Structure of mixture having fine and coarse aggregate dominant

### 9.2.2 Formulation of Void Model

The proposed void model is based on the concept discussed by Bui V.K.[ *Bui V.K.,2000*] that the void of binary mixture (V) is a function of separated void content of compacted coarse aggregate ($Vg_{min}$) and void content of compacted sand ($Vs_{min}$). It is assumed that the function of void content (V) corresponding to coarse-total aggregate ratios (Nga), which are lower and higher than minimum coarse-total aggregate ratio ($Nga_{min}$). $Nga_{min}$ is the ratio that corresponds to the lowest void content in coarse and fine aggregate binary mixture.

Experiments with four batches of aggregate were carried out in order to formulate the void model. The data is presented in Table 9.1.

Table 9.1 Void content of separate fine and coarse aggregate, minimum void content and corresponding coarse-total aggregate ratio

| Designation | $Vg_{min}$ | $Vs_{min}$ | $Nga_{min}$ | $V_{min}$ |
|---|---|---|---|---|
| Batch 1 | 0.4533 | 0.3480 | 0.40 | 0.2998 |
| Batch 2 | 0.4525 | 0.3807 | 0.45 | 0.3171 |
| Batch 3 | 0.4440 | 0.3807 | 0.55 | 0.2898 |
| Batch 4 | 0.4440 | 0.3480 | 0.50 | 0.2776 |

Where: $Vg_{min}$ = Void content of compacted coarse aggregate

$Vs_{min}$ = Void content of compacted fine aggregate, Sand

$Nga_{min}$ = Coarse-total aggregate ratio which gives the minimum void content in aggregate binary mixture

$V_{min}$ = Minimum void content in aggregate binary mixture

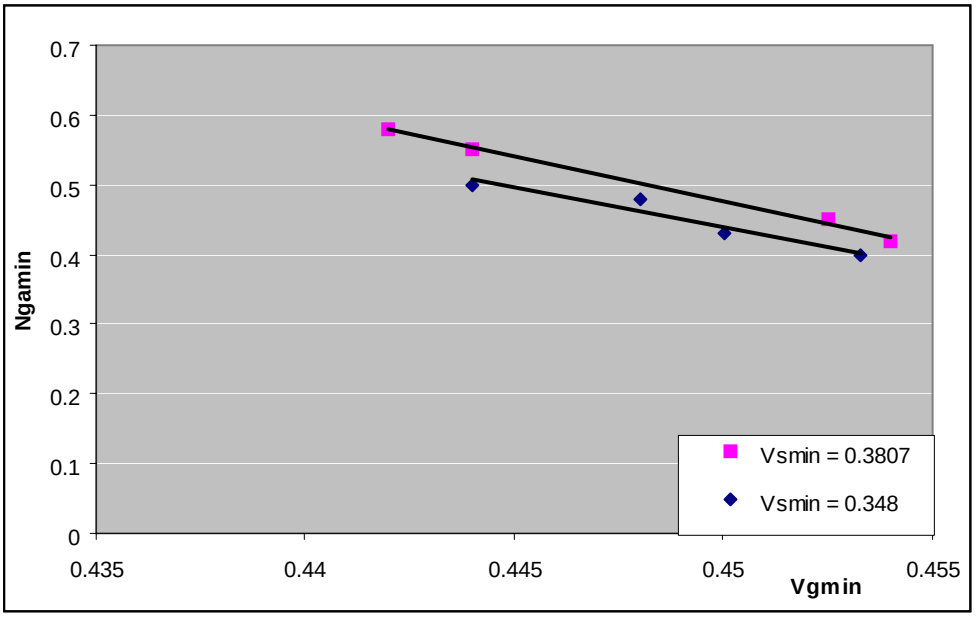


Fig. 9.3 Relation between $Nga_{min}$ and $Vg_{min}$

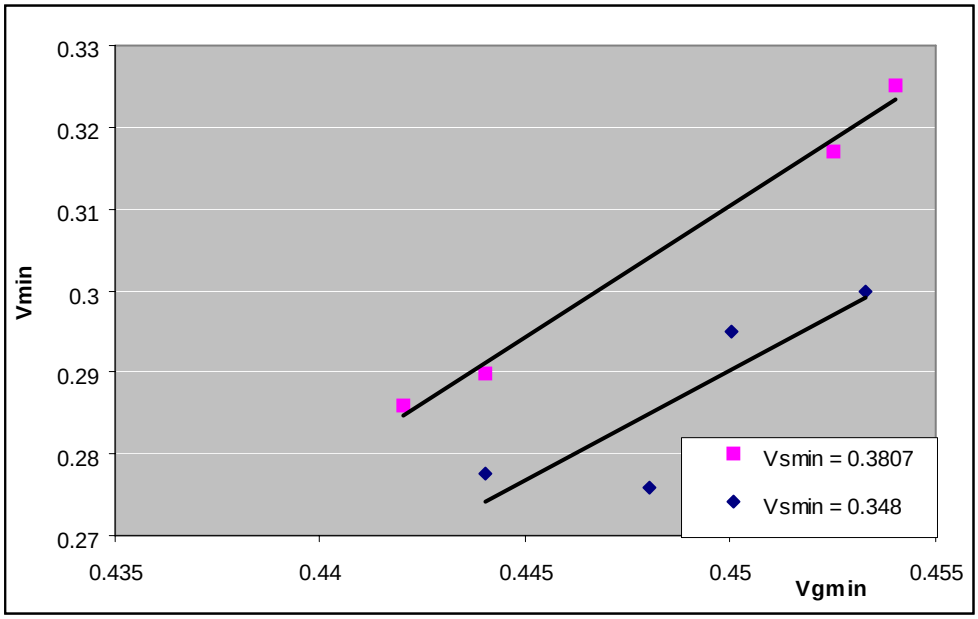


Fig. 9.4 Relation between $V_{min}$ and $Vg_{min}$

By analyzing the data from Table 9.1 and Fig. 9.3 to 9.4, it has been found that the functions for $Nga_{min}$ and $V_{min}$ are linear which plotted against two variables, ie. Void content of densely compacted fine aggregate ($Vs_{min}$) and that of densely compacted coarse aggregate

($Vg_{min}$). The functions of voids in the S-Zone and the G-Zone are parabolic with the variables that are $Nga_{min}$, $V_{min}$, Nga and $Vg_{min}$ or $Vs_{min}$, respectively. These functions are derived as follows:

- **Functions for $Nga_{min}$ and $V_{min}$**

The $Nga_{min}$ and $V_{min}$ are functions of $Vg_{min}$ or $Vs_{min}$. For every kind of aggregates, which have the known value of densely compacted void content, then $Nga_{min}$ and $V_{min}$ can be written as:

$$Nga_{min} = A + B*Vg_{min} \quad (9.1)$$

Where: A and B are functions of $Vs_{min}$

$$A = m_1 + m_2 * Vs_{min} \quad (9.2)$$

$$B = m_3 + m_4 * Vs_{min} \quad (9.3)$$

By using the least square exponential method and experimental data from Table 9.1,

$$Nga_{min} = 5.739 - 11.684 * Vg_{min} \quad \text{for } Vs_{min} = 0.3807 \quad (9.4)$$

$$Nga_{min} = 5.275 - 10.753 * Vg_{min} \quad \text{for } Vs_{min} = 0.3480 \quad (9.5)$$

Similarly, by using the least square exponential method and eq. (9.12) & (9.13),

$m_1 = 0.3296$ $m_2 = 14.209$

$m_3 = -0.845$ $m_4 = -28.272$

Substituting values of $m_1$, $m_2$, $m_3$ and $m_4$ into eq (9.9) to (9.11),

$$Nga_{min} = [0.3296 + 14.209 * Vs_{min}] - [(0.845 + 28.472 * Vs_{min}) * Vg_{min}] \quad (9.6)$$

Similar procedure was applied for calculating $V_{min}$ as;

$$V_{min} = C + D*Vg_{min} \quad (9.7)$$

$$C = n_1 + n_2 * Vs_{min} = 2.983 - 10.821 * Vs_{min} \quad (9.8)$$

$$D = n_3 + n_4 * Vs_{min} = -6.375 + 25.181 * Vs_{min} \quad (9.9)$$

$$V_{min} = [2.983 - 10.821 * Vs_{min}] - [(6.375 + 25.181 * Vs_{min}) * Vg_{min}] \quad (9.10)$$

- **Functions for Void content in Binary Mix**

As presented above, the void ratio can be expressed in terms of two different parabolic functions of S-Zone (Fine aggregate dominate) and G-Zone (Coarse aggregate dominate) with their center point lying on Nga = $Nga_{min}$ axis. The derivations of these functions are as follows [*Power. T.C., 1968*]:

**For S-Zone,**

When $Nga < Nga_{min}$

$$V - V_{min} = a\,(Nga - Nga_{min})^2$$

Thus, $$V = a\,(Nga - Nga_{min})^2 + V_{min}$$

When Nga = 0, then $V = Vs_{min}$, we get;

$$a = \frac{Vs_{min} - V_{min}}{(Nga_{min})^2}$$

$$V = V_{min} + \frac{Vs_{min} - V_{min}}{(Nga_{min})^2} * (Nga - Nga_{min})^2 \quad (9.11)$$

**For G-Zone,**

When $Nga > Nga_{min}$

$$V = a\,(Nga - Nga_{min})^2 + V_{min}$$

When Nga = 1, then $V = Vg_{min}$, we get;

$$b = \frac{Vg_{min} - V_{min}}{(1 - Nga_{min})^2}$$

$$V = V_{min} + \frac{Vg_{min} - V_{min}}{(1 - Nga_{min})^2} * (Nga - Nga_{min})^2 \quad (9.12)$$

Analyses of the above equations indicate that the variables for the void ratio equation of aggregate binary mixture are only $Vs_{min}$ and $Vg_{min}$. Those values can be determined according to ASTM C29/C29M-91a and usually they are standard properties of aggregates to be tested.

The experimental results and the void contents calculated from the proposed model on binary mixes using a combination of different batches of coarse and fine aggregate supplied agreed to certain extent. Especially, it was found that the experimental $Nga_{min}$ values are close to that of the value calculated from the proposed model. Thus, this void model can be used to determine optimum Nga. With the use of this model, the void content corresponding to every Nga can be determined. Thus, this model is useful in mix design.

### 9.2.3 Average Distance ($D_{ss}$) between Aggregate Particle

In this study, the average distance ($D_{ss}$) between the aggregate particles is defined as double the average thickness of the covering paste layer around the aggregate particle having the average diameter, $D_{av}$. (Fig 9.5) It is obvious that the fresh SCC must have a good deformability and segregation resistance in order to have a satisfactory filling ability. It should be noted that the blocking and segregation resistance of SCC around obstructions such as opening or spacing of reinforcing bars have a close relationship with particle-particle interactions and that of liquid paste, i.e. powder paste phase, can control such particle interaction.

Thus, the larger distance between aggregate particles causes smaller friction in the given aggregate group. This can lead to better deformability and flowability. Therefore, this

study is first carried out to calculate the average distance between aggregate particle in the mixtures with different paste volume ($V_{pt}$) and coarse aggregate to total aggregate ratio (Nga).

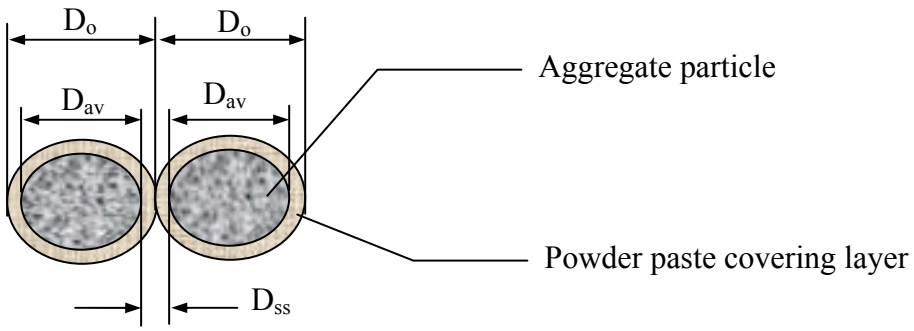


Fig 9.5 Thickness of paste around spherical shape aggregate particle

For simplicity, all the aggregate particles are first assumed to be spherical in shape. The average distance between aggregate particles ($D_{ss}$) is calculated from the typical grading curve of the combined aggregate.

Average diameter of aggregate ($D_{av}$) can be obtained from:

$$D_{av} = (\sum M_i * D_i) \Big/ (\sum M_i) \tag{9.13}$$

where $D_i$ = average sieve group size, $D_i = (d_i + d_{i+1})/2$

$M_i$ = percentage of retaining on the corresponding sieve of aggregate group i

Then, average particle volume ($V_{av1}$) is derived as

$$V_{av1} = \pi D_{av}^3 / 6 \tag{9.14}$$

Number of aggregate with diameter of $D_{av}$ in the mixture,

$$N_a = V_a / V_{av1} \tag{9.15}$$

Where $V_a$ = total aggregate volume

Volume of paste covering an aggregate ($V_{p1}$)

$$V_{p1} = (V_{pt} - V_v) / N_a \tag{9.16}$$

where $V_{pt}$ = Total paste volume; $V_v$ = Volume of void in compacted aggregate

Thus, equation (9.16) can be written as

$$V_{p1} = \pi\left(D_o^3 - D_{av}^3\right)/6 = \left(V_{pt} - V_v\right)/N_a \tag{9.17}$$

where $D_o$ = Diameter of aggregate which is already covered with paste

$$D_o = \left(6/N_a\pi\left(V_{pt} - V_v\right) + D_{av}^3\right)^{1/3} \tag{9.18}$$

From Figure 9.5, the average distance of two particles is 2 times the thickness of covering paste around the particle, that is,

$$D_{ss} = 2(D_o - D_{av}) \tag{9.19}$$

$$D_{ss} = D_{av}\left\{\left(\frac{V_{pt} - V_v}{V_t - V_{pt}} + 1\right)^{1/3} - 1\right\} \tag{9.20}$$

The relationship between coarse to total aggregate ratio (Nga) and void content in the aggregate binary mix is plotted in Figure 9.6. The void content will firstly decrease with an increase in coarse to total aggregate ratio (Nga), after Nga reaches a certain value, the void content of the aggregate binary mix starts to increase with further increases in the coarse to total aggregate ratio (Nga).

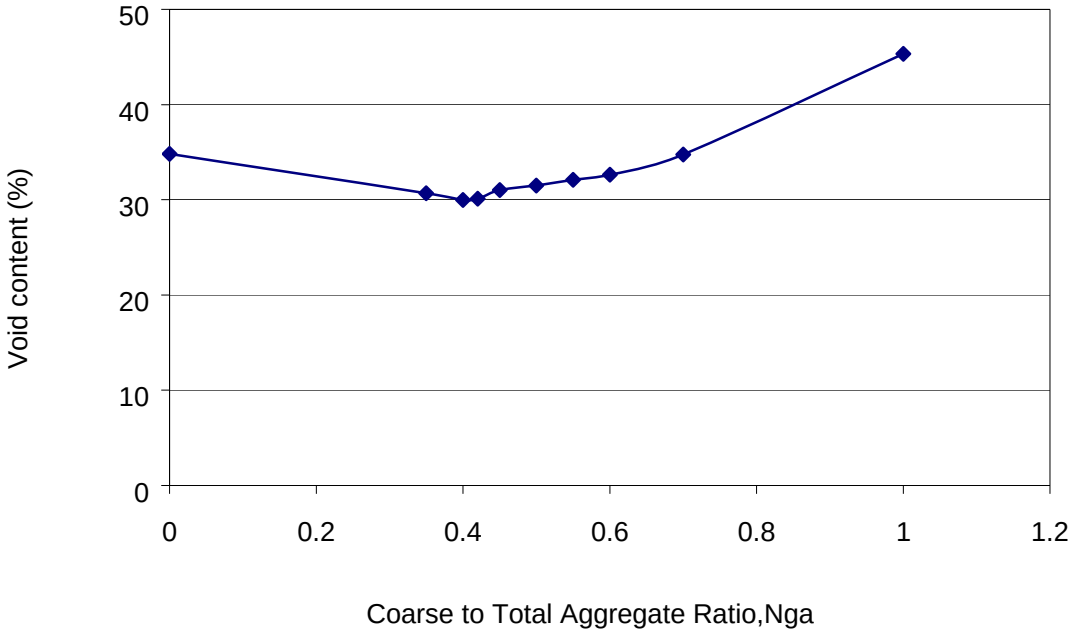


Fig 9.6 Relationship between void content($V_v$) and coarse to total aggregate ratio (Nga)

For the same aggregate binary mix, when the coarse to total aggregate ratio lies between 0.40 to 0.42, the void content within the aggregate binary mix approaches to a minimum at about 30% (Table 9.2).

Table 9.2 Measured void content of Binary Mixture

| **Nga** | 0.0 | 0.35 | 0.40 | 0.42 | 0.45 | 0.50 | 0.55 | 0.60 | 0.7 | 1.0 |
|---|---|---|---|---|---|---|---|---|---|---|
| **$V_v$ (%)** | 34.80 | 30.68 | 29.98 | 30.10 | 31.00 | 31.50 | 32.10 | 32.63 | 34.76 | 45.33 |

As discussed above, the required paste volume in SCC is not only to fill all the voids in the mix, but also to cover all the aggregate surfaces. To obtain the desired SCC with economic efficiency, the void content in the binary mix shall be minimized, at the same time the average inter-particle distance between the particles shall be maximized. Figure 9.7

indicates that for the same set of sand and coarse aggregate binary mix and for the same paste volume, the average particle distance Dss is different with respect to different coarse aggregate to total aggregate ratio (Nga). With a constant paste volume for all Nga, there can be found an optimum coarse to total aggregate ratio (opt. Nga) which will result in a maximum $D_{ss}$. It shall be noted that after coarse to total aggregate ratio Nga reaches a certain value, the average inter particle distance Dss will decrease with the further increases in the coarse to total aggregate ratio Nga. This is mainly due to the increase in void content in the aggregate binary mix which requires more paste volume to fill. Therefore the optimum coarse to total aggregate ratio shall lead to a void content as low as possible and a average inter particle distance as big as possible, which requires an optimum paste volume without sacrificing the fresh and hardened properties of the resultant SCC.

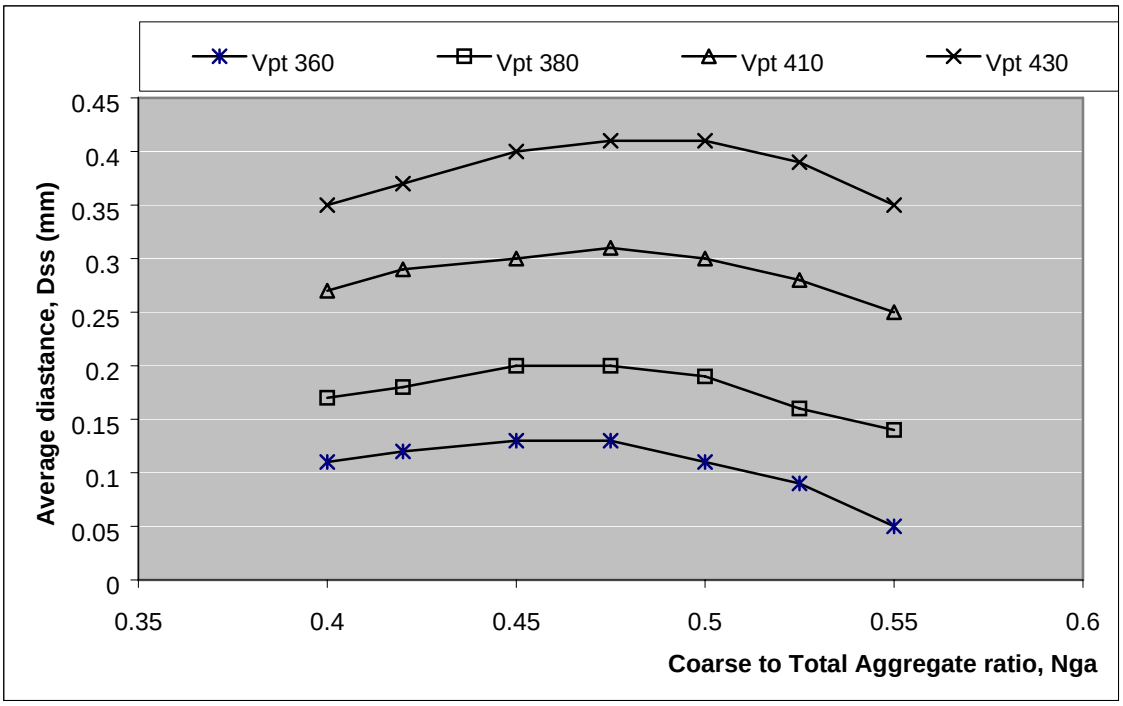


Fig. 9.7 Relationship between average inter-particle distance ($D_{ss}$) and coarse-total aggregate ratio (Nga)

From Fig 9.8, it is very clear that the average inter particle distance $D_{ss}$ increases linearly with an increase in the paste volume for the same aggregate binary mix with the

same coarse to total aggregate ratio. For the same set of aggregate binary mix with different coarse to total aggregate ratio, the average inter particle distance $D_{ss}$ increases faster for the bigger coarse to total aggregate ratio Nga. For example, when paste volume increases from 320 liters/$m^3$ to 460 liters/$m^3$, the average inter particle distance $D_{ss}$ increases from 0.1mm to 0.8mm (increases by 0.7mm) for coarse to total aggregate ratio 0.40; When the coarse to total aggregate ratio changes to 0.55, the average inter particle distance $D_{ss}$ increases from 0.03mm to 0.982mm (increases by 0.952mm). This is due to the fact that the surface area in the aggregate binary mix with a bigger coarse to total aggregate ratio Nga is smaller than that with a smaller coarse to total aggregate ratio.

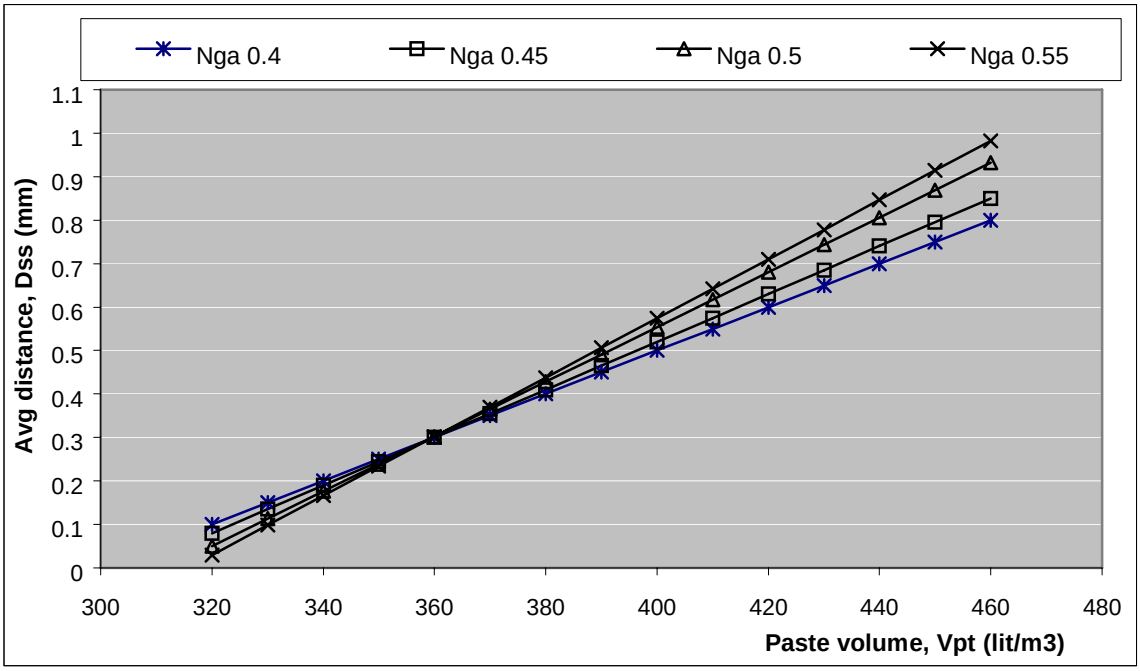


Fig. 9.8 Relationship between average inter-particle distance ($D_{ss}$) and different paste volume ($V_{pt}$)

Table 9.3 Optimum Coarse-Total Aggregate (opt. Nga) ratio and respective paste volume ($V_{pt}$)

| **Opt. Nga** | 0.40 | 0.45 | 0.50 | 0.55 |
|---|---|---|---|---|
| **Vpt (lit/$m^3$)** | 320 to 350 | 350 to 390 | 320 to 400 | 400 to 460 |

The assumption of spherical shape may be regarded as an ideal case. However, it can also be found from the experiments that even when the total surface area of the aggregate group is assumed to increase by 50% from the assumed value, the Nga ranges which produce the maximum $D_{ss}$ remains unchanged (Fig 9.9).

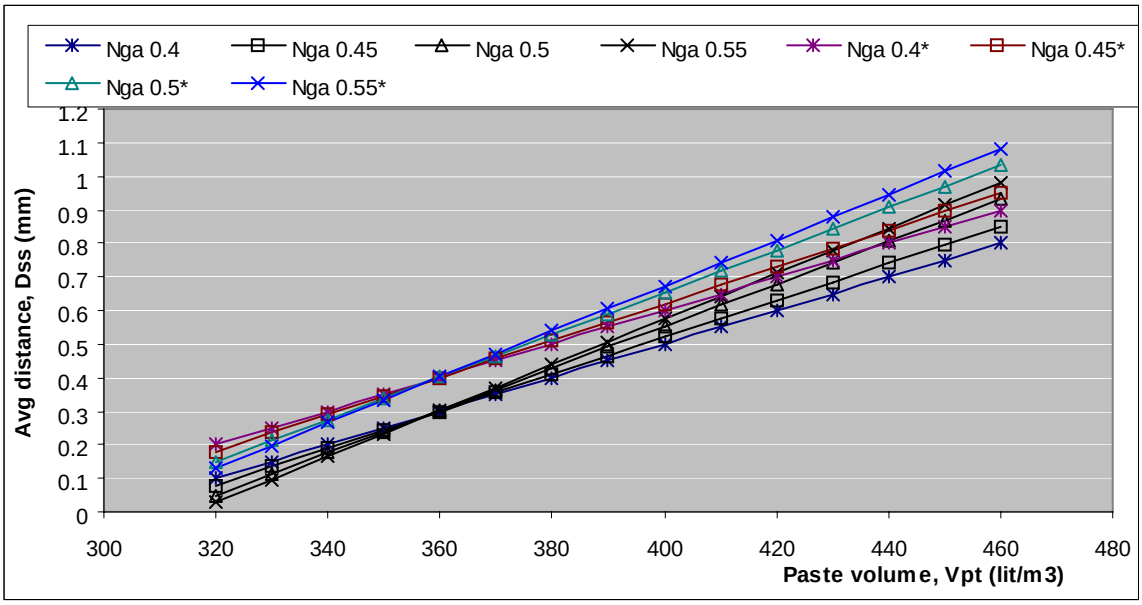


Fig. 9.9 Relationship between aggregate inter-particle distance ($D_{ss}$) and different paste volumes ($V_{pt}$) for 50% error in total aggregate surface area

## 9.2.4 Blocking Criteria Concept

The larger coarse aggregate volume results in the tendency of reducing paste volume, but this can lead to a tendency of higher blocking risk. The fresh SCC must have good deformability and segregation resistance in order to ensure satisfactory filling ability. The effect of aggregate on blocking depends on the aggregate mean size. Larger particle sizes lead to a higher risk of blocking. Ozawa [*Ozawa, K et. al, 1989*] and Tangtermsirikul [*Tangtermsirikul, S. et. al, 2001*] proposed the equation for calculating the blocking risk of multi-size aggregate as follows;

$$\text{Risk of blocking} = \sum \left( {}^{n_{si}} \big/ _{n_{sbi}} \right) \quad (9.21)$$

Where; $n_{si}$ is the volume ratio of aggregates of a single-size group i and $n_{sbi}$ represents the volume ratio, which would cause blocking, of aggregates of the single size group i. It was also found that the ratio between the size of opening and the size of particles is also an important factor in the blocking criteria of SCC.

The optimum ratio of coarse-total aggregate (Nga) results in a maximum average distance between the aggregate particles surfaces and the best deformability. However, if the optimum ratio is too high, fresh SCC will face blocking problems when passing through reinforcing bars. Therefore, in this study, a blocking criterion is suggested in order to determine the maximum total aggregate content to avoid blocking problem.

In practice, the blocking volume ratios are related to the ratio of reinforcement clear spacing to the average diameter of the aggregate particles of each size fraction and the viscosity of powder paste. In this study, the blocking criteria of SCC are discussed based on the approach suggested by Swedish Cement and Concrete Institute, CBI [*Billberg, P. and Österberg, T, 2002]*. The relation between blocking aggregate ratio ($N_b$) and the ratio ($D_{ca}$) of reinforcement clear spacing ($D_c$) to average diameter of aggregate ($D_{av}$) can be derived as follows;

$$D_{ca} = D_c/D_{av} \quad (9.22)$$

$$N_b = a1*(D_{ca}-1) = 0.35(D_{ca}-1) \quad \text{for } 1.0 < D_{ca} < 2.6 \quad (9.23)$$

$$N_b = a2*D_{ca} + b2 = 0.010484*D_{ca} + 0.533 \quad \text{for } 2.6 < D_{ca} < 15 \quad (9.24)$$

$$N_b = \text{constant} = 0.69 \quad \text{for } D_{ca} > 15 \quad (9.25)$$

Where:

$D_c$ : Reinforcement clear spacing

$D_{av}$ : Average aggregate diameter

$N_b$ : Blocking volume ratio between total aggregate volume ($V_a$) and total concrete volume ($V_t$)

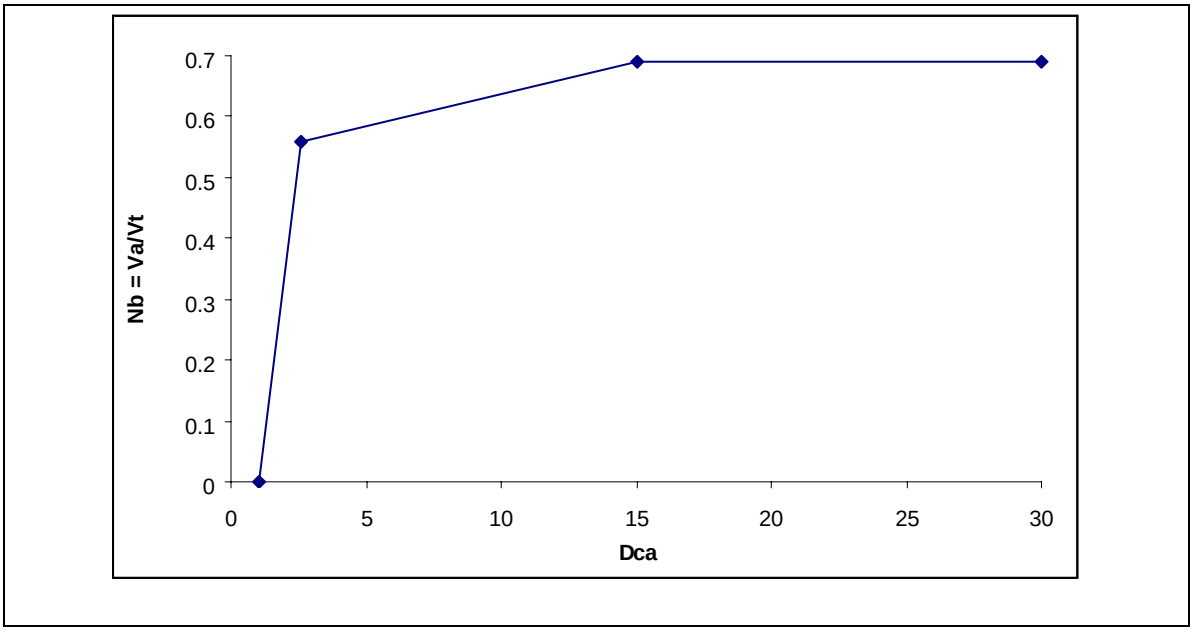


Fig 9.10 Relationship between blocking volume ratio (Nb) and ratio of reinforcement clear spacing to average particle diameter (Dca)

Using the equations (9.21) to (9.25), the equation for determining maximum aggregate volume corresponding to each coarse-total aggregate ratio (Nga) of each aggregate group type can be derived as;

$$\text{Risk of Blocking} = \sum\left[Nsi/Nsbi\right] = \sum\left[\frac{Vai/Vt}{Vbai/Vt}\right] = \sum\left[\frac{Vai}{Vbi}\right] = \sum\left[Vgm/Vbgm\right] + \sum\left[Vsn/Vbsn\right]$$

Where;

Vai : Volume of aggregate group i

Vbi : Blocking volume of aggregate i

Vgm : Volume of coarse aggregate group m

Vbgm : Blocking volume of coarse aggregate group m which can be calculated from eq (9.23) or (9.24) or (9.25)

Vsn : Volume of fine aggregate group n

Vbsn : Blocking volume of fine aggregate group m which can be calculated from eq (9.23) or (9.24) or (9.25)

Such blocking criteria can be utilized in combination with the proposed theory to determine the best Nga with satisfactory passing ability.

## 9.3 Optimization of Liquid Phase or Paste Portion

This section discusses the effect of the solid liquid phase, which contains cement, fillers, water, superplasticizer and air bubble. In order to design the paste volume, which satisfies the fresh flowability and segregation resistance, the proportion of powder, water and dosage of superplasticizer need to be optimized.

Proposed mix design concept focuses on the liquid phase including:

- Calculation of paste volume
- Selection of water content, cement content and w/c according to strength requirements
- Dosage of superplasticizer
- Air content in freshly mix concrete

### 9.3.1 Calculation of Paste Volume

The paste volume ($V_{pw}$) is needed not only to fill all voids among the aggregate particles but also to envelop all surface areas of aggregate particles. The paste volume of SCC can be obtained from the above presented methods by taking into account the aggregate inter-particle distance ($D_{ss}$), optimum aggregate ratio (Nga) and blocking criteria.

## o Cement Content

Different cements have different water requirements in concrete. The water requirement relates to cement properties such as particle size distributions, fineness and chemical compositions. A finer particle size results in an increase in water requirements. Ordinary Portland cement usually requires less water than rapid hardening cement. For the mix proportion of SCC, the different properties of different cement types can be adjusted by varying the dosage of water and admixtures of different kinds. It is important to select the cement content according to strength requirements as well as local climate condition. Ordinary Portland cement was used through out the study. In Singapore, due to the high temperature of tropical regions, the maximum amount used was limited to 470 kg/m$^3$ in this research.

## o Filler Content

It is clear that different filler materials show different flowability of SCC. Their physical characteristics and chemical composition play an important role not only in fresh stage workability but also in the hardened stage strength development and long-term durability. The content of fillers also influences the flowability of SCC A higher filler content results in higher water demand and poor workability. Thus, the optimum content of filler powders must be considered not only from the filling ability aspect but also from the other requirements such as compressive strength, durability, long-term deformations, etc.

In this research, due the strength requirements and limited OPC content because of tropical high temperature, the filler content was varied from 100 kg/m$^3$ to 230 kg/m$^3$ so as to meet the paste volume requirements.

- **Water Content**

Water content used was determined by taking into account for the fresh workabilities and strength requirements. A higher water content would lead to a potential for bleeding and segregation but lower water content results in using a higher dosage of superplasticizer to achieve the fresh workabilities of SCC.

Thus in this research, the maximum and minimum water content were fixed at 220 kg/m$^3$ and 170 kg/m$^3$ respectively.

- **Dosage of Superplasticizer**

It was reported that a higher dosage of superplasticizer results in better deformability, but excessive dosage could cause bleeding and increased segregation potential. Each type of cementitious powders favors only a certain kind of superplasticizer due to the possibility of slump loss and insufficient flowability of SCC.

The dosage of superplasticizer for each mix was calculated with regards to its respective saturation dosage of different powders. In this project, two types of superplasticizer were used. ADVA 108 that contains retarder was used to enhance the slump retention up to 90 min and ADVA 109, which does not have retardation properties, was also used to achieve the early age (24 hours) strength development. The proportions of these two types of superplasticizer were determined experimentally and it was found that 55% of ADVA 108 to 45% of ADVA 109 gave the best results with regards to requirements of slump retention and early age strength.

## 9.4 Proposed SCC Mix Design Steps

General consideration of mix design steps are proposed in order to give a framework of the proposed mixes. The flow chart for mix design is also presented in **Fig. 9.11**.

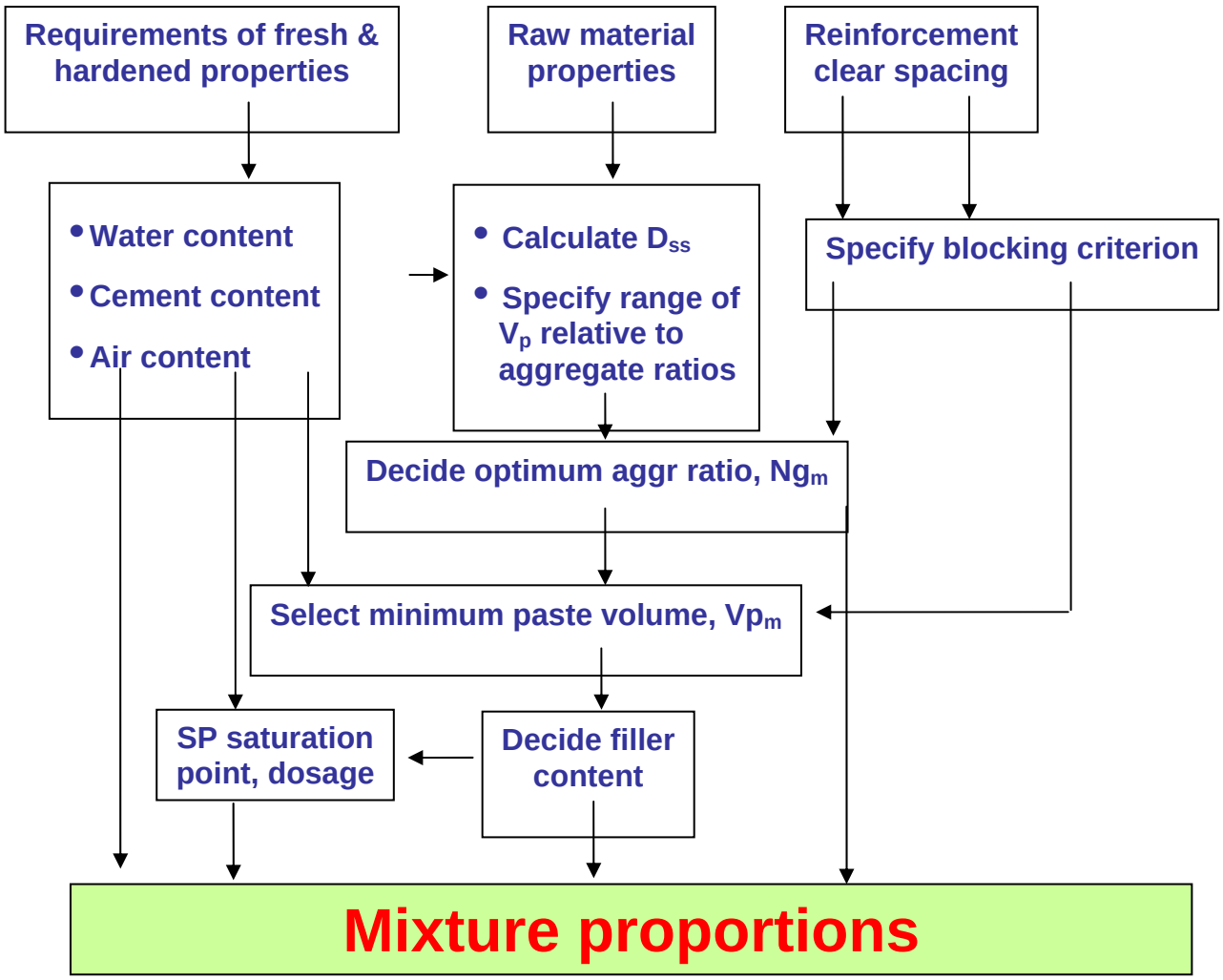


Fig. 9.11 Flow Chart for Proposed Mix Design Procedures

**Step 1: Characterization of raw materials**

- Cement and fine filler: specific gravity, fineness, size distribution, and chemical composition.

- Coarse (CA) and fine aggregate (FA) : specific gravity in dry and SSD condition, grading, surface moisture content, water absorption, voids content of separate CA and FA, voids content of binary aggregate mixture (i.e., CA+FA).

**Step 2: Requirements of concrete properties (fresh and hardened concrete)**

- Select OPC content suitable for the particular project
- Based on W/C, calculate water content which satisfies the fresh properties as well as hardened properties of SCC.
- Assume nominal air content (e.g. 1 to 2%)

**Step 3: Testing and finding the Optimum values of coarse-total aggregate ratio (i.e. Ng) and paste volume (i.e. $V_p$)**

- For various coarse-total aggregate ratios, Nga, (= CA/[CA+FA]), experimentally determine the voids content of each compacted binary mixture. Specify the optimum value of $Ng_{min}$

  (i.e **$Ng_{min}$**) which corresponds to the minimum voids content.
- For various ratios of Nga with assumed different paste volume ($V_p$), calculate the distance between the aggregate particles ($D_{ss}$)
- For each Nga, analyze and specify the ranges of $V_p$ which produce maximum $D_{ss}$.
- With reference to blocking criteria, i.e., spacing of reinforcing bars, select optimum paste volume (i.e. **$V_{pm}$**) from the above range of $V_p$

**Step 4: Dosage of Admixture**

- Determine the saturation point of superplasticizer with respect to water content, W/C, W/P and analyzed its effectiveness based on thickness of water film.

Saturation Point of the superplasticizer corresponds to the dosage of SP, beyond which there is no appreciable improvement in flow properties (flow diameter or funnel flow time) of the paste.

## 9.5 Example of Mix Proportions

According to the requirements and some restrictions due to our local conditions, the mix proportions of SCC for different target strength levels had been proposed. Table 9.4 presents such examples of some of the requirements of research objectives and limitation due to local conditions.

Table 9.4 Requirements of research objectives and limitation due to local conditions

| **Research Objectives** | **Restriction (based on local condition & experience)** |
|---|---|
| 1) Target strength 40, 60, 80 MPa | 1) OPC used cannot be more than 470 kg/m$^3$ due to concern over excessive heat of hydration |
| 2) Fine fillers used are Granite Dust (GR) and copper slag (DC) | 2) Available as waste product from aggregate quarry and ship blasting industry. Allowable usage of DC in concrete is 10% by weight of fine aggregate. |
| 3) Retention time for about 90 min | 3) Water content should not be lower than 170 kg/m$^3$. |

These includes 2 series designed as A and B. Series A (GR group) are the mix proportion for SCC using Granite Dust alone as filler. While in Series B (DC group), only Copper Slag Fines were used as filler with the restriction of 10% sand replacement by slag. For our current materials and local conditions, the following values were found from detail analysis of the above mix design steps. The detail mix design steps are presented in Appendix A.

Minimum paste volume**,** **Vpm = 410 lit/m$^3$ (bar spacing of 35 to 40 mm)**

Optimum coarse–total aggregate ratio, **Ngm = 0.49**

Extensive lab trials had been conducted to verify the proposed mix proportions for SCC and to find the possible solutions of some problems which might be encountered during casting of SCC in ready mix plants.

### 9.5.1 Verification of Proposed Mix Proportion for SCC

A series of trail mixes were conducted in order to verify the proposed mix proportions for SCC in terms of fresh flow characteristics and hardened compressive strength development.

- **Trial Mixes with Granite Dust (GR series)**

Trail mixes for three strength levels of SCC incorporating granite dust were conducted in order to justify the proposed mix proportions and suitability of granite dust in SCC. Table 9.5 to 9.6 presents the mix proportions used for 40 MPa, 60 MPa and 80 MPa SCC in which granite dust was used as filler.

Table 9.5 Mix proportion used for 40 MPa SCC

| OPC (kg) | Water (kg) | Granite (kg) | F-Agg (kg) | C-Agg (kg) | Adva 108 (ml) | Adva 109 (ml) |
|---|---|---|---|---|---|---|
| 400 | 200 | 170 | 790 | 760 | 800* | 700* |

Table 9.6 Mix proportion used for 60 MPa SCC

| OPC (kg) | Water (kg) | Granite (kg) | F-Agg (kg) | C-Agg (kg) | Adva 108 (ml) | Adva 109 (ml) |
|---|---|---|---|---|---|---|
| 450 | 180 | 150 | 790 | 760 | 1200* | 1000* |

Table 9.7 Mix proportion used for 80 MPa SCC

| OPC (kg) | Water (kg) | Granite (kg) | S- Fume (kg) | F-Agg (kg) | C-Agg (kg) | Adva 108 (ml) | Adva 109 (ml) |
|---|---|---|---|---|---|---|---|
| 470 | 170 | 130 | 23.5 | 790 | 760 | 1700* | 1000* |

*ml/100 kg of OPC

Table 9.10 summarizes the trial results on different strength levels of SCC which were prepared according to the proposed mix proportions.

Table 9.10 Trail results on different strength level of SCC

| Designation | Fresh Properties | | | Hardened Strength (MPa) | | |
|---|---|---|---|---|---|---|
| | S-flow (mm) | Blocking | V-funnel (s) | 1 D | 7 D | 28 D |
| GR 40 | 680 | 0.85 | 6 | 10 | 36 | 45 |
| GR 60 | 690 | 0.9 | 9 | 22 | 56 | 72 |
| GR 80 | 680 | 0.9 | 12 | 31 | 68 | 84 |

It can be observed from above table that all the proposed mixes satisfied both in the fresh flow characteristics and the hardened compressive strengths development. Thus, the proposed design procedure can be successfully used to design the required strength levels of SCC.

- **Trial Mixes with Copper Slag (DC slag series)**

A series of lab trials was conducted to verify the proposed mix proportions for SCC incorporating copper slag, DC slag. The amount of copper slag that can be added in concrete products was limited to 10% by weight of sand according to Ministry of Environment due to the concerns of leaching problems. Thus, in the trials, DC slag had been added either as part of sand or part of filler. The DC slag (10% by weight of sand) was added together with sand

if it was treated as part of sand. However, if DC slag was treated as part of filler, the delayed adding technique was adopted, i.e DC slag was added at the end of mixing sequence. Table 9.11 presents the mix proportions that were used to verify the proposed mix proportions of SCC incorporating DC slag.

Table 9.11 Mix proportions of SCC incorporating DC slag

| Name | OPC (kg) | Water (kg) | Granite (kg) | DC slag (kg) | F-Agg (kg) | C-Agg (kg) | Adva 108 (ml) | Adva 109 (ml) |
|---|---|---|---|---|---|---|---|---|
| DC 1 | 400 | 200 | 170 | 73 | 730 | 760 | 1500* | 1200* |
| DC 2 | 400 | 200 | 90 | 79 | 790 | 760 | 910* | 750* |

Table 9.12 Trail results on different strength level of SCC

| Designation | Fresh Properties | | | Hardened Strength (MPa) | | |
|---|---|---|---|---|---|---|
| | S-flow (mm) | Blocking | V-funnel (s) | 1 D | 7 D | 28 D |
| DC 1 | 665 | 0.9 | 10 | 9 | 33.5 | 42 |
| DC 2 | 660 | 0.9 | 12 | 9 | 34 | 45 |

*ml/100 kg of OPC

It can be seen from Table 9.11 that DC 1 mix, in which copper slag was treated as part of sand without adjusting total powder content, required a higher dosage of chemical admixture compared with the DC 2 mix, where copper slag was replaced as part of the filler and the total powder content was adjusted. It is clear that the finer particle DC slag behaves more like a filler rather than a sand in the mix and enhanced the total powder content resulting in a requirement for higher dosage of chemical admixtures. On the other hand in mix DC 2, the dosage of chemical admixture was dramatically lower than even the GR mixes, GR 40. Aside from the different dosage requirements of chemical admixture, both DC 1 and DC 2 mixes showed similar fresh flowability as well as hardened compressive strengths development.

Thus, it can be concluded from the trials reported that the proposed mix design of SCC incorporating granite dust (GR) and copper slag (DC slag) as powder offers satisfactory results in the desired fresh stage properties as well as hardened strength development..

# CHAPTER 10 CONCULSIONS AND RECOMMANDATIONS

## 10.1 Conclusion

Based on the present study, the following conclusions can be made:

(1) The physical properties and chemical characteristics of constituent materials influence the rheological parameters, yield stress and plastic viscosity of SCC. In the paste fraction of SCC, the particle shape and particle reactivity of incorporated powder influence significantly the rheological properties. For pastes without admixtures, the particle shape and size of filler powder has significant effects on the paste rheology. For paste with admixture; superplasticizer, the rheological parameters are more dependent on reactivity of the powder rather than on the particle shape. The decrease in yield stress due to increased dosage of admixture is more significant than the decrease in viscosity.

(2) The rheological model to predict especially the yield stress and the plastic viscosity of the paste fraction of SCC was proposed by taking into account the physical and chemical effect of powder (angularity factor and reactivity factor), type of chemical admixture used (repulsion factor) of the powders. It was found that the inter-particle distance, presented as thickness of water film around the powder particle, was the primary controlling factor for the rheology properties of the paste fraction. It seems that the proposed the rheological model is able to predict the yield stress and plastic viscosity of the paste fraction of SCC satisfactorily ($R^2$ = 0.94 and 0.92 respectively).

(3) There is a possible correlation between mortar rheology and its paste fraction by applying the suspension theory. The rheology of the mortar can be determined as a function of the rheology of its suspending medium and the inter-particle distance of the fine aggregate particle. It was found that the yield stress and plastic viscosity of mortar has a linear relation with those of its paste fraction by considering the contributory effect of physical characteristic such as angularity, surface modulus and specific surface area of the fine aggregate in the mix.

(4) Rheology of SCC could be correlated with its corresponding paste fraction through mortar rheology. By optimizing the mix constituents incorporated in the paste fraction, rheology of SCC can be predicted with minimum number experimental tests.

(5) Simple physical tests which can be carried out easily in the laboratory as well as on site showed some indication of the rheological characteristics of the mix. The physical characteristics and chemical compositions of the mix constituents have a great influence on the flow properties of SCC.

(6) The proposed mix design step, which is mainly based on the fundamental characteristics of the mix constituents, can be used to design the mix proportions of SCC with satisfactory fresh flow properties and hardened mechanical strengths. The proposed mix design method has the potential to optimize the mix proportions of SCC for the production process.

(7) With the understanding of the factors affecting on paste rheology, it is possible to predict the workability of SCC from its paste fraction in combination with additional physical effects of the aggregate. Thus, there may be a need to optimize the mix proportions of SCC during actual production.

(8) With the aid of paste rheology and parametric study, locally available powders especially industrial waste can be identified for appropriate incorporation into SCC so as to further reduce the cost of the powder fraction in SCC.

(9) The usage of OPC content to enhance cohesiveness of the concrete mix can be reduced by replacment with less active or inactive filler powders available locally. Thus for SCC, the potential of thermal cracking due to a higher temperature rise in the tropical environment by the usage of higher OPC content can be minimized.

The overall objective of this project is the development of the new technology on SCC that can be applied in tropical environments including Singapore. This research has provided the cement and concrete industries with a set of mix design guidelines for the production of SCC. The guidelines for mix proportioning of SCC include different types of fillers. With these proposed guidelines, the mix proportions of SCC can be selected with the help of minimal parametric study on the mix constituents. With an understanding of the physical and chemical properties of these mix constituents and their possible contributory effect on SCC, it is possible to establish the mix proportioning of SCC, which can be

successfully applied in tropical areas. Thus, the proposed mix design method has the potential for use in optimizing the mix proportions of SCC during actual production.

## 10.2 Recommendations for Future Works

The model for prediction of paste rheology proposed in this study has been concentrated on the internal factors which affect its rheology. Throughout the paste rheological study, the external factors such as temperature, humidity or moisture content of the surrounding environment, initial mixing conditions, shear history, during the rheology test, testing procedure such as test duration, measuring system were fixed in order to investigate the effects of internal factors on paste rheology. Therefore, it is recommended to explore the effects of external factors on paste rheology by controlling the internal factors. Besides filler powder, GGBS, LS, GR, DC, used in this study, other type of locally available powder such as cement sludge or PFA or other types of powder can be used to investigate the rheological characteristics of the paste fraction.

In the investigation of rheology of mortar as well as concrete, OPC with one type of filler mix was used as the corresponding paste fraction. Future work can be done with double blended filler powders. Besides the fine filler used in this study to achieve cohesiveness of SCC, viscosity modifying agents may also be included to study its behavior on the rheological properties of the paste, mortar and concrete.

Ambroise J, Rols S, and Pera J (1999), "Self-levelling Concrete - Design and Properties", *Concrete Science and Engineering*, 1(3), pp140-147.

Agarwal S.K., Masood I. and Malhotra S.K. (2000), "Compatibility of Superplasticizer with Different Cements", *Construction and Building Materials*, vol.14, 253-259

ASTM C114-83b (1983), "Test Method for Chemical Analysis of Hydraulic Cement", Annual Book of ASTM Standards, 04.01, *American Society for Testing Materials, Easton, MD*

ASTM C 150-84 (1984), "Specific Gravity for Cement", Annual Book of ASTM Standards, 04.01, *American Society for Testing Materials, Easton, MD*

ASTM E11-95 (1995e). "Standard Specification for Wire Cloth Sieves for Testing Purposes". Philadelphia, Pennsylvania: *American Society for Testing and Materials*. 241805.

ASTM C136-96a (1996d). "Standard Test Method for Sieve Analysis of Fine and Coarse Aggregates". Philadelphia, Pennsylvania: *American Society for Testing and Materials*. 241447.

ASTM C33-97 (1997g), "Standard Specification for Concrete Aggregates". Philadelphia, Pennsylvania: *American Society for Testing and Materials*. 239386.

ASTM C127-88 (1988) (reapproved 1993). "Standard Test Method for Specific Gravity and Absorption of Coarse Aggregate". Philadelphia, Pennsylvania: *American Society for Testing and Materials*. 241450.

ASTM C128-93 (1993), "Standard Test Method for Specific Gravity and Absorption of Fine Aggregate". Philadelphia, Pennsylvania: *American Society for Testing and Materials*. 241449

ASTM C 29/29M-91a (1991), "Test Method for Unit Weight and Voids in Aggregate", Annual Book of ASTM Standards, 04.01, *American Society for Testing Materials, Easton, MD*

ASTM C305-99 (1999), "Standard Practice for Mechanical Mixing of Hydraulic Cement Paste and Mortar of Plastic Consistency", Philadelphia, Pennsylvania: *American Society for Testing and Materials*.

ASTM C143-90a (1990) "Standard Test Method for Slump of Hydraulic Cement Concrete". Philadelphia, Pennsylvania: *American Society for Testing and Materials*. 232147

Banfill, P.F.G., Denis Beaupré,Frédéric Chapdelaine, François de Larrard,Peter Domone, Laurent Nachbaur,Thierry Sedran, Olaf Wallevik,Jon E. Wallevik (2000), "Comparison of Concrete Rheometers, Internal Tests at LCPC", *National Institute of Standard and Technology*, NISTIR 6819, 157 pages

Banfill, P.F.G.(1983), 'A Viscometric Study of Cement Paste containing Superplasticizers with a note on Experimental Technique', *Magazine of Concrete Research*, V.33, No. 114, pp.37-47

Barnes, H. A. Hutton, J. F. and Walters, F. R. S. (1989). "An Introduction to Rheology". *Elsevier science publishers*, Amsterdam.

Bartos, P. (1992). 'Fresh Concrete Properties and Tests'. *Elsevier science publishers*, Amsterdam.

Bartos, P. J. M. and Grauers, M. (1999). 'Self-compacting concrete'. *Concrete*, Vol. 33, No. 4, pp. 9-13.

Bennenk, W., (2001), "SCC as Applied in the Dutch Precast Concrete Industry", *Proc. Second International Symposium on Self-compacting concrete*, Tokyo, Japan, Ozawa K and Mashiro O Ed., COMS Engineering Corporation, 2001 pp625-632.

Betancourt, G. H. (1988). 'Admixtures, Workability, Vibration and Segregation'. *Materials and Structures*, Vol. 21, pp. 286-288.

Billberg P. (1999a), "Fine Mortar Rheology in Mix Design of SCC", *Proceedings of First International RILEM Symposium on Self-Compacting Concrete*, Stockholm, 1999, pp 47-58

Billberg, P., (1999b), 'Self-compacting concrete for civil engineering structures –the Swedish experience', *CBI rapport 2:99*, Swedish Cement and Concrete Research Institute, SE-100 44, Stockholm

Billberg P., (2001), "Influence of filler characteristics on SCC rheology and early hydration", *Proceeding of the second International Symposium on Self-Compacting Concrete*, Tokyo, October, 285-294

Billberg, P. and Österberg, T (2002), "Self-compacting Concrete - Technique of Application", Report of Swedish Cement and Concrete Research Institute, 154 p. Pris: 300

Bui V.K (2000)., "Penetration Test of Resistance to Segregation" ,in A.Skarendahl,O.Petersson(Eds.), *State of the Art Report of RILEM Technical Committee 174-on Self-Compacting Concrete*, ISB2-912143-23-3, RILEM Publications S.A.R.L, Cachan, France, Report 23,2000, pp.136–138.

BS 5328 (1997), "Concrete, Part 1. Guide to Specifying Concrete", *British Standards Institution*, London.

BS 8110 (1997), "Structural use of concrete, Part 1, Code of Practice for Design and Construction", *British Standards Institution*, London.

Chidiac S.E, Habibbeigi F. and Chan D (2006), "Slump and Slump Flow for Characterizing Yield Stress of Fresh Concrete", *ACI Materials Journal*, V.103, pp 413-418

Christensen B.J. and Ong F.S (2005), "The Performance of High-Volume Fly Ash Self-Compacting Concrete, (SCC)", *Proceedings of Foutrh International RILEM Symposium on Self-Compacting Concrete*, USA, pp 139-144

Cyr M., Legrand C., Mouret M. (2000), "Study of the Shear Thickening Effect of Superplasticizer on the Rheological Behavior of Cement Paste Containing Mineral Additives", *Cement and Concrete Research*, 30, pp 1477-1483

Day, K. W. (1995). 'Concrete Mix Design, Quality Control and Specification'. E. & F. N. Spon, London.

Dinesh, M. (2001), "Framework", Newsletter of the Building and Construction Authority, *Published by The Building and Construction Authority, Singapore*, Jan-Feb., 8 pages.

Domone P.L.J. (1999), "Properties of Mortar for Self-Compacting Concrete", *Proceedings of First International RILEM Symposium on Self-Compacting Concrete*, Stockholm, 1999,

Domone P.L.J., (2000), "Mix design": *State-of-the-art Report of RILEM Technical Committee Report*, 174-SCC, Self-compacting Concrete, RILEM report 23, RILEM S.A.R.L., 2000, pp 49 - 65.

Doraipandian, L. (2001), *Island Concrete (Pte) Ltd*, private communication.

EFNARC, (2002), "Specification and Guidelines for Self-compacting Concrete", *European Federation of Producers and Applicators of Specialist Products for Structures*, EFNARC, Norfolk, UK. February 2002, 32pp.

Ferraris, C.F., and Gaidis, J.M. (1992), "Connection Between the Rheology of Concrete and Rheology of Cement Paste", *ACI Materials Journal*, Vol. **89** No. 4, pp. 388-393

Ferraris C.F. and Larrard F. de (1998), "Testing and Modeling of Fresh Concrete Rheology", NISTIR 6094, *Building and Fire Research laboratory, National Institute of Standards and Technology*

Ferraris, C.F., Obla, K.H. and Hill, R., (2001), "The Influence of Mineral Admixture on the Rheology of Cement Paste and Concrete", *Cement and Concrete Research*, 31, 2001, pp245-255.

Ferraris, C.F., Larrard, F de. and Martys N. (2001), "Fresh Concrete Rheology: Recent Developments," *Materials Science of Concrete VI*, Sidney Mindess and Jan Skalny, eds., American Ceramic Society, 215-241

Ferraris C.F. and Martys N.S (2003), "Relating Fresh Concrete Viscosity Measurement from Different Rheometers", *Journal of Research of the National Institute of Standard and technology*, Vol. 108, pp 229-234

Gibbs J C and Zhu W. (1999), "Strength of Hardened Self-Compacting Concrete", *Proc. of the first international RILEM symposium on self-compacting concrete*, Stockholm, pp 199-209.

Hanehara S. and Yamada K. (1999), "Interaction between Cement and Chemical Admixture from the Point of Cement Hydration, Adsorption Behavior of Admixture and Paste Rheology", *Cement and Concreter Research*, vol. 29, 1159-1165

Hattori K. (1990), "A New Viscosity Equation for Non-newtonian Suspensions and Its Applications", *Proceedings of Int. Conf. On Rheology of Fresh Cement and Concrete*, Liverpool, pp181-191

Ho D W S, Sheinn A M M, Ng C C, Lim W B, and Tam C T (2001a), "Self-Compacting Concrete for Singapore", *Proc of 26th Conference in Our World in Concrete and Structures*, Singapore. August, 293-299

Ho D. W. S, Sheinn A. M. M., and Tam C. T. (2001b), "The Sandwich Concept of Construction with SCC", *Cement and Concrete Research*, 31(2001), Sept, No 9, 1377-1381

Ho D. W. S, Sheinn A. M. M., Lim W.B. and Tam C. T. (2001c), "Compatibility Between Conventional and Self-Compacting Concrete", *Proc. 2nd Int Symp on Self-Compacting Concrete*, Japan, October, 595-600

Ho D. W. S, Tam C. T. and Sheinn A. M. M. (2001d), "Some Major Issues of Self-Compacting Concrete", *Conspectus*, Nov 2001

Ho D. W. S, Tam C. T. and Loy. T. S. (2001e), "SCC – Here to Stay", *Singapore Concrete Institute*, Concrete News, Feb, 305.

Ho D. W. S, Sheinn A. M. M., Ng. C. C. and Tam C. T. (2002a), " The Use of Quarry Dust for SCC Application", *Cement and Concrete Research*, April 2002, Vol 32 No 4, pp 505-511.

Ho, D.W.S. Sheinn, A.M.M and Tam, C.T., (2002b), "Rheological Model for Self-Compacting Concrete – Paste Rheology", *Proc. 27th Conference on Our World in Concrete & Structures,* 29-30 August 2002, Singapore, CI-Premier Pte Ltd, Singapore, pp517-523.

Ho D. W. S, Sheinn A. M. M., Tam C. T. and Mak S. L (2003)., "Material for Sustainable Infrastructure Development", *Concrete Today*, Vol. 1, Jan-Apr , 10-17

Ho D. W. S, Sheinn A. M. M., Tam C. T., Quek S. T. (2004), "Utilization of Incinerator Ash", *Singapore Concrete Institute* (SCI)

Hu, C., DeLarrard, F., and Gjorv, O.E. (1995), "Rheological Testing and Modelling of Fresh High-Performance Concrete", *Materials and Structures*, Vol. **28**, pp. 1-7.

Hu, C., de Larrard, F., Sedran, T., Boulay, C., Bosc, F., Deflorenne, F. (1996), "Validation of BTRHEOM, the new rheometer for soft-to-fluid concrete," *Materials and Structures*, Vol. 29, No. 194, pp. 620-631

Jiang W. and Roy D.M., (1992), 'Microstructure and Flow Behavior of Fresh Cement Paste', *Materials Research society Symposium Proceedings Vol. 289,* November 30-December 2, Boston, U.S.A., 161-166

Katz A. and Baum H., (2006), "Effect of High Levels of Fines Content on Concrete Properties", *ACI Materials Journal*, V.103, pp 474-482

Karam G. N. (1992), "Theoretical and Empirical Modeling of the Rheology of Fresh Cement Pastes", *Material Research Society Symposium Proceedings Vol. 289*, Boston, U.S.A, November 30-December 2, pp167-172

Kim J. K., Han S. H., Park Y. D., Noh J.H., Park C. L., Kwon Y. H. and Lee S. G. (1996), "Experimental Research on the Material Properties of Super Flowing Concrete", in: Bartos P.J.M. , Marrs D.L. and Cleland D.J. (Eds.), P*roduction Methods and Workability of Concrete*, E&FN Spon, 271-284

Kurita M., Nomura T. (1999), "Highly Flowable Steel Fiber-Reinforced Concrete Containing Fly Ash", in: Malhotra V.M. (Ed.), *American Concrete Institute, Sp 178*, June, 59-175

.Khayat K.H, Hu C. and Monty H. (1999), "Stability of Self-Consolidating Concrete, Advantages and Potential Applications", *Proceedings of First International RILEM Symposium on Self-Compacting Concrete*, Stockholm, pp143-152

Kurokawa, Y., Tanigawa, Y., Mori, H., Komura, R. (1994), "A Study on the Slump Test and Slump-Flow Test of Fresh Concrete," *Transactions of the Japan Concrete Institute*, vol. 16, pp. 25-32, 1994

Lim, W.B. (2001), "Development of Self-compacting Concrete - Compatibility of SCC with Normal Concrete", *National University of Singapore*, Dept of Civil Engineering Dissertation, 51 pages.

Loudon, A.G., (1952-1953), "Computation of Permeability from Simple Soil Test", *Geotechnique*, 3, 165-183

Larrard F.De., (1999), "Concrete Mixture Proportioning, A Scientific Approach", Modern Concrete Technology Series, E & FN Spon

Marrs, D. L. (1998). 'Development of SIFCON for Use in Structural Applications'. *PhD thesis*, University of Paisley.

Martys, N.S. and Ferraris, C.F. (2003), "Simulation of SCC Flow", *First North American Conference on the Design and Use of Self-Consolidating Concrete*. Proceedings. Chicago, IL, November 12-13, pp. 27-30, 2003.

Matsuhisa M., Yamada K., Ishimori M. and Kaneda Y. (1998), "Effects of Cement Character on the Fluidity of Cement Paste Added with Beta-Naphthalene Sulfonate Type or Polycarboxylate Type Superplasticizer", *Proceedings of the Japan Concrete Institute* 20-2, 67-72

Mindess S.,.Young J.F (1981), "Concrete", Prentice Hall, Englewood Cliffs, 531NJ, 1981.

Murata, J., and Kikukawa, H. (1992), "Viscosity Equation for Fresh Concrete", *ACI Materials Journal*, Vol. **89** No. 3, May-June

Ng, C.C. (2001), "Rheology of Self-compacting Concrete: Influence of Filler Materials on Cement Paste", *National University of Singapore, Dept of Civil Engineering Dissertation*, 71 pages.

Neville A.M. (1995), "Properties of Concrete", *Fourth edition*, Longman, Harlow

Nishibayashi S., Yoshino A., Inoue S. (1996), "Effect of Properties of Mix Constituents on Rheological Constant of SCC", *In production methods and workability of concrete*, Edi. By P.J.M Bartos, D.L. Marrs and D.J. Cleland, London; E&FN Spon, pp 255-262

Nishizaki T, Kamada F, Chikamatsu R, and Kawashima H. (1999), "Application of High Strength Self-Compacting Concrete to Prestressed Concrete Outer Tank for LNG Storage", *Proc. of the first international RILEM symposium on self-compacting concrete*, Stockholm, pp 629 - 638.

Noguchi T., Oh S. G. Tomosawa F. (1999), "Rheological Approach to Passing Ability between Reinforcing Bars of Self-Compacting Concrete", *Proceedings of*

*First International RILEM Symposium on Self-Compacting Concrete*, Stockholm, pp 59-70

Okamur H., Ouchi M. (1999), "Self-Compacting Concrete. Development, Present Use and Future", *Proceedings of First International RILEM Symposium on Self-Compacting Concrete*, Stockholm, pp 3-14

Okamur H., Ouchi M. (2003), "Self-Compacting Concrete", *Journal of Advanced Concrete Technology*, Vol 1, No 1, April

Ong, W.S.S. (2002), "Compatibility of SCC and Normal Concrete using Different Chemical Admixtures and Casting at Fresh State", *BEng Thesis*, Department of Civil Engineering, National University of Singapore, 2002, 105pp.

Ozawa, K., Maekawa, K., Kunishima, M., and Okamura, H. (1989), "Development of High Performance Concrete Based on the Durability Design of Structures", *Proceedings of the 2nd East-Asia and Pacific Conference on Structural Engineering and Construction*, Vol. 1, pp. 445-450.

Ozawa, K. Maekawa, K. and Okamura, H. (1990). 'High Performance Concrete with High Filling Capacity'. *Proceedings of International RILEM Symposium on Admixtures for concrete – improvement of properties*, Barcelona, edited by Vazquez, E. pp. 51-62.

Popovics S. (1982), "Fundamentals of Portland Cement Concrete: A Quantitative Approach", *vol. 1: fresh concrete*, John Wiley & Son's Inc., New York, pp 27-91

Persson, B., (1999), "Creep, Shrinkage and Elastic Modulus of Self-Compacting Concrete", *Proc. 1st International RILEM Symposium of Self-compacting concrete*, Stockholm, RILEM S.A.R.L., 1999 786pp.

Petersson Ö (2000a), "Applications": *State-of-the-art Report of RILEM Technical Committee Report*, 174-SCC, Self-compacting Concrete, RILEM report 23, RILEM S.A.R.L., pp 95-109.

Petersson, Ö. (2000b), "L-shape Box Test", *Self-compacting Concrete State-of-the-Art Report*, Sweden, September 2000, pp 126-128.

Peter A. C, Philip L. and Mohammed A O. (2001), "Workability of Cement Pastes", *ACI Materials Journal*, Nov-Dec, Pp 476-482

Power. T.C. (1968), "The Properties of Fresh Concrete", John Wiley & Sons, Inc., 1968

Poppe A.M and Schutter G.De (2005), "Modeling of the Heat Development During Cement Hydration in Self-Compacting Concrete", *Proceedings of Forth International RILEM Symposium on Self-Compacting Concrete*, USA, pp 271-278

RILEM (1999), "First International RILEM Symposium on Self-compacting Concrete", Stockholm, Ed., A. Skarendahl and O. Pertersson, *RILEM S.A.R.L.*, 1999, 786pp

RILEM Report 23 (2000), "State-of-the-art Report of RILEM Technical Committee 174-SCC", *Self-compacting concrete*, Ed., A. Skarendahl and O. Pertersson, RILEM S.A.R.L., 2000. 154pp.

RILEM (2001), "Second International Symposium on Self-compacting concrete", Tokyo, Japan, 23-25 October 2001, Ozawa K and Mashiro O Ed., *COMS Engineering Corporation*, 2001 742pp.

Russel W.B., Saville D.A., and Schowalter W. R. (1989), "Colloidal Dispersions", *Cambridge University Press*, Cambridge3

Saak W., Jennings H. M. and Shaf S. P. (1999), "Characterization of Rheological Properties of Cement Pastes for use in Self-Compacting Concrete", *Proceedings of First International RILEM Symposium on Self-Compacting Concrete*, Stockholm, pp 83-94

Schober I. and Mader U. ( 2005), "Selecting the Optimum HRWR for SCC", *Proc. of the first international RILEM symposium on self-compacting concrete*, USA, pp 39-46

Sedran T. and Larrard F. (1999), "Optimization of Self-Compacting Concrete Thanks to Packing Model", *Proceedings of First International RILEM Symposium on Self-Compacting Concrete*, Stockholm, pp 321-332

Sedran R. (1999), "Rheometry and rheology of concrete. An application to Self Compacting Concrete," *PhD Thesis*, 220 p, Mars

Shoya M., Aba M., Sugita S., Tsukinaga Y. and Tokuhashi K. (1999)**,** "Self Compatibility of Fresh Concrete with Non-Ferrous Metal Slag Fines Aggregate", *Proceeding of the first Rilem International Symposium on Self-Compacting Concrete*, Stockholm, September, 579 – 589

Singapore Standard SS 31: (1998), "Aggregate from Natural Sources for Concrete", 20 pages

Skarendahl, Å., (2000a), "Development Objectives", Self-compacting Concrete, *State-of-the-art-report of RILEM Technical Committee* 174-SCC, *RILEM Publications S.A.R.L.*, pp. 9-13.

Skarendahl Å, (2000b), "Definitions", State-of-the-art Report of RILEM Technical Committee Report, 174-SCC, *Self-compacting Concrete*, RILEM report 23, RILEM S.A.R.L., pp. 3-5.

Skarendahl Å (2000), "Early Age and Hardened Properties": *State-of-the-art Report of RILEM Technical Committee Report*, 174-SCC, Self-compacting Concrete, RILEM report 23, RILEM S.A.R.L., pp 43-46.

Skarendahl, Å., (2001), *Swedish Cement and Concrete Research Institute*, private communication.

Sonebi, M. and Bartos, P. J. M. (1999). "Hardened SCC and its Bond with Reinforcement". *Proceedings of 1st International RILEM Symposium on Self-Compacting Concrete*, Stockholm, edited by Skarendahl, A. and Petersson, O. pp. 275-289.

Struble L.J. and Sun G.K.,(1993), "Cement Viscosity as Function of Concentration", *Flow and Microstructure of Dense Suspension*, Material Research Society, Pittsgurgh, pp173-178

Takada, K. (2000a), "Slump-Flow Test", *Self-compacting Concrete State-of-the-Art Report*, Sweden, September 2000, pp 117-119.

Takada, K. (2000b), "V-Funnel Test", *Self-compacting Concrete State-of-the-Art Report*, Sweden, September 2000, pp 120-122.

Takada, K. and Tangtermsirikul, S., (2000c), "Testing of Fresh Concrete", *Self-compacting Concrete, State-of-the-Art Report*, Sweden, September 2000, pp 25-39.

Takada K. (2000d), "Test Method Description": State-of-the-art Report of RILEM Technical Committee Report, 174-SCC, Self-compacting Concrete, *RILEM report 23*, RILEM S.A.R.L., pp 117 - 141.

Tan C K, Loh S, Logendran D, and Seow K H (2001), private communication, 2001.

Tangtermsirikul, S. (1998). 'Self-Compacting Concrete'. RILEM TC-SCC State f the art report (draft version), edited by Skarendahl, A. and Petersson, O. pp. 6-9.

Tangtermsirikul S., Khunthongkeaw J., Kaewkhluab T. (2001), "Deformability and Compressive Strength Models for Self-Compacting Concrete', *Proceeding of the second International Symposium on Self-Compacting Concrete*, Tokyo, October, 117 – 126

Talbot, A.N., discussion of paper by R.B. Young (1919), 'Some Theoretical Studies on Proportioning Concrete by the Method of Surface Area of Aggregates', *Proc. ASTM, vol. 19*, Part II, 483

Tam C. T., D. W. S and Sheinn A. M. M. (2002), "Potential Benefits of SCC in Precast Construction", *Asian Concrete Construction Conference*, Hong Kong, 26-27 November

Tam C.T., Sheinn A.M.M, Ong K.C.G and Chay C.Y (2005), " Modified J-Ring Approach for Assessing Passing Ability of SCC", *Proceeding of the Fourth International Symposium on Self-Compacting Concrete*, USA, pp 687-692

Tanigawa Y., Mori H. and Watanabe K. (1990), "Analytical Study on Flow of Fresh Concrete by Suspension Element Method", *Proceeding of RILEM Colloquium: Properties of Fresh Concrete,* Chapman and Hill, 301-8

Tattersall G.H.(1991), "Workability and Quality Control of Concrete", E&FN Spon, London

Tattersall G. H. and Banfill P. F. G. (1983), "Rheology of Fresh Concrete", *Pitman and advance publishing program*, Boston

Tattersall G.H. and Diamond S. (1976), "The Use of Coaxial Cylinders Viscometer to Measure Rheological Properties of Cement Paste", *Proceedings of Int. Conf. On Hydraulic Cement Paste*: Their Structure and Properties, Sheffield, pp 118-133

Trägårdh J. (1999), "Microstructural Features and Related Properties of Self-Compacting Concrete" *Proc. of the first international RILEM symposium on self-compacting concrete*, Stockholm, pp 175-186.

Urano S., Hashimoto C. and Tsuji C. (1999), "Evaluation of Flow of Self-Compacting Concrete by Visualization Technique", *Proceeding of the first Rilem International Symposium on Self-Compacting Concrete.*

Vachon, M., (2002), "ASTM puts Self-Consolidating Concrete to the Test", Standardization News, June 2002, ASTM International, W. Conshohocken, USA, pp34-37.

Wüstholz T, (2005), "A Model Approach to Describe the Fresh Properties of Self-Compacting Concrete (SCC)", Otto-Graf-Journal 79, Vol. 16, 2005, pp 79-94

Westerholm M., (2006), "Rheology of the Mortar Phase of Concrete with Crushed Aggregate", *Licentiate Thesis*, Luleå University of Technology, Department of Chemical Engineering and GeosciencesDivision of Mineral, Processing2006:06

Yahia A., Tanimura M., Shimabukura A., Shimoyama Y. (1999), "Effect of Rheological Parameters on Self Compatibility of Concrete Containing Various Mineral Admixture", Proceeding of the first Rilem International Symposium on Self-Compacting Concrete, Stockholm, September, 523-535

Yamaguchi O., Nakajuma H. and Takahashi M. (1995), "The Effect of Paste and Mortar Containing Various Type of Water Reducing Agents", JCA *proceedings of Cement & Concrete*, vol. 49, 216-221 Stockholm, September, 25-34

Zhang X.and Han J. (2000), "The Effect of Ultra Fine Admixture on the Rheological Properties of Cement Paste", *Cement and Concrete Research* 30, 827-830

Zukoski, C.F., and Struble, L.J. (1993), "Rheology of Cementatious Systems", *Mater. Res. Soc. Bul.,* 18:39-42

The following papers had been written and published based on the research work presented in this thesis:

1. Ho D. W. S, Sheinn A. M. M., and Tam C. T., *"Sandwich concept of construction with SCC"*, Cement and Concrete Research, 31(2001), 1377-1381

2. Ho D. W. S, Sheinn A. M. M., Ng. C. C. and Tam C. T. , *"The use of quarry dust for SCC applications"*, Cement and Concrete Research, 32 (4), 505-511.

3. Ho D. W. S, Sheinn A. M. M. and Tam C. T., "S*ome major issues of SCC"*, Conspectus, 2001, 74-81.

4. Ho D. W. S, Sheinn A. M. M., Tam C. T. and Loy. T. S., "*SCC – Here to Stay"*, Singapore Concrete Institute, Concrete News, Feb, 2002, 305.

5. Ho D. W. S, Sheinn A. M. M. and Tam C. T., "*Rheological Model on paste Fraction of SCC"*, Cement and Concrete Research, submitted for publication

6. Ho D. W. S, Sheinn A. M. M. and Tam C. T., "*Rheological model for self-compacting concrete – paste rheology*", Proc. 27th Conference on Our World in Concrete & Structures, 29-30 August 2002, Singapore, pp517-523. (Awarded paper for Young Concrete Researcher Award, 2002)

7. Ho D. W. S, Sheinn A. M. M. and Tam C. T., "*Compatibility between conventional and SCC"*. Proc 2nd Int. Sym. on SCC, Japan 2001, 595-600

8. Ho D. W. S, Sheinn A. M. M., Ng C. C., Lim W. B. and Tam C. T., "*SCC for Singapore"*, Proc. 26th Conf on Our World in Concrete and Structures, Singapore, 2001, 293-299

9. Ho D. W. S, Sheinn A. M. M. and Tam C. T., "*Influence of mix constituents on paste rheology of SCC"*, Proc. 15th KKCNN, 19-20 December 2002, Singapore, pp13-18

10. Ho D. W. S, Sheinn A. M. M. and Tam C. T., "*Potential Benefits of SCC in Precast Construction*", Asian Concrete Construction Conference in Hong Kong, 26-27 November 2002

11. Ho D. W. S, Sheinn A. M. M. and Tam C. T., "Effect *of Particle Shape on Paste Rheology of SCC*", Proc 3rd Int. Sym. on SCC, Iceland 2003

12. Ho D. W. S, Sheinn A. M. M., Tam C. T., Bartos P.J. and Zhu W., "*Investigation on Interfacial Transition Zone of SCC Pastes by Use of Depth-Sensing Micro-Indentation*", Proc. 16th KKCNN, 08-10 December 2003, South Korea (**Awarded paper for KKCNN CHOI AWARD for Outstanding Young Researcher**)

13. Ho D. W. S, Sheinn A. M. M., Tam C. T., Quek S. T. (2004), "*Utilization of incineration ash in self-compacting concrete*", The Proceedings of 1st International Conference on Sustainable Construction Waste Management, Singapore

14. Ho D. W. S, Sheinn A. M. M., Tam C. T., Quek S. T. (2004), "*Utilization of incinerator ash*", to be published in Singapore Concrete Institute (SCI)

15. Ho D. W. S, Sheinn A. M. M., Tam C. T., (2004), "*Comparative study on hardened properties of Self-Compacting Concrete (SCC) with Normal Concrete (NC*)", Proc. 29th Conference on Our World in Concrete & Structures, August 2004.

16. Tam C.T., Sheinn A.M.M, Ong K.C.G and Chay C.Y(2005), "Modified J-Ring Approach for Assessing Passing Ability of SCC", *Proceeding of the Fourth International Symposium on Self-Compacting Concrete*, USA, pp 687-692

# APPENDIX A

## Example of Mix Design Calculation

## Design Target and Available Materials

| | |
|---|---|
| **Fresh Properties** | Slump Flow > 600 mm,<br>Funnel Flow Time < 15 sec,<br>L-Box Blocking Ratio, H1/H2 > 0.8<br>Retention Time ~ 90 min<br>1 D Compressive Strength ~ 10 Mpa |
| **Hardened Properties** | 28 D Compressive Strength of 60 MPa |
| **Reinforcement Clear Spacing** | 40 mm |
| **Available Materials** | OPC, Granite Dust, River Sand, Crush Granite, ADVA 108 & ADVA 109 |

## STEP 1 : Characterization of Raw Materials

| | **OPC** | **Granite Dust** | **FA 1** | **CA 1** |
|---|---|---|---|---|
| Specific Surface Area | 836 $m^2/\ell$ | 674 $m^2/\ell$ | 185.21 $cm^2/cm^3$ | 89.76 $cm^2/cm^3$ |
| Surface Modulus, SM | | | 24.23 | 18.5 |
| Mean Diameter | 20 um | 59 um | 0.7 mm | 12.2 mm |
| Chemical Reactivity | Reactive | Inert | Inert | Inert |
| Angularity Factor | 1.63 | 2.14 | 0.73 | 1.15 |
| Reactivity Factor | 1.68 | 1.0 | 1.0 | 1.0 |
| Repulsivity Factor | 1.4 | 1.0 | 1.0 | 1.0 |
| Specific Gravity | 3.15 | 2.65 | 2.6 | 2.65 |
| Absorption (%) | | | 0.9 | 0.6 |
| Bulk Density ($kg/m^3$) | | | 1619 | 1492 |
| Void Content (%) | | | 35.8 | 45.4 |

:

## STEP 2: Requirements of Concrete Properties

| **Research Objectives** | **Restriction (based on local condition & experience)** |
|---|---|
| 1) Target strength 60 MPa | 1) OPC used cannot be more than 470 kg/m$^3$ due to concern over excessive heat of hydration |
| 2) Retention time for about 90 min | 2) Water content should not be lower than 170 kg/m$^3$. |

Amount of OPC selected : 450 kg/m$^3$

w/c : 0.4 (to achieve 28D compressive strength of 60 MPa,

Water content : 180 kg/m$^3$

Assume nominal air content : 2.0 %

## STEP 3: Testing and finding the Optimum values of coarse-total aggregate ratio (i.e. $Ng_{min}$) and paste volume (i.e. $Vp_m$)

Determine $\mathbf{Ng_{min}}$ based on void content of binary mixture.

Nga = CA/(CA+FA)

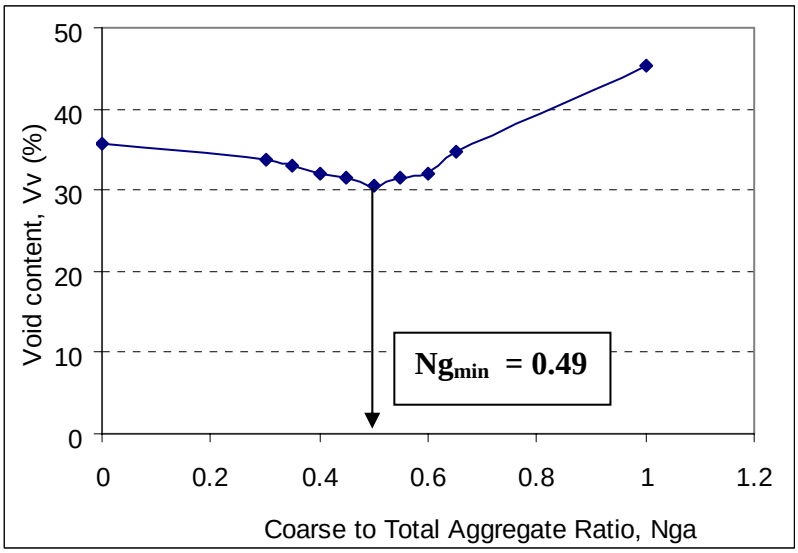


Fig A1. Relationship between void content (Vv) and coarse to total aggregate ratio (Nga)

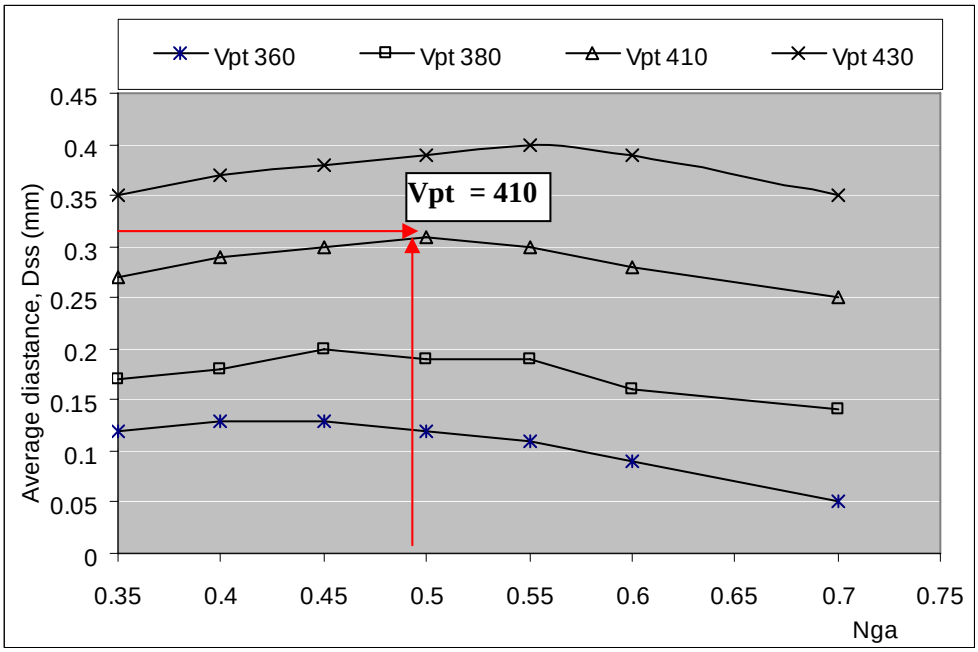


Fig. A2 Relationship between average inter-particle distance ($D_{ss}$) and coarse-total aggregate ratio (Nga)

For blocking criteria,

Dca = Dc/Dav = 40/6.53 = 6.13

Nb = Va/Vt = a2*Dca +b2 = 0.010484*6.13 + 0.533 = 0.597

Va = 0.597x1000 = 597 liter/$m^3$

From above analysis,

Total paste volume required to avoid blocking of aggregate,

Vp = Vt-Va = 409 liter/$m^3$ which is similar to the paste volume that gives the maximum Dss.

Therefore, optimum paste volume for this mix,

**Vpm = 410 liter/$m^3$**

Total aggregate volume = 1000-410 = 590 liter/$m^3$

0.49 = CA/(CA+FA)

**Volume of coarse aggregate = 287 liter /$m^3$ (760 kg/$m^3$)**

**Volume of fine aggregate = 303 liter /$m^3$ (790 kg/$m^3$)**

Total paste volume, = volume of OPC + volume of filler + Volume of water + Volume of Air + Volume of superplasticizer

$Vpm = V_{OPC} + V_{GR} + Vw + Vv + Vsp$

**$V_{GR}$ + Vsp = 410-142.86-180-20 = 67.14 liter/m$^3$**

At this point of time, ignore Vsp and volume of filler is assumed as 67.14 liter/m$^3$

## STEP 4: Dosage of Admixture

Saturation point of superplasticizer was determined with respect to water content, W/C or W/P.

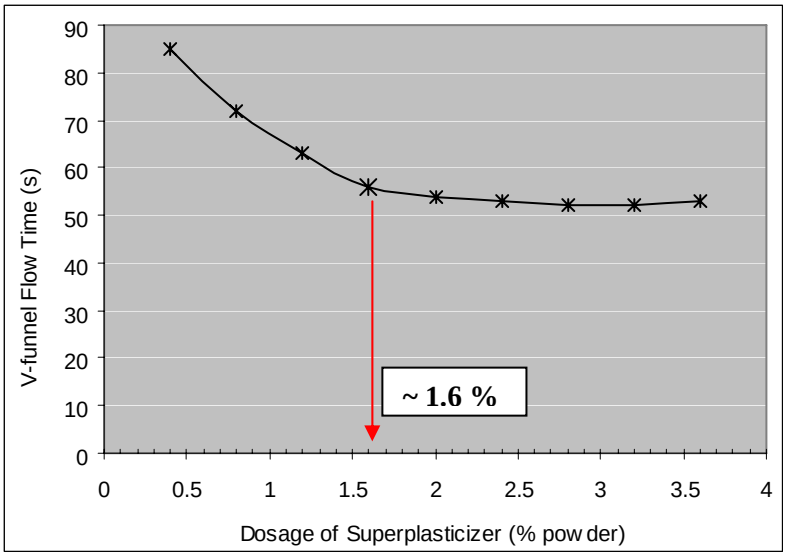


Fig. A3 Relationship between dosage of superplasticizer and V funnel flow time to investigate Saturation Point

Dosage of admixture, Vsp = 1.6% by volume of powder = 67.14x1.6x100/1.08 = 9946 ml

For requirement of 90 min retention time and 1D strength, 55% of ADVA 108 to 45% of ADVA 109 was used.

**Dosage of ADVA 108 = 5470 ml/m$^3$ (1215 ml per 100 kg of OPC)**

**Dosage of ADVA 109 = 4475 ml/m$^3$ (995 ml per 100 kg of OPC)**

**Total filler content, $V_{GR}$ = 67.14-9.946x1.08 = 56.4 liter = 150 kg/m$^3$**

From above mix design steps and calculation, the final mix proportion used for 60 MPa SCC incorporating granite fines can be presented in Table A1.

Table A1. Mix proportion used for 60 MPa SCC

| **OPC (kg)** | **Water (kg)** | **Granite (kg)** | **F-Agg (kg)** | **C-Agg (kg)** | **Adva 108 (ml)** | **Adva 109 (ml)** | **Air Content** |
|---|---|---|---|---|---|---|---|
| 450 | 180 | 150 | 790 | 760 | 1200* | 1000* | 2% |